Xylitol from low cost substrate and process optimization

A Thesis

Submitted in Partial Fulfillment of the Requirements for the Degree of

DOCTOR OF PHILOSOPHY

by

Harsh Vardhan

(176107107)

Department of Chemical Engineering

Indian Institute of Technology Guwahati

Guwahati - 781039, Assam (India)

June-2023

This thesis is dedicated to my Parents, Family Members and Mentors, who have motivated me to achieve my goal

DEPARTMENT OF CHEMICAL ENGINEERING

INDIAN INSTITUTE OF TECHNOLOGY GUWAHATI

STATEMENT

I do hereby declare that the content embodied in this thesis entitled "***Production of Xylitol from low cost substrate and process optimization***" is the result of investigations carried out by me at the Department of Chemical Engineering, Indian Institute of Technology Guwahati, Guwahati, India, under the guidance of **Prof. Kaustubha Mohanty and Dr. Soumya Sasmal.**

In keeping with the general practice of reporting scientific observations, due acknowledgements have been made wherever the work described is based on the findings of other investigators.

June, 2023 **Harsh Vardhan**

DEPARTMENT OF CHEMICAL ENGINEERING

INDIAN INSTITUTE OF TECHNOLOGY GUWAHATI

CERTIFICATE

This is to certify that **Mr. Harsh Vardhan** has been working under our supervision since January 2018. We here by forward his thesis entitled **"*Production of Xylitol from low cost substrate and process optimization*"** to be submitted for the award of the degree of Doctor of Philosophy to IIT Guwahati. We certify that he has fulfilled all the requirements according to the rules of this institute and the investigations embodied in his thesis have not been submitted elsewhere for a degree or diploma.

Date:
IIT Guwahati

Date:
Visva-Bharati

Dr. Kaustubha Mohanty
Professor and Head of the Department,
Department of Chemical Engineering
Indian Institute of Technology Guwahati

Dr. Soumya Sasmal
Assistant Professor
Department of Biotechnology
Visva-Bharati, West Bengal

ACKNOWLEDGEMENT

I would like to express my gratitude to everyone who made this possible and express my sincere gratitude to my supervisors Prof. Kaustubha Mohanty and Dr. Soumya Sasmal. This thesis would not have been possible without their valuable ideas, inspiration, and constant support during my research that helped me achieve this goal. Mohanty Sir has provided me the freedom and wisdom for research and allowed me to work in my own way. He has always cherished my new ideas and shown me the true pathway to approximate the research problem and implement to acquire the targets. I solemnly thanks to my thesis co supervisor Dr. Soumya Sasmal, for constant support, love, encouragement, scientific temperament, and true trust on me. It is very difficult to show my sincere gratitude to him with limited words. The best way to show my gratitude to him will probably be to follow the pathway which he has guided me to accomplish my goals.

I would like to thanks all my doctoral committee members Prof. Ramagopal V. S. Uppaluri, Dr. Partho Sarathi Gooh Pattader and Dr. Soumen Kumar Maiti for their valuable ideas and recommendations during my progress reviews and seminars that has led to the successful completion of this thesis. I would like to thanks present and former heads of the Department of Chemical Engineering, Prof. Kaustubha Mohanty, Prof. Anugrah Singh, and Prof. Bishnupadal Mandal, for supplying me with all the essential facilities.

I would also like to thanks all the staff members of the Department of Chemical Engineering for their true support and motivation. I am thankful to Chemical Engineering Department, School of Energy Science and Engineering, Department of Biosciences and Bioengineering, Central Instruments Facility (IIT Guwahati), Biotech Park and North East Centre for Biological Sciences and Healthcare Engineering (NECBH) for providing with the instrumental facilities.

I take the pleasure to thanks the present and former head of School of Energy Science and Engineering Department, IIT Guwahati, Prof. Kaustubha Mohanty and Prof. V.S.Mohalkar for allowing me to access the use of Laboratory and instrument facilities. I extended my heartfelt gratitude to Biofuels Laboratory (School of Energy Science and Engineering), IIT Guwahati and lab members for cell culture,

fermentation experiments and valuable suggestion during experiment.

I am grateful to the members of my research group for their selfless help and cooperation. Dr. Saran Sarangapany, Dr. Sounak Bera, Dr. Sanjeev Mishra, Dr. Bikashbindu Das, Dr. Madonna Roy, Dr. Vasu Chaudhary, Barasa Malakar, Sachankar Buragohain, Pranab Jyoti Sarma, Munmi Bhattacharya, Deepesh Singh Chauhan, Janaki Komandur, Saptaswa Biswas, Ankit Agarwal, Ananya Bardhan, Naveen Kumar A Yaranal, Aanisha Akhtar, Pooja Singh, Om Prakash, Anindita Das, Pikesh Kumar, Sanku Pratim Bora, Sachin Kumar Vaishya and Shubham Sharma. I would also like to acknowledge Suraj Kumar Panda, Saptarshi Gupta, Avinash Anand, Kaustubh Chandrakant Khaire, Shweta Kumbhar, Umesh, Aradhana Priyadarsini and Pushpita Das for their unconditional help and support.

This Ph.D. endeavor would not possible without support, love, trust, and blessings of my family members and parents. I owe my achievements to my family. I thank to my Sisters and Brothers for their constant support, love and encouragement. I thank my brother Raj Vardhan for their moral support and encouragement in achieving this level and always standing with me in all phases of my life. Finally, thanks to my one-stop solution, my wife Gayatri Khushbu for taking excellent care of me in my difficult times. I could not achieve this milestone without you.

I am forever grateful to Almighty God for giving me the strength to face life's challenges and make life beautiful.

Place: IIT Guwahati

Date: June 2023 **Harsh Vardhan**

ABSTRACT

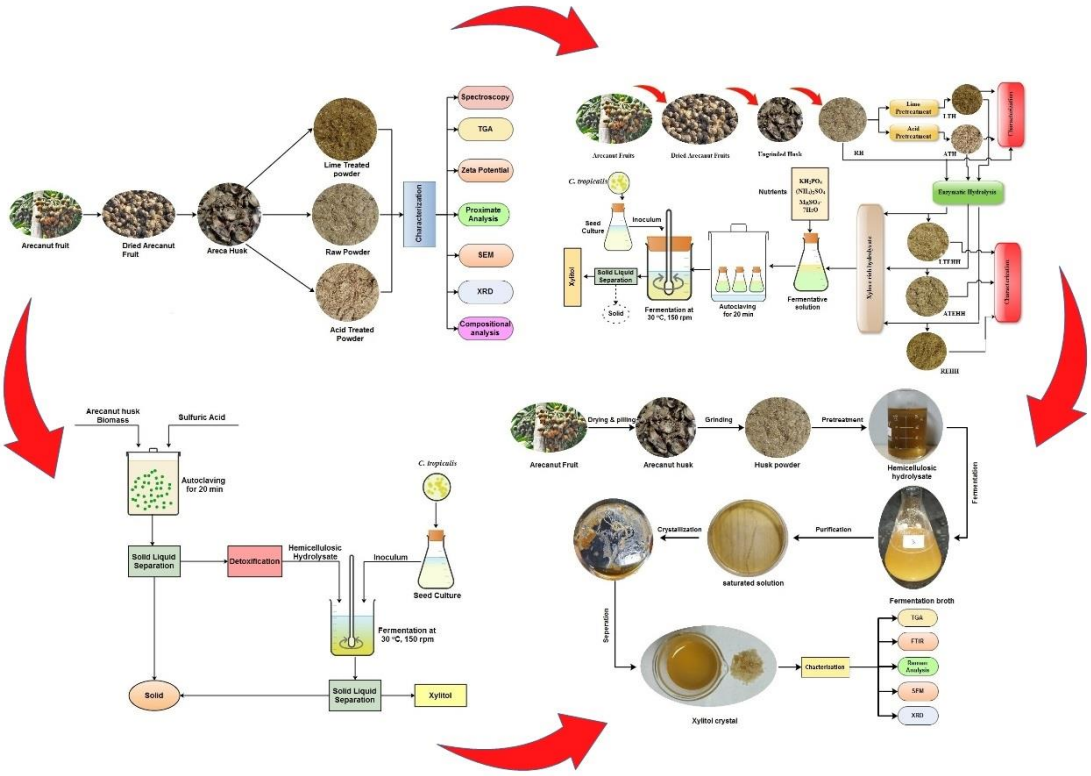

Xylitol is a high-quality polyalcohol, mainly used in pharmaceuticals, hygiene products, and food due to its functional properties such as anticarcinogenic, antibacterial, low-calorie, and hypoglycemic properties. At present, xylitol is primarily produced through chemical hydrogenation of xylose at high temperatures (150 °C) and pressure (5.5 MPa) on the reaction with metal catalysts such as Pl, Ru, Pt and Raney nickel. Separation and purification of xylitol is very expensive through this process. However, compared to this method, xylitol production through bioconversion of hemicellulosic hydrolysate by micro-organisms is an environment friendly, less energy-intensive, renewable, and overall economical process. This process ensures high safety, low production cost and high product selectivity.

The primary objective of this research is to utilize the agricultural bio-waste (such as areca nut husk) as a feedstock for the production of xylitol, preferably in a repetitive batch fermentation process, with *C. tropicalis* as the fermentative microorganism. Primary processes include, biomass characterization and pretreatment (Mainly dilute acid hydrolysis and lime treatment), Acidic and Enzymatic hydrolysis of biomass, detoxification of acidic hydrolysate by using activated charcoal and cation-anion

exchange resins, detoxified hydrolysate was fermented by *C. tropicalis* for xylitol production and finally downstream process was performed for product purification.

Lignocellulosic materials are inexpensive and readily available biomass in the form of either agricultural wastes or forest residues. These materials can be used as energy producer sources for solids (xylitol, etc.) liquids (ethanol, butanol, etc.) and gaseous (CO, H_2, etc.) as energy to meet increasing energy demands. Biomass pretreatment is a predetermined step to fragment lignocellulosic biomass into its basic components such as lignin and carbohydrate molecules. The first objective of present study is the pretreatment and characterization of lignocellulosic biomass namely Areca nut husk (*Arecan catechu*), which is widely available in the region of North-Eastern part of India. The study includes several physical characterizations like ultimate and proximate analysis, thermogravimetric analysis, crystallinity and chemical characterization that embraced Raman spectroscopy and FTIR. This study revealed that the Areca husk fiber contained 29.17% hemicellulose. Combination of all these properties revealed that Areca nut husk can be explored as the impending potential for low-cost source of xylose.

Direct biotransformation or saccharification of areca nut husk is very difficult because of recalcitrant nature of lignocellulose. To make biomass more amenable for saccharification, lime and acid pretreatment was conducted. But, before conducting the saccharification, compositional analysis was performed to know the initial available constituents in feedstocks. To improve the enzymatic hydrolysis of areca nut husk, various saccharification parameters like xylanase enzyme loading was varied. Results exposed that a highest yield (g/g) of reducing sugar about 90%, 83% and 15% were achieved for Acid Treated Husk (ATH), Lime Treated Husk (LTH) and Raw Husk (RH), at enzyme loading of 15.0 IU/g. Saccharification was performed at a substrate loading of 2% (w/V), 100 rpm agitation, 30 ◦C hydrolysis temperature for 12 h hydrolysis time at pH 4.5 to 5.0. Raman spectroscopy, Zeta potential, x-Ray diffraction (XRD), Field Emission Scanning Electron Microscopy (FESEM), Thermogravimetric Analysis (TGA), and Fourier Transform Infrared Spectroscopy (FTIR) were performed to know the structural changes in native, pretreated and saccharified residues. Structural analysis showed that major part of partial crystalline and amorphous cellulose in the areca nut husk biomass were hydrolyzed during saccharification. But, hydrolysis results the removal of amorphous substances, disruption of crystalline structure, and the transformation of crystalline zone to amorphous zone were noted.

Dilute acid hydrolysis is one of the most promising way for xylose production, which can be further use for xylitol production. But, detoxification is necessary before the fermentation of hydrolysate, because various toxic components present in the hydrolysate causes inhabitation problem. Various detoxification was performed and their effect on sugar loss and inhibitor removal was estimated. Detoxification includes series of treatments, primarily pH adjustment, activated charcoal treatment and Amberlit ion exchange resin treatment. Detoxification removed about 99% of toxic components present in the hemicellulosic hydrolysate. Further, fermentation parameters were optimized by using RSM and ANN techniques. The results of the ANN model showed that it was significantly more robust and accurate in estimating the values of the dependent variables compared to the RSM model. ANN has also been shown to be very accurate in finding optima and predicting optimal yields. RSM is recommended for modelling new processes, while ANN is better suited for modelling nonlinear systems with non-second-order interactions. Finally, Submerged fermentation process was performed by *C. tropicalis* for production of xylitol under the optimized conditions, which resulted the optimum yield of 0.74 g/g. It was concluded that detoxification by pH adjustment, activated charcoal and ion exchange resins are considered to be the most economical technique for removing toxic compounds from hemicellulosic hydrolysates and this medium is considered to have as huge potential for xylitol production.

Downstream processing of xylitol is one of the most important steps during xylitol production by microbial routes. The present research also highlights the product purification and separation from fermented broth. Xylitol crystals were separated by crystallization from fermented broth, accompanied by characterization of xylitol crystal such as X-ray diffraction (XRD), Differential scanning calorimetry (DSC), Thermogravimetric Analysis (TGA) and Raman analysis. DSC analysis revealed that the melting process of commercial xylitol crystals after crystallization (CXCAC) was observed at 93.71 °C with enthalpies of 210.7 J/g However, almost similar results were observed for xylitol crystals from fermentation broth (XCFB), having a melting point at 91.73 °C with enthalpies 220 J/g.

Keywords: Characterization, Pretreatment, Detoxification, Optimization, Fermentation, Crystallization

भारतीय प्रौद्योगिकी संस्थान गुवाहाटी
Indian Institute of Technology Guwahati

CONTENTS

LIST OF TABLES

LIST OF FIGURES

ABBREVIATIONS

AGU	Anhydroglucose Unit
AH	Acidic Hydrolysate
ANN	Artificial Neural Network Ann
ANOVA	Analysis of Variance
ATEHH	Acid Treated Enzymatic Hydrolysis Husk
ATFH	Acid Treated Fermentative Hydrolysate
ATH	Acid Treated Husk
ATH	Acid Treated Husk
CAGR	Compound Annual Growth Rate
CMC	Carboxy Methyl Cellulose
CRI	Crystallinity Index
CXCAC	Commercial Xylitol Crystals After Crystallization
DNS	Dinitrosalicylic Acid Method
DOE	Factorial Design of Experiment
DTG	Derivative Thermogravimetric
FBR	Fluidized Bed Reactor
FDA	Food and Drug Administration
FESEM	Field Emission Scanning Electron Microscopy
FTIR	Fourier Transform Infrared Spectroscopy
GA	Genetic Algorithm
HIS	High-Intensity Sweeteners
HMF	Hydroxymethyl Furfural
HPLC	High-Performance Liquid Chromatography
LCB	Lignocellulosic Biomass
LTEHH	Lime Treated Enzymatic Hydrolysis Husk
LTFH	Lime Treated Fermentative Hydrolysate
LTH	Lime Treated Husk
MB	Methylene Blue
MBS	Methylene Blue Staining

MLP	Multi-Layer Perceptron
NADH	Nicotinamide Adenine Dinucleotide
NADPH	Nicotinamide Adenine Dinucleotide Phosphate
ND	Not Detected
OTR	Oxygen Transfer Rate
OPEFB	Oil Palm Empty Fruit Bunch
OVAT	One Variable at a Time
REHH	Raw Enzymatic Hydrolysis Husk
RFH	Raw Fermentative Hydrolysate
RH	Raw Husk
RMSE	Root Mean Square Error
RSM	Response Surface Methodology
SP	Steam Explosion Pretreatment
SSFH	Synthetic Solution Fermentative Hydrolysate
TGA	Thermogravimetric Analysis
TPC	Total Phenolic Compounds;
XCFB	Xylitol Crystals from Fermentation Broth
XDH	Xylitol Dehydrogenase
XR	Xylose-Reductase
XRD	X Ray Diffraction Analysis
YPD	Yeast Extract Peptone Dextrose

SYMBOLS AND UNITS

g/L	Gram per liter
v/v	Volume/volume
µL	Microliter
mg mL^{-1}	Milligram per milliliter
°C	Degree Celsius
µm	Micrometer
g/L day^{-1}	Gram per liter per day
ΔX	Difference in biomass concentration
Δt	Cultivation period
mL	Milliliter
h	Hour
µg mL^{-1}	Microgram per milliliter
µM	Micromolar
rpm	Rotation per minute
µmol g^{-1} FW	Micromole per gram of fresh weight
g-force	Gravitational force
min	Minutes
$L_{content}$	Lipid content
W_{lipid}	Lipid weight
W_{sample}	Sample weight
w/v	Weight/volume
a.u.	Arbitrary unit
U mg^{-1} protein	Units per milligram of protein
mg g^{-1}	Milligram per gram
nm	Nanometer
wt.%	Weight percent

GW	Gigawatt
$\mu g\ mL^{-1}day^{-1}$	Microgram per millilitre per day
mV	Millivolt
ppm	Parts per million
µg/g FW	Microgram per gram of fresh weight
$mm^2\ s^{-1}$	Square millimeter per second
$MJ\ Kg^{-1}$	Megajoules per kg
$mol\ L^{-1}$	Mole per liter
kg^{-1}	Per kilogram
L^{-1}	Per liter
$kWh\ m^{-3}$	Kilowatt hour per cubic meter
g	Gram
K	Kelvin
$kJ\ mol^{-1}$	Kilojoule per mole
$kJ\ mol^{-1}\ K^{-1}$	Kilojoule per mole per kelvin
$kWh\ kg^{-1}$	Kilowatt hour per kilogram
$mmol\ g^{-1}$	Millimole per gram
cm^{-1}	Per centimetre
eV	Electronvolt
$m^2\ g^{-1}$	Meter square per gram
mL	Millilitre
$°C\ min^{-1}$	Degree Celsius per minute
$mL\ min^{-1}$	Millilitre per minute
Å	Angstrom

THESIS OUTLINE

The thesis is organized as per the guidelines of Indian Institute of Technology Guwahati. The thesis content has been divided into seven chapters following the objectives of this research study. The thesis is presented in the following seven chapters:

Chapter I: Introduction

Chapter II: Review of Literature and Objectives

Chapter III: Characterization and Pretreatment of Lignocellulosic Biomass

Chapter IV: Saccharification of Lignocellulosic biomass for production of fermentable sugar

Chapter V: Optimization of fermentation process for production of xylitol from detoxified dilute acid hemicellulosic hydrolysate

Chapter VI: Downstream process for separation of xylitol from fermentation fermentation broth and crystallization

Chapter VII: Overall Conclusions and Future Scope

A brief description of the content of each of the chapters is furnished below:

Chapter I: Introduction

This chapter starts with historical background of xylitol in the world, in which brief discussion about energy shortage during World War II and contributions of various country in its manufacturing process. It then describes the national and international scenario of xylitol, in terms of global market, production and consumption. Comparative analysis of Sugar substitute in India and world is also described vividly. Further, discussion on xylitol and it's natural occurrence, chemical structure and physical properties. Thereafter, discussion on different routes of xylitol production and various fermentation process optimization parameters. it then gives a brief idea about lignocellulosic biomass and its occurrence in India. Various Research challenges in xylitol production from lignocellulosic biomass have discussed in brief.

Chapter II: Review of Literature and Objectives

This chapter starts with Analysis of lignocellulosic biomass in India and

selection of suitable feedstock for xylitol production. Pretreatment is recognized as the most crucial step for biomass processing, in which physical, chemical and biological pretreatment are considered to be most prominent. later in this chapter, literature review on different mode hydrolysis of Lignocellulosic Biomass, like enzymatic and chemical hydrolysis. further, survey on various types of detoxification methodology like, biological, physical, chemical, solid-liquid and liquid-liquid. The chapter then discusses about xylitol process modelling and process optimization, followed by fermentation and separation of xylitol crystal. Based on the discussion in the chapter, knowledge gap was discussed and four objectives were decided and planned accordingly.

Chapter III: Characterization and Pretreatment of Lignocellulosic Biomass

Agricultural waste is a most promising renewable energy source and can be defined as complex polymers of cellulose, hemicellulose and lignin. Therefore, it is called lignocellulosic material. Various permutations and combinations of the three components, makes this biomass properties unique from another biomass. These properties vary from biomass to biomass. In addition to biofuel production, lignocellulosic biomass serves as a feedstock for the production of value-added chemicals such as xylitol. Therefore, characterization and pretreatment of varying compositions of biomass is necessary for their analysis. The primary objective of this chapter is to characterization and pretreatment of Areca nut husk (*Areca catechu*), which is widely available in the region of North-Eastern part of India. This analysis showed the potential of this biomass as a feedstock for the production xylitol. This lignocellulose matrix provides the basic structure of plants. It is composed of three main components such as cellulose, hemicellulose and lignin. The cellulose, hemicellulose and lignin concentration were determined as 43.28%, 29.17% and 12.64% for Raw Husk, 45.30%, 23.50% and 14.50% for Lime Treated Husk and 51.7%, 11.2% and 19.8% for Acid Treated Husk, respectively. The lignin concentration of three biomass samples was found to be between 11-23%. Various physical characterization (XRD, TGA, FESEM, Zeta Potential Raman and FTIR) and chemical characterization processes were applied in this study and their outcomes are also explained vividly.

Chapter IV: Saccharification of Lignocellulosic biomass for production of fermentable sugar

Areca nut husk was pretreated and then saccharified to convert hemicellulose xylose into fermentable sugars. Plant cell walls are solid lignocellulosic composites. Enzymes must act directly at the solid-liquid interface and participate in surface depolymerization of individual cellulose chains to hydrolyze carbohydrate polymers. This surface ablation process results in kinetics that are several orders of magnitude slower than freely diffusing enzymatic reactions because the conversion is limited by substrate accessibility. A dilute sulfuric acid and lime pretreatment procedure was performed to make the biomass more suitable for the enzymatic saccharification process. An enzymatic saccharification process using a xylanase enzyme was used to compare pretreated biomass samples. The activity of the xylanase enzyme was found to be 2.65 IU/mL. The pretreated lignocellulosic biomass was used for enzymatic hydrolysis at 50°C, 150 RPM for 96 hours at different enzyme loading (2, 5, 10 and 15 IU/g of biomass). The pH of the medium was maintained at 4.6. The yield of reducing sugar was higher in case of acid treated husk (about 89%) as compared to lime treated husk (about 83%).

Chapter V: Optimization of fermentation process for production of xylitol from detoxified dilute acid hemicellulosic hydrolysate

This chapter describes the process optimization for production of maximum hemicellulosic hydrolysate from areca nut husk by varying various dilute acid hydrolysis parameters. Detoxification of hemicellulosic acid hydrolysate were conducted by adjusting the pH, treatment with activated charcoal and ion exchange resins. Optimization of fermentation process was conducted by RSM and ANN modelling procedure. Various parameters were optimized such as substrate concentration, temperature, pH and fermentation time. The optimized condition of fermentation process for production of xylitol was achieved at temperature 40 °C, OLR 50 kg/L and pH 5.5 respectively. Fermentation was conducted by *Candida tropicalis* as per optimized conditions and observed that optimum yield of xylitol was found to be 0.66 g/g.

Chapter VI: Downstream process for separation of xylitol from fermentation broth and crystallization

This chapter describes the downstream process for separation of xylitol from fermentation broth and crystallization. The experiment was conducted as per literature. Thereafter, firstly purification of fermentation broth was conducted by adjusting the pH, treatment with activated charcoal and ion exchange resins. Purified fermented broth was concentred for crystallization by using vacuum rotavapor as per literature. Crystallization was performed by raising the temperature of solution by 10 °C above the saturation temperature followed by addition of negligible amount xylitol for initial crystal growth. Separation of xylitol crystal was performed, followed by characterization of xylitol crystal to compare properties of xylitol crystal obtained after fermentation and pure xylitol crystal.

Chapter VII: Overall Conclusions and Future Scope

This chapter summarizes the conclusions drawn from the current work and the recommendations for future work. The overall objective of this thesis is to produce xylitol from lignocellulosic biomass areca nut husk. The data revealed that areca nut husk have great potential for xylitol production by micro-organism species *candida tropicalis*. It can be concluded, that the research regarding obtaining the xylitol from lignocellulosic biomass can be enhanced by optimizing the metabolic activity of the micro-organism strain.

भारतीय प्रौद्योगिकी संस्थान गुवाहाटी
Indian Institute of Technology Guwahati

Chapter 1

Introduction

1.1. Historical background

Xylitol was first discovered in Finland in 1891 by German chemist Emil Fischer. This xylitol made chemically by using birch trees wood (D-xylose) [1,2]. However, its purity was doubtful because it contained small amounts of sugar alcohols in addition to xylitol. Its discovery was uneventful, and xylitol remained just a research chemical until the 1930s. But, during World War II, when Finland was suffering from a shortage of sucrose (table sugar). During this time, chemists and engineers find alternative sweeteners due to war-associated sugar shortages in countries in Finland and began using xylitol as a sugar substitute. In 1963, it was approved in the United States by the Food and Drug Administration (FDA) for use as a special dietary and nutritional additive [1]. The first large-scale production of sugar alcohols was carried out in 1975 by a Finnish company. At the same time, a Swiss company was interested in producing xylitol, so in 1976 the two joined forces and he founded a company called Xyrofin. While this was happening, other companies in the former Soviet Union, China, Japan, Germany and Italy were producing xylitol for the domestic market. Prior to 1970, it was primarily used in diabetic diets and parenteral nutrition [2]. In 1975, the first xylitol chewing gum was launched in Finland. A few months later, the first chewing gum containing xylitol was also launched in the United States [2].

1.2. National and international scenario of xylitol

Growing demand for xylitol in food and nutraceutical applications is expected to be a key driving factor for the market over the forecast period. The global xylitol market size was valued at USD 447.88 million in 2020 and is expected to expand at a compound annual

growth rate (CAGR) of 6.4% from 2020 to 2028 [3]. Asia Pacific led the global market in 2020 accounting for the largest revenue share of more than 39%. China is the leading producer of xylitol followed by Europe and the U.S. Whereas China, India, and Thailand are among the leading consumers of xylitol in the region. It is one of the versatile natural sweeteners, which is widely used in chewing gums, nutraceuticals, and diabetic foods. China is the key exporter across the globe. The U.S., Europe, India, and other South Asia countries are the key export destinations for China in the market [4].

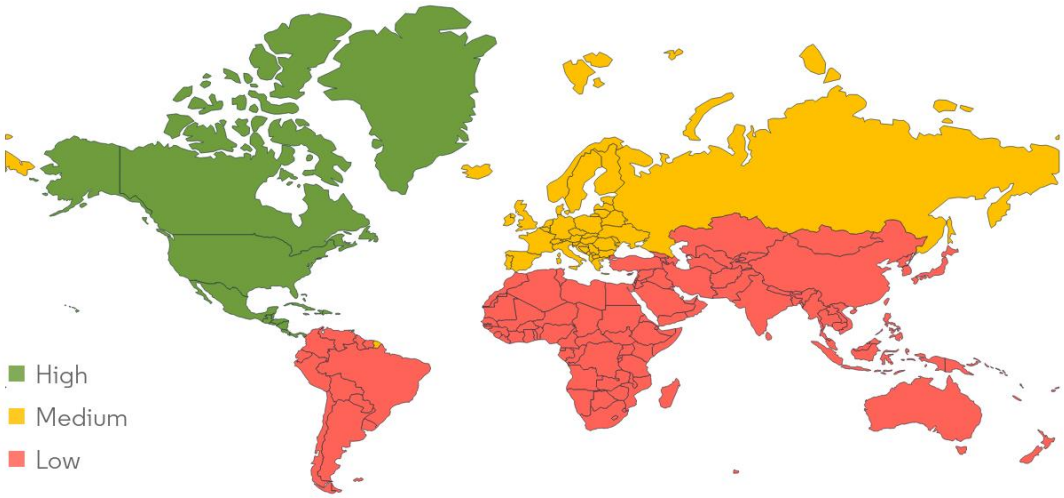

Figure 1.1 Xylitol Market size by region 2018 [4]

Xylitol has 40% fewer calories than regular sugar. A teaspoon of sugar contains 16 calories compared to a teaspoon of xylitol, which has 9.6 calories. It is used in chewing gum manufacturing as a sugar substitute due to its pleasant cooling effect. In America, Europe, and Asia, xylitol is widely used in chewing gums, mints, lozenges, and candies. It also has potential applications in bakery items, sauces, condiments, pharmaceuticals, and nutraceuticals [3].

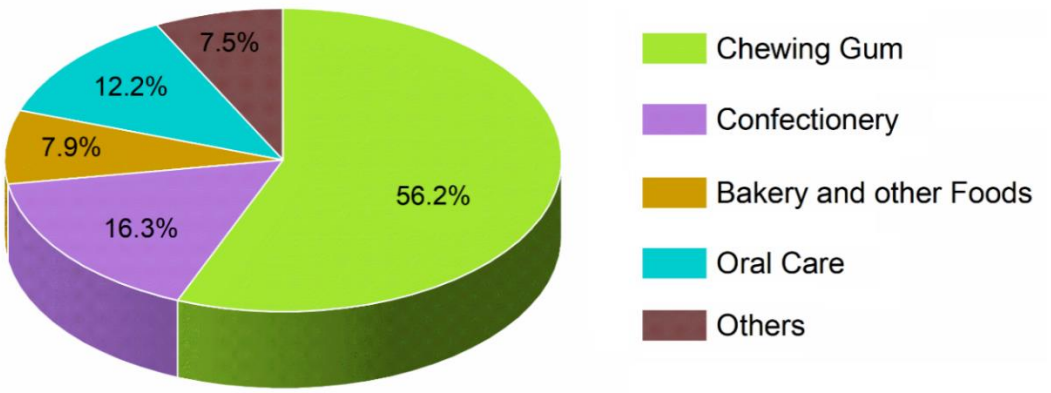

Figure 1.2 Nutraceuticals & Functional Foods chart [3]

The global market is characterized by the presence of several global and regional players. The production is concentrated in the U.S., China, and Europe. The market has a high potential for emerging and new players that require broad support across the world. Some of the prominent players in the global xylitol market include: DuPont de Nemours, Inc., Roquette Freres, Cargill, Incorporated, Ingredion Incorporated, Mitsubishi Corporation Life Sciences Limited, Thompson Biotech (Xiamen) Co., Ltd., ZuChem, Inc., Herboveda India, Godavari Biorefineries Ltd. and NovaGreen, Inc [3,4].

1.2.1. Comparative analysis of Sugar substitute in India and world

In the European region, Germany is the largest market for food sweeteners. An increase in the consumption of processed food products is driving the market's growth. Germany Food Sweeteners market is segmented by type which includes Sucrose, Starch Sweeteners and Sugar Alcohols, and High-Intensity Sweeteners.

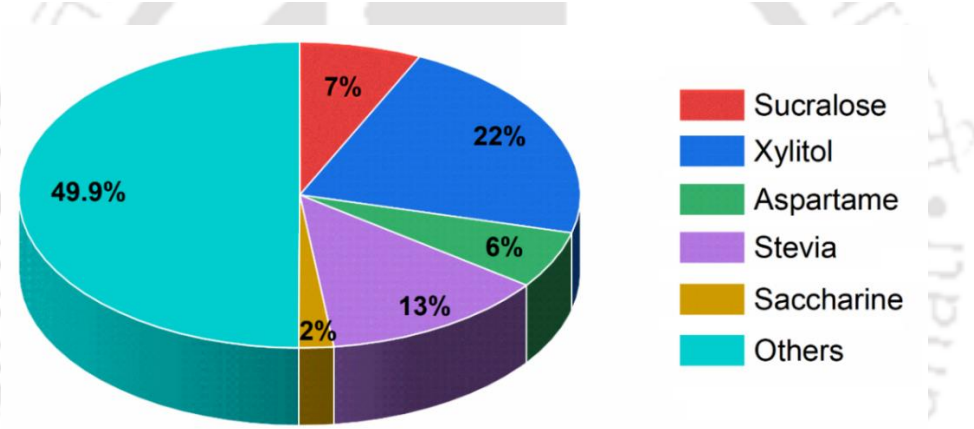

Figure 1.3 Sugar Substitute Market share by segment in Germany, 2018 [4]

India's food sweetener market is forecast to register a CAGR of 4.2 % during the forecast period (2022-2027). The market study of the Indian food sweetener market is segmented by sucrose, starch sweeteners and, sugar alcohols, high-intensity sweeteners (HIS). Starch sweeteners and sugar alcohols include xylitol, sorbitol, dextrose and others. By application as dairy, bakery, beverages, confectionery, and others [4].

More than 62 million Indians are currently affected by diabetes, which is more than 7.1% of the adult population. Furthermore, nearly one million Indians die due to diabetes every year. In terms of Gender, Females account for more than half of the diabetic population in India. People in the age group of 40-74 have shown a high risk of diabetes in India [3]. Consumers have adopted artificial sweeteners due to increasing awareness of the risks associated with diabetes. Day by day increasing Indian diabetic population makes xylitol to be the fastest-growing sweetener segment over the forecast period. The growing awareness

about the health benefits of xylitol over sugar has increased its demand. In 2013, the government approved xylitol production in the Indian subcontinent. Indian players trying to established industries based on production of sugar substitute and gain a competitive advantage. Major Indian players are Herboveda India, Godavari Biorefineries Ltd., NovaGreen, Inc and others [3,4].

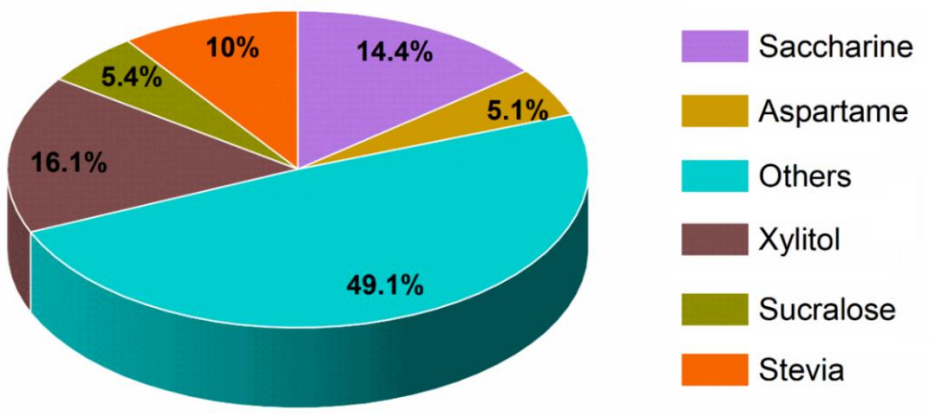

Figure 1.4 Sugar Substitute Market share by segment India, 2018 [4]

1.2.2. Economic analysis and market trends on the production of Xylitol

Xylitol is a major value-added chemical that can be produced from renewable resources such as hardwoods and maize. According to the International Market Analysis Research Consulting Group (IMARC), the global market for xylitol was valued at 921 million USD in 2020, and it is projected to reach 1.37 billion USD in the next five years [5]. In India, xylitol production is in its infancy, and the market is expected to grow rapidly in the coming years due to the increasing demand for sugar substitutes and rising health awareness among consumers. The Indian government has launched various initiatives to promote the use of renewable resources in the production of chemicals, which will boost the production of xylitol. However, India is still dependent on imports for most of its xylitol requirements.

DuPont, an American-based company, is the world's largest producer of xylitol, and it commercializes xylitol under the trade name xivia. Nearly 70% of xylitol production is used in the production of confectionery items and chewing gums, making it an essential ingredient in the food industry. Xylitol has been certified to be safe for consumption by the US Food and Drug Administration, which makes it a popular choice among consumers [5].

In the bioproduction of xylitol, techno-economic analysis and assessment of environmental impact must be done at every step of the production process. This will ensure that the biomass is valorized sustainably with minimal waste production. Integrating xylitol production with other products makes the bioconversion process industrially feasible and can lead to the creation of a circular bio-based economy. Life cycle assessments are crucial to

understanding the environmental impact of xylitol production.

Studies have been conducted to estimate the material and energy balance and carbon dioxide emission levels in the bioproduction of xylitol. These studies have shown that energy requirements and greenhouse gas emissions can be reduced by employing heat integration between processes. In India, research and development initiatives are underway to develop more sustainable and efficient processes for xylitol production.

Lastly, xylitol is a valuable chemical that can be produced sustainably from renewable resources. The global market for xylitol is growing rapidly, and India is expected to play a significant role in this growth. However, sustainable production processes and life cycle assessments are crucial for the long-term success of the xylitol industry.

1.3. Xylitol

Xylitol is a naturally occurring 5-carbon sugar alcohol found in the fibers of many vegetables, fruits, and produced by the reduction of D-xylose (from hemicellulose fraction of lignocellulose). Raspberries, yellow plum, strawberries, cauliflower, corn, lettuce, and corn husks all contain natural xylitol [6]. Xylitol is not an artificial sweetener, like aspartame or sucralose. It is produced by plants and animals. It was first produced from birch trees and now it is more commonly produced from lignocellulosic material. Xylitol can be found naturally in many unusual places. In fact, our bodies naturally make 5-10 grams of the stuff every day [7]. For commercial purposes, xylitol comes from lignocellulosic material such as corncob, sugarcane bagasse, areca nut husk etc. This product is unique due to its chemical structure as compared to other sugars. Unlike carbohydrates, such as monosaccharide (i.e., fructose, glucose and galactose) and disaccharides (i.e., maltose, sucrose and lactose), xylitol has a five-carbon structure.

On an average individual Indians consumes about 10 spoons sugar per day, which is about 18 kg of sugar per year [8]. In addition, all of us are consuming considerable amounts of sugar in hidden forms from different processed food items such as sweetened beverage which contains up to 40 g (10 teaspoon) of free sugars. Large sugar intake can lead to weight gain, which can lead to diabetes and obesity; Excess sugar consumption can also raise blood pressure, triglycerides, and bad cholesterol levels, all of which increase the risk of heart disease, among other systemic effects. Xylitol can be used by anyone trying to lower their sugar intake and reduce calories from sugar; it has about 75% fewer carbohydrates and 40% fewer calories than sugar [9]. It is compatible and complementary with all current oral hygiene recommendations and beneficial for all age groups of people. Many people (mainly

young children) are affected by tooth decay. Small child who is allowed to snack all day or an older patient who has exposed root surfaces; Many can be helped by introducing xylitol to their caregivers or to the patients themselves. Because xylitol comes in many forms, it's easy to incorporate into everyday life. Chewing xylitol gum or even using xylitol mint after meals can help reduce plaque and food debris, increase salivation, and inhibit bacterial growth. People with xerostomia can greatly benefit from taking xylitol regularly.

Another group of people who can greatly benefit from taking xylitol regularly are people with xerostomia. The patients taking prescription drugs where xerostomia is a common side effect where people suffer from dry mouth. Not only can dry mouth be uncomfortable, but it also carries other risk factors, such as mouth sores, thrush, chapped lips, poor chewing and swallowing, and increased tooth decay [7]. Recommending xylitol with the right guidelines can help patients deal with such issues. Xylitol can also be used in the diet of diabetics because it is slowly absorbed through the intestinal system, its initial metabolic steps are insulin-independent, and it does not cause rapid changes in blood glucose concentration [10]. Due to the insulin-independent nature of xylitol, it has been used as a sweetener in diabetic diets in Germany, Switzerland, Russia and Japan since the 1960s [9]. It can be metabolized in the absence of insulin and can replace sugar (sucrose) on a weight basis, making it a suitable sweetener for diabetics [11]. Obesity can also be reduced by regularly consuming xylitol [12]. According to some studies, xylitol also appears to have potential as a useful promoter of absorption and treatment of osteoporosis, acting as a chelating agent and complexing with cations such as calcium with intermediate stabilities [13,14]. Xylitol has many benefits as an ingredient or additive in nutritional formulas. It is not subject to the harmful Maillard reaction, which is responsible for both darkening and reducing the nutritional value of proteins due to the destruction of amino acids. It limits obesity tendencies when continuously supplied in the diet and improves the sensory properties of food products when added in formulations without physical instability and chemical deterioration during storage [12].

1.3.1. Physical Properties and chemical structure of Xylitol

Xylitol is a naturally occurring five-carbon sugar alcohol (Figure 1.5) that has the similar sweetness and one-third the caloric content of sucrose [15]. Xylitol is a pentavalent sugar alcohol with the empirical formula $C_5H_{12}O_5$ and MW 152.15. Xylitol is a meso compound that is completely devoid of optical activity in solution. Its structure is indicated in Figure 1.5. Its physical properties are listed in Table 1.1. It is found in small amounts in various plants,

fruits, and vegetables (Table 1.2) or can be produced by chemical or microbial reduction of D-xylose from xylan-rich hemicellulose hydrolysates (Figure 1.6). Hemicellulose, which accounts for 19-34% of plant biomass, is an abundant polymer in nature. It consists of several monomers including xylose, glucose, galactose, arabinose, mannose and glucuronic acid with side acetyl groups in its branched structure [16]. Sugar cane bagasse, corn fiber, oats, corn cobs, cottonseed hulls, rice straw, birch wood, and nut shells are xylan-rich substrates that can be used as feedstock for commercial xylitol production [17].

Table 1.1 Physical properties of xylitol [17,18]

Property	**Xylitol**
Formula	$C_5H_{12}O_5$
Molecular Weight	152.15
Melting Point (°C)	93 – 94.5
Boiling Point (at 760 mmHg)	216 °C
Density (bulk density) (15 °C)	1.50 g/L
Caloric value	4.06 cal/g (16.88 J/g)
Appearance	White, crystalline powder
Odour	None
Solubility at 20 °C	169 g/100 g H_2O
pH in water (1 g/10 mL)	5 – 7
Density (sp. gravity) of aqueous solution (20 °C), 10%	1.03
60%	1.23
Moisture absorption (%) (4 days, 20-22 °C at 60% relative humidity	0.05
at 92% relative humidity	90
Heat of solution,	Endothermic, 36.61 Cal/g (153.76 J/g)
Viscosity (cP) (20 °C) , 10%	1.23
40%	4.18
50%	8.04
60%	20.63
Relative sweetness	Equal to sucrose; greater than sorbitol and mannitol
Specific rotation	optically inactive

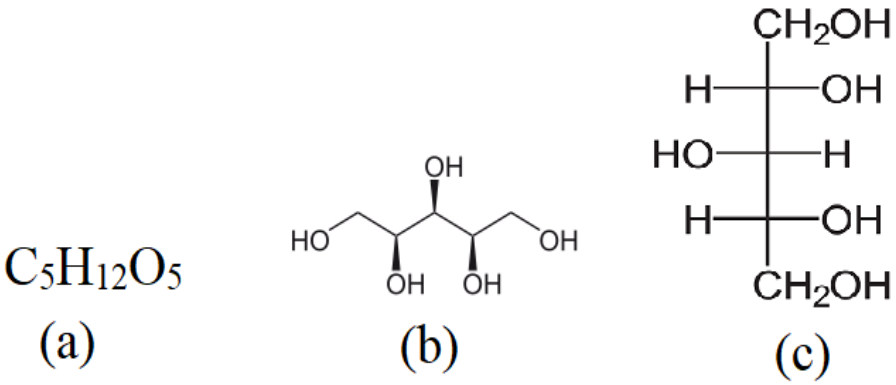

Figure 1.5 Chemical formula (a) and structure (b, c) of xylitol (IUPAC: Pentane-1,2,3,4,5-Pentol)

1.3.2. Production of xylitol on large scale

The production of xylitol by extraction from its natural sources is very difficult and uneconomical because of the relatively small occurrences. Xylose, a pentose that can be hydrogenated to xylitol, is known to be widespread in plant matter. It is not found in plants in the free state, but mostly in the form of xylan, a polysaccharide made up of D-xylose units found in association with cellulose. Xylose also occurs as part of glycosides [19].

Despite its widespread availability in nature, xylose is difficult to produce commercially due to the problems encountered in separating it, particularly from other carbohydrates such as glucose. However, the fact that xylan is more easily hydrolyzed than cellulose offers the technical possibility for xylose extraction and xylitol production. Accordingly, the extraction of xylose from plant material and its subsequent hydrogenation is the basic principle of xylitol production (Figure 1.6).

Table 1.2 Xylitol presence in fruits and vegetables [18]

Product	**Xylitol (mg/100 g dry substance)**
Leek	53
Carrot	86.5
Onion	89
Fennel	92
Brewer's Yeast	4.5
Carrot Juice	12
Chestnut	14
Banana	21

White Mushroom	128
Eggplant	180
Endive	258
Raspberry	268
Kohlrabi	94
Lettuce	96.5
Pumpkin	96.5
Spinach	107
Strawberry	362
Yellow Plum	935
Lamb's Lettuce	273
Cauliflower	300

Plant materials that contain a suitable amount of xylans for use in this process include hardwoods such as birch and beech, oat and cotton seed hulls, corn cobs, bagasse of sugar cane, straw and various nut shells. The xylan or xylose content of such materials is 2 & 30% of dry matter. The selection of raw materials for the production of pure xylitol is important. Most alternatives are bulky and low-density. Optimally, therefore, the raw material for large-scale production should be one that is centrally available in large quantities and with a relatively high xylan content. Agricultural by-products are used in some of the existing processes, e.g. B. Almond shells in Italy and apparently rice and cotton seed shells in China and the Soviet Union. The large Finnish production is based on birch wood chips, while in Germany other hardwood chips were used. Xylan-containing sulfite waste from the pulp and paper industry has been proposed as a more economical alternative to hardwoods. Production in the US is expected to be based on corn cobs. All of these raw materials contain relatively small amounts of polymers of other sugars such as glucose, mannose, arabinose and galactose in their hemicelluloses. The hydrolysates require extensive purification and separations to remove these sugars from xylose and xylitol. Nevertheless, it is possible to recover about 50-60% of the xylans as xylitol.

1.3.3. Existing industrial method of xylitol production in India and World

The industrial production of xylitol typically involves the hydrolysis of hemicellulose-rich materials, such as corn cobs, birch, or beech wood, to obtain xylose. The xylose is then fermented using a microorganism, usually a strain of yeast or fungus, to produce xylitol. The

following are some details on the existing industrial methods of xylitol production in India and internationally:

In India, the most common raw material used for the production of xylitol is corn cobs. The hydrolysis of corn cobs is carried out using dilute sulfuric acid at a high temperature and pressure. The resulting xylose is then fermented using a yeast strain, *Candida tropicalis*, to produce xylitol. The process is carried out in a batch or fed-batch mode, and the fermentation time ranges from 48 to 96 hours. The xylitol is then purified using methods such as ion exchange chromatography or crystallization [20].

The industrial methods of xylitol production used in other countries are similar to those used in India. The raw materials used include birch and beech wood, corn cobs, and sugarcane bagasse. The hydrolysis process varies depending on the raw material used, but typically involves the use of acid or enzymes. The fermentation process involves the use of different strains of yeast or fungi, such as *Candida guilliermondii*, *Candida parapsilosis*, and *Candida utilis*. The xylitol is purified using methods such as crystallization, recrystallization, or chromatography [21].

Overall, the industrial methods of xylitol production are well-established and have been optimized for high yields and purity. These methods have made xylitol production commercially viable, and xylitol is now widely used as a low-calorie sweetener in a variety of food and beverage products.

1.3.4. Routes of Xylitol production

Theoretically, xylitol can be obtained from extraction of fruits and vegetables, chemical and biotechnological processes. The comparison of chemical and biological methods of xylitol production with their advantages and disadvantages has been listed in Table 1.3. Various routes of xylitol production discussed in the following sections and shown in Figure 1.6.

Table 1.3 Comparison of Chemical and Biological method of xylitol production [22]

Factor	Biological	Chemical
Carbon Source	Xylose from lignocellulose	Pure xylose from lignocellulose
Catalyst	Yeast/bacteria/fungi that require xylose reductase and xylitol dehydrogenase enzyme	Nickel and hydrogenation
Process Steps	- Acid or enzymatic hydrolysis of lignocellulose	- Acid hydrolysis of lignocellulose

	- Detoxification of hydrolysate - Fermentation of hydrolysate to xylitol - Xylitol purification	- Purification of hydrolysate to obtain pure xylose - Hydrogenation of xylose to xylitol - Xylitol crystallization
Purification	Complex downstream process because of different microbial by-products	Ion-exchange resins
Advantages	- Uses renewable resources - More environmentally friendly - Lower energy and mild temperature - Lower setup and maintenance costs	- High yield of Xylitol production - Quick and efficient process - Can use a variety of raw materials - Provides highly purified xylose
Disadvantages	- Lower yield of Xylitol production - Longer production time - Requires more specialized knowledge and skills	- Harsh chemicals are required, which can be harmful to the environment - High energy consumption - Expensive setup and maintenance costs - Laborious and cost/energy-intensive - Use of extensive separation and purification steps - Requires high temperature and pressure - Low efficiency process - Not environmentally friendly
Cost	Lower due to lower energy and mild temperature	High due to the need for two steps of purification process, high energy required, and laborious

1.3.4.1. Extraction from fruits and vegetables

Xylitol is found naturally in vegetables and fruits, as well as in lichen, algae, yeast, and fungi. It can be recovered from these sources by solid-liquid extraction, but its quantity is very low in such raw materials (less than 900 mg/100 g) is a major economic disadvantage for this process [23].

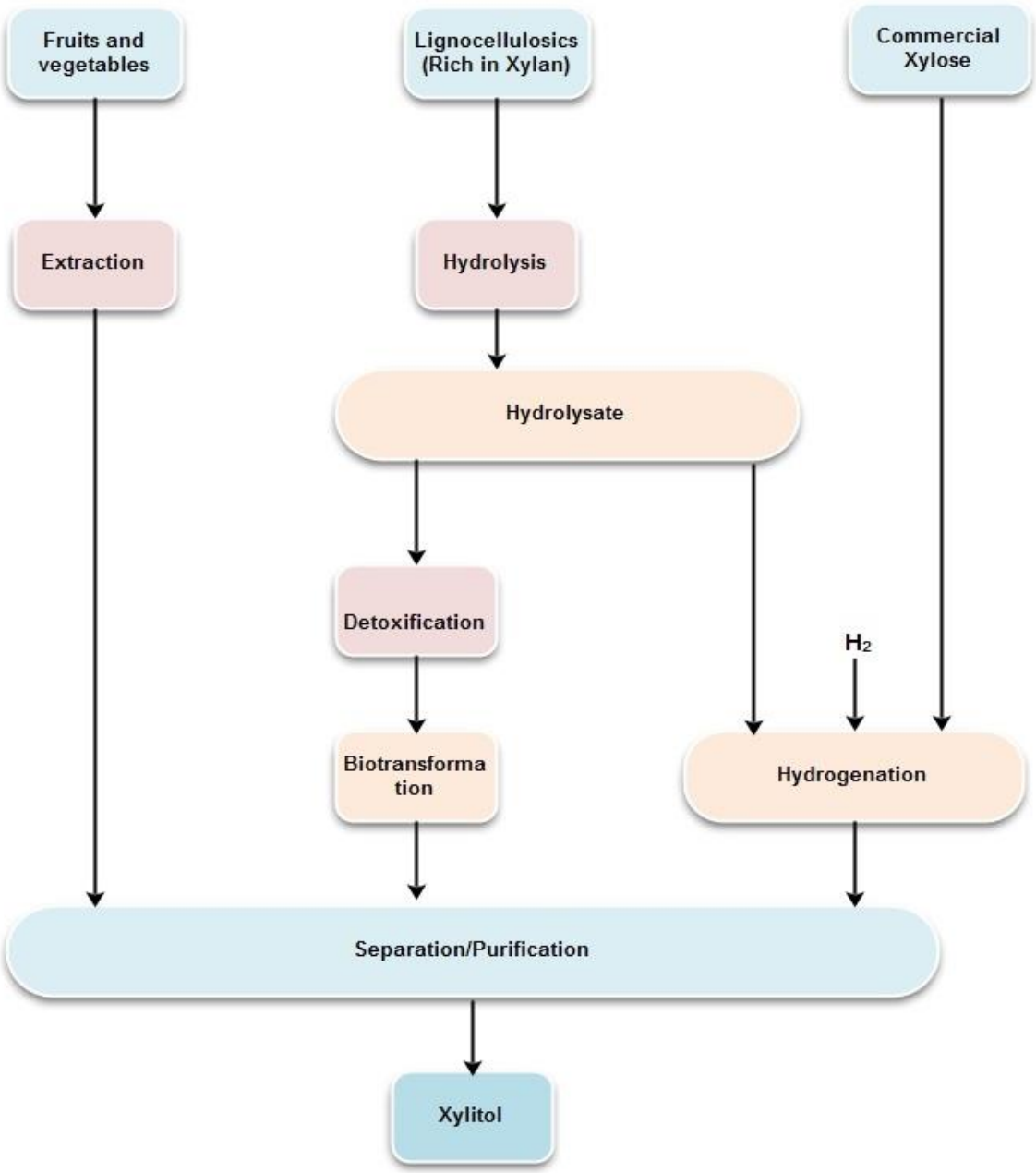

Figure 1.6 Xylitol production methods [12]

1.3.4.2. Xylitol from chemical source

The process starts with the acid-catalyzed hydrolysis of xylans (polysaccharides belonging to the hemicellulose fraction of plant biomass) for the production of xylose [17]. However, when other polymers other than xylan are present in the hemicellulose fraction of biomass, hydrolysis of the associated polymers produces hydrolysates containing various impurities such as glucose, arabinose, galactose and mannose. Costly purification steps are required if pure xylose is desired [24]. Most of the impurities consist of monosaccharides that cannot be removed by ion-exchange chromatography or activated carbon [25]. After purification and removal of dyes, metal ions, proteins, and other impurities, the xylose-

containing hydrolyzate is subjected to hydrogenation at 80-140° C. and a hydrogen pressure of about 5000 kPa in the presence of a metal catalyst. The xylitol solution produced by the reduction process requires further purification by chromatographic fractionation, followed by concentration and crystallization of the product to obtain pure xylitol [24]. Among all the steps, separation and purification are the costliest. The yield of xylitol is about 50-60% of the starting xylose [26]. The chemical process for xylitol production based on catalytic hydrogenation of xylose-rich hemicellulose hydrolyzate is briefly illustrated as follows.

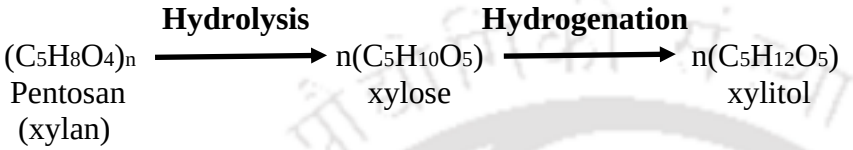

(1.1)

The major drawbacks of traditional production methods, particularly high contamination levels and waste disposal concerns, have led researchers to find alternatives to xylitol production. One of the most interesting methods is microbial production [25].

1.3.4.3. Xylitol production from microbial sources

Production of xylitol takes place from D-xylose by NADPH-dependent xylose reductase as a metabolic intermediate in xylose-utilizing microorganisms [27]. Table 1.4 shows that many yeasts and molds have the enzyme xylose reductase and are therefore able to produce xylitol. *Croquecera, Trichosporon, Pichia, Cryptococcus, Rhodotorula, Hansenula, Kluyveromyces, Paxsolen, Torropsis, Monilia, Ambrodiozyma,* and *Torula* are yeasts capable of producing xylitol [27].

Enterobacter licefaciens, Corynebacterium sp. and *Mycobacterium smegmatis* can also produce xylitol [28]. Microbial conversion of D-xylose to xylitol is important for industrial production and has been extensively studied in yeast compared to other microorganisms. In a seventh biochemical pathway, D-xylose is converted to xylitol as an intermediate (via xylose reductase activity), either to xylulose or directly to xylulose. Xylulose kinase activity then generates xylulose-5-phosphate, which proceeds down the pentose phosphate pathway.

Table 1.4 Microbial production of xylitol from pure xylose or from lignocellulosic hydrolyzate [20]

Microorganisms	Fermentation conditions	Raw material	Time (h)	P (g/L)	Yp/s (g/g)	Qp (g/L·h)
***Candida tropicalis* HPX2**	30°C, v/V 100/250 mL, X0 20 g/L, 200 rpm	D-Xylose	24	40	>0.90	1.67
***C. tropicalis* BSXDH-3**	30°C, v/V 1/2.5 L, X0 50 g/L, 300–500 rpm	D-Xylose, Glycerol	n.a.	n.a.	0.97	3.2
***C. guilliermondi* FTI-20037**	30°C, v/V 100/250 mL, X0 104 g/L, 200 rpm	D-Xylose	78	77.2	0.74	0.99
***C. tropicalis* IFO 0618**	30°C, v/V 200/250 mL, X0 172 g/L	D-Xylose	n.a.	n.a.	0.64	2.67
***C. tropicalis* DSM 7524**	30°C, X0 100 g/L, 300 rpm, pH 2.5	D-Xylose	800	220	0.70–0.73	0.28
***C. boidinii* NRRL Y-17213**	30°C, v/V 50/125 mL, X0 150 g/L, 125 rpm	D-Xylose	336	53.1	0.47	0.16
***C. mogii* ATCC 18364**	30°C, v/V 300/1000 mL, X0 53 g/L, 250 rpm	D-Xylose	n.a.	n.a.	0.62	n.a.
Debaryomyces hansenii	28°C, v/V 10/50 mL, X0 150 g/L, 180 rpm	Sugarcane bagasse	48	10.54	0.71	0.22
***Candida* sp.559-9**	30°C, v/V 10/30 mL, X0 200 g/L, 110 rpm	D-Xylose	120	173	0.90 (ca.)	1.44
Hansenula polymorpha	30°C, v/V 200/500 mL, X0 125 g/L, 150 rpm	D-Xylose, Glycerol	96	58	0.62	0.60 (ca.)
C. tropicalis	30°C, v/V 2/7 l, X0 150 g/L, 350–400 rpm, 14 recycle rounds	D-Xylose	284	110	0.81	5.4
***C. tropicalis* KCTC 10457**	30°C, v/V 2/5 l, X0 200 g/L, 350 rpm, 10 recycle rounds	D-Xylose, Glucose (20 g/L) (ca.)	152 (ca.)	1824 (ca.)	0.85	12
***Pichia* sp.**	28°C, v/V 100/250 mL, X0 40 g/L, 250 rpm	D-xylose	50	25	0.58	0.5 (ca.)
***D. hansenii* UFV-170**	30°C, v/V 25/125 mL, X0 10 g/L, 200 rpm	D-xylose	24	5.84	0.54	0.24
***C. tropicalis* JH030**	30°C, v/V 60/250 mL, X0 46 g/L, 150 rpm	Rice straw	71 (ca.)	31.1	0.71	0.44
***C. tropicalis* SS2**	X0 25 g/L Xylose, Glucose (25 g/L)	-	67 (ca.)	220	0.93	3.3

Note: Yp/s = xylitol yield on xylose consumed (g/g); Qp = xylitol volumetric productivity (g/L·h); P = maximum xylitol production (g/L); n.a. = not available; v/V = volume medium/volume system; X0 = initial xylose concentration (g/L); ca. = calculated.

1.3.4.3.1. Xylitol production by bacteria

Most bacteria have an enzyme called xylose isomerase that can specifically convert xylose to xylulose. In a second step, it is phosphorylated by xylulokinase to D-xylulose-5-phosphate, a common intermediate in prokaryotic and eukaryotic metabolism. D-xylulose-5-phosphate is either incorporated into the pentose phosphate pathway or converted to glyceraldehyde-3-phosphate and acetyl phosphate by xylulose-5-phosphate phosphoketolase.

Similar to glucose metabolism in yeast, this step produces glycolytic intermediates without the formation of nicotinamide adenine dinucleotide phosphate (NADPH) [29]. In addition to xylose isomerase, bacteria have an oxidoreductase system that reduces xylose to xylitol and further oxidizes it to xylulose. Using the *Enterobacter* strain in a xylitol production experiment yields 33.3 g/l of xylitol with a volumetric productivity of 0.35 g/l/h in the medium initially containing 100 g/l of xylose [30]. In contrast, *Corynebacterium* sp. Adding gluconic acid increases xylitol production.

1.3.4.3.2. Xylitol production by yeasts

Some yeast strains are able to convert xylose into D-xylulose through an oxidoreductive conversion consisting of two consecutive reactions. In the first stage, D-xylose is converted to the intermediate xylitol with xylose reductase (XR) in the presence of nicotinamide adenine dinucleotide (NADH) or NADPH [31]. In the second stage, xylitol is converted (oxidized) to D-xylulose by either NAD+-bound or NADP+-bound xylitol dehydrogenase (XDH) [32].

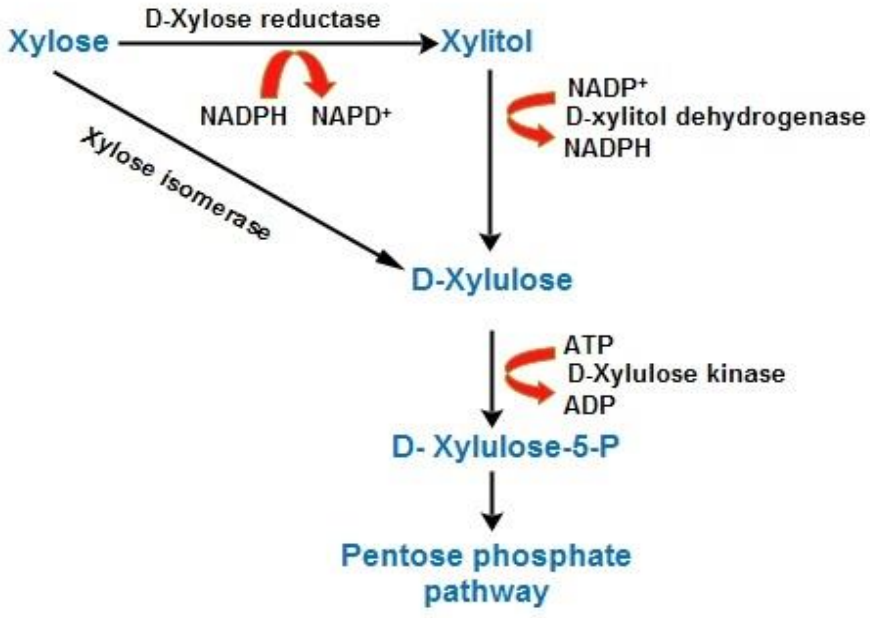

Figure 1.7 Pathway for bacterial xylose utilization [27]

Different yeast species show different abilities to ferment xylulose to ethanol or xylitol [33]. If the oxygen level is too low, a redox imbalance occurs because the NADH produced in the xylitol dehydrogenase step cannot be reoxidized back to NAD. This oxygen-depleted imbalance is due to a decreased breathing rate, which limits the production of NAD+. Therefore, at the end of the pentose phosphate pathway, the alternative ethanol pathway is chosen. However, since the pentose phosphate pathway is still active, the conversion of NADP+ to NADPH continues [34].

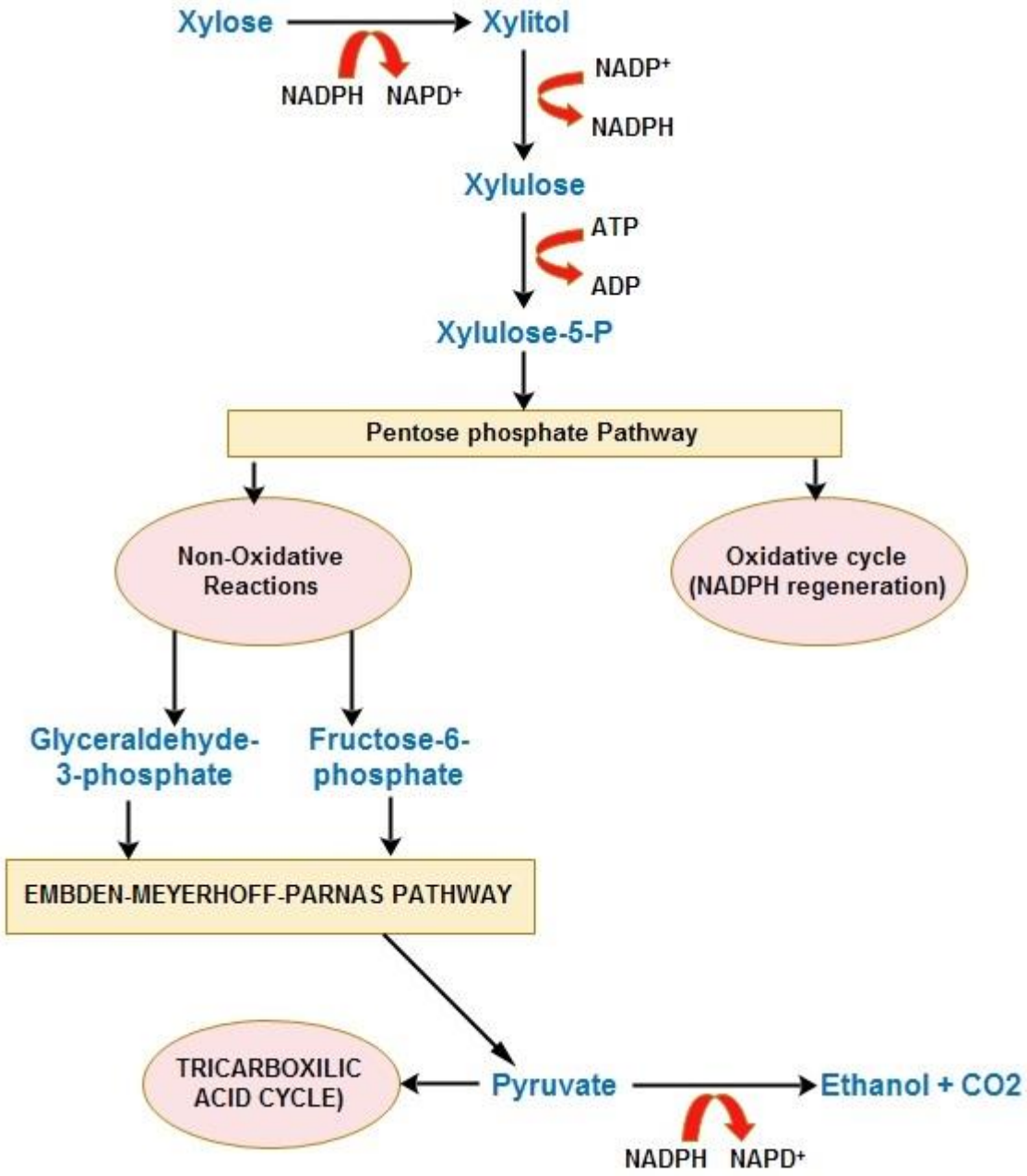

Figure 1.8 D-xylose metabolism in yeasts [35]

The resulting redox imbalance enhances xylitol accumulation in the XR/XDH system due to the limited supply of NAD+ for use by XDH. For higher xylitol accumulations in *D.*

hansenii, semi-anaerobic conditions were essential to lower the NAD/NADH ratio in the xylitol to xylulose oxidation step. The non-regeneration of NAD+ under oxygen-limited conditions thus leads to the accumulation of xylitol and its subsequent excretion into the medium [27]. Yeasts with XR activity associated with both NADH and NADPH, such as *Pichia stipitis*, can regenerate the NAD+ consumed in the second step of xylose metabolism under anaerobic and oxygen-limited conditions. Therefore, no xylitol accumulation occurs between the cofactors of XR and XDH and the main product in this situation is ethanol.

In contrast, yeasts such as *Debaryomyces hansenii*, which consume xylose through XR activity, are dependent on NADPH only in the first step of xylose conversion (in the complete absence of NADH-bound XR). They can produce xylitol as the main product [12]. In the second step, xylitol is oxidized to xylulose, mostly in the presence of NAD+ [36]. The presence of either high XR or low XDH activities is considered a criterion for the selection of xylitol-producing microorganisms [12]. Barbosa et al. calculated the xylitol yield when using NADH2+ as a cofactor for XR under aerobic conditions in nutritionally balanced media [37]. It appears as follows:

$$126 \text{ xylose} + 3\ O_2 + 6 \text{ ADP} + 6 \text{ Pi} + 48\ H_2O \longrightarrow 114 \text{ xylitol} + 6 \text{ ATP} + 60\ CO_2 \qquad (1.2)$$

At a theoretical product yield of 0.905 mol xylitol/mol xylose. Under a similar hypothesis, the same investigator reported the following mechanism of anaerobic conditions.

$$48 \text{ xylose} + 15\ H_2O \longrightarrow 42 \text{ xylitol} + 3 \text{ ethanol} + 24\ CO_2 \qquad (1.3)$$

with a theoretical product yield of 0.875 moles xylitol/mole xylose. Dissolved oxygen concentration is a control parameter affecting the operational aspects of xylitol production by yeast [38].

1.3.4.3.3. Xylitol production by molds

Biological production of xylitol by fungi has been less studied than by yeast and bacteria. *Petromyces albertensis* was used as a biocatalyst for xylitol reduction by Dahiya et al. A yield of 0.4 g/g xylose was obtained after 10 days of fermentation. A low xylitol yield was reported by Ueng et al. Fermenting with Mucor seeds. Hydrolyzate of sugarcane bagasse hemicellulose [39,40]. Chiang et al. reported that *Byssochlamys, Glicoladium, Penicillium, Rhizopus, , Myrothecium, Aspergillus,* and *Neurospora* spp. have the ability to produce a small amount of xylitol from xylose [41].

1.4. Optimization of fermentation process

Over the last few years, scientists have paid much consideration to the industrial production fermented products because of their anticipated potential in biological fields. Several factors influence the performance of fermentation processes, such as temperature, xylose concentration and pH [42]. The effects of these components are often characterized by experimentation, as the impacts of these parameters are very complicated, with feasible reciprocities among the different elements. Optimization techniques generally enhance fermented product yield by maintaining favorable fermentation conditions. In a laboratory, most of the methods for optimization of the fermentation process are mainly based on data obtained during experimental analysis, which cannot be utilized for industrial purposes.

Moreover, the statistic-based method, such as Response Surface Methodology (RSM) technique, cost enormous resources and workforce than expected because of designing experiments, making models, evaluating the effects of different factors, and finding the ideal operating conditions [43]. To report the synergistic impact of various components and to minimize the laborious experiments, Artificial Neural Network (ANN) is progressively being utilized. ANN is generic in configuration and has the ability to learn from recorded information. ANN attempts to determine and optimize important variables to identify the factors' levels to improve the response (productivity or product yield). The benefit of ANN is that it doesn't need earlier specification of an appropriate fitting function and has universal approximation capability, i.e., it can estimate practically a wide range of non-linear functions, including quadratic functions, whereas RSM approximates only quadratic expression. Therefore, the present study investigated the optimized parameters by application of Artificial Neural Networks (ANN) and Response Surface Methodology (RSM) theory. Additionally, after optimization, downstream processing was performed to separate xylitol crystal fermentation, followed by characterization of crystal.

1.5. Fermentation Parameters

The main stage in xylitol production is fermentation is fermentation process, which is controlled by several factors including carbon source, nitrogenous compounds, substrate concentration, aeration rate, inoculum, pH and temperature. All of these factors are explained in the next section.

1.5.1. Xylose concentration

Substrate concentration (D-xylose) has been proven to be an important parameter for yeast growth and fermentation. Xylitol cannot be produced in the absence of D-xylose, and the combination of aeration and xylitol concentration is an important and critical factor for xylose reductase and xylitol dehydrogenase activity and xylitol formation in yeast. Initial xylose concentration can affect its production by microorganisms. Increased xylose concentration in microbial cultures that can withstand high sugar and high osmolarity leads to increased xylitol yield and production rate. Increasing the initial xylose concentration usually reduces the growth rate, unless the aeration rate is increased [44]. Horitsu et al. studied the effect of D-xylose concentration on xylitol production in *C. tropicalis* by varying the concentration from 100 g/L to 300 g/L [28]. The maximum yield of xylitol was obtained at his D-xylose concentration of 172 g/L. Walther et al. reported that at high initial xylose concentrations and high aeration rates, *C. tropicalis* ATCC 96745 cells grew vigorously at the start of fermentation, leading to increased production rates [45]. However, the xylitol yield decreased when the initial xylose concentration was low and the dissolved oxygen level was high. They also found that this yield decreased at very high initial concentrations of xylose. This is attributed to the osmotic stress that can be induced in microorganisms at high sugar concentrations in the medium. It was also concluded that proper manipulation of initial substrate concentration and aeration would likely result in high levels of xylitol yield.

1.5.2. Carbon source

Studies have shown that carbon sources are more effective than xylose in producing xylitol. Yabashi et al. D-xylose was supplemented with D-glucose for cultivation of *C. tropicalis* [46]. During the early stages of fermentation, D-glucose is used for cell growth and then D-xylose is consumed. Xylitol yield and productivity increased 1.2-1.3-fold with the addition of glucose to the fermentation medium. These conditions resulted in 104.5 g/l of xylitol in 32 hours with a yield of 0.82 g xylitol/g xylose. In a study by Silva et al. For *C. guilliermondii* FTI 20037, the addition of glucose to the fermentation medium decreased the product yield from 0.66 g/g to 0.45 g/g [47].

Similar results were reported by Soleimani et al. Effect of glucose on xylitol yield and production rate of *C. guilliermondii* during fermentation [48]. Furthermore, it was observed that the process lengthened when glucose was used as a cosubstrate. In a study by Lee et al. Fed-batch fermentation using recombinant *S. cerevisiae* has been proposed to overcome this problem [49]. Very low glucose concentrations in the medium are required for *C. tropicalis*

to achieve effective xylitol production [45]. During fermentation, if the medium contains significant amounts of glucose, aerobic conditions should be employed to achieve higher yields and productivity. In the absence of glucose, microaerobic conditions improve the yield of xylitol. Arabinose appears to be an inducer of xylose reductase, in contrast to glucose as a cosubstrate. This is because, in our experiments, higher arabinose concentrations increased both xylitol yield and productivity.

1.5.3. Nitrogen source

One of the most important organic nitrogen sources for xylitol-producing yeasts is yeast extract. Depending on the yeast used as the biocatalyst, the yeast extract as a supplement in the medium may or may not be effective in xylitol formation. In some cases, a higher product yield can be achieved with urea or urea and casamino acids [50]. Microbial xylitol production and xylose utilization are affected by the type and concentration of the nitrogen source, and the yeast strain is an effective factor in his two parameters mentioned above [51]. Vandeska et al. Increased xylitol yield was observed in *C. boidinii* when fermentation media were supplemented with urea compared to those supplemented with ammonium sulfate (Table 1.3) [52].

Table 1.5 The effect of nitrogen source on xylitol yield and dry cell mass formed by *Candida boidinii*. [52]

Parameter	**Nitrogen source**					
	$(NH_4)_2SO_4$	KNO_3	NH_4NO_3	NH_4Cl	Urea	Urea and Casamino acids (5 g/l each)
Ccm (g/l)	5.88	4.96	4.31	5.07	6.25	9.03
Yx/s (g/l)	0.06	0.01	0.05	0.06	0.10	0.12

Yx/s: Xylitol yield coefficient (g xylitol per g xylose used) *Fermentation time was 4 days; C_{cm}: Dry cell mass and each source yielded 1.06 g/L nitrogen. The medium supplemented with (g/L): NH_4NO_3, 3.03; NH_4CI, 4.05; $(NH4)_2SO_4$, 5.00; KNO_3, 7.65; and urea, 2.27.

1.5.4. Inoculum age and concentration

Fermentation rate and yield are affected by inoculum age, which affects metabolic activity and cell viability [51].]. Improved xylitol yield using *C. guilliermondii* FTI 20037 was reported by Felipe et al., depending on inoculation time, inoculum dose (concentration), and hydrolyzate composition [53]. Pfeiffer et al. Low values of xylitol productivity and cell growth from *C. guilliermondii* inoculum less than 15 hours or older than 24 hours were

obtained, and the best conditions were achieved in the above ranges [54]. Cao et al. We studied the effect of initial cell concentration of *Candida* species. His B-22 on xylitol production from D-xylose showed a linear increase in xylitol formation rate and fermentation time he found to be significantly reduced at initial inoculum concentrations ranging from 3.8 to 26 g/L inoculum [55].

1.5.5. Aeration rate

Due to the different effective parameters and the wide range of aeration levels examined in the literature, it is difficult to conduct detailed studies of the effect of aeration on xylitol production. Intermediate aeration rate values generally provide the best conditions for xylitol yield and productivity. For example, *D. hansenii* shifts its metabolism towards xylitol production under low aeration conditions (4–22 mmol/L/min), with highest productivity at oxygen transfer rates (OTR) above 2 mmol/L/h. The literature confirmed that oxygen was an essential factor for xylose uptake, as switching to anaerobic conditions halted both xylose consumption and metabolic activity. In a related study, *C. tropicalis* had a maximum xylitol yield of 0.62 g/g (xylitol/xylose) under semi aerobic conditions, whereas the maximum yield under microaerobic conditions was 0.36 g/g (xylitol/xylose). / xylose). Medium with glucose gave higher yields and productivity under aerobic conditions, whereas under microaerobic conditions yields were improved in the absence of glucose. These results may be attributed to the increased oxygen demand due to the high cell densities achieved in the presence of glucose [45].

1.5.6. Temperature and pH

The optimum temperature for xylitol production by yeast is reported to be about 30 °C for *C. tropicalis* DSM 7524, small temperature fluctuations above this level do not significantly affect xylitol yield. The xylitol yield was independent of temperature when the cells were grown in the temperature range of 30 °C to 37 °C. However, temperatures above 37 °C significantly reduced xylitol yields [56]. Similarly, xylitol formation at *C. guilliermondii* FTI 20037 was the same at 30 and 35 °C, but decreased as the temperature increased to 40 °C [37]. The optimum initial pH for fermentation depends on the yeast used. Optimal pH for *Debaryomyces hansenii* and *Candida* spp. is 5.5 or 4-6 [55]. Best pH for *C parapsilosis, C. guilliermondii* and *C. boidinii* are 4.5-5, 6.0 and 7.0 respectively. If the pH is not controlled, it will drop during the fermentation process. Therefore, under such conditions, the initial pH value should be higher than under controlled conditions. For example, the

optimal starting pH for *C. boidinii* under controlled conditions is 5.5. Without control, initial pH should be 7.0 [50].

1.6. Genetic modification of microorganisms (engineered strains)

Genetic modification of microorganisms has been widely used to improve production and yield of various bio-based products. Xylitol, a five-carbon sugar alcohol used as a sweetener, is one such product whose production has been enhanced through genetic modification of microorganisms. Xylitol can be produced from xylose, a sugar obtained from lignocellulosic biomass, through chemical processes or microbial fermentation. However, chemical processes have several drawbacks, including high energy requirements, high substrate purification costs, and production of toxic byproducts. Hence, the use of microbial fermentation for xylitol production is preferred. Genetic modification of microbes can improve the efficiency of xylitol production, making it a viable alternative to chemical processes.

Several parameters need to be considered before designing gene manipulation on microbes for xylitol production. These parameters include genetic stability, regulatory and safety considerations, growth kinetics, expression levels of recombinant proteins, good productivity, high yield, and ease of product recovery. To achieve these parameters, various genetic engineering strategies have been employed, including transport optimization, xylose reductase overexpression, cofactor supply and engineering, gene deletion, and manipulation of bioprocess parameters [57]. Table 1.6 shows some of the important engineered microorganisms with enhanced xylitol production.

One strategy used to improve xylitol production is the disruption of xylitol dehydrogenase gene (xdh) in the recombinant strain of *Debaryomyces hansenii*. The disruption of xdh improved xylitol accumulation by almost 2.5-fold. Another strategy involves expressing a novel D-arabitol dehydrogenase-encoding gene (ardh) and xylitol dehydrogenase encoding gene (xdh) in *Escherichia coli* strains from *Gluconobacter* sp. JX-05. Co-biotransformation with both recombinant strains improved xylitol yield by two times in comparison with wild *Gluconobacter* sp. due to the utilization of other carbon sources along with xylose [57].

In another study, an endogenous aldose reductase gene GRE3 and a xylose transporter gene SUT1 gene were overexpressed in the industrial yeast strain of *S. cerevisiae* for xylitol production from agricultural biomass [57]. The developed strain was evaluated for xylitol production from corn cob hemicellulosic hydrolysate containing glucose as the cosubstrate. The engineered strain exhibited higher xylitol productivity than the control strain. Furthermore, the

replacement of glucose by glycerol as a cosubstrate increased xylitol productivity, although the conversion factor for glycerol was lower than for glucose.

In a more recent study, an engineered strain of *Saccharomyces cerevisiae* (YPH499-XR-BGL-XYL-XYN) was developed by expressing cytosolic xylose reductase (XR) along with β-D-glucosidase (BGL), xylosidase (XYL), and xylanase (XYN) enzymes co-displayed on the cell surface from various fungal and yeast resources. The cumulative expression of all these enzymes contributed to the bioconversion of kraft paper pulp to xylitol, with a conversion rate of 28% after 96 hours. Moreover, the use of multiple enzyme systems significantly reduced the need for enzymatic pretreatment. Further expression of XYL and XYN on the cell surface using an SED1 "SSS" cassette improved the xylitol yield by 44% [5,57].

In conclusion, genetic modification of microorganisms has shown promise in improving the production and yield of xylitol. Various genetic engineering strategies have been employed, including transport optimization, xylose reductase overexpression, cofactor supply and engineering, gene deletion, and manipulation of bioprocess parameters. These strategies have led to the development of more efficient and productive

1.7. Lignocellulosic biomass

Lignocellulosic biomass (LCB) refers to plant biomass composed primarily of cellulose, hemicellulose, and lignin. In reality, these polymers are organized to varying degrees into complex and heterogeneous three-dimensional structures, whose complex structures and compositions vary according to species and environmental conditions [58]. LCB is increasingly recognized as a valuable feedstock because lignocellulosic biomass refineries are similar to petroleum refineries. The structure and composition of LCB influence the hydrolysis of polysaccharides. Therefore, understanding each component is important for efficient utilization of lignocellulosic biomass.

There are various forms of LCB resources around the world, which can be divided into four categories: agricultural waste, forestry waste, energy crops and biological waste [59]. Global production of plant biomass composed of more than 90% lignocellulose is about 200×10^9 tonnes/year, with about $8–20 \times 10^9$ tonnes of primary biomass potentially available [59]. Lignocellulosic biomass is the most abundant, bio renewable, globally available, high xylitol yield and is a promising option for economical xylitol production. and other products with great potential for sustainable production.

Table 1.6 Engineered microorganisms for enhanced xylitol production [5]

Engineered Strains	Genetic Engineering Strategy	Xylitol Produced	Xylitol Productivity	Xylitol Yield
Escherichia coli	Insertion of NADPH-dependent Xylose reductase gene from *Candida boidinii*	-	-	Xylitol yield: 57.1 ± 2.6mM at 24 h
Escherichia coli	Cloned xylose reductase from *Candida tropicalis*	-	12 g/L.h	-
Escherichia coli	Insertion of xylulokinase (*Xyl3*) from *Pichia stipitis* and deletion of the *Escherichia coli* xylulokinase gene (*xylB*)	-	-	80mM xylitol produced from 110mM xylose in 72h
Escherichia coli	Insertion of plasmid with d-xylose/proton symporter *XylE* and the d-xylose ABC transporter XylFGH and xylose reductase from *Candida boidinii* (CbXR)	56 g/L	productivity from 24 to 96 h is ~0.33 g/h	-
Bacillus subtilis	Cloned Xylitol-phosphate dehydrogenase (XPDH) genes from several Gram-positive bacteria	-	-	23% xylitol yield
Lactococcus lactis	Insertion of D-xylose reductase from Pichia stipitis CBS 5773 and xylose transporter from Lactobacillus brevis ATCC 8287	160 g/L	2.72 g/L.h	Xylitol yield- −2.5mol/mol
S. cerevisiae	Insertion of xylose reductase from *Candida tenuis*	-	1.16 g/L.h	-
K. marxianus	Cloned xylose reductase from *Neurospora crassa*	-	4.43 g/L.h	-
Candida tropicalis	Insertion of xylose reductase from *Neurospora crassa*	-	1.44 g/L.h	96% at 44 h
S. cerevisiae	Insertion of xylose isomerase from *Piromyces* sp.	-	-	0.002 g/g.h
Candida tropicalis	Insertion of NADH preferring Xylose reductase from *Candida parapsilosis*	-	5.09 g/L.h	-
Saccharomyces cerevisiae	Expression of xylose isomerase from *Thermus thermophilus*	-	-	4.9± 1.0 mmol of xylitol, after 70 h of fermentation

1.7.1. Structural features of lignocellulosic biomass

LCB is primarily consists of three components; Cellulose, hemicellulose, lignin and small amounts of proteins, pectin, and some inorganic materials. In addition, the composition of these components varies depending on conditions such as age and growth stage, even for the same plant species. Polysaccharides (cellulose and hemicellulose) and lignin are found mainly in wood tissue and in the cell walls of grasses. Cellulose fibrils are embedded in a network of hemicellulose and lignin. The elasticity of LCB is due to the crystallinity of cellulose, the hydrophobicity of lignin, and the encapsulation of cellulose by a lignin-hemicellulose matrix [60]. This removes water from the cell wall and limits access for hydrolytic enzymes.

1.7.1.1. Cellulose

Cellulose is the main building material in lignocellulosic biomass. Cellulose is a very important polysaccharide as it is the most abundant organic compound on earth. Cellulose has a unique structure containing a linear chain of β-(1,4)-D-glucopyranose units in his 4C1 conformation. Each glucose unit rotates 180° with respect to its neighbors and the resulting disaccharide is called cellobiose [60]. The repeating unit of the cellulose chain is the disaccharide cellobiose, and long cellulose chains are arranged parallel to each other and held together by hydrogen bonding to form microfibrils. An extensive intra- and intermolecular hydrogen-bonding network exists in cellulose, which binds glucose units tightly together, making cellulose a relatively stable polymer and endowing cellulose fibrils with high tensile strength. Cellulose is a polymer that is insoluble in water. The chemical structure of cellulose is shown in Figure 1.9.

Cellulose is composed of long chains of hydro-D-glucopyranose units (AGUs), and each cellulose molecule has three hydroxyl groups per AGU, except at the ends [61]. The polymer contains three reactive hydroxyl groups at C-2, C-3, and C-6 atoms and is usually susceptible to transformation of typical primary and secondary alcohol OH groups [62]. Unbranched β1-4 linkages result in linear chains stabilized by intra- and inter-chain hydrogen bonds.

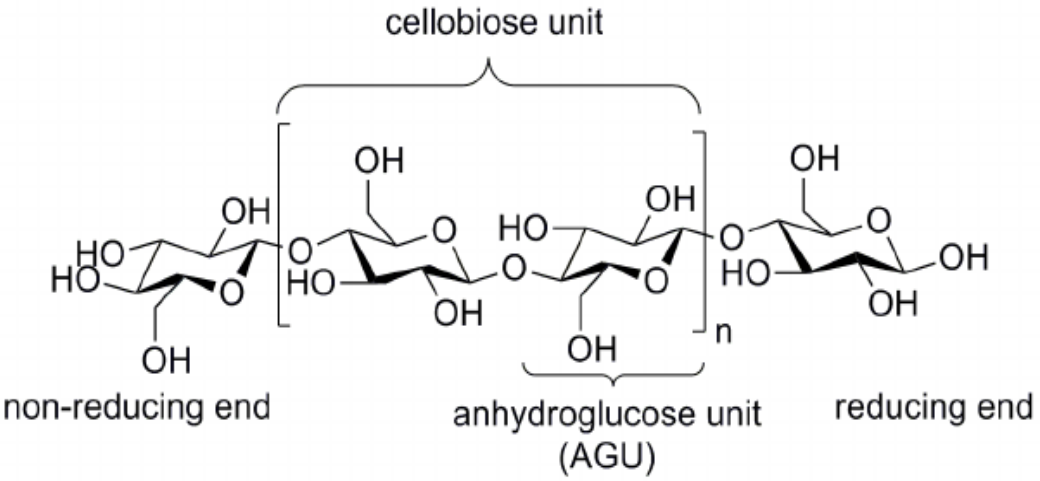

Figure 1.9 The cellulose polymer chain structure [63]

1.7.1.2. Hemicellulose

After cellulose, hemicellulose is the second most common natural polysaccharide. Hemicellulose is a heterogeneously branched polymer of pentoses (xylose, arabinose), hexoses (mannose, glucose, galactose), and sugar acids, and is found next to cellulose as an amorphous mass. Hemicellulose differs from cellulose in that it is primarily composed of xylose and other five-carbon monosaccharides. In plant cell walls, hemicellulose forms a complex connective network, connecting cellulose fibers into microfibrils and cross-linking them with lignin, providing the best combination of mechanical support and transport properties [64,65]. Hardwood hemicellulose mainly contains xylan, while coniferous hemicellulose mainly contains glucomannan. Unlike cellulose, hemicellulose has a branched amorphous structure. The structure and composition of hemicelluloses vary among plant types (particularly broad-leaved trees, conifers, and grasses) [66]. The degree of polymerization and concentration of building blocks such as monosaccharides vary from plant to plant. Hemicellulose xylan can be extracted very well in an acidic or alkaline environment, whereas glucomannan is poorly extractable in an acidic environment and requires a more alkaline environment than xylan for extraction [67].

1.7.1.3. Lignin

Lignin is the hydrophobic “glue” and insulator of plant cell walls. Next to carbohydrates, lignin is another natural source of aromatic polymers [68,69]. Lignin is an amorphous, aromatic hybrid polymer made from monolignols (aromatic alcohols), also called phenylpropane. The lignin structure is mainly composed of three different phenylpropane units such as p-coumaryl alcohol, coniferyl alcohol and sinapyl alcohol. These monolignols

are incorporated into lignin polymers in the form of p-hydroxyphenyl (H), guaiacyl (G), or syringyl (S) [70]. The concentration of these alcohols varies from plant to plant. The phenylpropanoid units present in lignin are held together by both ether and carbon-carbon bonds. Depending on the source of lignocellulosic biomass, the relative proportions of H, G, and S lignins differ [71]. It has been observed that coniferous lignin is composed mainly of G units, with a small amount of H units. Hardwood lignins usually contain G and S monolignins with trace amounts of H units, and herbaceous plants contain all three G, S, and H lignins in significant amounts, but in proportions. is different [72].

In LCB, lignin content, structure, subunits and association with polysaccharides are critical for cell wall resistance. It also influences the transport of water, nutrients and metabolites and plays an important role in plant cell development. Lignin builds the complex structures of lignocellulose that protect plants from attack by pathogens and insects [73].

1.7.1.4. Other constituents of lignocellulosic biomass

LCB also contains small amounts of other substances such as pectin, extracts, proteins and ash.Pectin is a complex mixture of polysaccharides and is rich in galacturonic acid. The structural types of pectin are homogalacturonan, rhamnogalacturonan I, and rhamnogalacturonan II [74]. Their composition and structure vary depending on the source and conditions of extraction, location, and other environmental factors. They are found in most primary cell walls and are particularly abundant in the non-woody parts of land plants. The highest concentration of pectin is found in the intermediate lamellae of the cell wall, which aids in cell adhesion and wall hydration. Their cross-linking also influences wall porosity and plant morphogenesis [75].

LCB extracts are low molecular weight compounds. These include resins (terpenes, lignans, and other aromatics), fats, waxes, fatty acids, alcohols, steroids, and higher hydrocarbons. These substances are chemically polar and non-polar in nature. It gives color and smell and protects plants from termites and microorganisms. The content and composition of extracts vary according to plant type, geographical location, season and age of growth. In plants, they are mainly found in resinous ducts, radial parenchymal cells, middle lamellae, intercellular and cell walls of tracheids, and in small amounts in ribbed fibers [76]. The functions of extracts are diverse and the functions of many extracts are not yet fully understood. Some are involved in crop protection and are precursors to certain chemicals [77].

1.7.2. Lignocellulosic biomass in India

Among all the renewable energy sources available, only lignocellulosic biomass can be used to generate heat, electricity, and fuels in formats and scales compatible with existing transportation and power generation infrastructure. It can also be used to create chemicals and materials. In rural areas, lignocellulosic biomass plays a very important role as it is the main source of energy for the majority of households in India. In India, biomass still accounts for 32% of total primary energy consumption, with over 70% of the population relying on biomass for their energy needs. LCB has the potential to create significant employment in rural areas [78].

The availability of large amounts of LCB in India is due to agriculture, as many states in India have agriculture-based economies. A summary of the report shows that while India has a significant amount of forest land, most of it is under government jurisdiction. Conservation policies and thus forest biomass was reported as zero. Again, another proportion of his LCB in India comes from indigenous resources such as solid waste residues, the timber industry, farm trees, and virgin land grass [79]. Lignocellulosic biomass, including agricultural residues, wood, grass, etc., is therefore available in large quantities in India.

However, in India, LCB is still not a suitable renewable energy source for biofuel production due to the following challenges in ensuring a reliable LCB supply chain: (I) variations in LCB availability throughout the year depend on cultivation patterns; (II) lack of an organized and formal biomass market; Lack of a robust business model for Another major challenge is the cost of biomass storage and transportation to biorefineries, which has steadily increased over time [80].

To maintain a constant supply of LCB all year round, industrial biomass can be grown from a number of plant species including miscanthus, bamboo, napier grass, and a variety of plants ranging from eucalyptus to oil palm (oil palm). Tree species can be grown in marginal or degraded areas. soil. The plant used in each case is usually not critical to the final product, but does affect the processing of raw materials.

1.8. Research challenges in xylitol production from lignocellulosic biomass

The benefits of xylitol production from lignocellulosic biomass have been widely reported. Here are the steps to produce xylitol using a biochemical approach:

Pretreatment, enzymatic hydrolysis, microbial fermentation, purification and crystallization of xylose. The cost of large-scale production of xylitol from lignocellulosic

biomass mainly depends on the technology used in the conversion methodology [81]. However, pretreatment of LCBs is essential for all other important aspects of the overall biochemical transformation, from selection of starting materials to size reduction, enzymatic hydrolysis, fermentation, product recovery, residue handling and possible by-products. It has a wide range of effects on steps [82]. Pretreatment of LCB involves degradation of the lignocellulose structure, reducing cellulose crystallinity, increasing biomass surface area, breaking the lignin barrier and minimizing the formation of inhibitors for subsequent fermentation steps. increase. Pretreatment includes physical, chemical, thermal, biological processes and combinations thereof. Pretreatment is one of the most expensive processing steps for xylitol production from lignocellulosic biomass [83]. Therefore, the pretreatment process is a major bottleneck in xylitol production and marketing. In addition, xylitol production technology includes other bottleneck parameters such as enzymatic saccharification of pretreated biomass and fermentation of hexose and pentose sugars released by hydrolysis and saccharification.

Therefore, to develop optimized new technologies in a cost-effective way to improve the production of xylitol from lignocellulosic biomass, it is necessary to study the optimization and parameters of pretreatment, saccharification, and fermentation technologies. Extensive research is required. Other issues also require significant research and development efforts to improve process efficiency and economics.

भारतीय प्रौद्योगिकी संस्थान गुवाहाटी
Indian Institute of Technology Guwahati

Chapter 2

Review of Literature and Objectives

2.1. Availability of lignocellulosic biomass in India and selection of suitable feedstock for xylitol production

Biomass can be defined as complex polymers of cellulose, hemicellulose and lignin. Therefore, it is also called lignocellulosic material. Various permutations and combinations of the three components, he mentioned earlier, impart unique properties to the biomass. These properties vary from biomass to biomass. In addition to biofuel production, lignocellulosic biomass also serves as feedstock for the production of value-added chemicals. Adequate supply of lignocellulosic biomass is a key factor for commercial production of value-added chemicals (such as xylitol) in India. Biomass sources vary, depending on environmental conditions, geographic location, or the dietary habits of the local population. It could be agricultural waste, forestry waste, dedicated energy crops, or a combination of all. A major advantage of generating energy from agricultural or forest waste is that raw material costs are negligible. This is a win-win situation for both energy producers and raw material harvesters. Agriculture plays an important role in the Indian economy. Therefore, the search continues for suitable agricultural wastes or forest debris that can be used as renewable energy sources. About 500 million tonnes of crop residues are generated annually from all agricultural production and are commonly used as animal feed, bedding, packaging material, direct fuel for domestic cooking, sold to industries such as the paper industry, or incinerated. To do. Harvest farms[84]. About 23% of India's area is also covered by forests [84]. Large amounts of forest debris and other agro-industrial wastes are readily available in India and are potential sources of lignocellulosic materials for xylitol production.

The main lignocellulosic biomass species available in northeastern India are arecanut husk, bamboo, peanut husks and sugarcane. All of these biomass materials are proven sources of bioenergy. Although these materials are abundant in nature, it is not profitable for the inhabitants of northeastern India to strain these materials for energy production. knowledge to grow.

The current economic, social and geographic scenarios of Northeast India may not accommodate such systematic cultivation systems. Northeast India is world-renowned for its biodiversity, there are some forests and agricultural wastes here, firewood plays an important role in the highland-dwelling societies of Northeast India, and cooking alone It is also used for heating and other daily activities. A significant lack of knowledge about the biomass properties of native tree and shrub species found in the forests of Northeast India and some states has delayed the establishment of biomass-based energy plants. Harvested biomass from northeast India for fermentable sugars and other valuable chemicals requires an understanding of lignocellulose chemistry.

This study focused on the biomass, namely the betel nut shell. Areca nut husks are known as agricultural waste in northeastern India. The betel nut (Arecan catechu) is also known as the betel nut (Figure 2.1). It is widely used in veterinary and human medicine, and is used in the paint and leather industries [85]. Areca is a genus of about 50 single-stemmed palms in the palm family found in humid tropical forests. The most famous representative of this genus is *Areca Catechu* from areca palm. Known for their bitter and zesty flavors, several varieties of areca nut are routinely chewed fresh or dried. The fruit has a smooth, yellowish-orange exocarp, a fibrous mesocarp, and a woody endocarp that is an edible nut (Figure 2.1). In India, the betel nut is eaten raw or as a chewing ingredient. The integument covers the edible part and consists of numerous short staple fibers embedded in a matrix of thin parenchyma [86]. A shell covering the chewing material, i.e. is the husk endocarp is discarded into the environment and constitutes approximately 60-80% of the total weight of the betel nut [87]. These nuts are commonly used as a popular chew in India and Pakistan. India is the largest consumer and producer of betel nut, accounting for up to 52.8% of global production [86]. India is estimated to produce at least 5,35,262 tonnes of areca nuts per year [88]. The total planted area is estimated at 2.7 million hectares and the annual production is estimated at about 3.3 million tons, with Karnataka, Kerala and Assam accounting for about 83% of the planted area and betel nut production. Assam is the third largest producer among them [86,89]. More than 6 million people involved in the cultivation, processing and trade of areca nut. More than 85% of cultivation land consists of small and marginal farms [90]. Areca nut shells are considered agricultural waste. Seashell disposal is one of the biggest problems for local commercial businesses in many parts of India, especially in Assam. There are limited studies on the uses of betel nut shells, such as in the manufacture of thick cardboard and wrapping paper [86,91]. The nuts are of commercial importance and are processed by cooking the whole nut. The skin of the fruit is removed and has no other

traditional uses. Leave the shells in a pile to dry. It's often annoying to the processor. The betel nut shell contains approximately 44% cellulose, 28% hemicellulose, and 11% lignin [92]. But is high in ash and not susceptible to enzymatic digestion, making it a raw material for biofuel production. use as is restricted [92]. The large amount of hard pericarp formed during the separation of the stones from the fruit, which is discarded without treatment, contains a significant amount (21%) of fermentable sugars in this lignocellulosic material [93]. Therefore, there are number of wide prospects exist where this agricultural waste material used as a feedstock for bio-energy and bio chemical production.

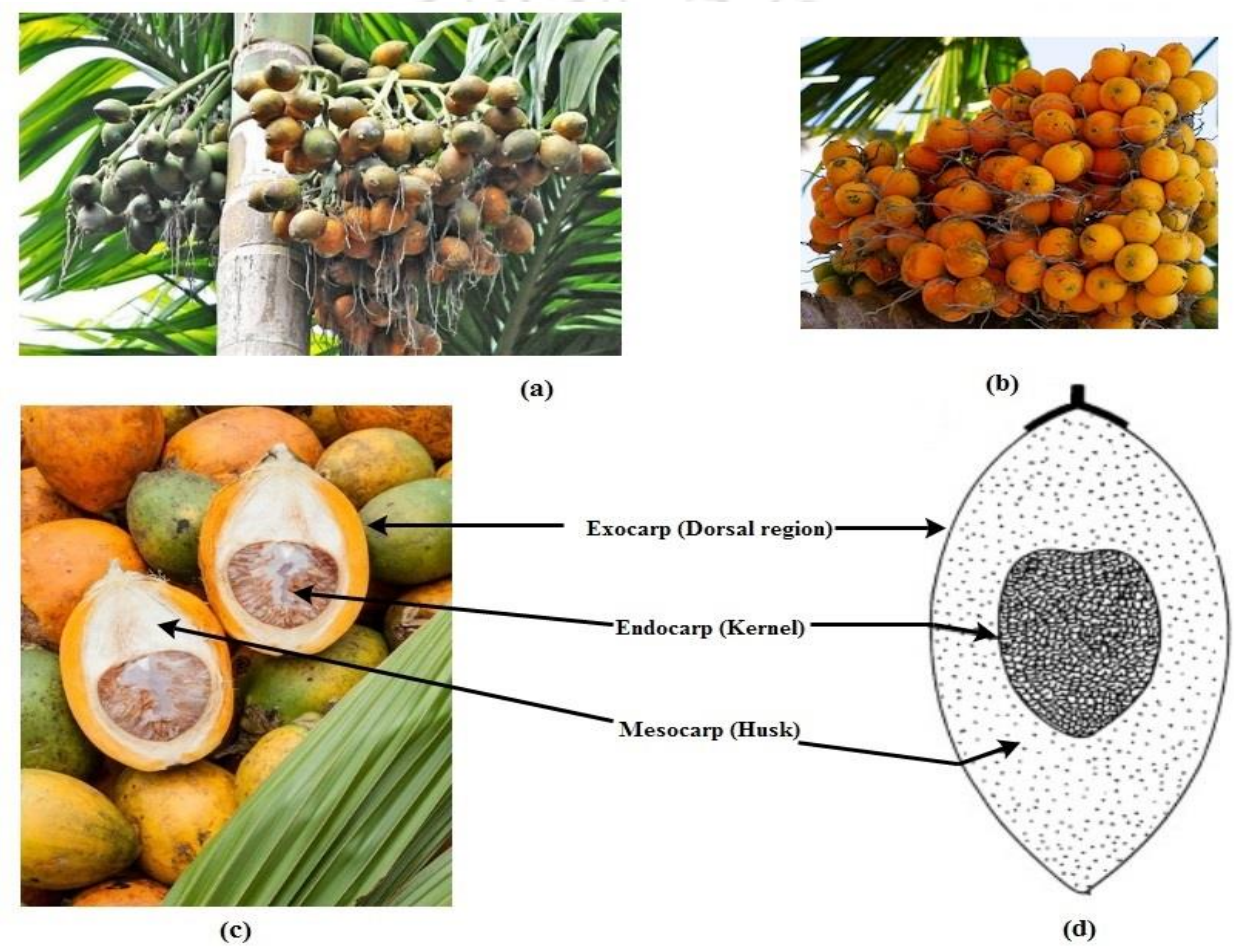

Figure 2.1 Areca nut and its various parts pictorial views [94]

2.2. Pretreatment

The complex structure of lignocellulose behaves as a protective barrier for plant cell walls from attack by potentially pathogenic organisms and provides resistance to mechanical forces. Digestibility of cellulose or other polysaccharides present in lignocellulosic biomass to monomers or fermentable sugars is hindered by many chemical, structural, or

physicochemical factors. Modern biotechnology research develops enzymes or mixtures of several enzymes that hydrolyze crude lignocellulosic material to produce monosaccharides, but this process is time consuming and economically viable. It's not technology. To speed up the hydrolysis process, scientists want to include an additional step known as "pretreatment." A pretreatment process rapidly breaks down lignocellulose into its parent components i.e. cellulose, hemicellulose and Lignin. Therefore, a key step in producing biofuels from lignocellulosic biomass is pretreatment. This step facilitates the enzymatic hydrolysis process by altering the structural features and increasing the surface area and porosity of the lignocellulosic biomass [95]. In general, the goals of the pretreatment process are:

1. Consumption of fewer chemicals
2. Minimum energy requirement
3. Reduction of by-products formation like furfural
4. Reducing the cost of feedstock size reduction
5. Preserve the hemicellulose fraction in biomass
6. Production of reactive cellulose fiber, which is suitable for enzymatic hydrolysis

2.2.1. Classification of pretreatment process

The pre-treatment process can be roughly divided into physical, chemical and biological pre-treatment processes (Figure 2.2). Each pre-treatment process has its own advantages and disadvantages. Table 2.1 shows the advantages and disadvantages of different pre-treatment methods. Among all the pre-treatment methods, the chemical pre-treatment method leads to fast and good sugar yield after enzymatic hydrolysis. Biological pretreatment sounds good, but the slower conversion rate and expense of enzymes doesn't make the process popular. In addition to irradiation, other physical pre-treatment methods require a high energy input in order to make the pre-treatment process successful. The present study focused on two pretreatment processes to achieve high product yields in subsequent enzymatic hydrolysis and fermentation processes. The dilute sulfuric acid pretreatment method and the lime pretreatment method were carried out and compared respectively.

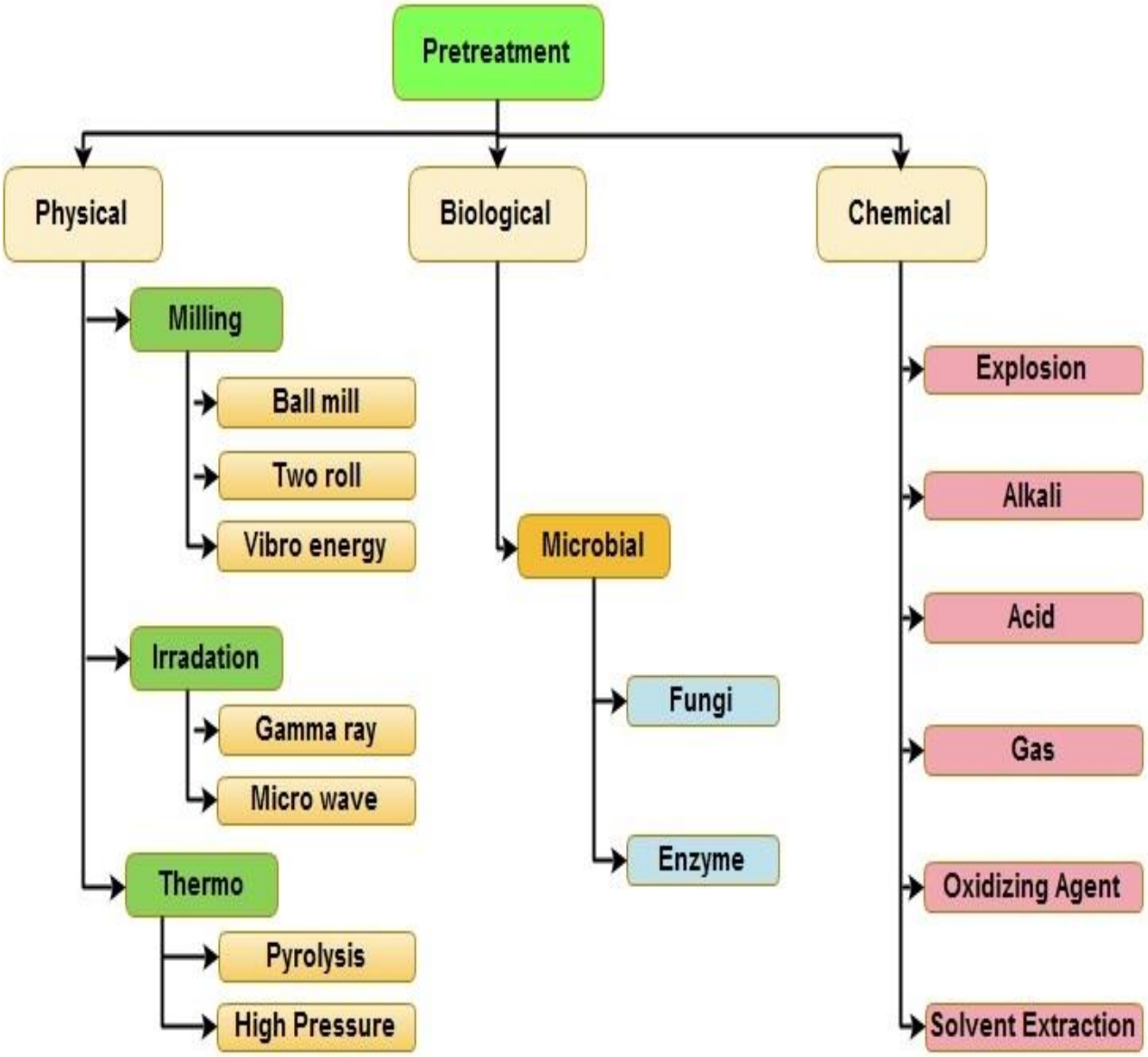

Figure 2.2 Different methods of biomass pretreatment [95]

2.2.1.1. Physical Pretreatment

2.2.1.1.1. Mechanical Size Reduction

Most lignocellulosic biomass require mechanical size reduction processing to increase the surface area for reaction with acids/bases or enzymes. Mechanical comminution methods include dry comminution, wet comminution, milling, vibratory ball milling, and compaction [96]. This step is typically performed before other steps are used to facilitate subsequent processes. Chopping reduces the size of biomass to 10–30 mm, whereas crushing and milling can reduce particle size to 0.2–2 mm [65]. The energy required for mechanical processing of lignocellulosic biomass depends on both biomass properties and final particle size. For example, hardwoods require more energy than agricultural waste [97].

Table 2.1 Advantage and disadvantages of different pretreatment processes [98,99]

Process	Characteristics	Pretreatment	Advantages	Disadvantages
Chemical process	-Partial hydrolysis of hemicellulose - Increase in accessible surface area and size of pores -Decrease in degree of polymerization and crystallinity of cellulose -Partial depolymerization of lignin	Dilute acid Hydrochloric acid, Sulfuric acid	High yield of pentose sugar, Operation time is less	Acid Recovery and formation of furfural
		Explosions -Steam explosion -Ammonia fiber explosion (AFEX) -CO_2 and SO_2 explosion	No inhibitory compounds, High yield of pentose sugar	Recovery of ammonia is not effective. Less effective process with increasing lignin content
		Sodium Hydroxide, Alkali,Lime	No Inhibitory compounds	Operation time is more
		Organosolvosis: Ozone, H_2O_2	High yield of pentose sugar	Solvent recoveryis expensive
		Gas; Chlorine dioxide Nitrogen dioxide	usually rapid treatment rates and most effective methods	Requirements of chemicals Typically need harsh conditions
		Cellulose solvents: -Ethanol-water extraction	most effective methods usually rapid treatment rates	Requirements of chemicals Typically need harsh conditions
Physical process	-Partial or complete hydrolysis of hemicellulose -Reduction in degree of polymerization and crystallinity of cellulose -Delignification	Milling -Colloid milling -Hammer milling -Ball milling	Operationtime is less	High energy requirements The overall yieldis poor.
		Irradiation -Gamma-ray irradiation -Electron beam irradiation	No inhibitory compounds; High yield of sugar	Specific design of process and equipment required
		High pressure	No Inhibitory compounds	Challenge in maintain high pressure
Biological process	-Reduction in degree of polymerization of hemicellulose and crystal -Delignification	Microorganisms Fungi Actinomycetes	No production ofinhibitory compound Mild operation conditions Low energy requirement	Rate of reaction is slow

2.2.1.1.2. Microwave Treatment

Microwaves are an alternative to traditional heating. Microwaves generate heat through direct interaction of objects with applied electromagnetic fields and are suitable for wet biomass [100]. It also alters the structure of cellulose, destroying the silicified surface, degrading hemicellulose, partially removing lignin, and finally improving the accessibility and reactivity of cellulose. Microwaves of plant fibers. Pretreatment requires high temperatures (above 160 °C) [101]. Microwave alkaline acid pretreatment of bagasse has also been reported. Results showed a significant effect on lignin removal. Although this technology is expensive, it has the advantages of (1) energy efficiency, (2) reduced processing time, and (3) ease of use [102].

2.2.1.2. Chemical Pretreatment

2.2.1.2.1. Acid Pretreatment

Acid pretreatment involves the use of concentrated and dilute acids to break bonds in lignocellulosic biomass. The most commonly used acids are inorganic acids (sulfuric acid, nitric acid, hydrochloric acid, and phosphoric acid) [103–105] and organic acids (formic acid, acetic acid, and propionic acid) [106]. However, sulfuric acid is most commonly used. Acid pretreatment can be performed with either low acid concentration (0.5-2%) and high temperature (100-240 °C) or high acid concentration (>30%) and low temperature [107]. Therefore, the dilute acid pretreatment process can be defined as a brief exposure to high temperature (e.g. 180°C). or at lower temperatures (e.g. 120 °C) for longer retention times (30-90 min) on the lignocellulosic material [108]. Treatment with dilute vs. concentrated sulfuric acid is currently receiving considerable attention [109]. Dilute sulfuric acid treatment has been commercialized for various types of biomass such as poplar, spruce (conifers), and switchgrass [110–112]. Little attention has been paid to high concentrations of acid because of drawbacks such as toxicity, equipment corrosion, and acid recovery [82]. The main application of acid pretreatment is to fractionate the components of lignocellulosic biomass and remove soluble hemicellulose [113]. The weaker binding to the remaining lignin after pretreatment makes the sugars more accessible to enzymes and microorganisms. The dilute acid used to hydrolyze the hemicellulose fraction and increase the biomass porosity makes the cellulose more accessible to enzymes. An advantage of the dilute acid pretreatment process is the ability to recover hydrolyzed sugars from hemicellulose. In addition to the hydrolysis/depolymerization of hemicellulose, treatment with dilute sulfuric acid is expected

to cleave some of the ether linkages, and under sufficiently harsh treatment conditions, the cleaved linkages form other linkages, i.e. lignin re-condensation.

2.2.1.2.2. Alkaline Pretreatment

Alkaline pretreatment uses bases such as sodium, potassium, calcium, ammonium hydroxide, and lime to modify lignocellulosic biomass. Alkaline pretreatment is mainly used because of its effective digestibility of cellulose and hemicellulose as opposed to acidic and hydrothermal processes [114]. During this pretreatment, a saponification reaction of the ester bond takes place. This disrupts the cross-links between hemicellulose and other components, thereby enlarging the lignocellulose pore structure [115]. The main advantage of this method is the removal of lignin and acetyl groups that inhibit enzymatic hydrolysis of cellulose [96].

Alkaline pretreatment can be performed at relatively low temperatures and does not require complex reactors [116]. The drawbacks of this process are the long residence times of hours to days and the need for neutralization of the slurry [117].

2.2.1.2.3. Organosolv Pretreatment

Organic solvents like ethylene glycol, methanol, ethanol with or without acid catalysts (HCl, H_2SO_4) are used to extract the hemicellulose separately along with lignin and cellulose. This pre-treatment is particularly efficient for lignocellulosic biomass with a high lignin content as it is able to break the inner lignin and hemicellulose bonds. In addition, relatively pure lignin can be obtained as a by-product from this process [117] which is usually carried out at high temperatures (100 - 250 °C). Acetylation renders the slurry acidic, so no acid addition is necessary [65]. To reduce costs, the solvent must be recovered by evaporation and condensation for further use. This is also very important as solvents can inhibit microbial growth, enzymatic hydrolysis and fermentation or anaerobic digestion [118,119].

2.2.1.2.4. Steam Explosion Pretreatment (SP)

In this process, the biomass is heated with pressurized steam (160–270 °C, 0.69–4.83 MPa) for a few seconds to a few minutes, and then the system is rapidly depressurized to atmospheric pressure as the condensed moisture evaporates. This causes the materials to undergo explosive decompression, causing hemicellulose to become solubilized in the liquid phase. The lignin structure is also transformed by the high temperatures. The cellulose in the solid fraction becomes more accessible [120,121]. Extensive research has been done on vapor explosion pretreatment, which has also been commercialized [114,122].

This pretreatment method improves cellulose digestibility, sugar extraction and pentose recovery while minimizing the formation of inhibitor products [123]. The pre-hydrolyzate enriched with sugar can be fermented directly into bioethanol [124]. It is reported that hot liquid water pretreatment is able to solubilize biomass hemicellulose up to 80% [125]. Cellulose digestibility rises with the removal of hemicelluloses.

2.2.1.3. Biological Treatment

Biological pre-treatment primarily includes the use of wood-degrading microorganisms, such as soft rot, white and brown fungi. It also includes bacteria that break down lignin and hemicellulose [126]. It has been reported that white rot fungi are the most effective microorganisms for biological pretreatment of biomass [127]. This method requires mild conditions and low cost. Due to restrictions such as However, due to the long pre-treatment times required for industrial processes, little attention has been paid to this method.

Biological pre-treatment could be effectively combined with other pre-treatment processes. If the biomass has a low lignin content, biological pre-treatment is often recommended [128].

2.3. Applications of Hemicellulose

Regarding biochemical conversion, it is important to utilize all components of the lignocellulosic biomass to make the process economical. Extensive research on cellulose has been carried out in various fields [129,130]. The high cost of cellulose, xylitol has always been a major obstacle for biochemical industries because of the costs associated with pretreatment, hydrolysis, and detoxification of lignocellulosic hydrolysates [131]. Also, fuel and energy production from biomass is commonly referred to as a carbon “dead end” because carbon is released into the atmosphere. A circular bio economy promotes a cascading use of biomass, with energy use coming last [131]. Attention should be paid to value-added bioproducts from all components of lignocellulosic biomass. Hemicellulose, a natural water-soluble polymer, has great potential for biochemical production. Some of the possible products from xylose bioconversion, including those studied in this paper, are described below.

2.3.1. Production of Xylitol from Hemicellulosic Biomass

Cellulose, hemicellulose, and lignin is the prime components of lignocellulosic biomass and its composition varies depending on the type of plant. The complex structure of

plant lignocellulose forms a protective barrier against cell destruction by fungi and bacteria. To make this structure suitable for transformation in fermentation processes, cellulose and hemicellulose must be hydrolyzed to their corresponding monomers (sugars) for use by microorganisms [132]. A major component of the hemicellulose portion of hardwoods and agricultural residues is xylan, a polymer of xylose units that is hydrolyzed to this sugar by mineral acids or xylanases. Under selected conditions, the solid residue from acid hydrolysis contains both cellulose and lignin fractions, which can be separated in further reaction steps and used for various product applications. Most fermentation studies focus on hydrolysates derived from acid hydrolysis, but hydrolysis of biopolymers can be done enzymatically. Hemicellulose has a low degree of crystallinity, a low degree of polymerization, and a heterogeneous structure compared to cellulose, which makes it easier to break down into structural units during the hydrolysis process [133]. On the other hand, lignin (phenolic fraction), which remains as a solid residue in acidic media for both cellulose and hemicellulose, can be hydrolyzed by stronger acids. Due to its open branched structure, hemicellulose is more susceptible to catalytic hydrolytic effects than cellulose. Raw material polysaccharides (lignocellulosic substances) must be hydrolyzed to the corresponding sugars in order to obtain a microbial carbon source in the fermentation process. The acid catalysts most commonly used for this purpose are H_2SO_4 and HCl.

The liquid phase produced by hydrolysis (containing xylose, by-products and compounds derived from other fractions of the raw materials such as extracts or lignin) can be used to make the fermentation media suitable for xylitol production. Like the defined media formulated by chemicals according to the biocatalyst requirement, the concentration of xylose as a substrate is an important factor affecting the production of xylitol, so the increased concentration of xylose leads to improved yield and productivity. However, when using lignocellulose hydrolysates in the preparation of culture media, some additional effects related to the concentration of the substrate have to be considered. The increase in the concentration of xylose through evaporation inhibits the microbial metabolism and reduces cell growth, which is dependent on a simultaneous increase in the concentration of other non-volatile compounds [134]. Inhibitors in the hydrolyzates produced by acid hydrolysis can be divided into several groups including: a) minerals or metals resulting from equipment corrosion or ions contained in the lignocellulose; b) compounds such as furfural and hydroxymethylfurfural derived from the breakdown of sugars at high temperatures; c) acetic acid released from the acetyl groups in biopolymers; and d) chemicals such as aldehydes, phenolic compounds and aromatics derived from lignin degradation and compounds derived

from extractive. Other important and potent inhibitory compounds in hydrolysates are organic acids such as syrindic, caproic, caprylic, vanillic, pelargonic and palmitic acids. Several factors such as the microorganism used, the adaptability of the microorganism, the mechanism of the fermentation process used, and the co-presence of several other inhibitors are the main parameters that determine the maximum permissible concentration for each process [135,136]. Therefore, in order to make the hydrolyzate suitable as a fermentation medium, acid hydrolysis should be carried out in the following manner. b) Concentration of inhibitory by-products in the range acceptable to microorganisms. c) High selectivity for cellulolysis [35].

2.4. Hydrolysis of Lignocellulosic Biomass

During hydrolysis, cellulose and hemicellulose polymers break down into monomeric subunits. Complete hydrolysis of cellulose yields glucose and hydrolysis of hemicellulose yields several hexoses and pentoses sugar. The predominant sugar in hemicellulose from hardwoods and crop residues is usually xylose, whereas in softwoods it is mainly mannose [137].

Prior to hydrolysis, biomass was pretreated to degrade micro- and macrofibrils, release polymer chains of hemicellulose and cellulose, and modify the pores therein for chemical or enzymatic hydrolysis. Allow chemicals and/or enzymes to enter the fiber [138]. There should be no decomposition, loss of carbohydrates, and formation of inhibitory by-products during pretreatment. There are various physical, chemical and biological pretreatment methods. Most of the hemicellulose is removed from the material, making it more susceptible to chemical or enzymatic digestion. After pretreatment, cellulose and hemicellulose are next hydrolyzed to monosaccharides in two ways.

- Enzymatic hydrolysis
- Chemical hydrolysis

2.4.1. Enzymatic hydrolysis/ saccharification

Conversion of lignocellulosic materials to useful products like xylitol requires hydrolysis of hemicellulose biomass to liberate fermentable sugars, which are then fermented to xylitol. The hydrolysis process is carried out by xylanase enzymes, breaking down structural carbohydrates into monomeric sugars, mainly xylose. Lignocellulosic materials have cellulose, hemicellulose, and lignin tightly bound together in a complex crystalline structure. As a result, the hydrolysis efficiency is reduced due to the restricted access of the

enzyme to the substrate i.e. Cellulose, reduced. Therefore, the degree of saccharification can be used as a benchmark to compare different pretreatment processes.

2.4.1.1. Enzymes

Enzymes are typically high molecular weight proteins (15000 < MW < millions of daltons) that act as catalysts. Enzymes are specific, versatile and highly potent biological catalysts that lead to much faster reaction rates compared to chemically catalyzed reactions under ambient conditions. Over 2000 different enzymes are known. Some enzymes require non-protein groups for their activity. This group is either a cofactor such as the metal ions Mg, Zn, Mn, Fe, or a complex organic molecule or a coenzyme such as some vitamins. Enzymes that catalyze the same reaction, although there are several different molecular forms, are called isoenzymes.

Cellulose and hemicellulose can be hydrolyzed by certain enzymes. Substrate quality, substrate concentration, enzymatic activity, pretreatment process used, and hydrolysis conditions such as pH and temperature are key factors in enzymatic hydrolysis. The optimum temperature and pH conditions for various enzymes are 40–50 °C and pH 4–5 [137]. The use of surfactants can also affect hydrolysis by changing the properties of the cellulose surface. This can be taking place by adsorption of surfactants to lignin, thereby reducing non-productive binding of enzymes to lignin [139,140].

2.4.1.2. Xylanases

Xylanases (endo-β-1,4-xylanase) are primarily responsible for hydrolyzing the β-1,4 bonds of plant xylans (Fig. 2.3), the main component of hemicellulose [141]. Since hemicellulose constitutes about 30% of the plant cell wall [142], and xylan is an important component of hemicellulose, xylanases play an important role in the bioconversion of agricultural industrial wastes into biomass that can be used as animal feed [143]. Industrial-scale xylanase production can be achieved using SSF from fungi, mainly *Trichoderma* and *Aspergillus* and. Fungi secrete enzymes into the medium, and their enzyme levels are generally much higher than yeasts and bacteria, which may be useful for xylanase production [144,145].

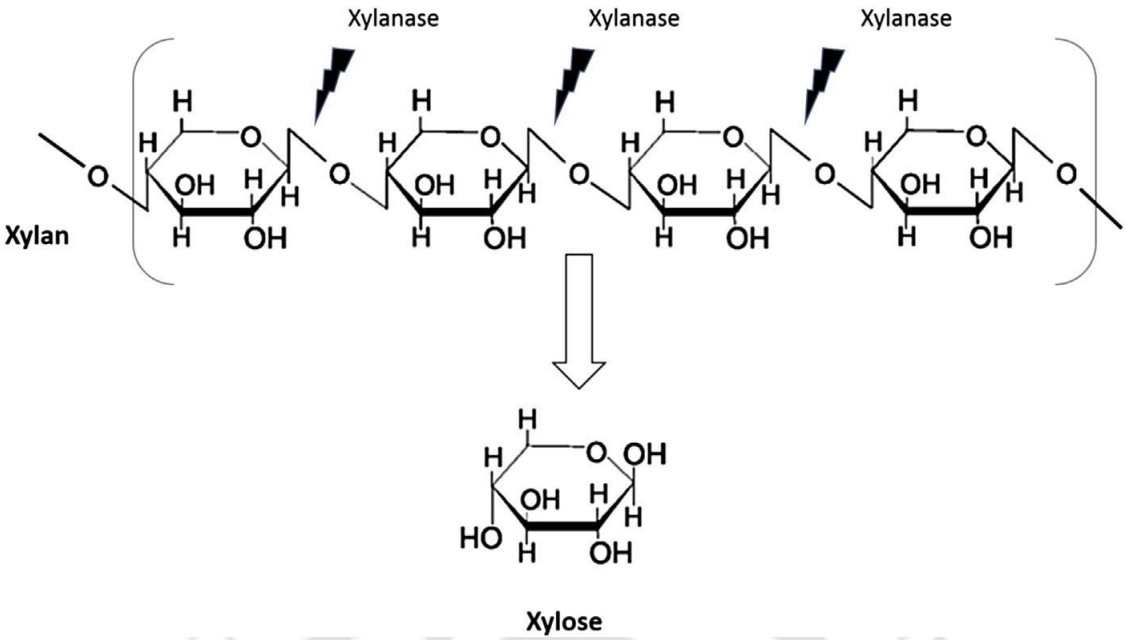

Figure 2.3 Mechanism of action of the xylanases enzyme [146]

Efforts to enhance nutrient digestibility in ruminant and monogastric animals may impact the profitability of the feed industry [147]. Supplementing dairy and beef cattle with exogenous enzymes can significantly improve feed efficiency and animal performance [148]. Enzyme products are various enzymes mixed with unknown amounts of each enzyme. Several studies have reported that a mixture of accessory fibrillolytic enzymes with high xylanase activity induced positive responses in captive dairy cows [149,150]. Other studies have explored the use of xylanases to improve nutrient digestibility in other ruminants and pigs [151].

2.4.1.2.1. Mechanism of action of the xylanases

It has often been proposed that the catalytic mechanism of glycosidases is similar to that of lysozyme. Hydrolysis reactions catalyzed by xylanases and cellulases proceed via an acid-base mechanism involving two residues. The first residue acts as a general catalyst, protonating the oxygen of the oxidic bond. The second residue functions as a nucleophile that interacts with the oxocarbonium intermediate in the case of retention enzymes or facilitates the formation of OH3 ions from water molecules as observed in reversal enzymes. The configuration retention reaction involves a two-step mechanism involving proton transfer to and from the oxygen atom at the equatorial position of the anomeric centre [152]. This reaction mechanism is similar to that of lysozyme [153]. As observed in the case of L-amylase, reactions leading to configuration inversion proceed via a single substitution [154]. Therefore, it is possible that a single amino acid residue (acid/base catalysis) is involved in

both proton transfer steps. Xylanases predominantly exhibit a double-displacement mechanism involving a glycosyl enzymatic intermediate that is formed and hydrolyzed via an oxocarbonium ion-like transition state.

2.4.2. Chemical hydrolysis

Chemical hydrolysis exposes materials to chemicals at specific temperatures for specific times to produce sugar monomers. The predominant chemicals used are acids, but alkalis (NaOH) are also used. The most studied acid is sulfuric acid, but other acids such as HCl have also been used [155]. Depending on the acid concentration used, acid hydrolysis is divided into two categories.

- Concentrated-acid hydrolysis
- Dilute-acid hydrolysis

2.4.2.1. Concentrated-acid hydrolysis

Concentrated acid hydrolysis is a comparatively older technique. This method gives a higher yield of sugar (e.g. 90% of the theoretical glucose yield) and can be operated at lower temperature compared to the dilute method. On the other hand, since the concentration of the acid is very high, typically 30-70% by volume, its dilution and heating during hydrolysis makes it very corrosive. Therefore, the process requires special expensive materials of construction such as alloys or non-metals such as ceramic or carbonaceous linings. Acid recovery is also a very energy-intensive process. In addition, large amounts of gypsum are formed during neutralization with sulfuric acid. In addition, the environmental impact severely restricts acid applications. High maintenance and investment costs have severely limited the commercial use of this process [156,157].

2.4.2.2. Dilute acid hydrolysis

This is the most commonly used technique among chemical hydrolysis methods. This process can be used as a pretreatment before enzymatic hydrolysis or as the main hydrolysis process. Most often it is run in batch mode with a retention time of a few minutes. Most hemicelluloses are hydrolyzed at temperatures below 200°C, but temperatures above 220°C are required for maximal glucose yields. Acid concentrations are typically 0.5–2% by volume [157,158]. A dilute acid pretreatment process can be defined as a brief exposure to high temperature (e.g. 180°C). Alternatively, for longer holding times (30-90 minutes), set the lignocellulosic material to a lower temperature (eg 120 °C) [158]. At present, treatment with

dilute sulfuric acid versus concentrated sulfuric acid is receiving considerable attention [137]. Dilute acid hydrolysis has many advantages over concentrated acid, including: shorter reaction times, Less corrosion, and faster reaction rates [159]. The main drawback of this process, especially in one step, is the breakdown of sugars and the formation of unwanted by-products. Not only does this reduce sugar yield, but by-products can inhibit the formation of the main product during subsequent fermentation. To avoid this degradation and inhibitor formation, the hydrolysis process can be carried out in two (or more) steps under different conditions.

2.4.2.3. Theory of acid hydrolysis process

The molecular mechanism of acid-catalyzed hydrolysis (breaking of β-1-4 glycosidic bonds) of cellulose follows the pattern outlined in Figure 2.4. Cellulose matrices are composed of microcrystalline bundles bound together by quasicrystalline domains and surrounded by a charged water boundary layer resulting from dipole-dipole interactions induced by the alignment of water molecules around the polar surfaces of the cellulose faces[160]. Water molecules and H^+ ions (from the acid) must penetrate the cellulose fibers for the hydrolysis reaction to proceed effectively. Otherwise hydrolysis will only occur on the surface of the cellulose.

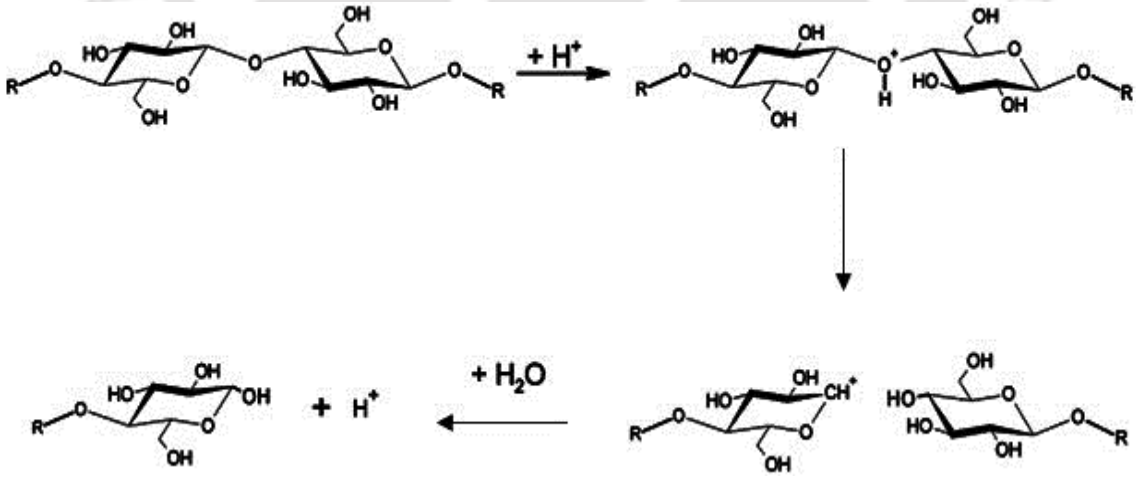

Figure 2.4 Mechanism action of acid hydrolysis of cellulose [160]

Acid catalyzes the disintegration of long cellulose chains to form smaller chain of oligomers and then sugar monomers that the acid can break. Cellulose hydrolysis begins with the reaction of acidic protons with oxygen to combine two glucose units to form the corresponding conjugate acid. This C-O bond is then cleaved, breaking the conjugate acid into a

cyclic carbonium ion and adopting a semi-chair conformation. Rapid addition of water releases free sugars and protons. Intermediate carbonium ion formation occurs faster at the ends than in the middle of the polysaccharide chain.

2.5. Detoxification of Hemicellulose Hydrolysate/Pre-hydrolysate

As mentioned above, acid/alkaline thermochemical processes are necessary to break down the structure of lignocellulosic biomass and obtain fermentable sugars. On the other hand, the pretreatment or hydrolysis processes result in the formation of toxin by-products that inhibit enzymatic hydrolysis and microbial fermentation. The formation and concentration of inhibitor products from pretreatment and hydrolysis vary depending on the input material and pretreatment process [161]. Substances that inhibit microbial growth include phenolic compounds and other aromatics, aliphatic acids, furan aldehydes, and inorganic ions. Phenolic compounds are degradation products of lignin, while carbohydrates are the main source of furanaldehydes and aliphatic acids (acetic, formic, and levulinic).

Acetic acid is primarily the result of hydrolysis of the acetyl groups of hemicellulose. However, levulinic acid and formic acid are formed by thermochemical pretreatment/hydrolysis involving acids [162]. Degradation of pentose and hexose sugars forms the furanaldehydes furfural and HMF, respectively. These chemicals are commonly found in lignocellulose hydrolysates/prehydrolysates. It is worth noting that some of these degradation products, such as levulinic acid, are in very high demand on the market [163]. Successful removal and separation of these by-products is therefore important as they can make a positive contribution to the economics of the process. Detoxification methods have been proposed that convert inhibitors to inactive compounds or reduce their concentrations. Some of these methods are described below.

2.5.1. Biological Detoxification

Biological treatment methods include the use of microorganisms or enzymes to convert toxic compounds present in the hydrolyzate/prehydrolysate [164]. Detoxification of hemicellulose hydrolysates usually involves enzymes such as laccase and peroxides. Certain enzymes of the white rot fungus Trametes versicolor modify the acidic and phenolic compounds contained therein. Oxidative polymerization of low-molecular-weight phenolic compounds was described as a possible mechanism for these enzymes [165]. Using microorganisms, wild microorganisms (yeast, fungi, bacteria) and/or recombinant microorganisms expressing laccase or peroxidase enzymes can also be used directly to

selectively remove inhibitors from lignocellulose hydrolysates. has been reported [166]. A fungal isolate, Coniochaeta ligniaria (NRRL30616), has also been reported to metabolize furfural, HMF, aromatic and aliphatic acids, and aldehydes present in corn straw hydrolysates [167]. Despite the effective results, the high cost of enzyme production and the time required for incubation are major obstacles to the large-scale application of this method for detoxification [168].

2.5.2. Physical Detoxification

2.5.2.1. Vacuum Evaporation

Vacuum evaporation is a suitable physical process for removing furfural, acetic acid, and other volatile compounds from hemicellulose hydrolysates. This method has been used successfully in several studies to remove acetic acid and furan inhibitors. About 80% of acetic acid removal from rice straw hydrolyzate using vacuum evaporation has been reported [169]. In most cases, detoxification was performed by vacuum evaporation at temperatures below 70 °C. A major drawback of this process described in the literature is the inability to remove non-volatile toxic compounds at elevated temperatures [170].

2.5.3. Chemical Detoxification

2.5.3.1. Alkali or Reducing Agent

Alkali-based techniques involve the removal of toxic compounds by applying alkali such as ammonium hydroxide, calcium hydroxide [161,171]. However, for lignocellulosic biomass prehydrolysates and dilute sulfuric acid pretreatment hydrolysates, hypercalcification (calcium hydroxide) is a commonly used detoxification process. In this cost-effective method, Ca(OH)2 is added to raise the pH value to 10 and H2SO4 to lower it to 6.5 [172]. This procedure has been reported to effectively remove volatile inhibitory compounds such as furfural and hydroxymethylfurfural (HMF) with ~10% sugar loss [166]. Sugar loss and the influence of alkali on inhibitors are the main drawbacks of this method. The use of reducing agents such as dithionite, dithiothreitol, and sulfite has also been reported. This chemical in situ detoxification helps skip additional steps to detoxification [173].

2.5.3.2. Liquid-Solid Extraction

2.5.3.2.1. Activated Charcoal treatment

Activated carbon is widely used to remove compounds from liquid phases by adsorption to purify or recover chemicals. The use of this high-capacity absorbent is known

to be a cost-effective detoxification method without affecting the sugar content of the hydrolyzate/pre-hydrolysate. Various process variables such as pH, activated carbon concentration, contact time, and temperature have a significant impact on the efficiency of the treatment [170]. It was reported that 27% of phenolic compounds were removed from rice straw hemicellulose hydrolyzate in the hydrolyzate. The activated carbon ratio was 40 g/g. The lack of recyclability of activated carbon is a major drawback for its large-scale use[170].

2.5.3.2.2. Ion-Exchange Resins

Anion exchange resins have been extensively studied for their effectiveness in efficiently removing inhibitors from hydrolysates. Both cationic and anionic resins can be used based on the inhibitor [174]. Chandell et al. reported that 63.4% of furan (g/L) and 75.8% of total phenols in sugarcane bagasse acid hydrolyzate were removed using an ion-exchange resin [175]. Despite the advantages of using ion exchange resins, including reusability and recyclability, the high cost associated with this process limits its application to lignocellulose-derived products on an industrial scale[166].

2.5.3.3. Liquid-Liquid Extraction

This procedure uses solvents to remove toxic chemicals. Important factors to consider when choosing an effective solvent are the partition coefficient, immiscibility, and boiling point of evaporation [176]. Various solvents have been used to remove inhibitors from lignocellulose hydrolysates/prehydrolysates, including ethyl acetate [177], toluene, chloroform [178], and hexane [179]. Low molecular weight phenolic compounds were found to be the major toxic compounds in the ethyl acetate extract. This may be due to the high solubility of phenol in ethyl acetate [180]. Ethyl acetate extraction was shown to be more effective than using a rotary evaporator in removing all toxins in lignin derivatives as revealed by Wilson et al., although acetic acid was partially removed [181].

2.5.3.4. Combined Methods

A single detoxification procedure may not be adequate to remove various types of inhibitors from lignocellulose, as each procedure is specific to a particular class of compounds. Two or more different methods can be used in combination for better results. Rodriguet et al. revealed that the removal of volatile and nonvolatile compounds from sugarcane bagasse hemicellulose hydrolyzate using activated carbon treatment before or after vacuum evaporation [182]. They reported that phenolic compounds were effectively removed

using activated charcoal prior to evaporation, whereas acetic acid removal performed better using post-evaporation treatment [182]. An integrated detoxification technique involving vacuum evaporation and solvent extraction was recently developed in our laboratory and was able to effectively remove acetic acid and furfural using toluene as a solvent [183].

2.6. Fermentation process modelling and optimization

The most commonly used modelling and optimization technique for fermentation and bioprocess is RSM, one variable at a time approach (OVAT) and factorial Design of Experiment (DOE) [184,185]. For the successful utilization of the RSM technique in optimization, a prototype, namely a comprehensive second-order polynomial, needs to be calculated to find out the comparative impact of the respective medium component. L_N (N factor at L levels) is the number of experiments configured by RSM; however, in each procedure, merely two or three groups can be implemented, and the plotting is confined to two variants at a time. Designing of this stringent models which illustrate the high non-linearity and stability is a crucial problem, because of the metabolic complexity of microorganisms and the various types of parameters involved [186]. By effective implementation of RSM, numbers of fermentation systems can be reasonably approximated by second-order relation. ANN is frequently utilised as "black box" models of key variants whose affinity to different processing units is neither established nor formally explained [187]. ANN has been effectively used for modelling, optimization, system design and control, because of its ability to learn and strain boisterous signals. Furthermore, ANN easily universalize information using a training procedure [188].

RSM, OVAT, DOE and other optimization techniques are widely used and their concepts and drawbacks are commonly known. Such as, in the case of OVAT, the interactive effect of parameters does not consider in the process; hence, the optimal set points may be neglected [189]. Whereas in case of DOE, as the number of simulation data increases, this technique becomes time consuming, labor-intensive and resource-demanding, which make this process not much more attractive. However, in the case of RSM, it ignores the less significant variables with a confined understanding of their possible interactive effects on the bioprocess output [190]. Nowadays, the most promising technique for modelling and optimization of bio-processes is Artificial intelligence tools. Some of them are Genetic Algorithm (GA), Artificial Neural Network (ANN), Particle Swarm Optimization (PSO), Fuzzy Logic and Ant Algorithm. All of these are mainly used in research and development for designing of bio-process [113,191]. In the last few years, ANN has mainly been used in research and development for

covariant bio-processes. Bioprocess models developed by ANN are lacking of previous information concerning of metabolic fluxes and kinetics that happen inside the cells and surrounding. ANN models pretend the linkage that exists in biological neurons with outstanding capability for analysis, association, adaptation and learning [189].

ANNs can be explained by the mathematical understanding of the neurological functioning of the human brain. They copy the brain's learning process by arithmetically modelling the network structure of interconnected nerve cells [113,191]. ANN is a structure like a multiprocessor computer system, consisting of simple processing components known as neurons. Like neurons in the brain, the ANN shows the connection and adapt properties among the elements. Moreover, previous knowledge of the events that govern the process is not required in ANNs because it is an entirely data-based process. The first layer of the ANN structure is known as the input layer. Further, one and more hidden layers are there, followed by an output layer. Formation of multi-layer neurons occurs when a set of single-layer neurons is connected. Figure 5.1 demonstrates the framework of multi-layer ANN [186]. The sources of info are provided to the first layer of neurons, which thus is associated with the second layer and subsequent layers. The hidden layer's neurons help establish a complex network between the input and output parameters. Usually, bio-process modelling and optimization are difficult for fermentations because it exhibits non-linear relationships. Applying the ANN model detects process non-linearities and defines a model that connects process inputs to appropriate output parameters [192].

2.7. Fermentation and separation of xylitol

2.7.1. Fermentation process

The word fermentation derives from the Latin verb " *fevere* " which means "*to boil*". However, boiling occurs when the gas bubbles break up on the surface of a boiling liquid during alcoholic fermentation, giving it the wart-like appearance. The fermentation process can be described as a process in which cellular energy is generated from the breakdown of nutrient molecules, where there is no net change in the oxidation state of the products compared to that of the reactants [193]. This definition of fermentation made little sense until the metabolic process was known. The metabolic pathways that produce energy are basically similar in nearly all organisms. The oxidation reaction to produce ATP can be carried out in the presence of oxygen (for aerobic bacteria) or in the absence of oxygen (for anaerobes). Thus, in aerobic microorganisms, the process of ATP generation is known as cellular

respiration, while in anaerobes, or aerobic organisms operating under anaerobic conditions, it is known as anaerobic respiration or fermentation.

Fermentation (such as brewing and winemaking) has been practiced for hundreds of years, but it was his L. Pasteur who observed the microorganisms associated with fermentation. In 1815, Gay-Lussac formulated the conversion of glucose to ethanol. Since 1940, the manufacturing of large-scale industrial solvent fermentation and distillation plants has developed rapidly. Biological routes are alternative methods of producing biofuels. Growing environmental concerns and periodic crises in some large oil exporters are making biofuels a viable and viable alternative in the energy market. The focus is on the production of ethanol and other biofuels from cellulosic biomass, and additional biotechnological methods of generating energy are also being explored [194]. All lignocellulosic biomass is biodegradable and, to varying degrees, can be biologically converted into various biofuels such as ethanol and hydrogen in anaerobic digestion processes.

Valuable and interesting research has been published, especially on the production of fuel ethanol and biohydrogen from lignocellulosic biomass. To produce biofuel from starch, this carbohydrate chain must be broken to yield a glucose syrup that can be converted to ethanol by yeast. This type of feedstock is most commonly used for ethanol production in North America and Europe. Corn and wheat are mainly used for these purposes. [195]. In tropical countries, other starchy crops such as tubers (such as cassava) can be used for commercial fuel ethanol production. Gnansounou et al. (2005) investigated the feasibility of producing fuel ethanol from sweet sorghum juice under conditions in northern China [196]. However, analysis of the integrated features of the entire process of producing fuel ethanol from different feedstocks together with biohydrogen production was not the main purpose of these reports. The aim of this work is therefore to study the co-production of bioethanol and biohydrogen and their integration as an important method of process improvement in the production of this liquid biofuel.

2.7.2. Xylitol production by Fermentation process

Applying appropriate techniques for biotechnological xylitol production is a critical step for the successful biotransformation of substrates into valuable products. This technology has several advantages such as economy, environmental friendliness, high productivity and high yield [197]. Carvalho et al. investigated the efficiency of xylitol production by varying several parameters of the fermentation process. *C. guilliermondii* FTI 20037 cells were incorporated into calcium alginate and used for xylitol production from

sugarcane bagasse hemicellulose hydrolyzate [198]. The optimization of the process was performed by a screening design and response surface methodologies. Using a hydrolyzate concentrated five times, values of 47.5 g/l, 0.81 g/g and 0.40 g/l/h were obtained for xylitol production, xylitol yield and volumetric productivity, respectively, in 120 h fermentation at an air flow rate of 1 .30 vvm, stirring speed of 300 rpm, initial cell concentration of 1.4 g/L and initial pH of 6.0. The metabolic behaviour of Ca-alginate bead-encapsulated *C. guilliermondii* cells for discontinuous xylitol production in a stirred-tank reactor from sugarcane-bagasse hydrolyzate was studied by Carvalho et al. (2005) [199]. Xylitol production of 47.5 g/L, yield of 0.81 g/g, and productivity 0.40 g under conditions including agitation speed (300 rpm), air flow (1.3 vvm), initial cell concentration, and initial pH (6.0) was obtained. /L/h from a fivefold concentrated hydrolyzate during a 120-hour fermentation. Therefore, the lower xylitol productivity in this system compared to that reported for free *C. guilliermondii* using different fermentation modes could be attributed to intraparticle mass transfer limitations.

Santos et al. (2005) investigated the effects of carrier concentration and aeration rate on the bioproduction of xylitol using *C. guilliermondii* cells immobilized on porous glass in a fluidized bed reactor (FBR) [200]. The results show that aeration rate positively affects volumetric productivity (Qp) and negatively affects product yield (Yp/s), while carrier concentration negatively affects both fermentation parameters. showed. Highest xylitol concentration (13.1 g/L) and highest product yield (0.38 g/g) were obtained with aeration rate of 0.03 vvm and carrier concentration of 62.5 g/L, while xylitol productivity was lowest. value (0.18 g/l/h). Only increasing the aeration rate to 0.093 vvm reduced the yield to (0.25 g/g) but had the highest volumetric productivity (0.44 g/L/h). This may be due to increased cellular metabolism.

Xylitol yield and concentration were at the lowest level and cell concentration was highest when the highest level of aeration rate and vehicle concentration was applied. This is because in this state cell metabolism is directed towards cell regeneration. On the other hand, increasing the carrier concentration ruptured the bubbles in the reactor and reduced xylitol accumulation. This is because it promoted cell proliferation (Santos et al. 2005a). As is known, good performance of immobilized cell lines depends primarily on the correct choice of immobilization support. Santos et al. (2003) used *C. guilliermondii* cells immobilized on porous glass to study xylitol production from hemicellulose hydrolyzate in a fluidized bed reactor, and found that inhibitory effects and/or mass transfer limitations were such. reported

that it can impair the performance of biological systems. Therefore, experimental optimization is required [198].

2.7.2.1. Xylitol Recovery from Fermented Broth

2.7.2.1.1. Purification of Fermented Broth

One of the most complex steps in industrial fermentation processes is product recovery and purification [201]. Impurities in xylitol fermentation broth come in different molecular sizes. Most of these contaminants are residual nutrients from fermentation and include yeast extracts, polypeptides, sugars, sugar alcohols, and inorganic salts. Knowing the properties of the xylitol molecule is very important in understanding extraction methods. The size of the xylitol molecule has been reported to be about 0.96–0.99 nm in length with a maximum radius of 0.3–0.33 nm [202]. Yeast extracts composed of amino acids, peptides, oligopeptides, proteins, and other metabolites are present as additives in the medium and are considered impurities in the culture medium during subsequent processing. The main recovery methods for xylitol include ion exchange resins, activated carbon, and chromatography. Grugel et al. Xylitol was purified from fermented sugarcane broth using activated charcoal, anion and cation exchange resins [201]. Xylitol has an affinity for strong cation exchange resins (Amberlite 200C) and weak anion exchange resins (Amberlite 94S), with xylitol sticking to the surface of the resin resulting in 40-55% product loss. The best medium clarification material was activated charcoal (25 g in 100 ml of fermentation broth), and xylitol had a lower affinity (20 %) for activated charcoal than resin at 80 °C and pH 6.0 for 60 min. It has also been shown that the most important factor in color removal is the concentration of activated carbon. The effect of activated carbon concentration is smaller at higher temperatures and is greater at pH 6.0 than at pH 9.0. In another study, Silva et al. Activated charcoal and polyaluminum chloride were evaluated to purify xylitol from fermentation media [203]. The results show that 5.2 g/L of polyaluminum chloride in combination with activated carbon at pH 9 and temperature of 50 °C for 50 min reduced phenolic compounds by 93.5% and promoted 9.7% loss of xylitol from fermentation media.

2.7.2.1.2. Crystallization of solution

Crystallization is a process in which randomly arranged molecules, atoms or ions assemble and form an ordered solid structure called crystal [204]. Since molecules that have same or similar structures are more likely to come together, crystallization is a good

separation and purification technique. It is an important separation technology for the separation of crystals from homogeneous solution mixture.

The fundamental concepts of crystallization are solubility and supersaturation and these terms essential towards developing and characterizing the behaviour of a crystallization system [205]. The solubility, which is a thermodynamic property, can be defined as the maximum amount of substance (i.e. solute) that can be dissolved in a given amount of solvent under certain temperature and pressure conditions when thermodynamic equilibrium does apply. Typically, the solubility of solute in a solvent does increase by raising the temperature within the bulk and consequently it is commonly considered as a function of temperature [206,207]. A phase diagram of a crystallization system is depicted in Figure 2.5, where the solubility curve is illustrated by a solid blue line. A solution which is located on the solubility curve is called saturated. Under certain conditions, however, a solution can dissolve more solute than is determined by the saturation condition, in which case a supersaturated solution is obtained. A necessary, but not sufficient condition for the formation of a new phase is the existence of supersaturation, a thermodynamically metastable state [204]. In more detail, supersaturation, which typically depends on the solute concentration and bulk temperature, is the decisive driving force of the crystallization [206]. Therefore, optimal supersaturation control is a prerequisite for the economical production of crystals with desired quality attributes, such as size, shape and purity.

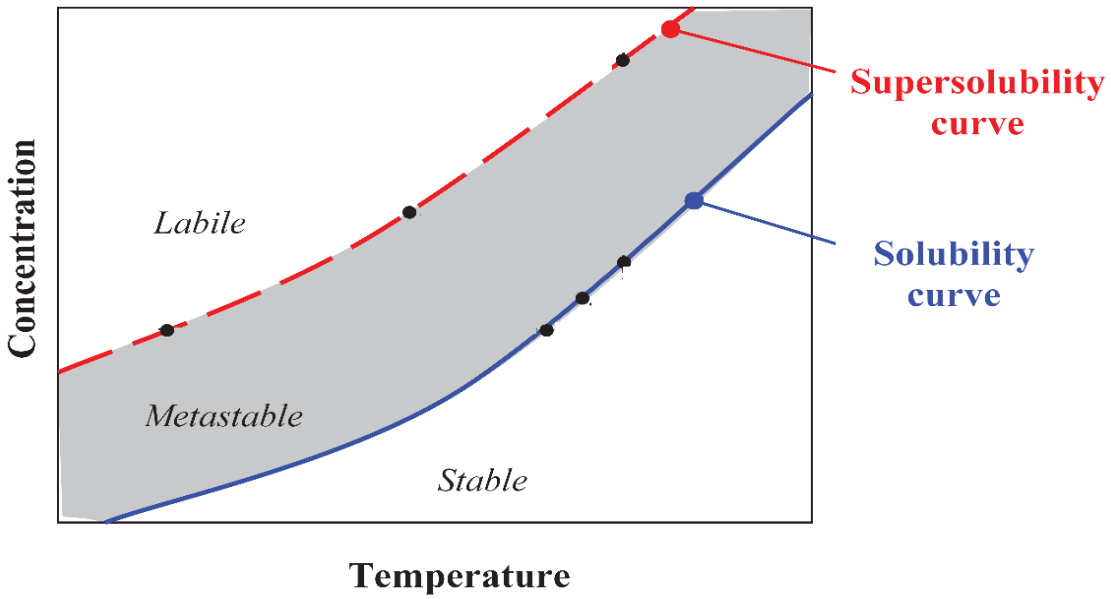

Figure 2.5 Solubility - Super solubility diagram [208]

2.8. Knowledge Gaps and Objectives

2.8.1. Problem Statements

The above literature survey showed that agricultural bio waste products have been studied extensively for their potential in the production of value-added chemicals through biotechnological routes, there is still a need for improvement in terms of cost-effectiveness and efficiency. While various agricultural feedstocks have been investigated for the production of xylitol, there is limited research on the use of Areca nut, which is composed of valuable fibers including xylan that can be converted to xylitol through fermentation. Furthermore, existing production techniques require high energy and operational costs, and there is a lack of information on optimizing the production methodology, investigating detoxification and optimization of hemicellulosic acid hydrolysate, and downstream processing and purification techniques. The objective of this research is to address these gaps in knowledge through an integrated process.

2.8.2. Research Questions

In light of this, it is important to explore sustainable and eco-friendly methods for the production of value-added chemicals such as xylitol. With this in mind, the present study aims to address the following research questions:

- Can locally available lignocellulosic biomass, specifically Areca nut husk, be used as a potential feedstock for xylitol production?
- How Can saccharification of pretreated biomass using varying enzyme loading result in the production of fermentable sugars for xylitol production?
- What are the optimal fermentation parameters (such as pH, temperature, inoculum concentration, and agitation) for the production of xylitol from detoxified dilute acid hemicellulosic hydrolysate?
- Can downstream processing and purification techniques be applied to the fermentation broth to produce purified xylitol crystals, reducing health hazard risks and other health-related issues?

The above questions reflect the gaps in knowledge identified in the literature survey, such as the limited research on the production of xylose through saccharification of biomass with varying enzyme loading, the need for investigation on the detoxification and

optimization of areca nut hemicellulosic acid hydrolysate, and the lack of reported works on downstream processing and purification of xylitol crystals.

2.8.3. Research Hypotheses

The specific research hypotheses of the present research work are as follows:

- Areca nut husk has the potential to be a viable feedstock for xylitol production, and optimizing the fermentation process can improve its economic efficiency.
- Varying enzyme loading during saccharification of biomass can improve xylose production, leading to higher yields of xylitol.
- Detoxification and optimization of areca nut hemicellulosic acid hydrolysate can improve xylitol production yield.
- Downstream processing and purification techniques can be applied to reduce health hazards and improve the purity of xylitol crystals.

2.8.4. Objectives of the Research

The overall objective of present research work is to employ an integrated process to address and study the above-mentioned gaps in knowledge. The specific objectives of present research work are as follows:

1. Characterization and pretreatment of locally available lignocellulosic biomass (Areca nut husk) to identify its potential for xylitol production.
2. Saccharification of pretreated biomass for production of fermentable sugar, followed by fermentation for xylitol production.
3. Optimization of fermentation process for production of xylitol from detoxified dilute acid hemicellulosic hydrolysate.
4. Study on downstream processing of fermentation broth for production of purified xylitol crystal and product characterization.

By addressing these research questions and achieving these objectives, the aim of this study is to contribute to the knowledge gap in the efficient and cost-effective production of xylitol from agricultural waste, specifically Areca nut husk.

भारतीय प्रौद्योगिकी संस्थान गुवाहाटी
Indian Institute of Technology Guwahati

भारतीय प्रौद्योगिकी संस्थान गुवाहाटी
Indian Institute of Technology Guwahati

Chapter 3

Characterization and Pretreatment of Lignocellulosic Biomass

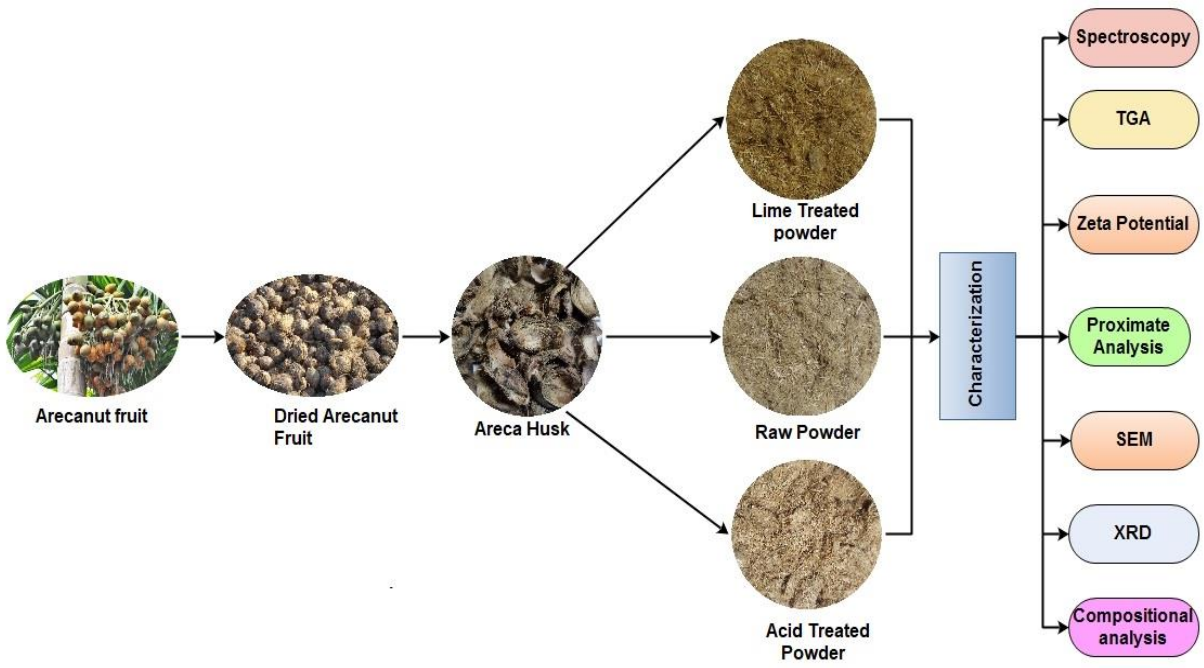

3.1. Overview

Lignocellulosic materials are abundant and affordable, either in the form of agricultural waste or forest residues, and can be utilized for energy production in various forms such as gaseous, liquid, or solid fuels, including xylitol. The use of lignocellulosic materials for energy production is a well-established fact in today's energy research. However, pretreatment of the biomass is a crucial step for the breakdown of the lignocellulosic structure into its basic components, such as lignin and carbohydrate molecules. Although several pre-treatment technologies exist to extract valuable chemicals from biomass, selecting the appropriate biomass remains a challenge. In this study, the focus was on the pretreatment and characterization of Areca nut husk, a lignocellulosic biomass widely available in the North-East region of India. The physical and chemical properties of Areca nut husk were investigated, including proximate and ultimate analysis, thermogravimetric analysis, crystallinity, and chemical characterization using FTIR and Raman spectroscopy. The study found that Areca nut husk fiber contains 29.17% hemicellulose and has the potential to be a low-cost source of xylose. However, there is still a need to optimize the pretreatment process to improve the yield and purity of xylitol. Additionally, future studies should focus on exploring the use of other lignocellulosic biomasses in the North-East region of India for energy production, and on developing efficient strategies for scaling up the production process.

3.2. Materials and methods

3.2.1. Materials

Husks of Areca nut were collected from the local vendors of Guwahati city. All the necessary chemicals were purchased from Hi-Media, India. Areca nuts husk fibers were separated manually followed by washing with tap water to eliminate the loosely adhered impurities followed by drying for 8 h at 70 °C temperature to remove the moisture content. After this, the dried husks were ground to fine particles and screened to collect the homogeneous particles of size lower than 0.5 mm, and placed in an air tight container till further use. The powdered biomass samples were used as a starting material for characterization. The characterization scheme of biomass samples is shown in Figure 3.1.

3.2.2. Lime Pretreatment

The lime pretreatment process comprised slurring of lime with water in desired proportion (1.25 g lime mixed with 5 g raw biomass). The slurryed mixtures of biomass and

lime were distributed (triplicate) in wide mouth reagent bottles and kept in an orbital shaker for seven days at 30° C temperature. After seven days, the mixture was washed with distilled water till pH of the slurry reaches nearly 7.0. The solid biomass samples thus obtained were send for different analysis to characterize using different instrumental techniques such as Fourier transform infrared spectroscopy (FTIR), Thermogravimetric analysis (TGA), Raman spectroscopy, Field emission scanning electron microscopy (FESEM), X-ray diffraction analysis (XRD) and Zeta-potential analysis.

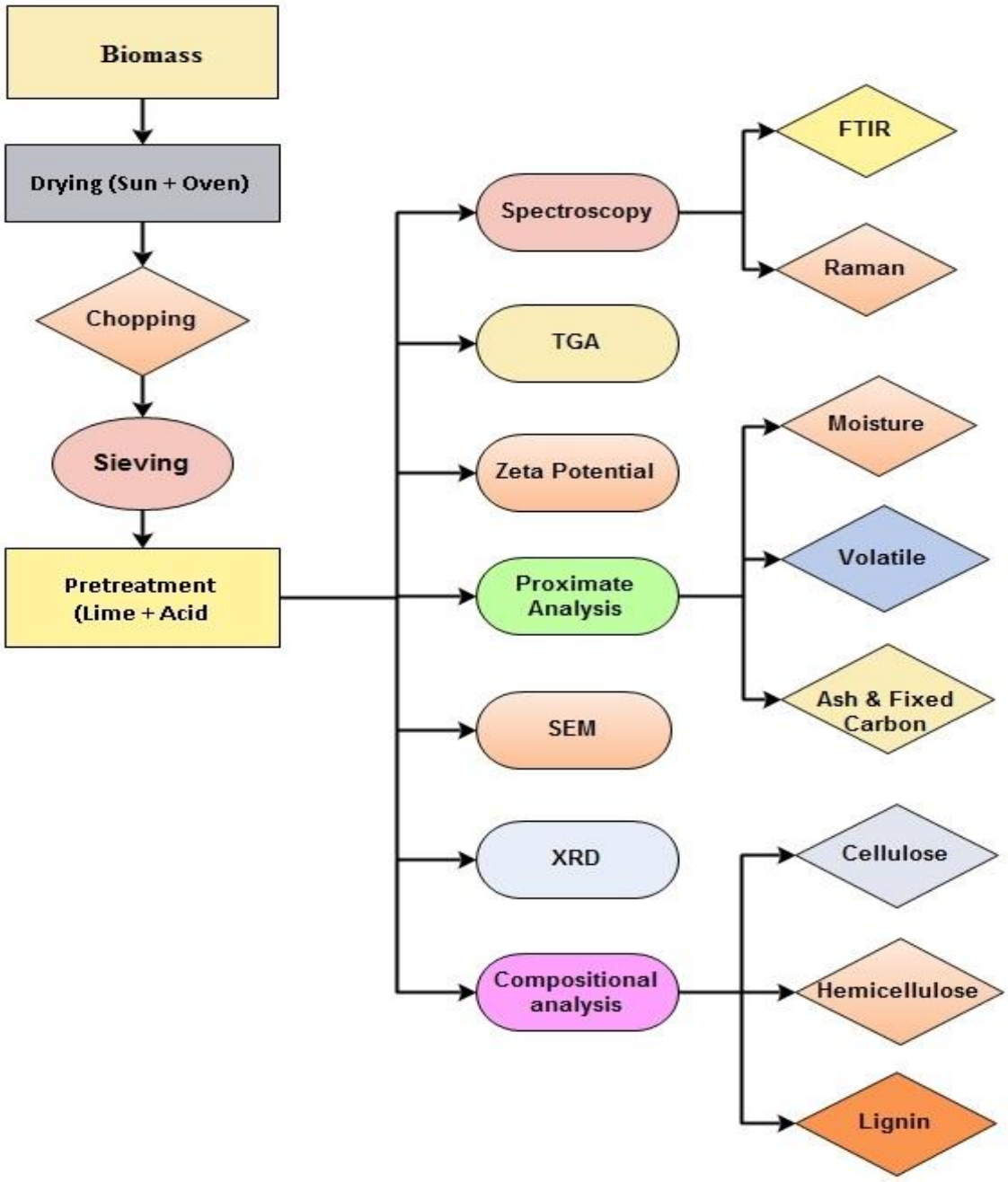

Figure 3.1 Scheme for characterization of biomass samples

3.2.3. Dilute Acid Pretreatment

The acid pretreatment process was conducted using sulphuric acid (H_2SO_4) to hydrolyze areca nut husk biomass. Biomass (5 g) was mixed into 500 mL water followed by addition of 12.5 g (i.e. 6.79 mL) of H_2SO_4 (density 1.84) into it. The solution was then properly mixed and transferred to an autoclave for hydrolysis for 30 min at 121°C. After completion of 30 min, the resultant solution was cooled to room temperature and the left-over biomass material was harvested followed by drying at room temperature. The dried biomass thus obtained was further send for characterization by different instrumental techniques as mentioned in previous section.

3.2.4. Compositional analysis of areca nut husk feedstock

Thermogravimetric analyser was used to determine the composition (cellulose, hemicellulose, and lignin) of areca nut husk sample (treated and untreated biomass). Results were reconfirmed by using conventional methods of structural analysis of lignin and carbohydrates, as discussed in NREL protocol [209]. All samples were hydrolyzed in 72% H_2SO_4 (specific gravity about 1.63 at 20 °C) at 30 °C for one hour. Hydrolyzed samples were further diluted with acid up to concentration of 4%, followed by autoclaving at 121 °C for an hour. Resultant solution was cooled at ambient temperature and passed through a filter. Presence of total acid insoluble lignin in the sample was directly proportional to the amount of retention. HPLC analysis of the permeate was performed to know the sugar content. With the help of sugar profile, the concentration of cellulose and hemicellulose were determined.

3.2.5. Fourier transform infrared spectroscopy (FTIR) Analysis

FTIR spectra of each sample was recorded using FTIR analyser (Model: Perkin Elmer Spectrum two) to study the functional groups present in the biomass samples. All the husk samples were mixed thoroughly with potassium bromide (KBr) at room temperature followed by scanning between the ranges of 4000 cm^{-1}-500 cm^{-1}.

3.2.6. Thermogravimetric Analysis (TGA)

Thermal stability of the native and pretreated areca nut husk samples was analysed using thermogravimetric analyzer (Hitachi, TA-7000). Approximately 8-9mg biomass samples was kept in a ceramic crucible and the thermal analysis was performed under inert atmosphere at 5 °C/min heating rate from temperatures 20 °C to 900 °C with 50 mL min^{-1} flow rate of nitrogen gas.

3.2.7. Raman spectra Analysis

The areca nut husk samples (both raw and pretreated) were scanned from 4000 cm^{-1} to 500 cm^{-1} using a Laser Micro Raman system equipped with JobinVyon, Model LabRam HR at room temperature.

3.2.8. Scanning Electron Microscopy (SEM)Analysis

SEM pictures of each biomass samples were captured using Horiba Zeiss SEM (Model-Sigma). The SEM pictures were analysed to find the texture, surface morphologies, topologies and elemental information of each studied samples at altered magnifications.

3.2.9. XRD Analysis

XRD analysis of all the biomass samples were carried outusing a broad angle X-ray diffractometer (Brucker D8 Advanced X-ray diffraction measurement system, Kolkata, India). Areca nut husk samples (raw, and pretreated) were kept in the sample holder and analysed under plateau conditions. The radiation (X-ray) was generated at a voltage of 40 kV and 40 mA current flow. The spectrum of scan was set between the ranges of $7^{o}$and $40^{o}$with a step size of 0.02° and residence time was set at 1 s/0.02°. Crystallinity index (CRI) along with the intensity of the main crystalline plane (002) and the amorphous fraction was calculated using the intensity value at 18° of 2θ for amorphous fraction and maximum intensity of (002) plane at 22° of 2θ for crystalline fraction [210]. Data points of experimental X-ray diffraction patterns of raw and pretreated areca nut husk was illustrated in Figure 6.

3.2.10. Zeta-Potential Analysis

The zeta potential of each biomass sample was examined using Zetasizer Nano ZS (Model No.: Delsa Nano C; Make: M/s Beckman Coulter, Swtizerland). The instrument was set to measure the Zeta Potential and particle size analysis (0.6 nm to 7.0 micron) with forward 15º and back scatter 165º**.** Phase analysis light scattering technique was used for the measurement of zeta potential of biomass.

The titration unit was associated with a sample compartment, which was linked with a capillary system, and peristaltic pump. 0.1 M NaOH and 0.1 M sulphuric acid solutions were used for the titration of biomass from pH value 7.5 to 2.5 under steady stirring. Freshly prepared biomass samples were suspended in water and filtered using 0.45 μm PVDF filter followed by titration. All the analysis was performed using biomass solution with a concentration of 0.5 gL^{-1}.

3.2.11. Proximate Analysis

The principle steps of this analysis were precisely determined by the American Society for Testing and Materials in addition to desirable level of error among different other laboratories. Proximate analysis provides idea about the quality of agricultural bio-waste. This is a set of methods to know the information about the content of moisture, volatile matter, ash, and fixed carbon.

3.2.12. Moisture Content

The moisture content was measured by ASTM E871 – 82 technique. Calculated amount of sample (1 g) was kept in a crucible and dried in oven for 5 h at 105 ± 2 ^{o}C. Analytical balance was used to measure the initial and final moisture content of the biomass. This procedure was repeated until constant weight was obtained. Moisture content was determined by the Equation 1.

$$\textbf{\textit{Moisture (\%)}} = \left(\frac{Weight_{sample.as.received} - Weight_{dry.sample}}{Weight_{sample.as.received}} \right) \times 100 \qquad (3.1)$$

3.2.13. Volatile Solid Matter Content

The major benefits of high volatile solid is that it has low ignition temperature and highly reactive in nature. High VM also causes smooth burning of biomass and less unburnt carbon release in the ash and low pollutant emission such as CO [211]. Volatile component of biomass mainly consists of combustible and non-combustible species such as C_2H_2, H_2, CO CH_4 and H_2S (combustible species) and NaOH, SOx, NaCl, and KOH (in combustible species) [212]. VM was estimated by using ASTM E872 – 82. 1.0 g of moisture less biomass sample was placed in a covered crucible or in some other container which stop the oxidation of the carbon residue at 975 ± 5 ^{o}C for 7 minutes. Difference in initial and final weight loss gives the percentage volatile solid and can be calculated by Equation 2.

$$\textbf{\textit{Volatile Solid (\%)}} = \left(\frac{Weight_{Initial} - Weight_{Final}}{Weight_{Initial}} \right) \times 100 \qquad (3.2)$$

3.2.14. Ash and Fixed Carbon Content

Ash and fixed carbon comprise the third and fourth parameters of the proximate analysis. Lower ash containing biomass has greater benefits such as easier biochemical and thermochemical conversion and suffers from less deposition, fouling problems [106]. Ash

content was measured by using ASTM D1102 – 84. 1.0 g of moisture free biomass sample was placed in crucible at 575 ± 5 ^{o}C for 4 h. The exact amount of ash was measured by Equation 3.

$$\textbf{\textit{Ash content (\%)}} = \left(\frac{Weight\ of\ \ Ash\ \ Left}{Weight\ of\ \ Biomass\ taken}\right)\times 100 \qquad (3.3)$$

The low values of fixed carbon have considerable importance for cutting down the CO_2 emission. The fixed carbon content of the biomass was calculated by Equation 4.

$$\textbf{\textit{Fixed Carbon (\%)}} \quad = 100 - \left[MC\ (\%) + VM\ (\%) + Ash\ Content\ (\%)\right] \qquad (3.4)$$

where, MC = Moisture content (%), VM = Volatile Matter (%)

For more accurate result, each analysis was repeated three times, and the mean values are presented in the present study.

3.3. Results and Discussion

3.3.1. Pretreatment

The structure of lignocellulosic biomass is very compact and dense, which is extremely difficult to hydrolyze. Hemicellulose were covalently bonded with lignin and cellulose and hemicellulose was rooted between them [213]. Hydrolysis process get intervene due to formation of mesh like structure. Efficiency of saccharification process indirectly depends on the constituents of areca nut husk such as cellulose, hemicellulose and lignin content. Therefore, compositional analysis of raw and pretreated feedstock husk was performed, which are shown in Table 3.1. Pretreatment causes to change in the concentration of cellulose, hemicellulose and lignin, observed from Table 3.1. A common pattern in compositional changes was observed that there is decrease in hemicellulose and lignin content, while an increase in cellulose content. Approximately 0.55 and 0.79 g/g of solid residue obtained after acid and alkaline pretreatment process respectively. Amount of solid fraction is higher in case of alkaline pretreated residue as compare to acid treated residue. This analysis revealed that there is less conversion of hemicellulose in case of alkaline pretreatment and most of hemicellulosic fraction was remained in it. According to Table 1, acid and alkaline pretreatment causes to increase the amount of cellulose content by 19.45% and 4.66%, respectively. But, parallelly there was reduction in the amount of hemicelluloses

content was observed by 61.7 and 19.43%, for acid and alkaline pretreatment respectively. The pretreatments results reported in the present work is similar to the results reported by other researcher in the literature [214,215].

Table 3.1 Compositional analysis of Areca nut husk feedstock

Sample\Composition	Cellulose	Hemicellulose	Lignin
Raw	43.28 ± 0.4%	29.17 ± 0.3%	12.64 ± 0.1%
Lime Treated	45.30 ± 0.2%	23.50 ± 2%	14.50 ± 0.5%
Acid Treated	51.7 ± 0.6%	11.2 ± 0.1%	19.8 ± 0.3%

3.3.2. Thermogravimetric Analysis (TGA)

TGA was performed to discern the degradation characteristics of raw and pretreated areca nut husk. Derivative thermogravimetric (DTG) and Thermogravimetric (TG) curves of raw biomass, lime treated biomass and acid treated biomass are presented in Figure 3.2 and Figure 3.3. Initial reduction in weight started at 35 °C and continuously increased up to around 200 °C corresponded to the release of moisture as vapor from the surface and the inter molecular hydrogen bonded chemisorbed water. The significant reduction in weight of areca nut husk, lime treated husk and acid treated husk was noticed at around 220 °C, 260 °C and 245 °C respectively which happened due the itemization of glycosidic linkages of cellulose and the thermal depolymerization of hemicelluloses [216,217]. The following stage of degradation was probably due the main binding material lignin which decomposed over a broader temperature range than cellulose and hemicelluloses [218].

The thermogram demonstrated that the degradation of acid treated pulp started at 230 °C and the rate of degradation accomplished most extreme at 360 °C because of the decomposition of cellulose but in the event of lime treated biomass the decomposition began at 200 °C. At 360 °C, highest rate of degradation was observed [219]. The ascent in the beginning temperature of degradation of lime treated pulp was because of the confiscation of non-cellulosic parts which made the cellulose thicker and more compact. This change in the degradation temperature from raw biomass to homogenized was due to the fact that in raw biomass the cellulose were entrenched in the lenient matrix consisting of hemicelluloses, lignin and pectin [220]. These components could form free radicals and may start the degradation effectively. The higher degradation temperature after the chemo-mechanical treatment draws out the enhanced thermal behaviour of biomass.

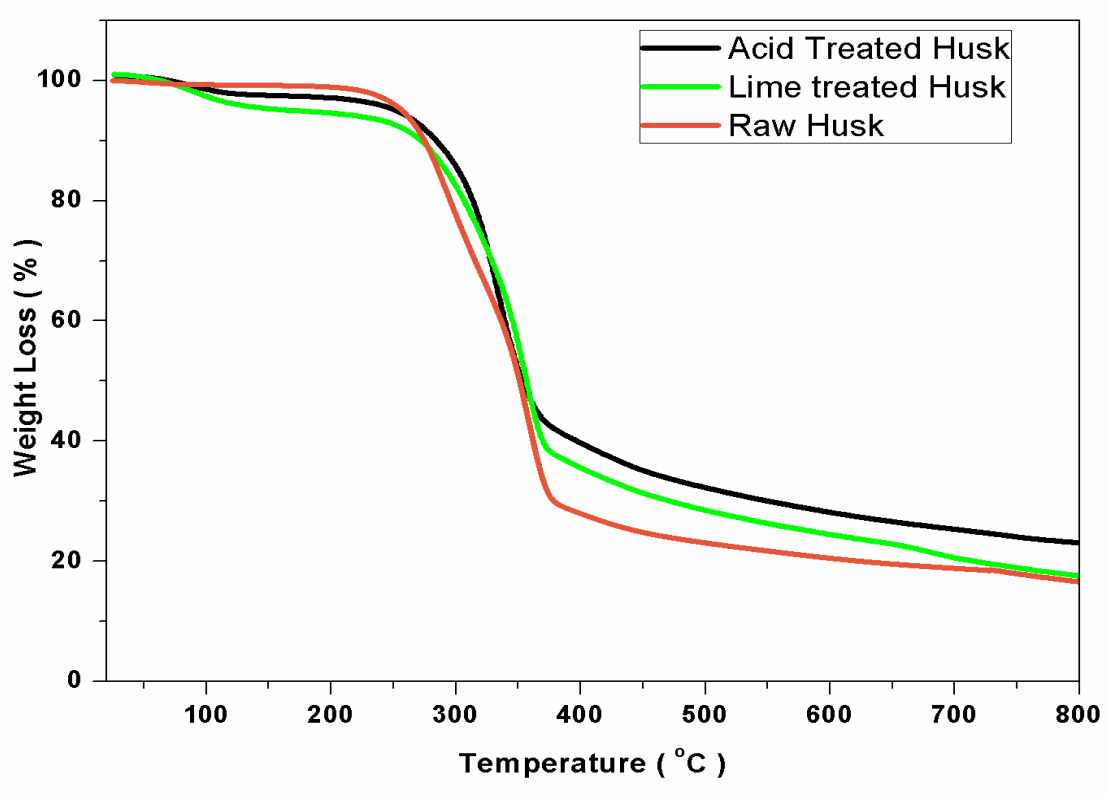

Figure 3.2 Thermogravimetric analysis of biomass samples

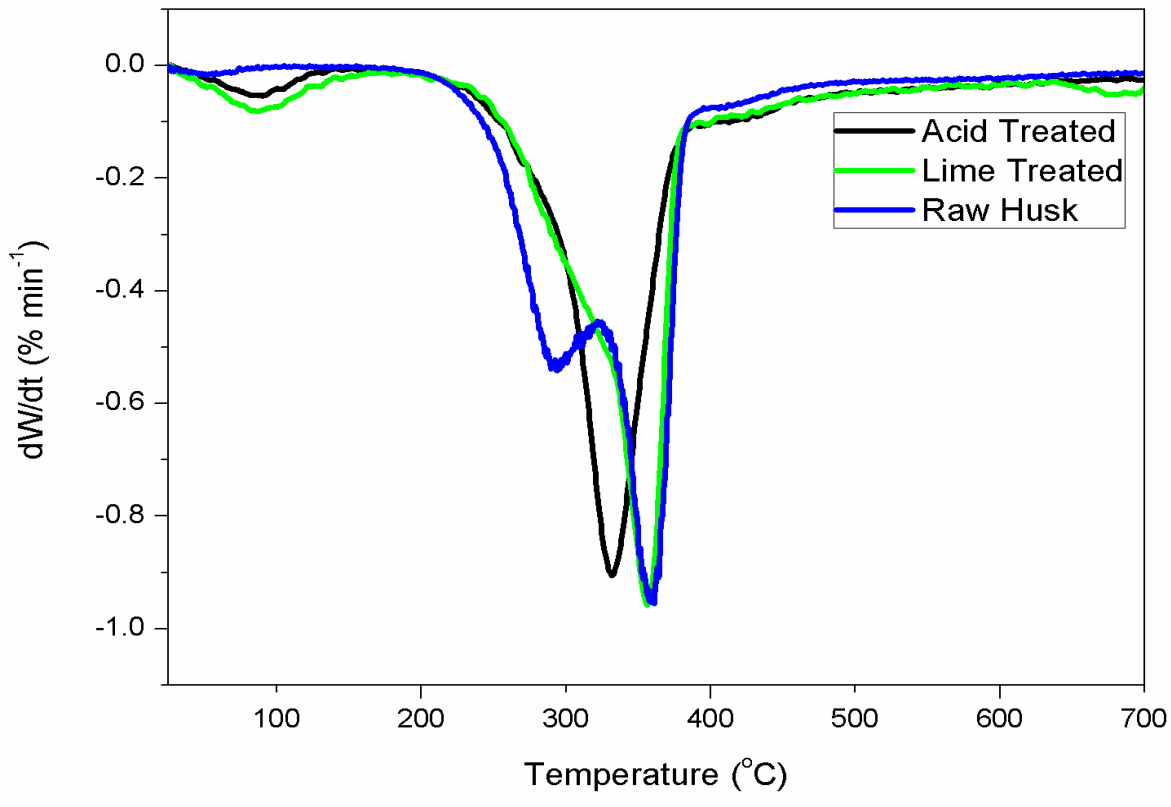

Figure 3.3 Differential thermogravimetric analysis of biomass samples

The DTG of raw biomass showed two major grooves, one at 80 °C, and another groove at around 290 °C – 360 °C and goes on till 600 °C. The grooves in the DTG graphs corresponded to the mass loss at respective zones, which are described below. The first groove was formed due to moisture loss and release of few volatiles having low molecular weight at temperature below 80 °C. The second groove (at the region between 290 °C and 360 °C) indicated weight loss due to burning of cellulose and hemicellulose fiber respectively, the lignin degradation started at around 500 °C [221].

3.3.3. FTIR analysis

Twisting, bending, rotating, vibrational motion connected with various functional groups available in the molecules results in significant information about the functionalities, configurations, molecular structures, exact predictions of the chemical composition and interactions. FTIR spectrum of three different materials such as raw areca nut husk, acid treated areca nut husk and lime treated areca nut husk are shown in Figure 3.4. The lowest transmittance showed lime treated areca husk followed by raw areca nut husk and acid treated areca nut husk in the range between 4000 cm^{-1} - 3300 cm^{-1}. The absorbance peaks were noticed at around 3253 cm^{-1} which were assigned to C-H, O-H stretching vibrations. The sharp peak at 2922 cm^{-1} signified the -C-H bond stretching in alkanes and alkyls group and asymmetric stretching vibration of CH_2 in cellulose, lignin and hemicellulose. The peak at 2348 cm^{-1} assigned to -H-C=O stretching in aldehydes group, 1722 cm^{-1} (C=O stretching in ketones) assigned to the uronic and acetyl ester groups or the ester linkage of the carboxylic group of p-coumaric acid and ferulic acid of hemicellulose. The band at 1509 cm^{-1} and 1243 cm^{-1} corresponded to the aromatic skeletal vibration and methoxyl groups of lignin present throughout the biomass materials [221]. Acid treated areca husk demonstrated the most astounding transmittance among all the three studied samples between the range of 3000 cm^{-1} -200 cm^{-1} due to higher density of hemicelluloses in acid treated areca nut husk fiber than the native and lime treated areca husk [222]. The absorption bands between 1243 cm^{-1} and 1052 cm^{-1} were due to the stretching vibration of C–O group of esters and phenols.

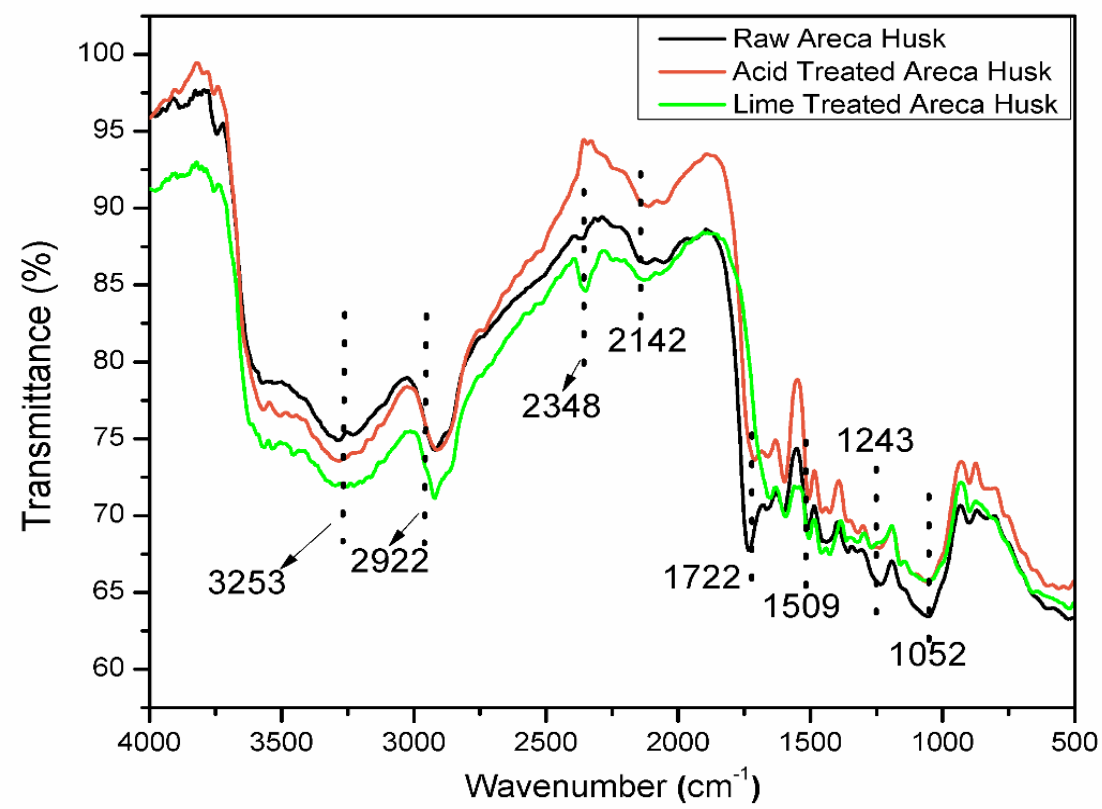

Figure 3.4 FTIR spectra of raw areca husk, acid treated areca husk and lime treated areca husk

Table 3.2 Evaluation of the FTIR spectrum.

Absorption Frequency cm^{-1}	Tentative assignments
3253	C-H, O-H stretching vibration
2922	-C-H stretching in alkanes and alkyls group
2348	-H-C=O stretching in aldehydes group
1722	C=O stretching in ketones
1509	aromatic skeletal vibration and methoxyl
1243	groups of lignin, the stretching vibration of
1052	C–O group of esters and phenols

3.3.4. FESEM analysis

The FESEM micrographs of untreated raw, acid treated and lime treated areca nut husk fibers were shown in Figure 3.5. The pictures (Figure 3.5) revealed the layered structure, irregular arrangement of the molecules, cavities like structure in areca nut husk fibers. FESEM observations indicated that there was a considerable difference in raw areca nut and lime treated areca nut husk fiber. In case of lime treated areca nut husk, fibers showed

hole like structure and agglomerated molecules. After treating with acid and lime, the morphological structures have changed completely due to the destruction or removal of the impurities present in the raw areca nut husk fibers (Figure 3.5 D, E, F and G, H, I).

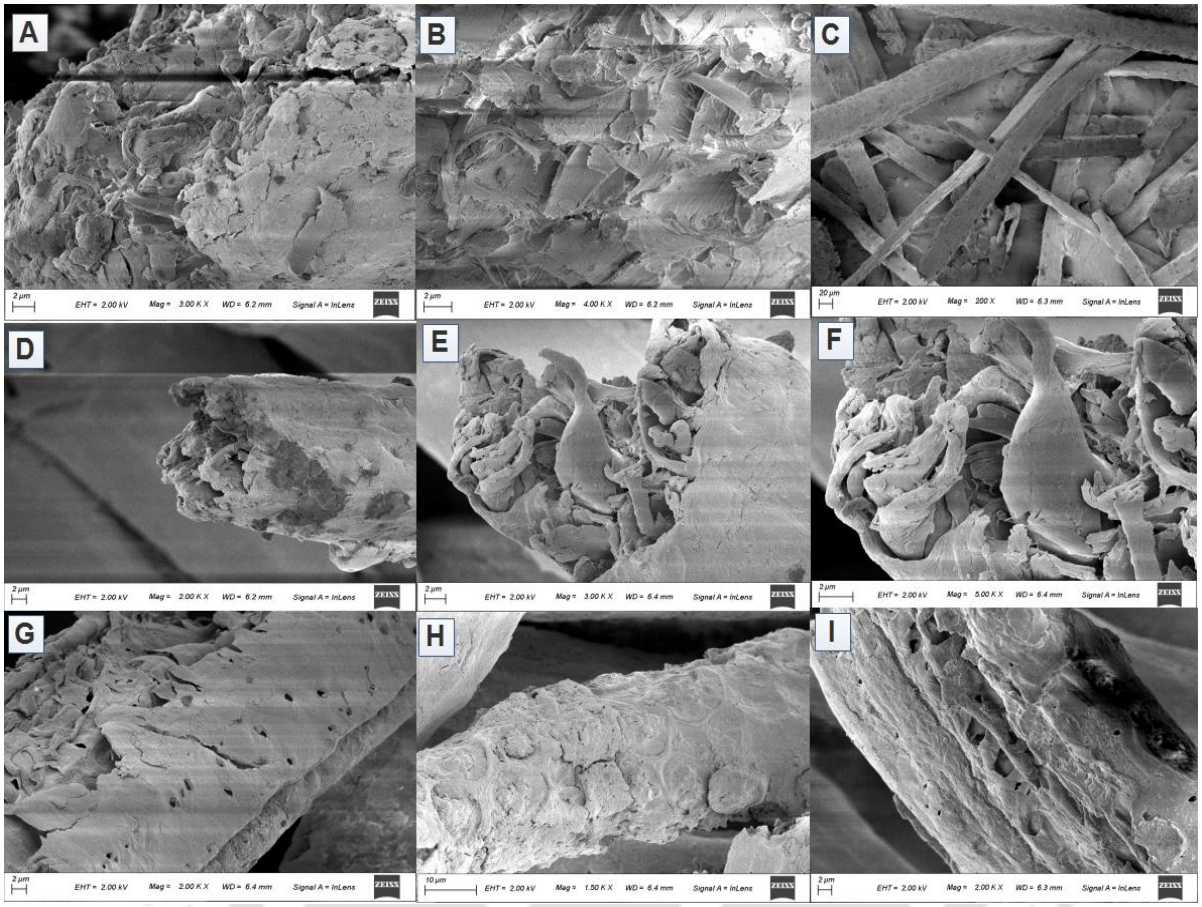

Figure 3.5 SEM micrographs of Raw areca nut (A, B, C), Acid treated areca nut (D, E, F) and Lime treated (G, H, I) at different magnifications

3.3.5. Zeta Potential

The outcome of Zeta potential of raw, acid treated and lime treated Areca nut husk were tabulated in Table 3.3. The Zeta-potential analysis techniques helps to quantify the amount and type of adsorbed or dissociated charged species, hydrophobicity, hydrophilicity present on the surface of lignocellulosic fibers. Hydrophilic polymers like cellulose have the tendency to absorb water which results significant swelling in it. Formation of hydrogen bonds between hydroxyl group of polymer and water molecules observed during the cellulose water interaction. The water permeates into the cellulosic fiber and split the H-bonding between the cellulosic molecules and disengage the polymeric structure [223]. Swelling of polymeric structure causes the decrease the value of zeta potential with time. Figure 3.6 showed that pretreatment process removed the majority of the non-cellulosic compounds. The

accessibility of functional group and active size of the surfaces were increased due to removal of waxes which causes more negative zeta-potential. Alkali treatment causes swelling of the fiber surface, consequently diminishing the zeta-potential of the fiber. The values of zeta potential (Table 3.3) of raw areca nut husk was more negative than acid and lime treated areca nut husk shown in Figure 3.6. The zeta potential of all samples was negatively charged in the acidic and basic medium [224].

Table 3.3 Zeta potential analysis

Samples	Zeta Potential (mV)	Droppler Shift (Hz)
Areca Nut Husk	-36.79	20.76
Acid treated areca nut	-20.57	11.60
Lime treated areca nut husk	-18.59	10.45

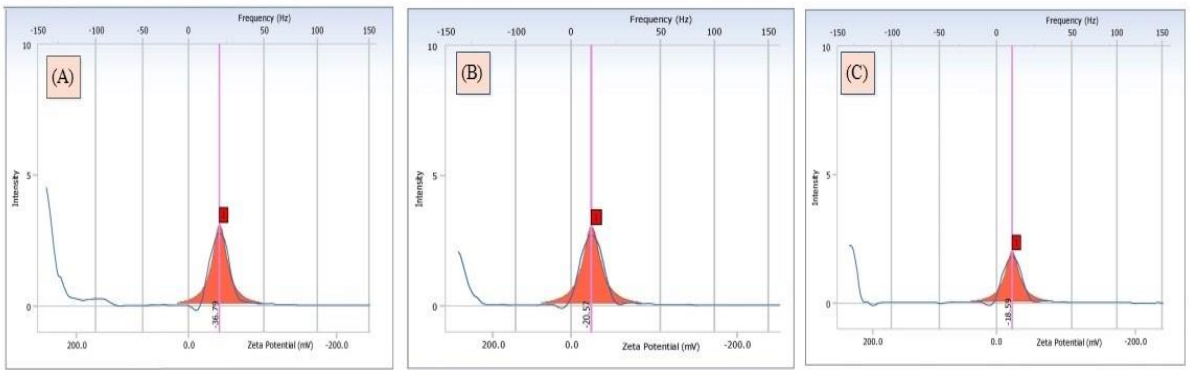

Figure 3.6 Zeta potential analysis: (A) Raw Areca nut Husk (B) Lime treated Areca nut Husk (C) Acid treated Areca nut Husk

3.3.6. Raman Spectra

This procedure used to look at rotational, vibrational and other low-frequency modes in a system. Raman spectroscopy is usually a type of spectral finger print to recognize the electrically symmetrical bond. Raman spectra generally comprises of two imperative groups, in particular, the G band (G for graphite) and D band (D for defect). The Raman spectra of areca nut husk shows the presence of D and G bands at 1300 cm^{-1} and 1585 cm^{-1} respectively (data not shown here). Raman intensity relies upon the change in polarizability of the bond, while the intensity of IR absorption relies upon the change in dipole snapshot of the bond.

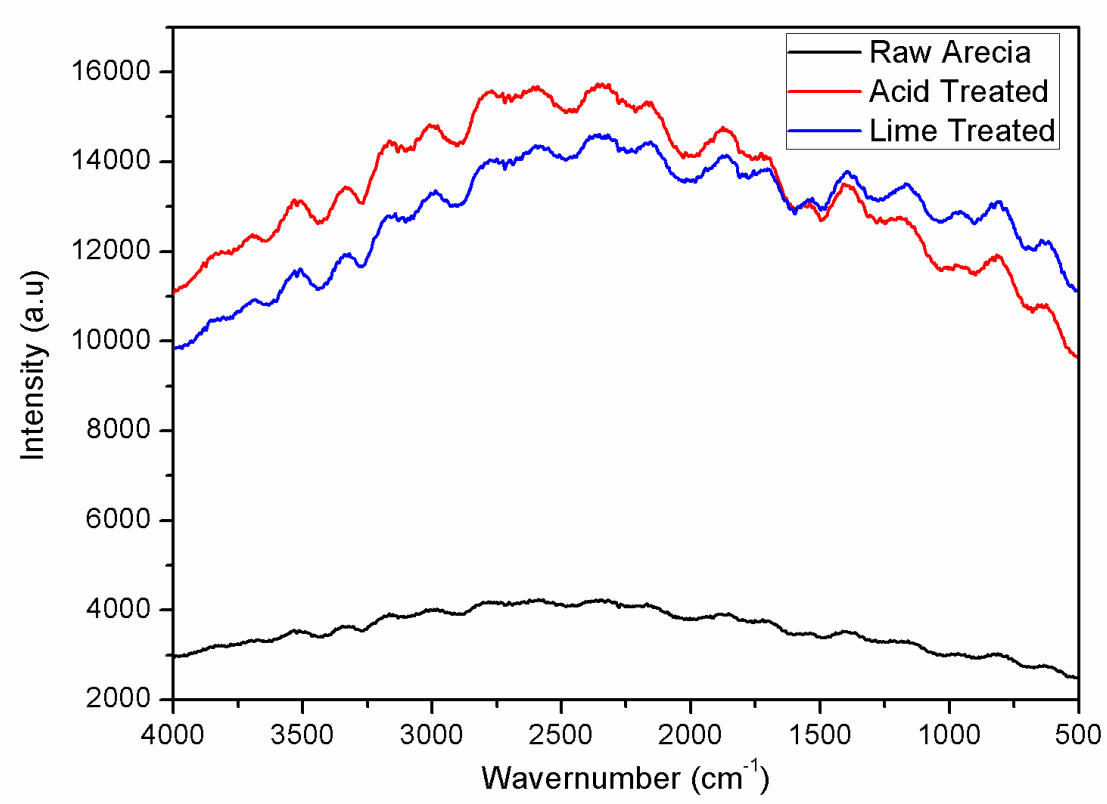

Figure 3.7 Raman spectra of raw areca nut, acid treated areca nut and lime treated areca nut

The Raman spectroscopy of the biomass samples were performed to perceive electrically symmetrical bonds (for example having no dipole minute) present in lignin and other polymers present in areca nut husk fiber. The increment in a particular peak of a Raman spectrum generally indicates that the fraction of substance (might be polymerized material for present case) in the sample contributing to that vibrational mode increased. From Figure 3.7, it was revealed that the intensity of acid treated areca nut was more than lime treated and raw areca nut husk which indicated that pretreatment process increased the vibrational frequency.

3.3.7. XRD

Biomass chain arrangements, internal stress and lattice parameters could be observed by using X-ray powder diffraction. The crystalline structure of areca nut husk can be well considered by XRD patterns. Figure 3.8 showed the XRD patterns of raw, acid treated and lime treated husk. The data conveyed the characteristic peaks at around (2θ =21.7, 22.1 and 22.3). The peaks represent the crystalline structure of areca nut husk [169]. The intensity of peak for raw areca nut husk (CRI=43.38±2.4) was more than acid treated (CRI=37.35±3.2) and lime treated husk (CRI=39.31±3.7) due to the number of planes (corresponding to each peak) exist within the material. The quantity of plane is specifically relative to the intensity of

peak.

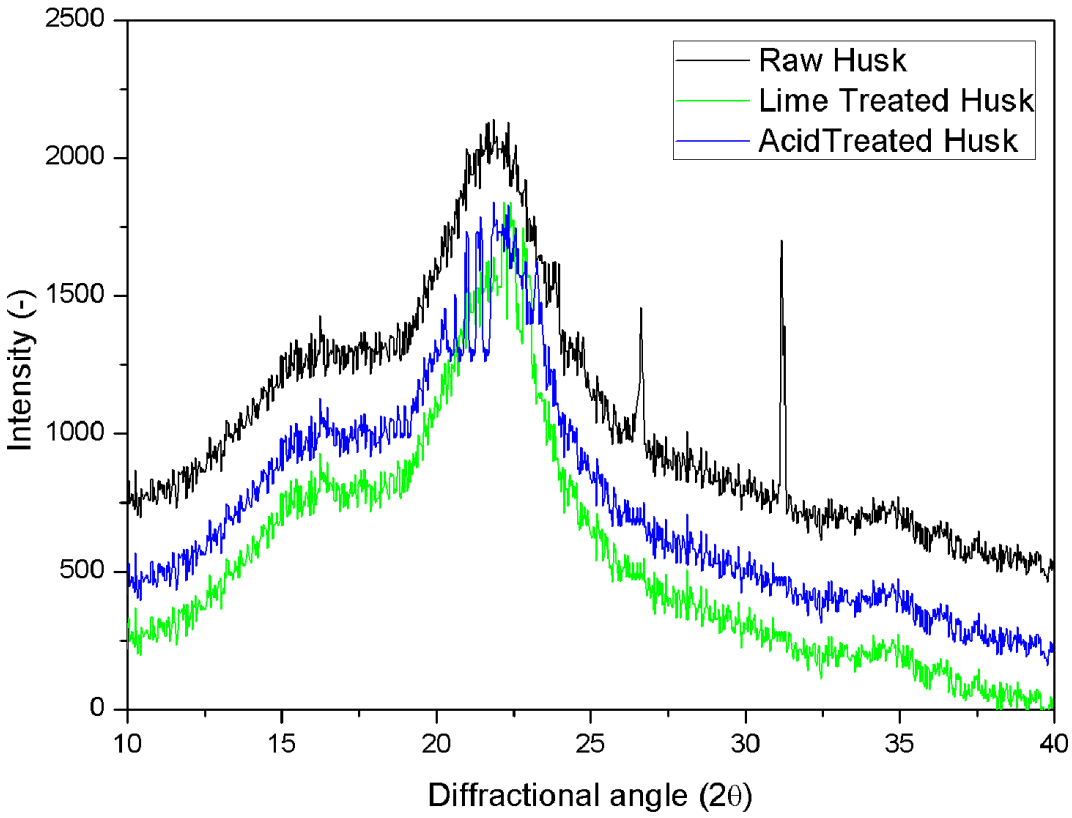

Figure 3.8 XRD pattern of raw areca nut, acid treated areca nut and lime treated areca nut

The homogeneous crystalline arrangement in the all biomass samples shows up due to the configuration of inter and intermolecular –H bonding due to hydroxyl group. The H-bonding limits the free movement of the lignocellulosic chains and adjust near one another in an arranged manner which results crystallinity. In the case of raw fiber, these crystalline spaces were surrounded in the matrix of amorphous components like hemicelluloses, lignin and cellulose along these lines a low crystallinity was observed [220]. It was obvious from the figure that the crystallinity diminished with the successive acid and lime treatments of areca nut husk.

3.3.8. Proximate Analysis

Table 3.4 represents the proximate analysis of areca nut husk biomass. Areca husk contained good amount of cellulose (43.28±0.4 %), hemicellulose (29.17±0.3%) and lignin (12.64±0.1%). High ash content retards the saccharification of biomass samples [225]. From Table 3.1, it was observed that areca nut husk contained about 5 % ash which indicated that the biochemical and thermochemical conversion will be easier. As the temperature of the

system increased from 75 °C, the rate of moisture removal also increased and attained the maximum rate at 105 °C but it was quite harder to eliminate all the moisture content of the material because lignocelluloses are hydrophilic in nature. According to vassilev *et al.* 2015 the moisture content varies in the range of 3% - 63% and can go up to 91% [211]. Higher fixed carbon content in biomass signifies greater the carbon content which is directly related to the heating value.

Table 3.4 Proximate analysis of biomass samples

Biomass	**Moisture (%)**	**Volatile Matter (%)**	**Ash (%)**	**Fixed Carbon (%)**
Areca nut husk	5.6 ± 0.04	80 ± 0.1	5 ± 0.03	9.4 ± 0.05

3.4. Conclusions

The study focused on the pretreatment and characterization of areca nut husk, which is a readily available and inexpensive source of lignocellulosic material in North East India. The findings indicate that this material has great potential for the production of xylose, which can then be further used for the production of value-added chemicals such as xylitol through fermentation. The pretreatment techniques of acid and lime resulted in a reduction in crystallinity index, making the biomass more accessible for saccharification and thus xylose production. These results suggest that areca nut husk could be an important resource for green and sustainable chemical production.

भारतीय प्रौद्योगिकी संस्थान गुवाहाटी
Indian Institute of Technology Guwahati

भारतीय प्रौद्योगिकी संस्थान गुवाहाटी
Indian Institute of Technology Guwahati

Chapter 4

Saccharification of Lignocellulosic biomass for production of fermentable sugar

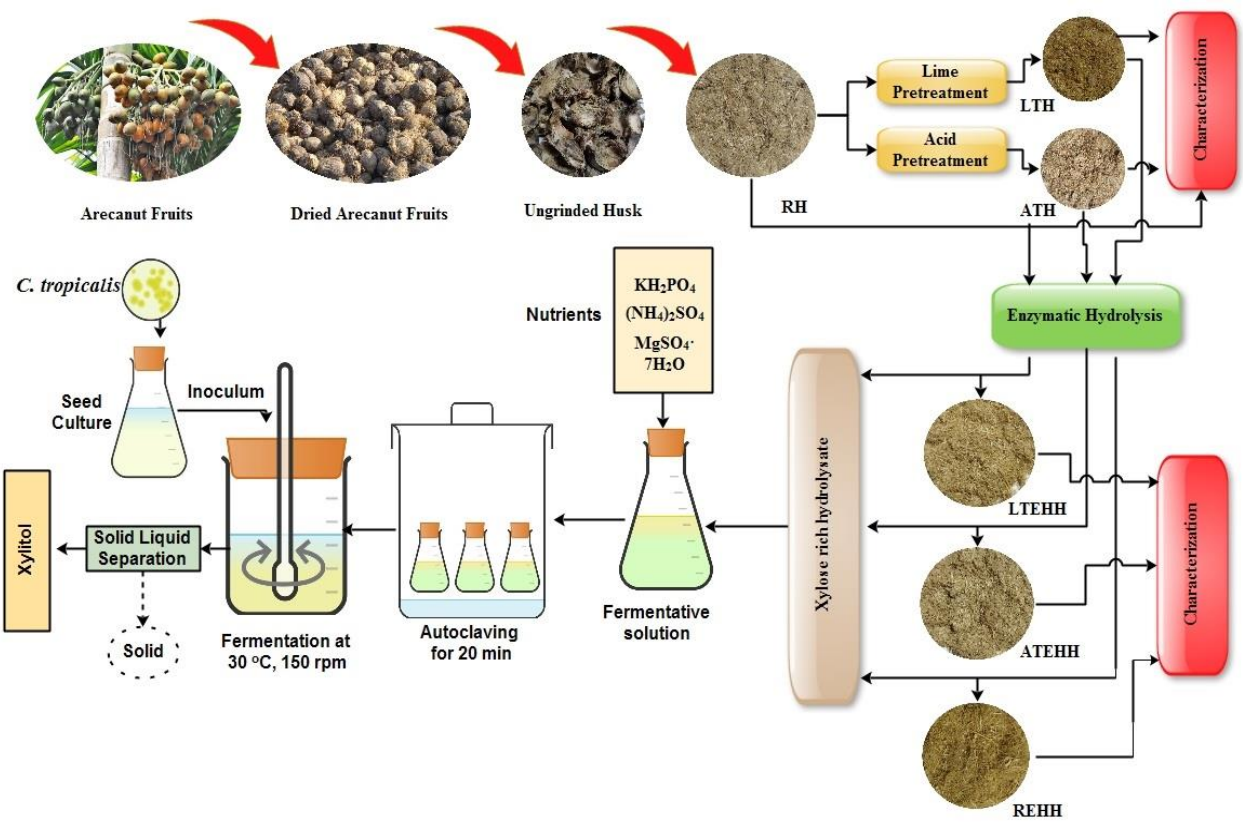

4.1. Overview

Areca nut husk has the potential to produce xylose, which can be used in the production of various biochemicals. However, the lignocellulose nature of the biomass makes it difficult to produce xylose by direct biotransformation or saccharification. To make the biomass more amenable to saccharification, lime and acid pretreatment were conducted. Before the saccharification process, compositional analysis was carried out to determine the initial constituents of the feedstocks. Enzymatic saccharification parameters such as xylanase enzyme loading were varied to improve the enzymatic hydrolysis of the areca nut husk. The highest yield of reducing sugar (90%, 83%, and 15% for ATH, LTH, and RH, respectively) was achieved at an enzyme loading of 15.0 IU/g. Saccharification was carried out at a substrate loading of 2% (w/V), 100 rpm agitation, 30 °C hydrolysis temperature for 12 hours hydrolysis time at pH 4.5 to 5.0. To understand the structural changes in native, pretreated, and saccharified residues, various analytical techniques such as Raman spectroscopy, Zeta potential, Field Emission Scanning Electron Microscopy (FESEM), X-Ray Diffraction (XRD), Thermogravimetric Analysis (TGA), and Fourier Transform Infrared Spectroscopy (FTIR) were performed. Structural analysis showed that during saccharification, a major portion of partial crystalline and amorphous cellulose in the areca nut husk biomass was hydrolyzed. However, it also resulted in the removal of amorphous substances, disruption of crystalline structure, and the transformation of the crystalline zone into an amorphous zone.

4.2. Materials and methodology

4.2.1. Raw materials and Chemicals

Areca nut husk were collected from nearby market of IIT Guwahati (Assam, India). Analytical grade chemicals were used in the present study and purchased from Sigma Aldrich. All the analysis was performed in triplicate for maintaining the accuracy in results.

4.2.2. Biomass pretreatment

Areca nut husk were manually pilled and separated from fruit. Fibrous husk was washed with running water to remove freely attached impurities followed by drying for overnight at 70 °C to eliminate the moisture present in the sample. The dried husk was finely grinded to obtain the husk powder and sieved (mesh size-BSS 30) to collect homogeneous particles less than 1 mm in size and kept in an air locked container for further application.

Lime pretreatment was performed in a 250 mL screw cap bottle by slurring 20% (w/w) lime with 80% (w/w) areca nut husk substrate in the desired ratio with water. Prepared

slurryed solution were kept in an orbital shaker at 30 °C for 7 days. On completion seven days, separation of solid residue from mixture was performed followed by washing with running water until the pH of the slurry was reached about 7.0. Biomass residue was dried for overnight in an oven at 60 °C and kept in an air locked container for further use [6].

Dilute acid (H_2SO_4) hydrolysis of areca nut husk was performed in a 250 mL screw cap bottle comprising 1% (w/V) of areca nut husk biomass loaded with 1.2% (v/v) H_2SO_4. Solution was autoclaved at 120 °C for 20 min. Acid hydrolyzed resultant solution was kept at room temperature for cooling. Finally, separation of solid residue was performed from resultant solution by vacuum filter and washed with running water until approximately pH 7 was achieved. Resultant residue was dried for overnight in an oven at 60 °C and stored in an air locked tube for further use [6].

4.2.3. Enzymes and Enzyme Activity Assays

The enzymes used were commercial Xylanase from Trichoderma viride and were procured from Sigma Aldrich, India. Commercially available xylanase enzyme activity was measured using CMC (Carboxy Methyl Cellulose) or birchwood xylan as substrates for xylanase and cellulase activity, respectively. Dinitrosalicylic acid method (DNS) method was used to monitor rate of polymer hydrolysis, which was measured by estimating the reducing sugars produced by enzymatic activity at 540 nm [226].

4.2.4. Optimization of saccharification process

The saccharification process was optimized by varying the xylanase enzyme concentration and analyzing the reaction at different time intervals. To conduct hydrolysis, 2% (w/V) of raw and treated (both lime and acid) solid biomass samples were mixed with sodium citrate buffer (pH 4.8) solution. The xylanase enzyme was loaded at different concentrations (2.5, 5.0, 10.0, and 15.0 IU/g). The reactions were carried out at 30 °C, 150 rpm, and between pH 4.5-5.0. Duplicate samples were taken at desired time intervals, and the sample solutions were kept at 80 °C for 10 minutes before further analysis. The hydrolysis process was optimized by monitoring the reducing sugar yield with respect to time and enzyme concentration. The optimal conditions for saccharification were determined based on the highest yield of reducing sugars obtained. The results showed that the highest yield of reducing sugars (90%, 83%, and 15%) were achieved for Acid Treated Husk (ATH), Lime Treated Husk (LTH), and Raw Husk (RH), respectively, at an enzyme loading of 15.0 IU/g. The xylose yield was calculated with the help of the following equation,

$$Yield\ (\%) = \frac{Xylose\ amount\ after\ enzymatic\ hydrolysis}{Theoretical\ xylose\ amount\ in\ the\ feedstock} \times 100 \quad (4.1)$$

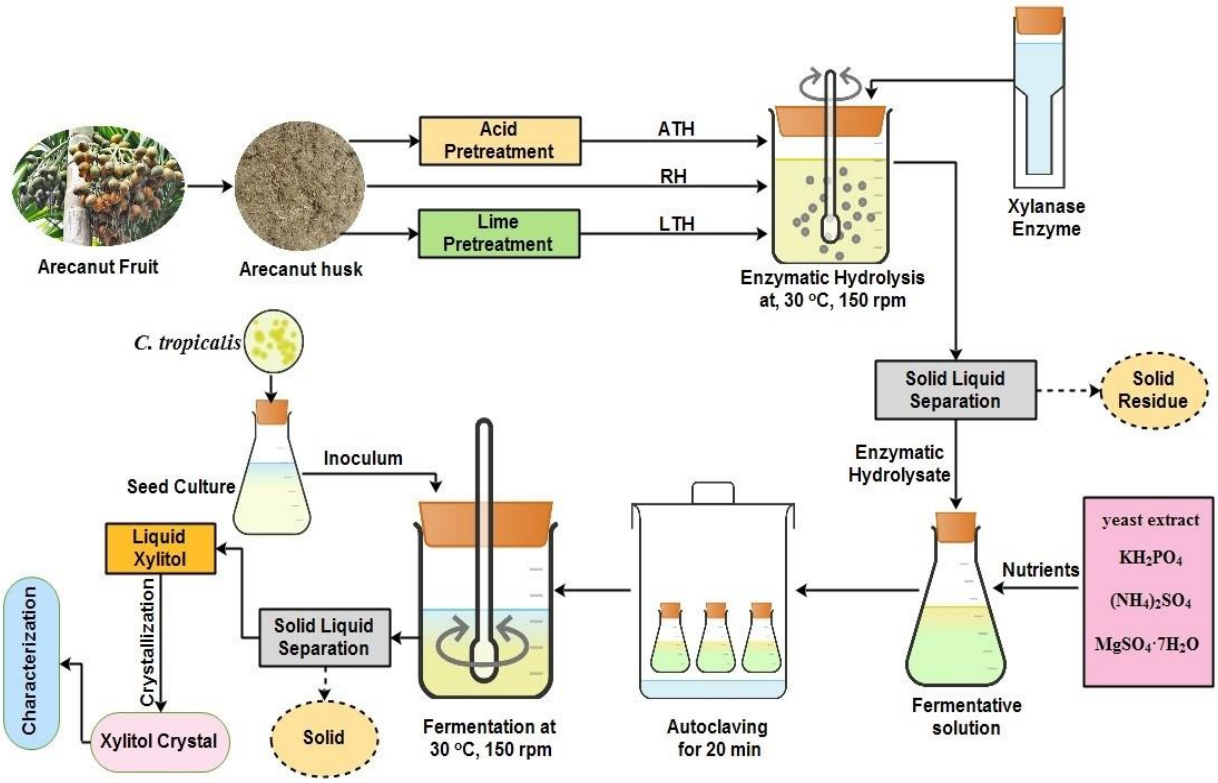

Figure 4.1 Complete methodology used for saccharification to obtain xylose and to convert it to xylitol

4.2.5. Thermal stability/degradation

TGA was performed with the help of thermogravimetric analyzer instrument (Hitachi, TA7000) under high purity nitrogen (About 99%) at heating rate of 10 °C min^{-1} with 50 mL min^{-1} of nitrogen low rate. Sample was kept in open platinum pan in the range of 5 mg to 10 mg and the temperature was ranged between ambient to 650 °C. The decomposition temperature was also analyzed by measuring the first derivative (T_{der}) of the TGA scan at the highest temperature.

4.2.6. Structural characterization of biomass

4.2.6.1. Raman spectra analysis

Raman spectra was analysed by using a Raman Laser Micro system (JobinVyon, Model LabRam HR spectrometer). All sample such as raw (Raw husk (RH)), pretreated (Lime treated husk (LTH), Acid treated husk (ATH)) and saccharified (Raw enzymatic hydrolysis husk (REHH), Lime treated enzymatic hydrolysis husk (LTEHH) and Acid treated enzymatic hydrolysis husk (ATEHH)) solid biomass were scanned in the range of 4000 cm^{-1}

to 500 cm^{-1}. The analysis was performed using a low power (10 mW) near-infrared diode laser that emits a wavelength of 785 nm with an incident power of 5 mW at room temperature. All spectra were scanned for 20 s each and performed in triplicate.

4.2.6.2. FTIR analysis

FTIR spectrum of raw, pretreated and saccharified samples were examined using an FTIR analyzer (Model: Perkin Elmer Spectrum). FTIR analysis was performed in the scanning range of 4000 cm^{-1} to 500 cm^{-1}. All samples were properly mixed with potassium bromide (KBr) in desired ratio before pelleting. Pelleted samples were further analysed in the range 4000 cm^{-1} to 500 cm^{-1}.

4.2.7. Field Emission Scanning electron microscopy (FESEM) analysis

Shape and surface topography of raw, pretreated and saccharified biomass were analysed by field emission scanning electron microscope (Gemini 500 FESEM). The device was equipped with a LaB6 field emission electron gun and three types of detectors: InLens, SE2 and ESB. Analysis was conducted by fixing the sample on an aluminium stub (G301, Agar Scientific, UK) through two-way carbon tape (G3347N, Agar Scientific, UK). Electrical conductivity of the sample surface was increased by spraying the chromium under argon vacuum with the help of sputter coater (Edwards S 150B sputter coater, layer thickness 12 nm). This analysis was conducted with a probe current of 10 mA and acceleration voltage of 5kV. Different magnification was used for taking the photographs under utmost conditions.

4.2.8. X-ray diffraction analysis (XRD)

XRD study of raw, pretreated and saccharified samples were performed in broad angle X-ray diffractometer (9KW Powder X-Ray Diffraction System, Make: Rigaku Technologies, JAPAN, Model: Smartlab). Samples (raw, pretreated and saccharified) were examined under plateau conditions by placing sample in sample holder. X-ray radiation were generated by passing 40 mA current and 40 kV voltage through instrument. Scanning spectrum was fixed in the range of 7–40° with residence time of 1 s / 0.02° and step size of 0.02°. Fig. 4 shows the XRD analysis of raw (RH)), pretreated (LTH, ATH) and saccharified (REHH, LTEHH and ATEHH) solid biomass. Crystallinity index (CrI) of the amorphous fraction and the main crystalline plane were determined by using the following equation.

$$Crystallinity\ Index = \frac{I_{cr}}{I_{cr} + I_{am}} \times 100 \qquad (4.2)$$

Where, I_{am} = Area of all amorphous peaks and I_{cr} = Area of all Crystalline peaks

4.2.9. Zeta potential analysis

The zeta potential of raw, pretreated and saccharified samples were analyzed with the help of Zetasizer Nano ZS (brand: M / s Beckman Coulter, Switzerland; Model Number: Delsa Nano C). All samples were analyzed in water at 25 °C in triplicate. Measurement of zeta potential and particle size (0.6 nm to 7.0 microns) was conducted by setting the instrument 15° forward and 165° backscatter. Zeta potential of the sample was measured by phase analysis light scattering technology. The titration unit was connected to the sample compartment and also coupled with the peristaltic pump and capillary system. Biomass titrations from pH 7.5 to 2.5 were performed using 0.1M NaOH and 0.1M H_2SO_4 solutions with constant agitation. The freshly prepared biomass sample was appropriately diluted, sonicated in water for 10 minutes, filtered using a, 0.45 µm (Polyvinylidene difluoride) filter and then titrated. All analyses were conducted in concentration of 0.5 g/L of biomass sample.

4.2.10. Microorganism and inoculum preparation

Candida tropicalis (MTCC 6192) culture was procured from Microbial Type Culture Collection and GeneBank (MTCC), India and maintained at 4 °C on YPD (Yeast Extract, Peptone and Dextrose) agar medium. Microorganisms were subcultured in every 15 days. The composition of the media used in this study as follows yeast extract 10.0 (g/L), peptone 20.0 (g/L) and dextrose anhydrous (glucose) 20.0 (g/L). 1N HCL solution was used to maintain the pH of the medium about 5.0. Cell culture process was conducted in a 250 mL Erlenmeyer flask (50 mL of medium) on a rotary platform shaker for 48 hours at 30 °C with 150 rpm [227,228].

4.2.11. Cell Dry Weight Measurements

Dry weight measurements were made by pipetting 5 mL of a well-mixed broth sample into a dry centrifuge tube. Cells from broth was separated by performing centrifugation for 5 minutes at 10,000 g. Separate the cell paste from broth by carefully scrapping the clear broth. Subsequently, separate the cell pastes from the centrifuge tube and kept in a weighing pan. Dry the cell paste for overnight in an oven at 60 ºC. Calculation of dry cell weight was performed by using following equation [229].

$$Dry\,cell\ weight\ (g/mL) = \frac{CW_3 - CW_2}{V_1} \tag{4.3}$$

Where: CW_3 = Weight of the sample including blank tube, CW_2 = Weight of the blank tube, V_1 = Volume of culture sample

4.2.12. Microbial fermentation

Xylitol production was carried out by preparing fermentative media (as shown in Figure 4.1) from REH, LTEH, ATEH and SSFH (synthetic solution fermentative hydrolysate), having initial xylose concentration (g/L) about 2.5, 5.9, 3.8 and 7.0, respectively. Xylose concentration act as main sugar substrate in the hydrolysate and was supplemented with yeast extract, 10 g/L; $(NH_4)_2SO_4$, 5 g/L; KH_2PO_4, 15 g/L; and $MgSO_4 \cdot 7H_2O$, 1 g/L. pH of the fermentative medium was kept between 4.5 to 5.0. About 4.0% (v/v) yeast strain culture were trasferred (inoculated) into the fermentation medium prepared from different enzymatic hydrolysate [228]. Fermentation was carried out at 30 ± 1 °C for 90 h at 200 rpm. Samples were withdrawn after every 6 h of time interval and stored in cold place after centrifugation for 15 min, 10,000 rpm.

4.2.13. Fluorescence Microscopy

Candida cells were visualized under Inverted Microscope with Fluorescence (Nikon, Ti-S with camera, Model: DS-Fi2-U3). Stock solution of Methylene Blue (MB) was prepared For fluorescent labeling. Prepared solution was diluted two fold followed by filtration by passing through a 0.22 µm membrane filter (MILLEX GP 0.22 µm; Merck Millipore Ltd., India). A 2.5 µL sample volume was pipetted onto a glass slide (VWR, India) and mixed with 2.5 µL filtered MB solution to a final concentration of 25 µg/mL. Imaging was performed for RFH (raw fermentative hydrolysate), LTFH (lime treated ferentative hydrolysate), ATFH (Acid treated fermentative hydrolyste) and SSFH (synthetic solution fermentative hydrolysate) samples under constant laser irradiation.

4.2.14. High-Performance Liquid Chromatography (HPLC) Analysis

Identification and quantitative measurment of various components such as, glucose, xylose and xylitol were performed by HPLC using an AMINEX ion exchange column (BioRad, HPX87C, Richmond) and a refractometer (BioRad, 1770, Richmond). A 5 mM sulfuric acid (H_2SO_4) - aqueous solution was used for the analysis as a mobile phase media. The analysis was performed on 0.6 mL min^{-1} flow rate at 60 °C.

4.3. Results and discussion

4.3.1. Enzymatic Hydrolysis

Reducing sugars obtained during enzymatic hydrolysis of raw (RH) and pretreated (LTH and ATH) biomass feedstocks exposed to various doses of xylanase enzyme load was shown in Figure 4.2. Treated biomass shows more efficient to enzymatic hydrolysis as compare to untreated (raw) biomass, when exposed to various dose of enzyme loading. After completion of saccharification process, it was observed that the yield of reducing sugar was higher for ATH as compared to all other feedstocks. It was also observed that higher for both low (2.0 IU/g of biomass) and high (15 IU/g of biomass) enzyme loadings. Yields of reducing sugar for RW, LTH, and ATH were 52.62%, 135.51%, and 126.16% higher at 15 IU/g biomass than at 2.0 IU/g biomass, loaded with xylanase enzyme. But, with an enzyme load of 2.0 IU/g biomass, the reducing sugar yields of ATH were 293.96% and 12.80% higher than the RW and LTH respectively. On the other hand, with an enzyme load of 15.0 IU/g, the yields of reducing sugars were 438.79% and 8.32% for RW and LTH, respectively. It is interesting to note that as the enzyme load increased from 5.0 IU/g to 10 IU/g, a dramatic increase in reducing sugars yield were observed for both LTH and ATH. However, in the case of RW, when the enzyme load was changed from 5.0 IU/g to 10 IU/g, only 6.91% of the reducing sugar content was released. This result highlights the role of pretreatment before enzymatic hydrolysis.

Enzymatic hydrolysis was positively affected by the acidic and alkaline pretreatment of biomass. This may be as a result of structural modification in the lignocellulosic polymer lattice due to huge energy irradiation. Similar results have been previously reported by other researcher for the other cellulosic materials [230]. Chosdu et al., 1993 reported that Enzymatic hydrolysis of corn stalk biomass treated with alkaline solution which yields 20% higher xylose in comparison with the untreated, after hydrolysis 48 h. However, Bak et al., 2009 performed similar type of work and reported that about 30% increase in xylose yield was absorbed when alkaline pretreated rice straw feedstocks were hydrolyzed enzymatically after 132 h of hydrolysis. In this research work, increase in reducing sugar yield was observed about 483% and 438% at 30 IU/g of enzyme loading for acid and lime treated sample as compare to raw sample. In the present research work, hydrolysis was performed by using xylanase enzyme and its efficiency may be improved by using more efficient enzyme. It also depends on the enzyme preparations used and load factors. Hydrolysis can be further enhanced by using pretreated cellulosic materials with an efficient xylanase enzyme system.

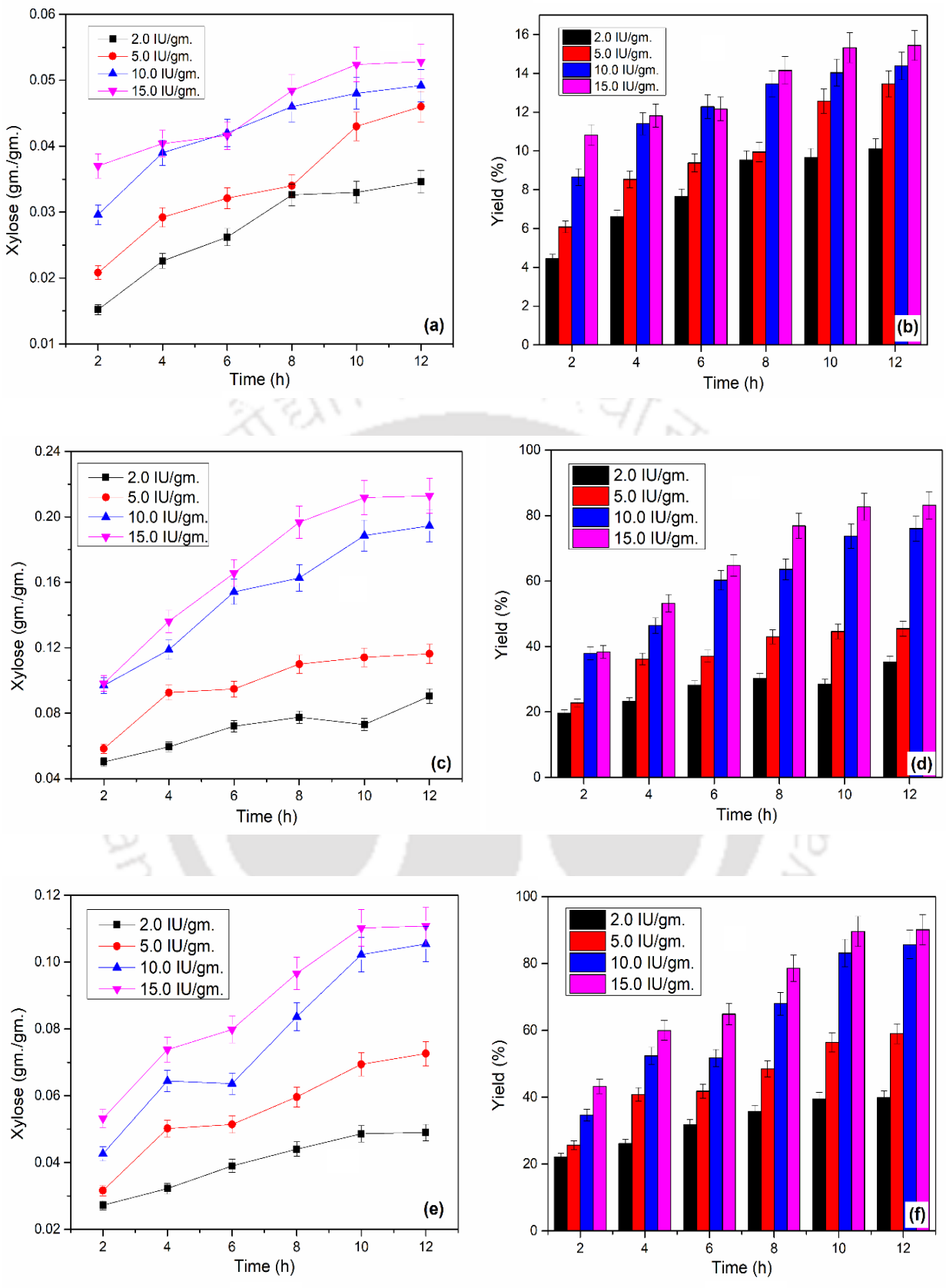

Figure 4.2 Xylose concentration and Yield during the enzymatic hydrolysis of: (A) RH, (B) LTH, (C) ATH, (D) REHH, (E) LTEHH, (F) ATEHH

4.3.2. Characterization of saccharified biomass

4.3.2.1. Thermogravimetric analysis (TGA)

The TG and DTG curves of raw, pretreated and saccharified residue are illustrated in Figure 4.3. TGA thermograms revealed that an initial weight loss occurs at room temperature to 100 °C in RH, LTH, ATH, REHH, LTEHH and ATEHH. This loss is mainly due to removal of the free and bound water molecules [6]. Due to a variation in its chemical structure, it generally decomposes at different temperature. Weight loss occurred between 100 °C to 250 °C is due breakdown of glycosidic bonds of cellulose and depolymerisation of the hemicellulose [233]. Lignin and cellulose have higher thermal stability as compared to hemicellulose [217]. Various saccharides (such as xylose, glucose, galactose, etc.) combined together to form hemicellulose. It forms a random amorphous structure having huge branches. This branch can be easily removed from the main steam to degrade to volatile evolving out (such as CO, CO_2 etc.) at low temperatures. Cellulose degradation was noted in the temperature range of 250 °C to 400 °C. Among cellulose, hemicellulose and lignin, the decomposition of lignin is quite difficult. Decomposition of lignin started from ambient temperature to 800 °C and its degradation happened throughout whole temperature [6,225,234].

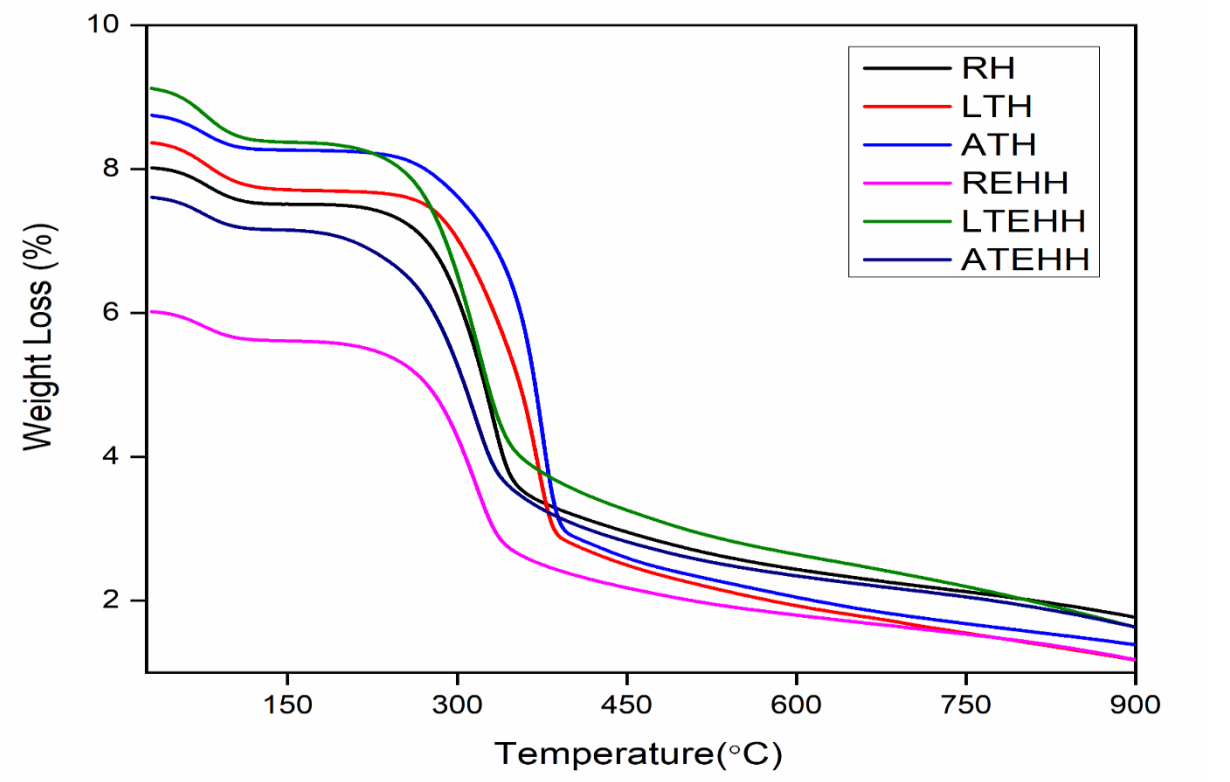

Figure 4.3 TGA curve of: (A) RH, (B) LTH, (C) ATH, (D) REHH, (E) LTEHH, (F) ATEHH

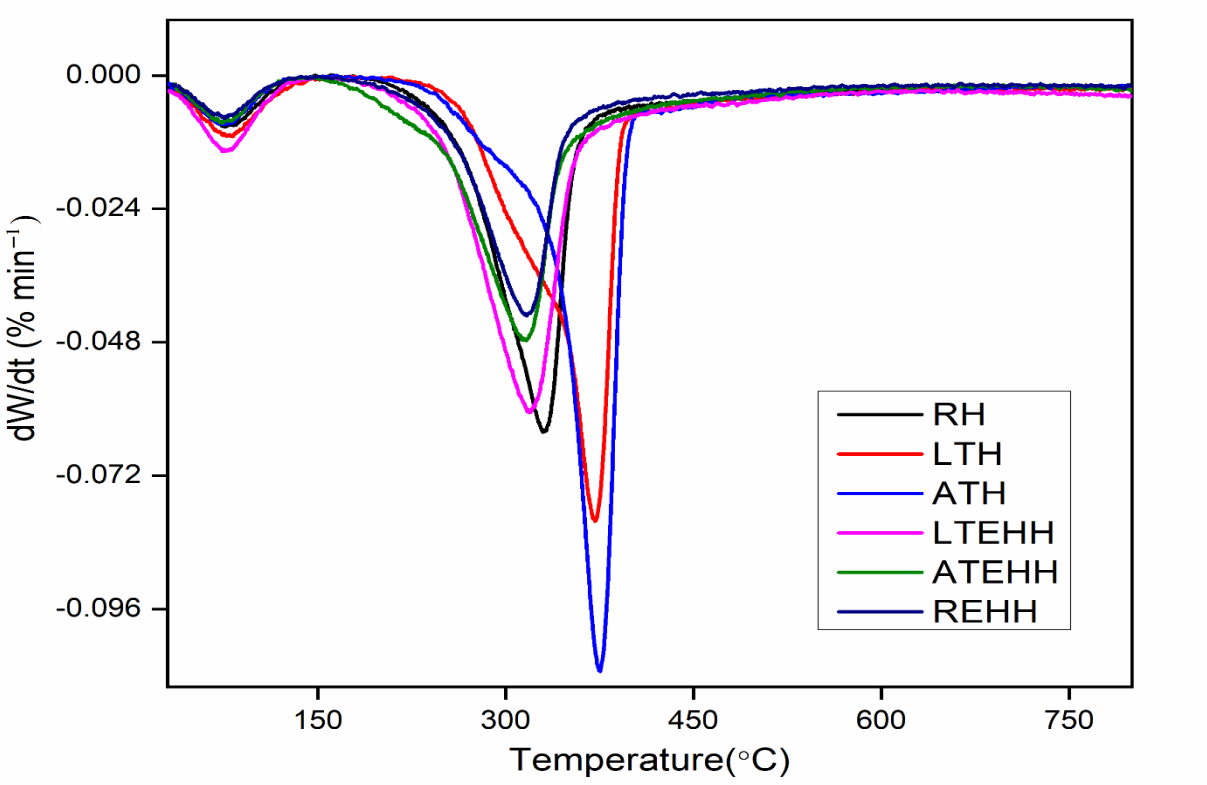

Figure 4.4 DTG curve of: (A) RH, (B) LTH, (C) ATH, (D) REHH, (E) LTEHH, (F) ATEHH

DTG analysis is the first derivative of thermogravimetric curve. DTG analysis for raw, pretreated and saccharified samples were analyzed and summarized in Figure 4.4. In this analysis, one major peak was observed for all sample in the temperature range of 35 °C to 150 °C. This loss is most probably associated with the evaporation of water and other volatile components [235]. Similar type of weight loss pattern was observed for all enzymatic hydrolyzed solid residue such as REHH, LTEHH and ATEHH. The decomposition peak at around 320 °C for all saccharified residue shows the degradation of the hemicellulose and α-cellulose component of the fibers. Sharp decrease in weight occurred between 200 °C to 400 °C, this decrease is most probably due to the decomposition of cellulose. At 400 °C almost all cellulose content was pyrolyzed [236]. After analysis of DTG curve, it was observed that there is a shift in the degradation curve of saccharified residue from raw and pretreated husk. The saccharified residue showed little bit lower degradation temperature which is around 50 °C lower than raw and pretreated. Enzymatic hydrolysis confirms that the saccharified residue has lower decomposition temperature because of decrease in molecular weight and crystallinity of residue [225,235].

4.3.2.2. XRD Analysis

XRD diffractogram of the raw, pretreated and saccharified residue showed peaks at 2θ, which represents amorphous and crystalline nature (Figure 4.5). Cellulosic biomass generally showed crystalline nature together with lignin and hemicellulose components. Hydrogen bond interactions and vander waal forces between the molecules are mainly accountable for the crystalline nature of the cellulose [235]. The XRD pattern of the resulting cellulosic biomass such as RH, LTH and ATH represents low and diffuse peaks at 15.94°, 15.66, 15.78 and a sharp peak at 22.02°, 22.12, 22.2. Saccharified residue such as REHH, LTEHH and ATEHH show low and diffuse peaks at 16.54°, 16.24, 15.94 and a sharp peak at 22.22°, 22.26, 22.36, representing the crystalline nature of typical cellulose [236]. Other researcher reported similar results in the literature [237]. Crystallinity percentage [CrI (%)] of these samples was observed to be 64.72, 61.91 and 54.81% for RH, LTH and ATH and 62.07, 60.20 and 51.37 for REHH, LTEHH and ATEHH respectively, reported in Table 4.1. This analysis revealed that the crystallinity of cellulose decreases after enzymatic hydrolysis. This reduction was may be due the disruption of crystalline structure which results the transformation of crystalline zone into amorphous zone during enzymatic hydrolysis. Higher reduction in crystallinity index was observed in the case of ATEHH. Higher reduction in CrI in case of ATEHH may be due to the lower cellulose and hemicellulose content in ATEHH feedstocks before hydrolysis [236,238]. Due to this, saccharification effect was more intense and cause huge disruption of crystalline regions in case ATEHH as compare to other feedstocks. The results are correlating from TGA analysis that Lower crystallinity of cellulose is most probably responsible for low degradation temperature in TGA. As a result of enzymatic hydrolysis, the structure of biomass was partially disrupted leading to the release of significant amount of xylose.

Table 4.1 Crystallinity index measured by X-ray diffraction (XRD)

Sr. No.	Name of Samples	2θ (main peaks)	Crystallinity index (%)
1	RH	22.36	64.72
2	LTH	22.06	61.91
3	ATH	22.44	54.81
4	REHH	22.34	62.07
5	LTEHH	22.02	61.20
6	ATEHH	22.42	52.37

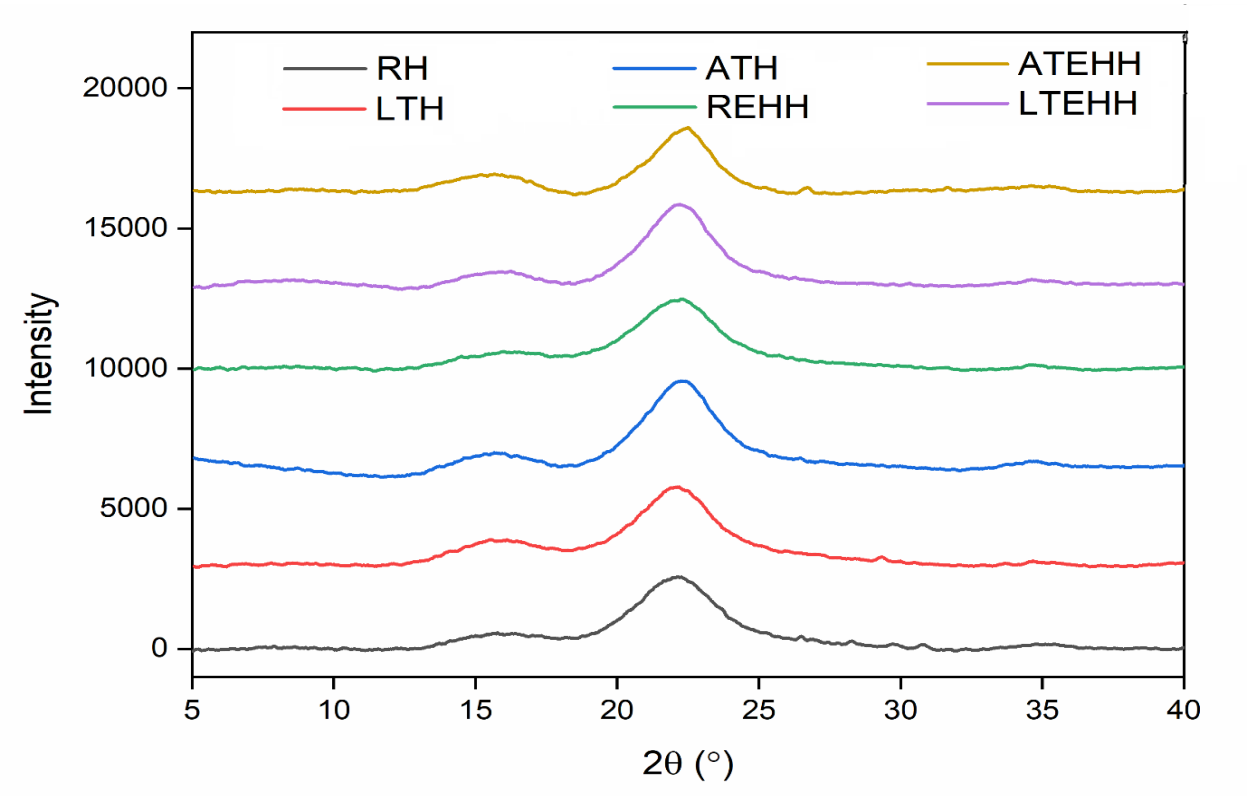

Figure 4.5 XRD curve of: (A) RH, (B) LTH, (C) ATH, (D) REHH, (E) LTEHH, (F) ATEHH

4.3.2.3. Raman Analysis

Raman spectroscopy is generally performed to examine the structural characteristics of samples, this characterization is sensitive to both amorphous and crystalline structures. If the electron cloud of the molecule, changes their polarizability during interaction with light then the molecule is considered to be "Raman active". Generally, change in vibrational modes (such as H–C–C, C = C, C–O–H, H–C–H, C–H, C–C, C–O, etc.) can be predicted from Raman analysis [239,240]. Strongest Raman signals is for the symmetric bonds which have the largest changes in polarizability. Table 4.2 represents the list of vibrational mode and their respective band assignments measured in the sample. On the other hand, O-containing functional groups in carbonaceous materials can be detected by FTIR analysis. However, it has limited use in exploring the low-polarity aromatic structures. "IR active" molecules in IR spectroscopy mainly depends on the dipole moment. Therefore, IR spectra have strong peaks for asymmetric bonds.

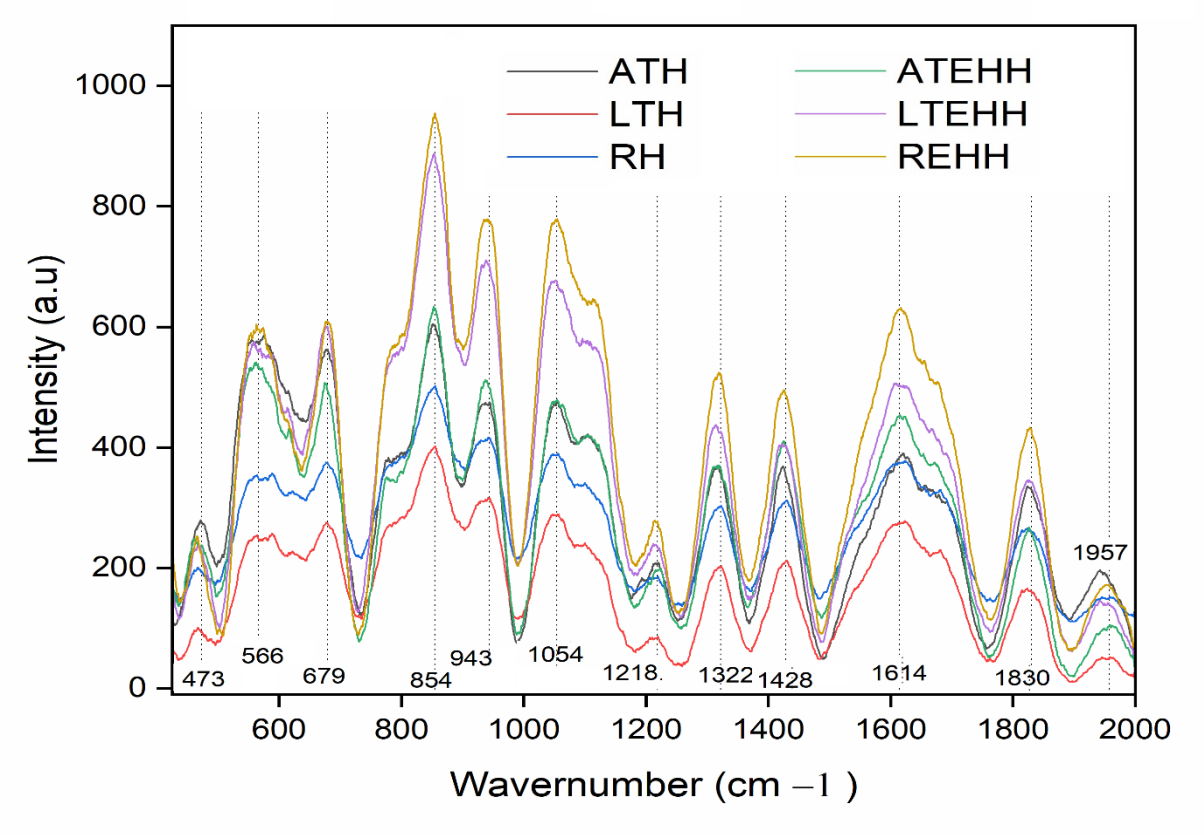

Figure 4.6 Raman curves of (A) RH, (B) LTH, (C) ATH, (D) REHH, (E) LTEHH, (F) ATEHH

Raman spectra analysis for raw (RW), treated (LTH and ATH) and saccharified (REHH, LTEHH and ATEHH) biomass were shown in Figure 4.6. Relative intensity of peak and its position were similar to previous data reported by many researcher [239,241]. Raman Spectra analysis from Figure 4.6 revealed that the major vibrations at 1614 cm^{-1} were due to lignin [241]. Whereas, in the spectral range at 906 cm^{-1} and 181 cm^{-1} mainly cellulose and hemicellulose components occurred. Kačuráková et al., 1999 reported that peak at 1,510 cm^{-1} mainly due to the existence of aromatic skeletal lignin. Whereas, peak at 1,329 cm^{-1} is due to presence of guaiacyl and syringyl condensed lignin in switchgrass. Weak vibration at 1471 cm^{-1} is attributed to the aromatic skeletal vibrations, methyl bending and lignin methoxy deformation. Strong bands for combinations of stretching of CO or CC ring and COC glycosidic linkages were noted at 1054 cm^{-1} and 1120 cm^{-1} respectively. Raman peak assigned at 943 cm^{-1} and 1,119 cm^{-1} is for the stretching of amorphous and crystalline cellulose. Furthermore, C–H distortion in hemicellulose and cellulose were noticed at 1,375 cm^{-1}, while C–O stretching in hemicelluloses and cellulose were observed at 1,054 cm^{-1} [241,242]. Xylan and cellulose have many common peaks in the analysis of Raman spectra. This is due to the similarity of local functional groups in the monomeric carbohydrate units; connections and repetitions in the polymeric structure is the only major difference between

them. Characteristic of phenolic group in the lignin were observed at in the Raman spectra range of 1598 cm^{-1} and 1629 cm^{-1}. As the concentration of hemicellulose and lignin increase in the physical mixture; bands at1096 cm^{-1} and 1121 cm^{-1} for xylan and cellulose decrease drastically [243].

Table 4.2 The band assignments for the main Raman peaks

Raman Shift (cm^{-1})	**Biomass constituent**	**Raman Vibrational Intensity**	**Assignments (Vibrational modes)**
473	Lignin	Weak	Ring deformation
566	Lignin	Strong	CCO and CCC in-plane bend
679	α-Pinene	Strong	Ring deformation
779	Lignin		CO stretches of lignin aromatic skeletal vibrations
854	Pectin	Weak	(C–O–C) Skeletal mode of α-
943	Lignin	Moderate	Lignin CCH wag; aromatic skeletal vibrations [240]
1054	Cellulose	Strong	CC and CO stretching
1119	Lignin		CC and CO stretching
	Cellulose		CC and CO stretching , COC, glycosidic; ring breathing,
1218	Lignin	Strong	Aryl-O of aryl OH and aryl-OCH_3; ring deformation
1322	NCSPs	Moderate	CH, COH
1428	Lignin	Weak	Lignin methoxy deformation, methyl bending, aromatic skeletal vibrations
1614	Lignin	Weak	Lignin aromatic skeletal vibrations
1682	β-Pinene		C = C stretch
1830	NCSPs	Moderate	C = O stretch
1957	Pectin	Weak	C = O stretch

4.3.2.4. Zeta potential

Zeta potential of the particles can quantify the stability of the particles in the solution. This is the potential present on the shear plane of the particles associated with both local environment of the nanoparticles and the surface charge. The particles are neutral and stable

if the value of zeta potential lies between -10 and + 10 mV [6]. The results of the zeta potentials of all samples are summarized in Figure 4.7 and Table 4.3. Hydrophobicity, hydrophilicity and dissociated or adsorbed charged species existing on the surface of lignocellulosic fibers can be quantify by this methodology. Tendency of hydrophilic cellulose polymer to absorb water which causes considerable swelling into it. During the cellulose water interaction, it was observed that polymer and water molecules forms H-H bonding. H-bonding between the cellulosic (fiber) molecules can be rupture by permeation of water molecules into it, which causes detachment of polymeric structure (Glaser 1999). The value of zeta potential (mV) for RH, LTH, ATH, REHH, LTEHH and ATEHH were -61.87, -60.36, -51.76, -35.56, -35.13 and -26.35 respectively. From this result, it can be observed that the value of zeta potential decreases progressively for more intense pretreated fibers and saccharified residue. This decrease was most probably due to swelling of polymeric structure. Figure 4.7 revealed that the majority of non-cellulosic compounds was removed by the pretreatment process. Removal of the wax causes to increase the accessibility and active surface area of the functional groups, results additional reduction in the value of zeta potential. Alkaline pretreatment also causes to further reduction in the value of zeta potential due to swelling of the fiber surface.

Table 4.3 Zeta potential analysis before and after enzymatic hydrolysis

S No.	Samples	Zeta potential (mV)	Doppler shift (Hz)
1	RH	-61.87	25.81
2	LTH	-60.36	25.27
3	ATH	-51.76	21.69
4	REHH	-35.56	14.42
5	LTEHH	-35.13	14.66
6	ATEHH	-26.35	10.19

However, treated biomass was further use for saccharification which results huge reduction in value of zeta potential. This huge reduction is most probably due to further degradation and disruption cellulosic fiber which causes more swelling of polymeric structure. Figure 4.7 showed that the value of zeta potential was more negative for ATEHH as compared to others, which is due to great degradation and disruption cellulosic fiber. In acidic and basic medium, value of zeta potential was negatively charged for all sample [6].

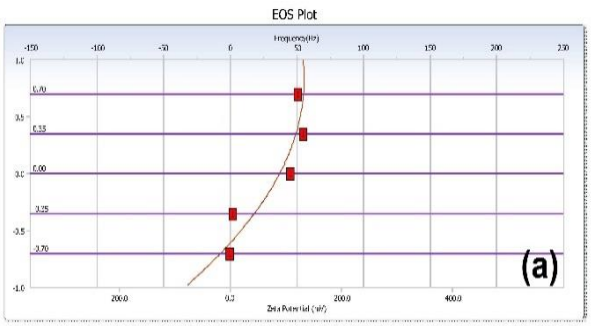
EOS Plot
(a)

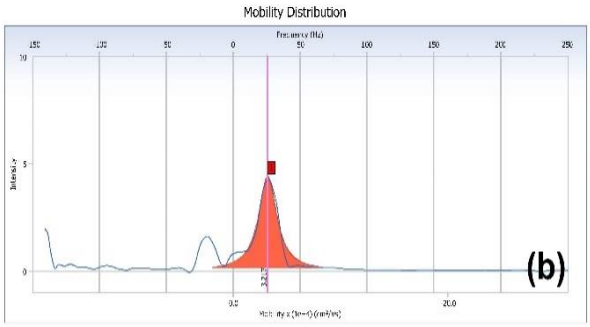
Mobility Distribution
(b)

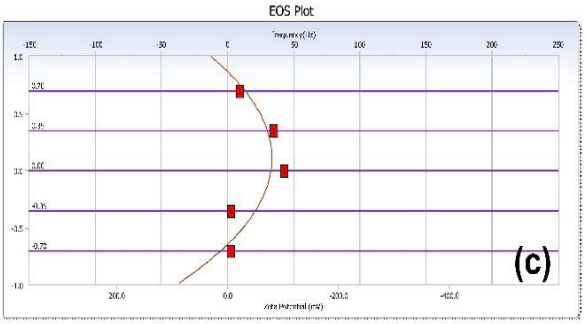
EOS Plot
(c)

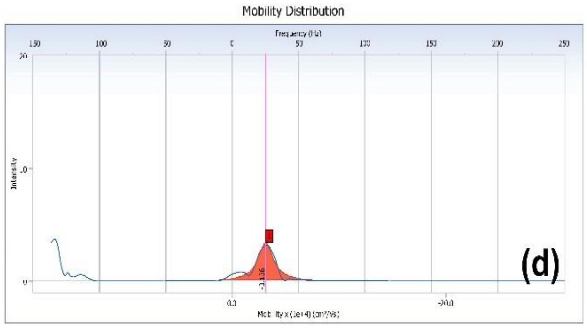
Mobility Distribution
(d)

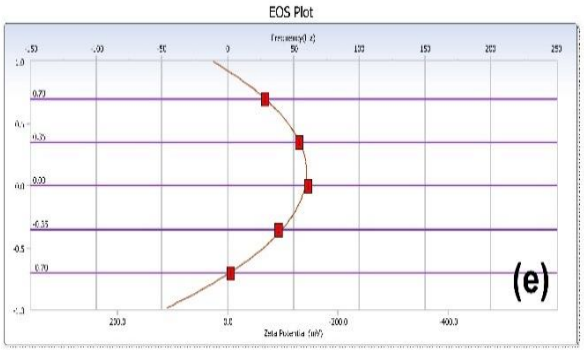
EOS Plot
(e)

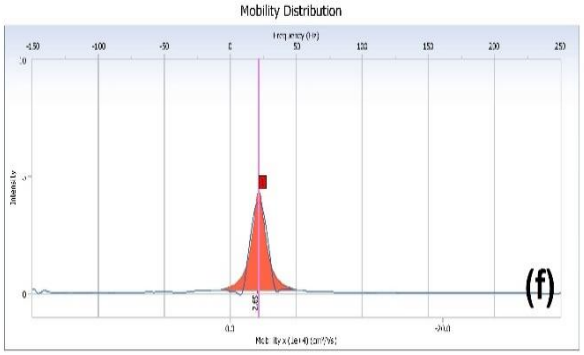
Mobility Distribution
(f)

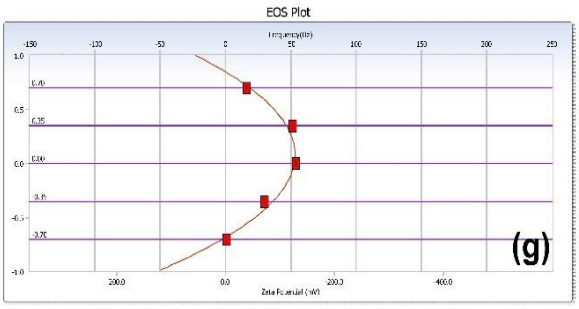
EOS Plot
(g)

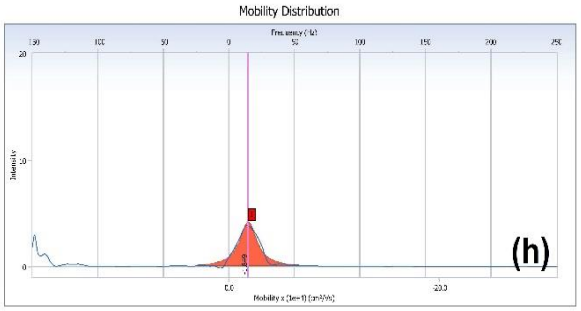
Mobility Distribution
(h)

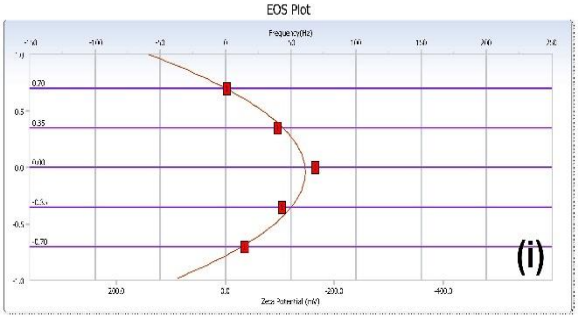
EOS Plot
(i)

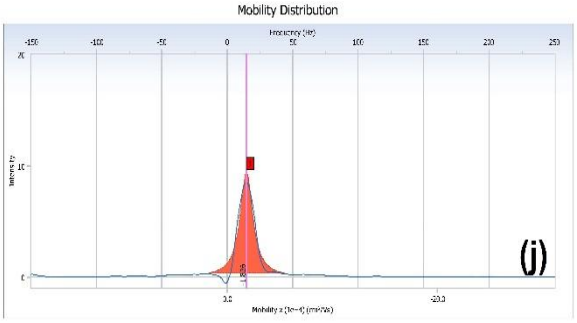
Mobility Distribution
(j)

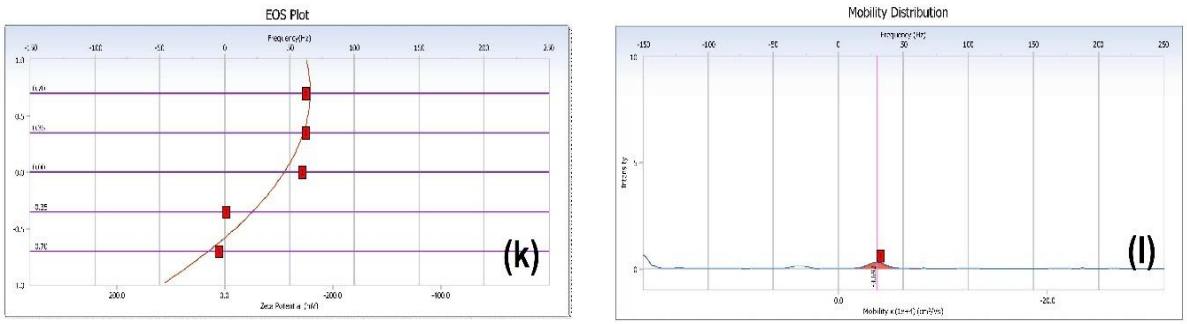

Figure 4.7 Zeta potential analysis of RH (a, b), LTH (c, d), ATH (e, f), REHH (g, h), LTEHH (i, j), ATEHH (k, l)

4.3.2.5. FTIR Analysis

Vibrational, bending, twisting and rotation motion associated with the several functional groups present in the molecule provide important information on functionality, molecular structure, precise chemical composition and correlations predictions. FTIR spectrum of raw, pretreated and saccharified biomass sample were shown in figure 4.8. The IR spectral absorption peaks at 3356 and 2921 cm^{-1} for the poplar material and its components, which is due to the strong O-H and C-H stretching, respectively. These two strong absorption peaks represent the presence of many CH bonds and hydroxy groups in the three main constituents of biomass (such as cellulose, hemicellulose and lignin) structure. Expansion and contraction of C=O in hemicellulose and lignin were absorbed at wavenumber of 1744 cm^{-1} [221]. In addition, a band was noted at 1420 cm^{-1} due to the carboxyl vibration of glucuronic acid containing xylan, symmetrical CH_2 bending vibration of cellulose and the in-plane deformation of CH with the elongation of the aromatic ring of lignin. Spectra at 1591 and 1508 cm^{-1} were assigned for the expansion and contraction (C = C) of the aromatic ring of lignin [244]. CH bending of cellulose, hemicellulose and lignin (aliphatic CH stretches of phenolic and methyl alcohols) were noticed at 1370 cm^{-1}. Bands at 1160 and 873 cm^{-1} are due to COC expansion and contraction at the $\beta(1 \rightarrow 4)$ glycosidic bond of hemicellulose and cellulose. Band noted at 1053 cm^{-1} due to the COH stretching of cellulose and hemicellulose. Although, IR spectrum of the sample is important for understanding the applied biomass treatment, such as chemical composition changes, biomass functionalization, and other transformations. Transmittance of saccharified husk is different among all the studied samples in the range of 3000 to 500 cm^{-1}, this is due saccharified husk has lower density of hemicellulose as compare to raw and treated husk [6].

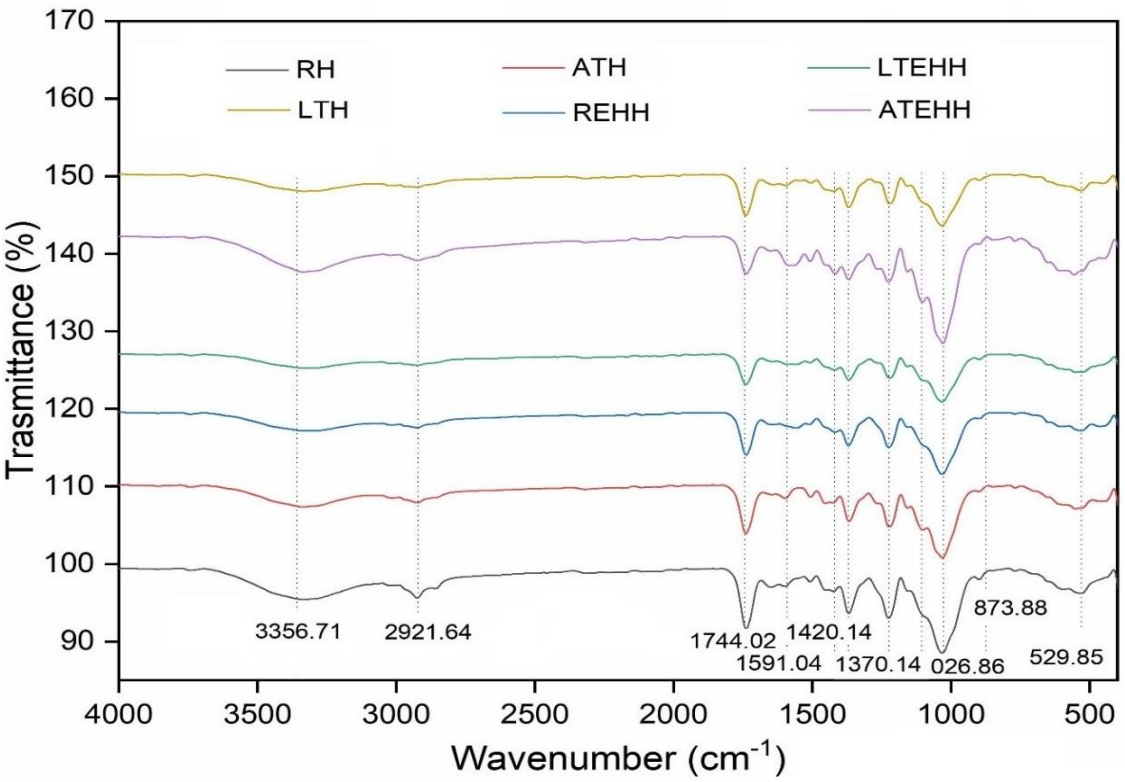

Figure 4.8 FTIR spectra of: (A) RH, (B) LTH, (C) ATH, (D) REHH, (E) LTEHH, (F) ATEHH

Table 4.4 The band assignments for the FTIR spectrum

S. No.	Wavenumber [cm^{-1}]	Assignment	Components
1	3356	O-H stretching	Cellulose, Hemicellulose, Lignin
2	2921	C-H stretching	Cellulose, Hemicellulose, Lignin
3	1744	C=O stretching	Hemicellulose, Lignin
4	1649	Aromatic skeletal vibration, C=O stretching, adsorbed O-H	Hemicellulose, Lignin
5	1591	C=C-C aromatic ring stretching and vibration	Lignin
8	1420	Symmetric CH_2 bending vibration, symmetric stretching band of carboxyl group, C-H deformation	Cellulose, Hemicellulose, Lignin
9	1370	C-H bending, C-H stretching in CH_3	Cellulose, Hemicellulose, Lignin
10	1152	C-O-C stretching	Cellulose, Hemicellulose, Lignin
12	1026	C-O stretching, aromatic C-H in plane deformation	Cellulose, Lignin
13	873	C-O-C stretching	Cellulose, hemicellulose
14	846	Aromatic C-H out of plane bending	Lignin

4.3.2.6. FESEM Analysis

FESEM analysis showed the morphological changes in raw, pretreated and saccharified biomass. Figure 4.9 revealed the uneven arrangement of the layered structure in these fibers. Before pretreatment cellulose crystals were plenty in number which get diminished after the pretreatment and make cellulosic fibers more amenable to enzymatic saccharification. Morphologies of the areca nut husk fibers that were subjected to the alkaline and acid pretreatment were almost identical, but showed the delicate differences when correlated to the morphologies after enzymatic saccharification [6]. FESEM analysis of the residue sample revealed the changes in morphology especially after saccharification at 15 IU/g biomass residue, which shows the level of change morphologies and structure in the crystalline cellulose fibers (Figure 4.9). Enzymatically treated biomass residue has many localized damages, which was observed from these micrographs. The rigidity of the cellulosic fibres was also lost and structure of saccharified residue became distorted due to removal of the hemicellulose content from the husk fibre. This analysis revealed the effect of saccharification on the areca nut husk morphology when pretty much hemicellulose and lignin are solubilized.

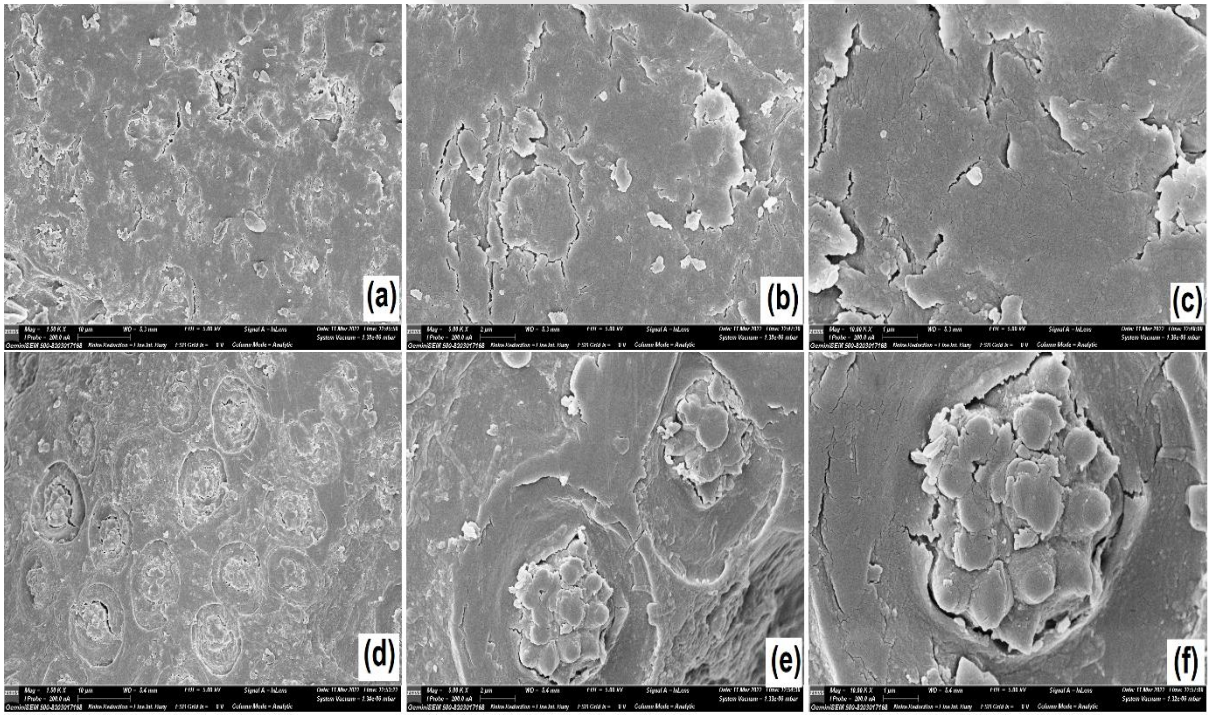

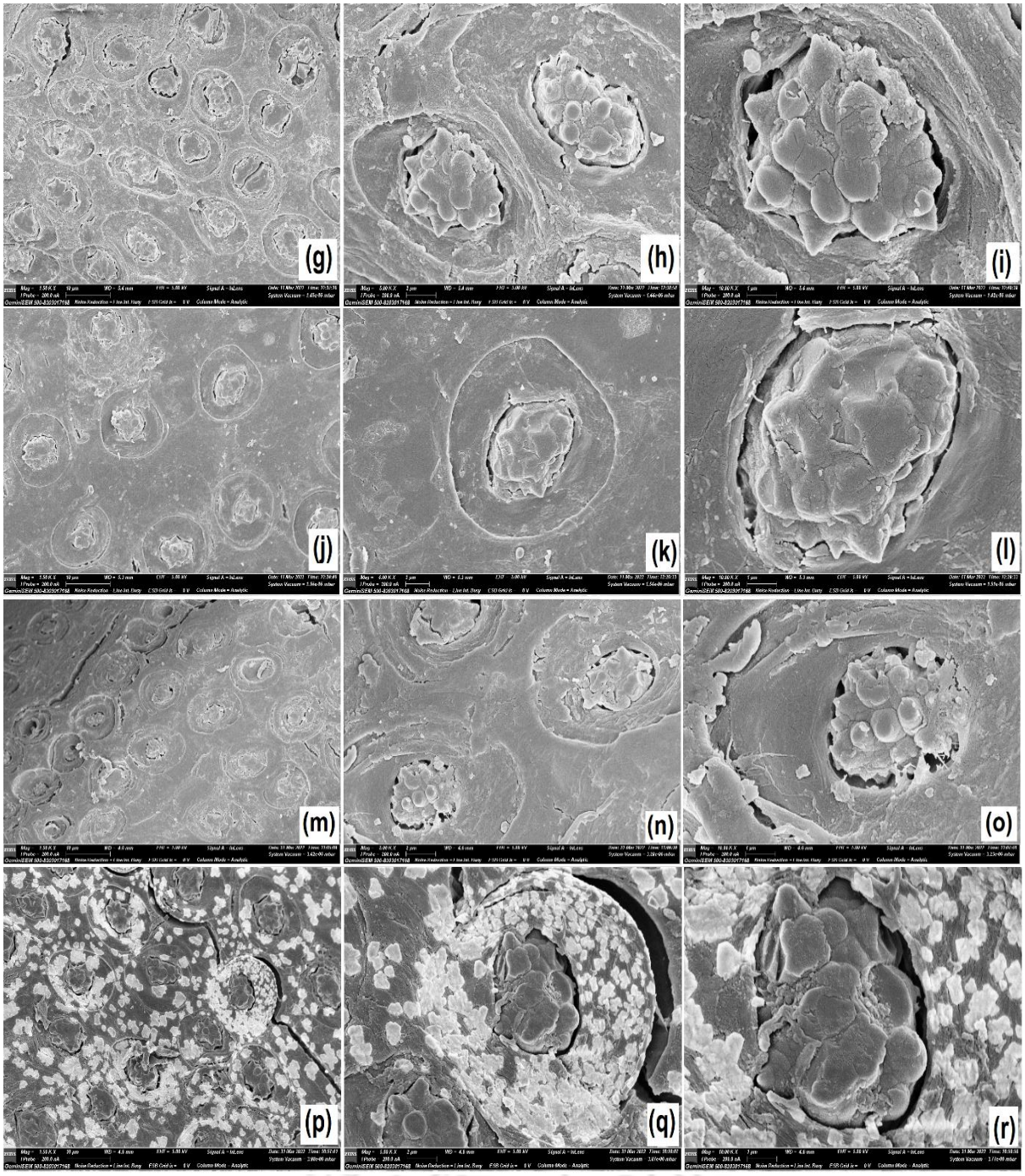

Figure 4.9 SEM images of: RH (a, b, c), LTH (d, e, f), ATH (g, h, i), REHH (j, k, l), LTEHH (m, n, o), ..ATEHH (p, q, r)

4.3.3. Production of Xylitol from enzymatic hydrolysate

4.3.3.1. FTIR analysis of hydrolysate

FTIR spectroscopy was performed in the region of 500 – 4000 cm^{-1} to compare the molecular conformational changes in the enzymatically hydrolyzed RH, LTH and ATH hemicellulosic hydrolysate. FTIR spectra was demonstrated in Figure 4.10, the absorbance at 3356 cm^{-1} was due to the hydroxyl group. This usually results due to hydroxyl group of the

cellulose forms intermolecular hydrogen bonds in the solution [245]. Moreover, a band was detected at 2338 cm^{-1}, indicating CH expansion and contraction vibrations because of presence of CH_3 and CH_2 functional groups. In contrast, the extracted hemicellulose signal appeared at 1757 cm^{-1}. This was due to the hemicellulose fraction dissolved during the water treatment and contains a small amount of acetyl, ester bonds of the carboxyl groups [246]. Absorbance signal around 1630 cm^{-1} was observed due to water absorbed by xylan type polysaccharides [247]. A reduction at the 1554 cm^{-1} due to vibrations and streatching of lignin aromatic ring, this attributed to lignin removal [248]. In addition, the lower absorbance at 1529 cm^{-1} appeared due to aromatic skeletal oscillations of the associated lignin [245]. In contrast, band at 1358 cm^{-1} was due to the presence of CH bending vibration in hemicelluloses and cellulose chemical structures [246]. The sharp absorption peak around at 1143 cm^{-1} shows the COC streatching in the cellulose and hemicellulose content. The sharp absorption peak around at 1051 cm^{-1} depicted typically for xylan which was mainly arises due to the CO and CC stretching oscillations having glycosidic bonds. FTIR spectral analysis confirmed that toxic components (such as ester and carboxyl groups) were significantly removed after various detoxification modes.

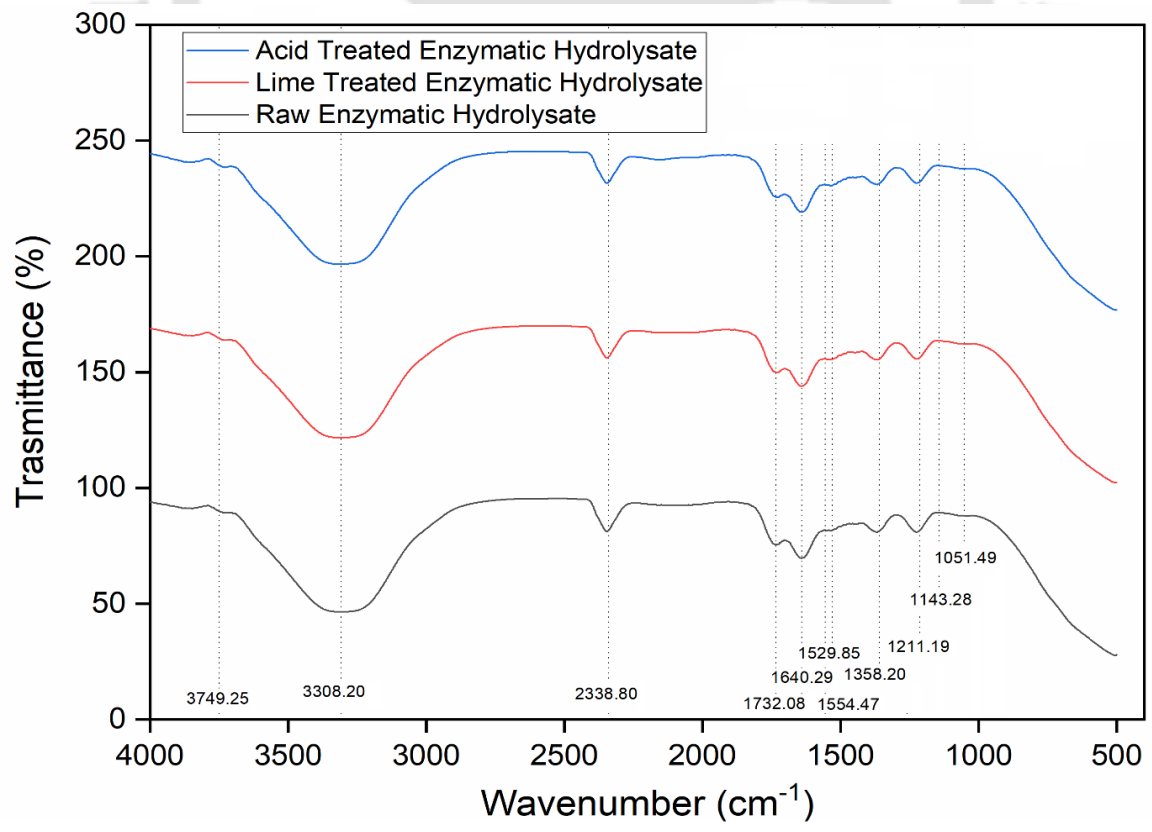

Figure 4.10 FTIR analysis of Enzymatic hydrolysate

Table 4.5 The band assignments for the FTIR spectrum [1, 35, 36]

S. No.	Wavenumber [cm^{-1}]	Assignment	Components
1	3356	O-H stretching	Cellulose, Hemicellulose, Lignin
2	2921	C-H stretching	Cellulose, Hemicellulose, Lignin
3	2338	C-H stretching	Cellulose, Hemicellulose, Lignin
3	1732	C=O stretching	Hemicellulose, Lignin
4	1640	Aromatic skeletal vibration, C=O stretching, adsorbed O-H	Hemicellulose, Lignin
5	1554	C=C-C aromatic ring stretching and vibration	Lignin
8	1529	Symmetric CH_2 bending vibration, symmetric stretching band of carboxyl group, C-H deformation	Cellulose, Hemicellulose, Lignin
9	1358	C-H bending, C-H stretching in CH_3	Cellulose, Hemicellulose, Lignin
10	1143	C-O-C stretching	Cellulose, Hemicellulose, Lignin
12	1051	C-O stretching, aromatic C-H in plane deformation	Cellulose, Lignin

4.3.3.2. Cell growth analysis of C. tropicalis

The growth curve of *C. tropicalis* in the growth media is illustrated in Figure 4.11, indicating the growth rates (per unit time) of 1.35, 0.69, 0.46, 0.42, and 0.56 for YPD, SSF, LTFH, ATHF, and RHF, respectively. This analysis observed that maximum growth of *C. tropicalis* in YPD is about 10.16 g/L after 36 h of incubation. Further extending the time of growth, it became stationary. However, the rate of growth was not same for the obtained hydrolysate after saccharification. Maximum growth of *C. tropicalis* in RFH (raw fermentated hydrolysate), LTFH (lime treated fermented hydrolysate), ATFH (acid treated fermented hydrolysate) and SSFH (synthetic solution fermented hydrolysate) were 3.28 g/L , 3.9 g/L , 4.3 g/L and 5.1 g/L respectively. The varaiation in growth of *C. tropicalis* in different fermentative medium is most probably due to uneven xylose concentration in the fermentative medium and also might be presence of some other by products in the case of RFH, LTFH and ATFH. However, in the case of RFH, LTFH and ATFH, the concencentation of cell is about 35.68%, 23.52% and 15.68% lower than the concentration of SSFH. Inspite of that stationary phase reached by all the sample in the same time [249].

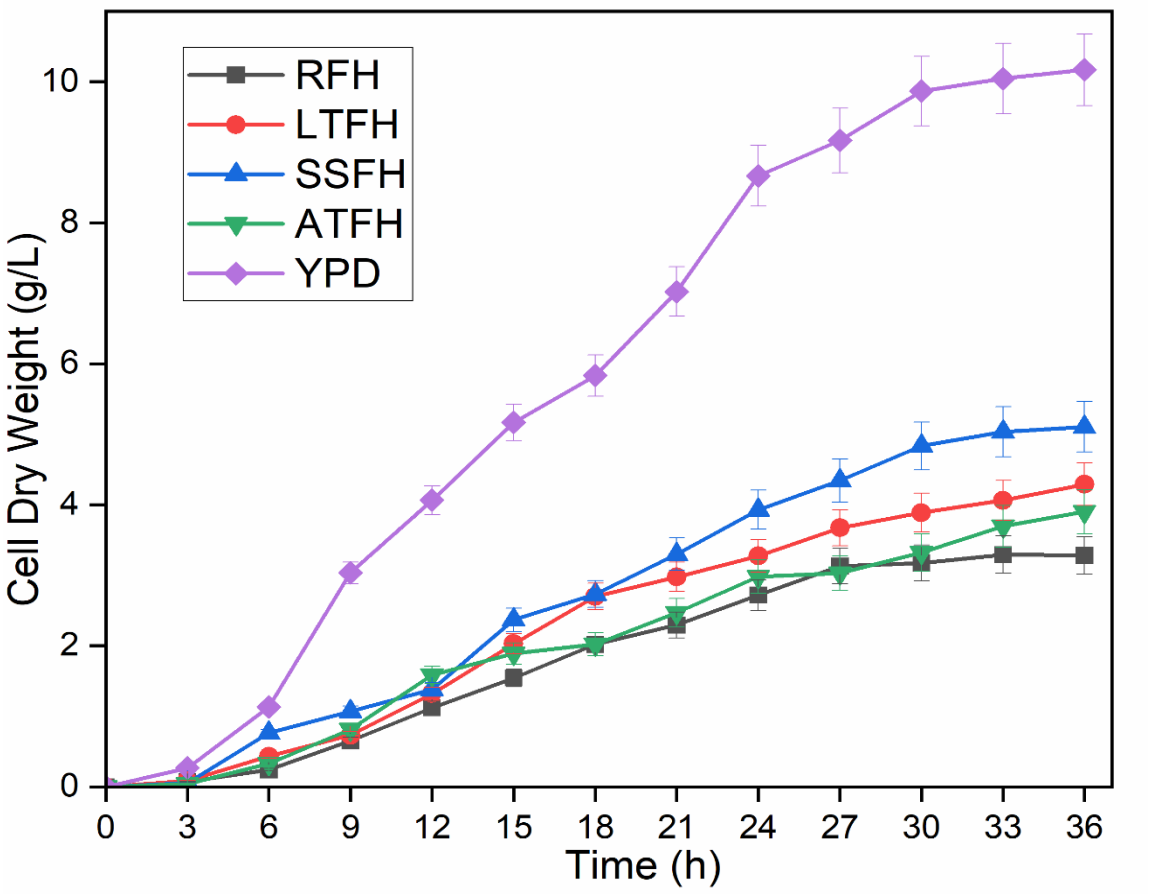

Figure 4.11 Growth curve of *C. tropicalis* in different fermentation and YPD medium

4.3.3.3. Xylitol production from enzymatic hydrolysate

Areca nut husk hemicelluosic hydrolysate obtained after enzymatic saccharificaation was used for xylitol production by *C. tropicalis*. As shown in Figure 4.12, the fermentation process was carried out for RFH, LTFH, ATFH and SSFH. Highest xylitol concentration obtained was about 1.80 g/L , 2.97 g/L , 4.60 g/L and 6.08 g/L for RFH, ATFH, LTFH and SSFH respectively, after 90 h of fermentation. The yield of xylitol was about 71.02%, 76.78%, 79.68% and 85.67% for RFH, ATFH, LTFH and SSFH respectively. In addition to that the initial concentration of xylose in the fermentative medium is about 2.47 g/L , 3.83 g/L , 5.88 g/L and 7.09 g/L respectively for RFH, ATFH, LTFH and SSFH. From this analysis, it can be noted that low concentrtion of xylose in the hydrolysate could affect the xylitol production and cause the lower yield of xylitol [52]. According to the present results, the xylitol yield was increases by 9% from RFH to LTFH when there was increase in xylose concentraation from 2.47 g/L to 5.88 g/L . But the yield of xylitol is about 17.10%, 10.37% and 6.98% lower for RFH, ATFH and LTHF as compare to yield of SSFH. The most

probable reason for lower yield of xylitol was concentration of xylose in the fermentative medium and also might be chance of presence of some toxic components in the fermentative medium.

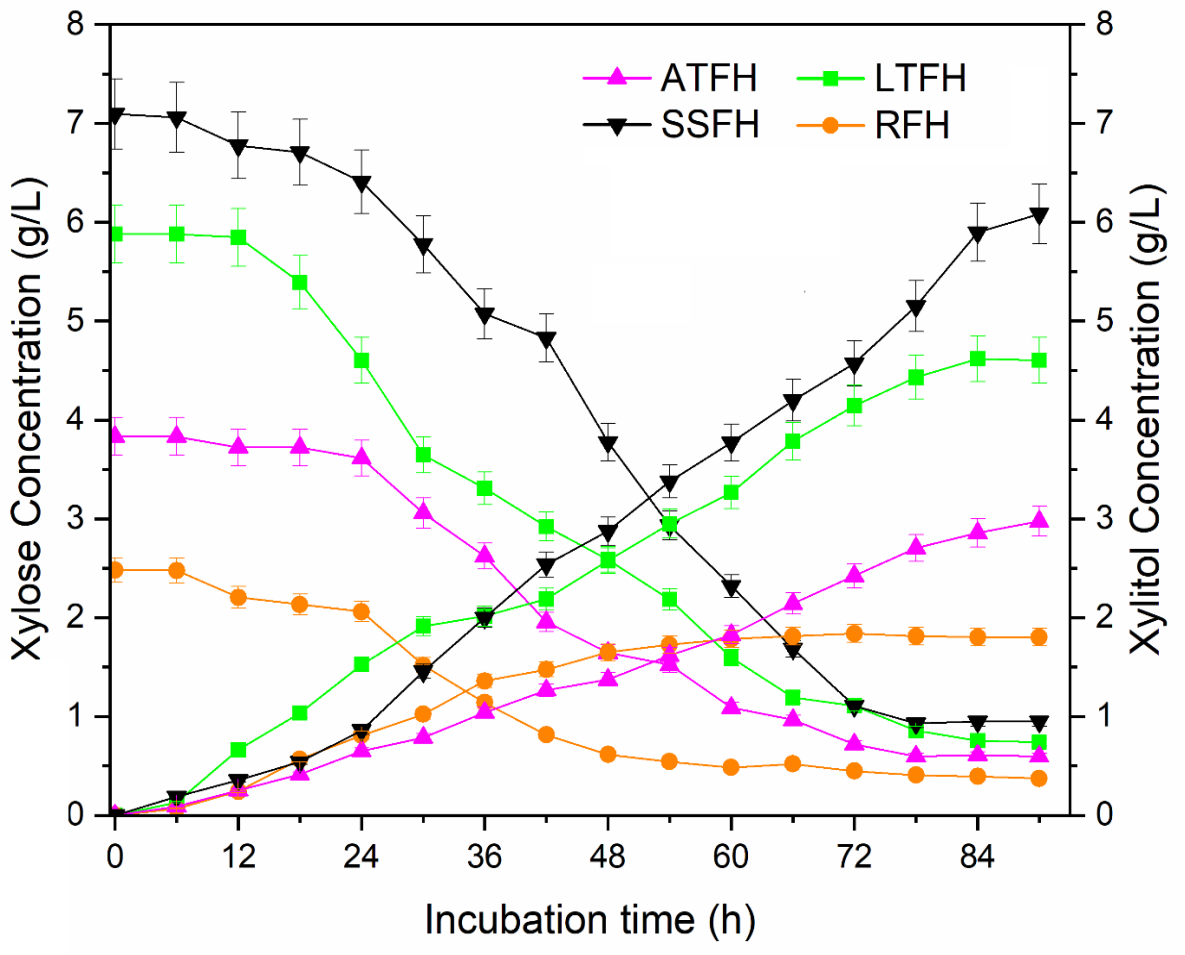

Figure 4.12 Xylose consumption and corresponding xylitol production profiles

Some literature reported the production of xylitol by fermentation process from lignocellulosic hydrolysate obtained from various biomasss sources, shown in Table 4.6. From literature it was observed that mainly dilute sulfuric acid hydrolysis was used to get xylose rich hydrolysate followed by detoxification and fermentation for production of xylitol. The maximum xylitol yield eported was in the range of 0.3-0.8 g/g xylose. But this study able to obtain the optimium yileld of xylitol 0.78 g/g by the frermentation of hydrolysate obtained from enzymatic hydrolysis instead of sulfuric acid process [250]. Very less literature available on over all yield of xylitol from lignocellulosic biomass. It was noted from literature that *D.hansenii* can catabolize glucose to ethanol under anaerobic condition with glucose/xylose ratio above 30%. Higher glucose concentration in the hydrolysate, diverts the process to ethanol production instead of xylitol [12]. In order to avoid byproduct formation (such as ethanol), higher xylanase specificity and lower cellulase activity enzyme would be

needed for maximum production xylose rich hydrolysate followed by xylitol production by fermentation process [251].

Presently production of xylitol in industry mainly based on the chemical hydrogenation process in presence of nickel supported catalyst [227]. major drawbacks of this process is that xylitol yield is relatively low due to chemical reduction of produced by products. Therefore xylitol production by fermentation of xylose rich hydrolysate obtained after saccharification of lignocellulosic biomass appears to be a promising alternative. In this research, yeast strain *C.tropicalis* ws used for xylitol production from enzymatic hydrolysate, the optimium yield achived was 79.68% which was near about same as reported by other researcher. Morover, the process used in this study was simpler than other methodology because dispensable use of detoxification process. Therefore production of xylitol by this methodolgy, makes process more economical, and enviroment friendly.

4.3.3.4. Viability analysis of *C. tropicalis* in fermentation media

The proposed analysis can provide an effective tool for research and development in food, brewery and pharmaceutical industry. This analysis may be incorporated in product manufacturing to monitor the micro-organism growth (yeast cell) and viability analysis during the fermentation process. Monitoring of *C. tropicalis* during fermentation and propagation in an industry is a very important and crucial task [249]. By using the fluorescence microscopy analysis of fermented broth, number of viable cells in culture (fermentation) medium can be easily estimated. In Figure 4.13, 4.14, 4.15, 4.16 and 4.17, the dotted point shows the intensity of living and viable cell. Cell viability analysis was conducted by using methylene blue staining (MBS). However, Figure 4.17 shows the growth of *C. tropicalis* in YPD medium and almost all cells are living in this analysis. Cell viability test by MBS revealed that the different concentration of xylose in REH, LTEH, ATEH and SSEH shows different viability. Moreover, one can clearly observe a decrease of the number of viable cells with decrease in concentration of xylose in fermentation medium. But, as the concentration of xylose increases, the proportion of living cells get increased which causes to enhancement in xylitol production during fermentation [52,55].

Table 4.6 Sugar and xylitol yield Comparative analysis for different biomass feedstock

Raw materials	Pretreatment	Hydrolysis	Xylose	Detoxification	Xylitol yield (g /g)	Ref.
OPEFB	Autohydrolysis (120 °C; 15 min)	Enzymatic hydrolysis	0.08 g/g	No	0.41	[251]
OPEFB	Autohydrolysis (120 °C; 15 min)	Enzymatic hydrolysis	4.63 g/L	No	0.24	[252]
Corn cob	Non-isothermal autohydrolysis to reach 202 °C followed by post hydrolysis with 0.5% H_2SO_4 (125 °C; 165 min)	Acid hydrolysis with 2% H_2SO_4 (130 °C; 15 min)	35.30 g/L	Yes	0.73	[253]
Corn cob	-	Acid hydrolysis with 1% H_2SO_4 (121 °C; 60 min)	0.25 g/g	Yes	0.75	[254]
Cashew apple bagasse	-	Acid hydrolysis with 6% H_2SO_4 (121 °C; 15 min)	19.02 g/L	No	0.32	[255]
Corn cob	-	Acid hydrolysis with 1% H_2SO_4 (121 °C; 40 min)	31.25 g/L	Yes	0.74	[21]
Brewery spent grain	-	Acid hydrolysis with 3% H_2SO_4 (130 °C; 15 min	24 g/L	No	0.58	[256]
Rice straw	-	Acid hydrolysis with 1.5% H_2SO_4 (130 °C; 20 min)	17.40 g/L	Yes	0.53	[257]
Corn cob	0.1% H_2SO_4 (room temperature;24 h)	High temperature steaming (HTS) (160 °C; 120 min)	0.18 g/g	Yes	0.71	[258]
Sugarcane straw	-	Acid hydrolysis with 1% H_2SO_4 (121 °C; 20 min)	18.60 g/L	Yes	0.67	[259]
Corn cob	Soaking in 10% aqueous ammonia (70 °C; 10 h)	Acid hydrolysis with 1% H_2SO_4	33.42 g/L	No	0.60	[260]
Corn cob	-	Acid hydrolysis with 1% H_2SO_4 (121 °C; 30 min)	21.98 g/L	Yes	0.37	[261]
Areca nut	Dilute Acid pretreatment (H_2SO_4)	Enzymatic hydrolysis	3.83 g/L	No	0.76	This study
Areca nut	Lime pretreatment	Enzymatic hydrolysis	5.88 g/L	No	0.79	-Do-

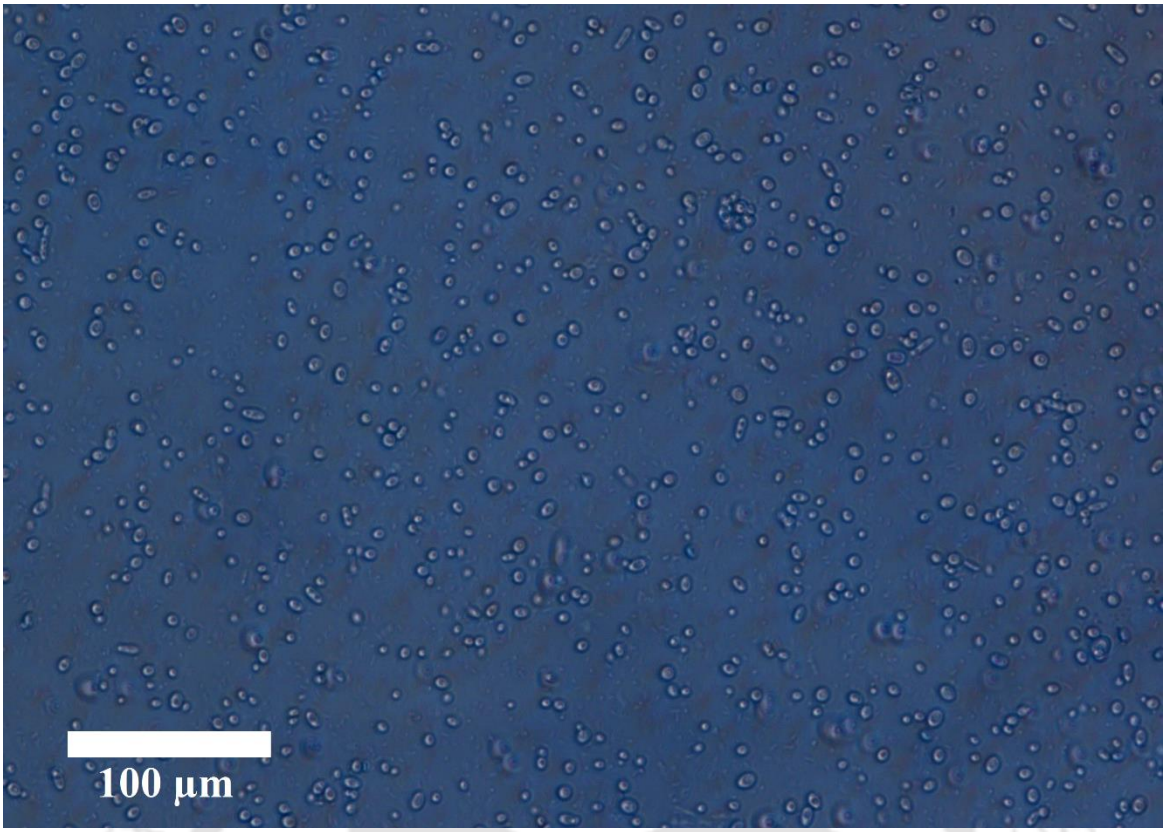

Figure 4.13 Viability analysis of *C. Tropicalis* in REH growth media

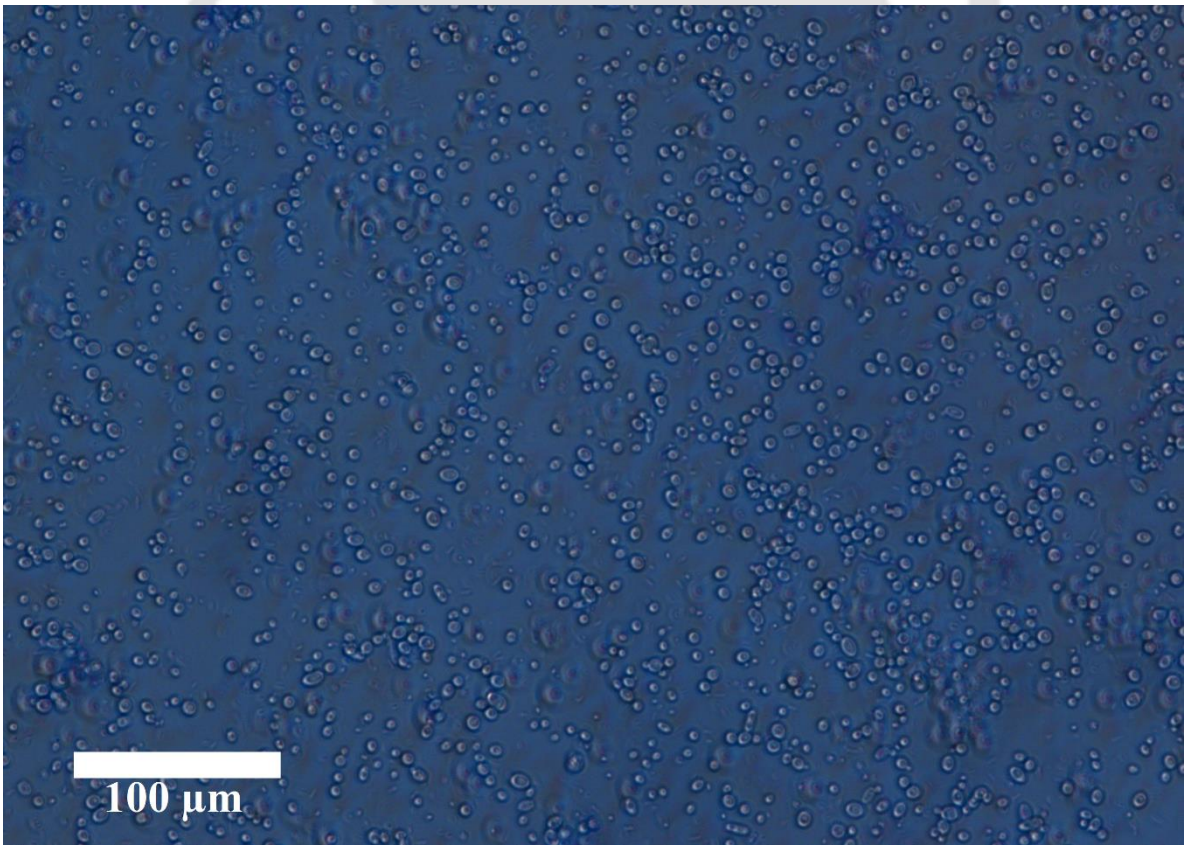

Figure 4.14 Viability analysis of *C. Tropicalis* in LTEH growth media

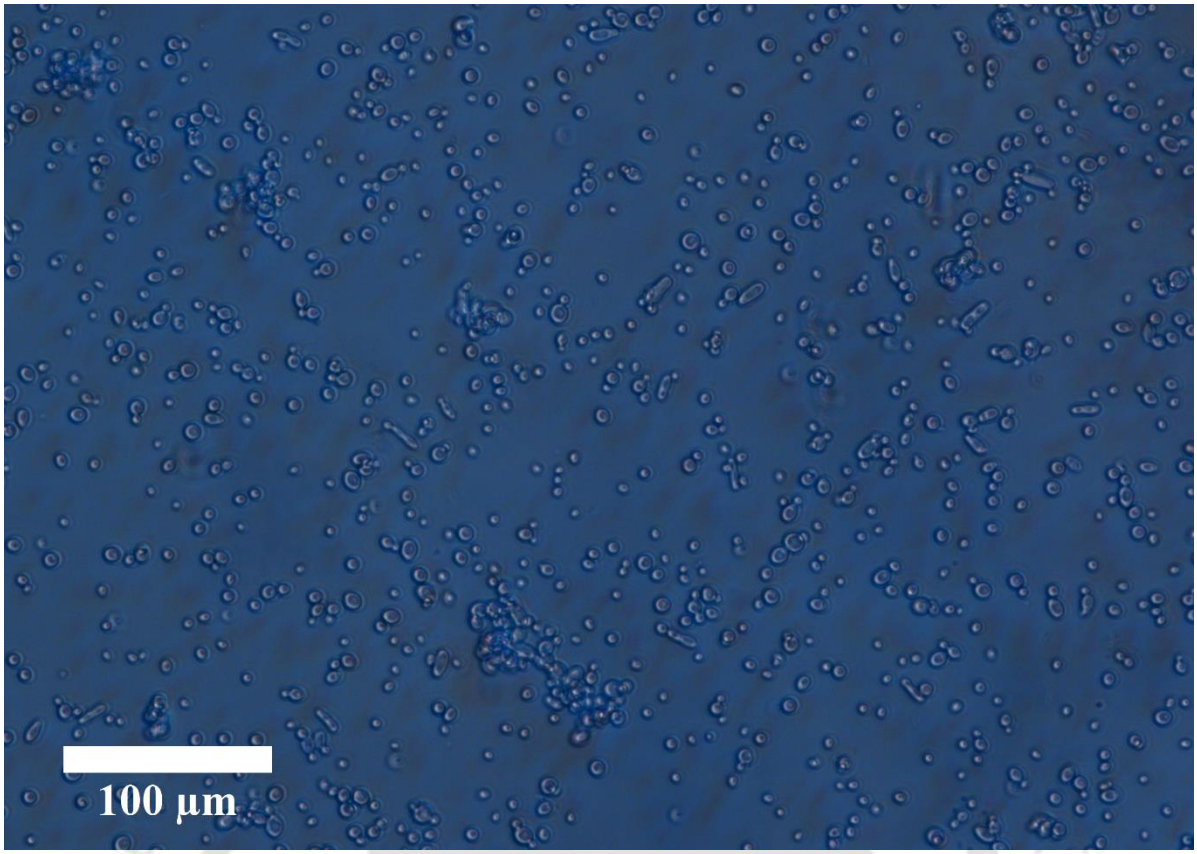

Figure 4.15 Viability analysis of *C. Tropicalis* in ATEH growth media

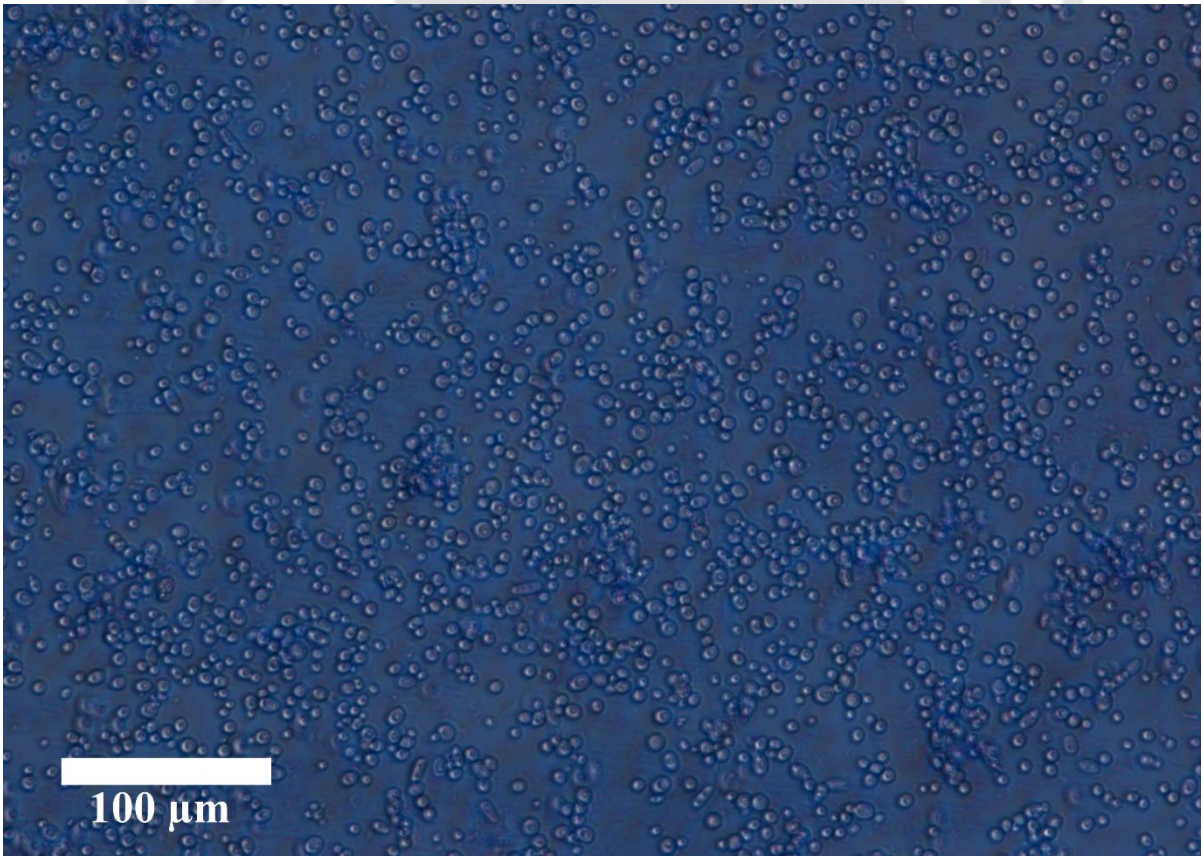

Figure 4.16 Viability analysis of *C. Tropicalis* in SSEH growth media

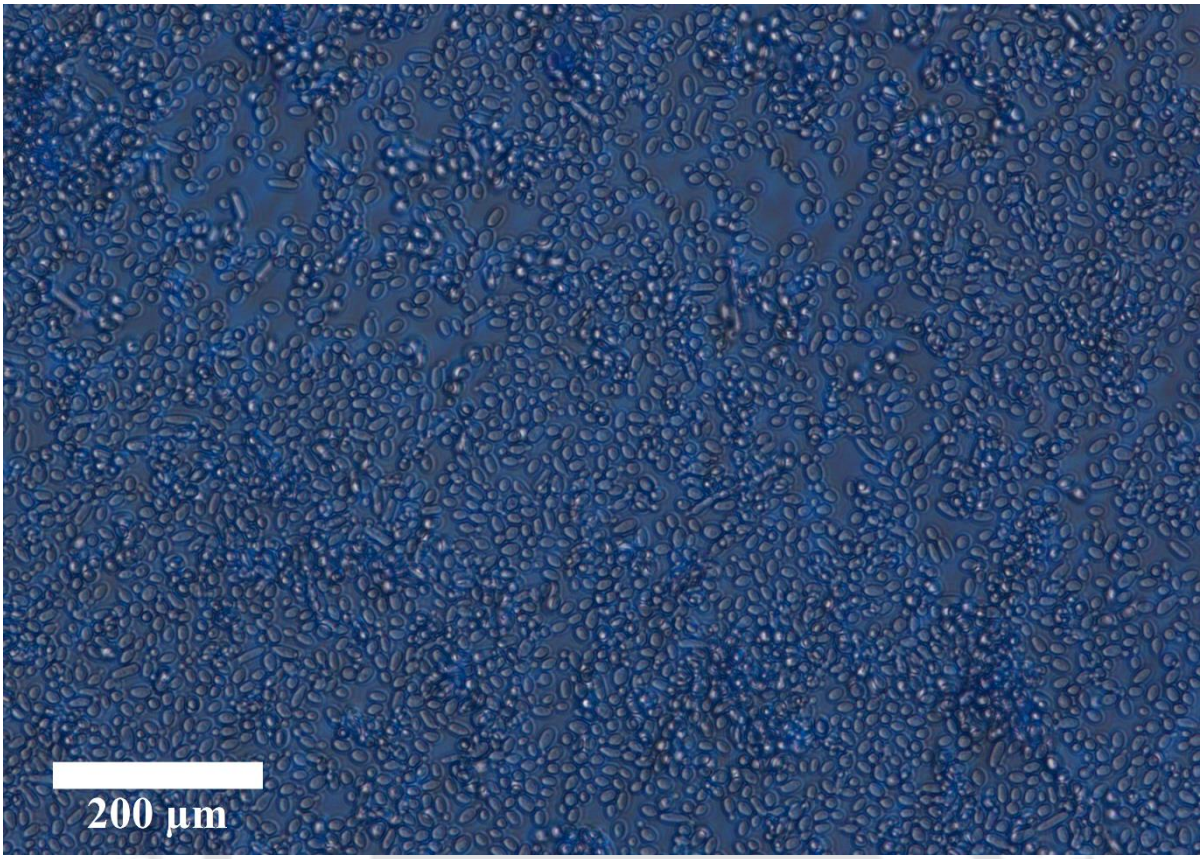

Figure 4.17 Viability analysis of *C. Tropicalis* in YPD growth media

4.4. Conclusions

The research work conducted in this study aimed to utilize areca nut husk as a potential source of xylose and xylitol. The use of pretreatment methods such as dilute acid (H_2SO_4) and alkali (lime) helped to increase the digestibility of the biomass, leading to the production of a xylose-rich hemicellulosic hydrolysate through enzymatic saccharification.

The results showed that the concentration of xylose sugar produced from the enzymatic saccharification of RH, LTH, and ATH was 0.034 g/g, 0.089 g/g, and 0.049 g/g of feedstocks, respectively. This xylose-rich hemicellulosic hydrolysate was then subjected to fermentation with C. tropicalis, which resulted in a yield of xylitol ranging from 0.71 g/g to 0.79 g/g for RFH, ATFH, and LTFH.

Overall, this study highlights the potential of areca nut husk as a renewable hemicellulosic substrate for the production of value-added biochemicals and bioproducts such as xylitol. The findings of this study could be useful in developing a sustainable and efficient lignocellulosic biorefinery for the production of biofuels and other high-value chemicals.

भारतीय प्रौद्योगिकी संस्थान गुवाहाटी
Indian Institute of Technology Guwahati

भारतीय प्रौद्योगिकी संस्थान गुवाहाटी
Indian Institute of Technology Guwahati

Chapter 5

Optimization of fermentation process for production of xylitol from detoxified dilute acid hemicellulosic hydrolysate

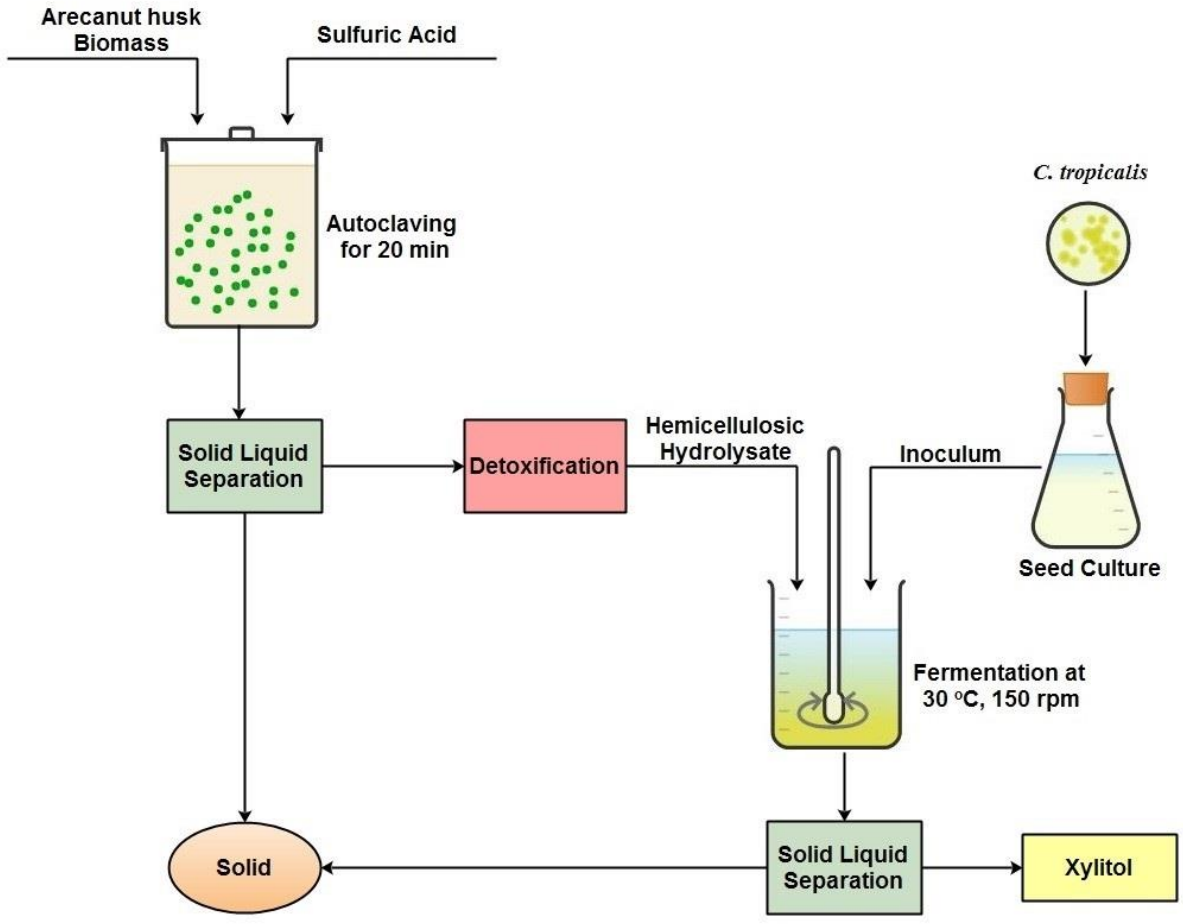

5.1. Overview

This research aimed to evaluate the detoxification and fermentation procedures of hemicellulosic hydrolysate obtained from areca nut husk for the microbial production of xylitol. Areca nut husk is a renewable and widely available raw material having high xylan content, making it an ideal substrate for xylitol production. However, the presence of inhibitors in the hemicellulosic hydrolysate obtained from the areca nut husk can hinder the fermentation process. To overcome this challenge, various techniques of detoxification were performed, including pH adjustment, treatment with activated charcoal, and Amberlit ion exchange resin. The effect of these techniques on sugar loss and inhibitor removal was estimated. Detoxification by a series of treatments removed about 99% of inhibitors present in the hemicellulosic hydrolysate, making it suitable for fermentation.

Fermentation was carried out by *C. tropicalis* using the detoxified hemicellulosic hydrolysate of areca nut husk, and the optimum yield of xylitol obtained was 0.66 g/g. This result confirms the potential of areca nut husk as a renewable and low-cost raw material for xylitol production. The study concluded that detoxification by pH adjustment, activated charcoal, and ion exchange resins are considered to be the most economical technique for removing toxic compounds from hemicellulosic hydrolysates, and this medium has huge potential for xylitol production.

5.2. Materials and Method

5.2.1. Materials

Areca nuts were purchased from nearby market of Guwahati city, India. All the chemicals used in this experiment were analytical grade and purchased from Sigma Aldrich. Experiments were conducted in triplicate to maintain the accuracy in result.

5.2.2. Pretreatment Method

Areca nuts were initially dried for a day under sunlight for preliminary drying followed by pilling to separate fibres. Separated husk fibres were washed with running tap water to discard the lightly bound contaminants and impurities. Washed husk was dried in an oven at 70 ºC for a day to remove the moisture content in it. To achieve particle sizes of around 1-5 mm in length and 1 mm in thickness, oven-dried samples were sliced into small pieces, ground into a fine powder, and then sieved (mesh size-BSS 30). Powder sample were kept in an airtight container for further use.

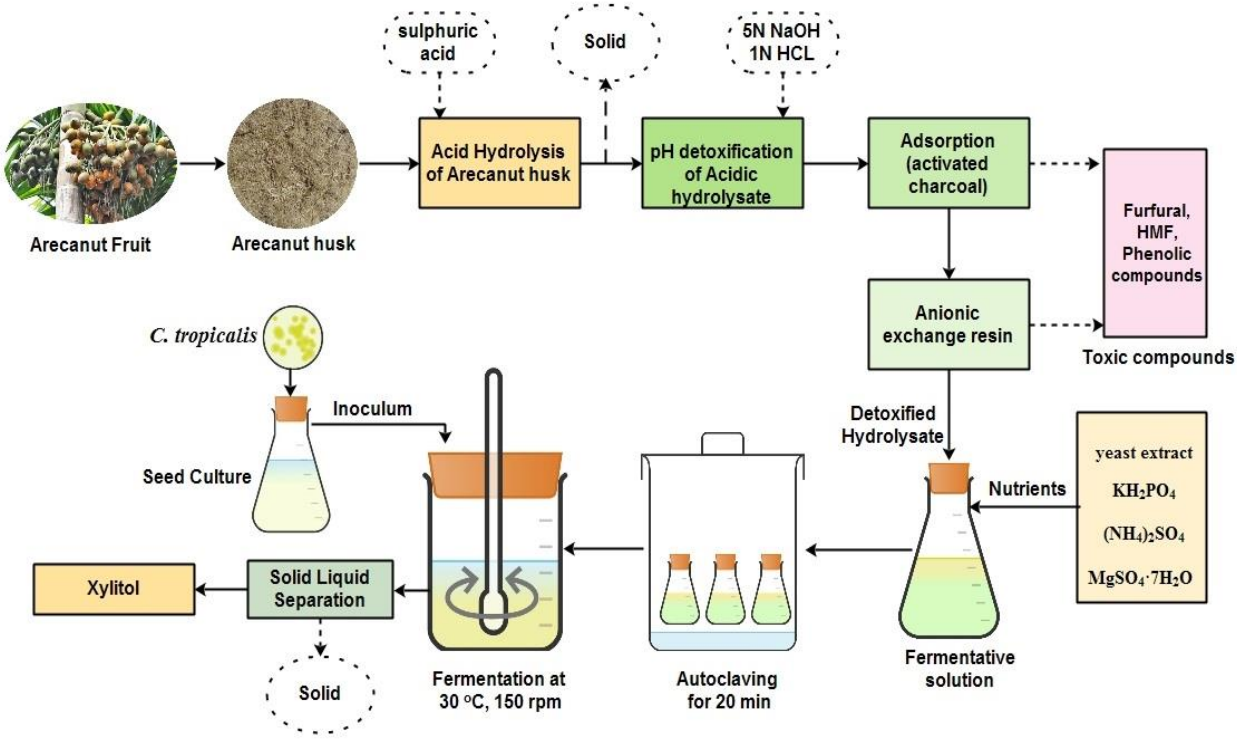

Figure 5.1 General Structure of a multilayer an artificial neural network [17]

5.2.3. Preparation of Areca nut husk hydrolysate and process optimization

Dilute acid hydrolysis (H_2SO_4) was conducted on a powder sample of areca nut husk following the protocol outlined in a previous study. The process involved blending 1% w/v (5 g) of biomass with 1.35% v/v (6.75 mL with density 1.84 g/mL) of H_2SO_4 to produce a 500 mL water solution, which was then subjected to hydrolysis in an autoclave for 20 minutes at 121 °C. Once the hydrolysis process was completed, the solution was allowed to cool to room temperature, and the hydrolysate was separated from the resulting solution using a vacuum filter (between 0.01 to 0.02 MPa) to remove any biomass residue. In order to evaluate the effect of hydrolysis on the release of xylose and toxic components during the hydrolysis of ANH, various parameters were examined during acid hydrolysis, including the solid-to-liquid ratio (1, 5, 10, and 15% w/v), H_2SO_4 concentration (1.35, 2, 2.70, and 5% v/v), and hydrolysis time (20-60 minutes).

5.2.4. Detoxification of hemicellulosic hydrolysate

The acidic hydrolysate obtained was subjected to various detoxification techniques as shown in Figure 5.1. Chemical detoxification involved adjusting the pH of the hydrolysate using 5N NaOH until it reached pH 10, maintaining the solution at that pH for an hour, and then performing centrifugation at 2000g for 10 minutes. The resulting hydrolysate was

referred to as PD10. Another hydrolysate, PD5.5, was obtained by subjecting the hydrolysate to NaOH treatment (as described above) and subsequently treating it with 1N HCl, adjusting the pH to 5.5 and maintaining it for an hour, followed by centrifugation at 2000g for 10 minutes. The hydrolysate obtained after chemical detoxification was further treated with activated charcoal at a rate of 5.0% (w/v) for an hour at 30 °C and 200 rpm, and the resulting hydrolysate was referred to as charcoal detoxified hydrolysate (CDH). The CDH was then treated with a series of strong ion-exchange resins (Amberlite IRA 120 and Amberlite IRA 410) that had been hydrated for 24 hours in distilled water, resulting in the resin detoxified hydrolysate (RDH). The CDH was first treated with Amberlite IRA 410 at a ratio of 2:1 (hydrolysate volume to resin mass) for 30 minutes at 30 °C and 200 rpm, followed by separation of the hydrolysate from the resultant solution using a vacuum filter. The hydrolysate was then treated with Amberlite IRA 120 at a ratio of 2:1 for 30 minutes at 30 °C and 200 rpm. Finally, the detoxified hydrolysate was separated and stored in a freezer at 4 °C for future use.

5.2.5. Microorganism and inoculum preparation

Candida tropicalis (MTCC 6192) culture was procured from Microbial Type Culture Collection and GeneBank (MTCC), India and maintained at 4 °C on YPD (Yeast Extract, Peptone and Dextrose) agar medium. YPD agar contains peptone as a source of carbon, nitrogen, vitamins, and minerals, while yeast extract provides B-complex vitamins to promote bacterial growth. Dextrose serves as the carbohydrate source, and agar is added to solidify the medium. Microorganisms were subcultured every 15 days. The composition of the media used in this study as follows yeast extract 10.0 (g/L), peptone 20.0 (g/L) and dextrose anhydrous (glucose) 20.0 (g/L). 1N HCL solution was used to maintain the pH of the medium at about 5.0. The cell culture process was conducted in a 250 mL Erlenmeyer flask (50 mL of medium) on a rotary platform shaker for 48 hours at 30 °C with 150 rpm.

5.2.6. Cell Dry Weight Measurements

Dry weight measurements were made by pipetting 5 mL of a well-mixed broth sample into a dry centrifuge tube. Cells from broth was separated by performing centrifugation for 5 minutes at 10,000 g. Separate the cell paste from broth by carefully scrapping the clear broth. After this separate the cell pastes from the centrifuge tube and kept in a weighing pan. Dry the cell paste for overnight in an oven at 60 ºC. Calculation of dry cell weight was performed by using following equation.

$$Dry\,cell\ weight\ (g/mL) = \frac{CW_3 - CW_2}{V_1} \quad (5.1)$$

Where: CW_3 = Weight of the sample including blank tube, CW_2 = Weight of the blank tube, V_1 = Volume of culture sample

5.2.7. Experimental design and fermentation process

The fermentation process was carried out in a 5 L bioreactor containing a 1.5 L fermentation medium. The Response Surface Methodology (RSM) was used for the modelling and optimization process (Minitab 16) with input parameters of temperature (18–42 °C), substrate loading (13-37 g/L), pH of the medium (3.8-6.1), time of operation (46-96 h) and agitation (82-318 rpm) (Table 5.1). The corresponding range of input parameters has been carefully selected according to previous studies on lignocellulosic waste [7]. The inoculum loading was fixed at 10% (w/v) since it is the standard acceptable quantity usually implemented for xylose fermentation processes [262]. The central composite design was generated using MINITAB 16 software. The design matrix had 32 cubic points, eight center points in a cube and ten axis points. The α value was calculated to be 2.366. A total of 54 independent runs with different combinations of parameters at different levels were designed. Each experiment (run) was experimentally evaluated, and xylitol concentration was recorded, respectively. Experimental data was used to fit the polynomial model equations to explain the effect of the considered parameters on xylitol concentration.

Table 5.1 Design parameters and their level in RSM

Level	Parameters				
	Agitation (rpm)	**pH**	**Temperature (℃)**	**Time (hr)**	**Xylose (g/L)**
	A	**B**	**C**	**D**	**E**
-α	82	3.81	18	46	13
-1	150	4.5	25	60	20
0	200	5	30	70	25
1	250	5.5	35	80	30
+α	318	6.18	42	94	37

5.2.7.1. Study of optimization using Response Surface Methodology (RSM) and Artificial Neural Networks (ANN)

For the utilization of the RSM technique in optimization, a prototype, namely a comprehensive second-order polynomial, needs to be calculated to find out the comparative impact of the respective medium component. L_N (N factor at L levels) is the number of experiments configured by RSM; however, in each procedure, merely two or three groups can be implemented, and the plotting is confined to two variants at a time. Because of the metabolic intricacy of microorganisms and the commonly diverse range of parameters involved, designing stringent models to illustrate the high non-linearity and stability is a crucial problem [186]. By effective implementation of RSM, numbers of fermentation systems can be reasonably approximated by second-order relation. ANN is frequently utilized as "black box" models of key variants whose affinity to different processing units is neither established nor formally explained [187]. ANN has been effectively used for modelling, optimization, system design and control because of its ability to learn and strain boisterous signals. Furthermore, ANN easily universalizes information using a training procedure [188].

The most commonly used modelling and optimization technique for fermentation and bioprocess is RSM, one variable at a time approach (OVAT) and factorial Design of Experiment (DOE) [184,185]. These methodologies are broadly utilized, and their concepts and drawbacks are commonly known. Such as, in the case of VAT, the interactive effect of parameters does not consider the process; hence, the optimal set points may be neglected [189]. On the other hand, DOE is not much more attractive because it is time, labor-intensive, and resource-demanding when the number of simulation data is increased. However, in the case of RSM, it ignores the less significant variables with a confined understanding of their possible interactive effects on the bioprocess output. Nowadays, the most promising technique for modelling and optimization of bio-processes is Artificial intelligence tools. Some of them are Genetic Algorithm (GA), Artificial Neural Network (ANN), Particle Swarm Optimization, Fuzzy Logic and Ant Algorithm, all of these are mainly used in research and development for designing bio-process [113,191]. In the last few years, ANN has mainly been used in research and development for multivariate bioprocesses. Bioprocess models developed by ANN are devoid of previous information concerning metabolic fluxes and kinetics that happen inside the cells, and surrounding seals pretend the connection that exists in biological neurons with unique zing ability of association, analysis adaption and learning [189].

ANNs can be explained by the mathematical understanding of the neurological functioning of the human brain. They emulate the brain's learning process by arithmetically modelling the network structure of interconnected nerve cells [113,191]. ANN is a structure like a multiprocessor computer system, consisting of simple processing components known as neurons. Like neurons in the brain, the ANN shows the connection and adapt properties among the elements. Moreover, previous knowledge of the events that govern the process is not required in ANNs because it is an entirely data-based process. The first layer of the ANN structure is known as the input layer.

Further, one and more hidden layers are there, followed by an output layer (Figure 5.1). Formation of multi-layer neurons occurs when a set of single-layer neurons is connected. Figure 5.1 demonstrates the framework of multi-layer ANN [186]. The sources of info are provided to the first layer of neurons, which thus is associated with the second layer and subsequent layers. The hidden layer's neurons help establish a complex network between the input and output parameters. Usually, bioprocess modelling and optimization are difficult for fermentations because it exhibits non-linear relationships. Applying the ANN model detects process non-linearities and defines a model that connects process inputs to appropriate output parameters [192].

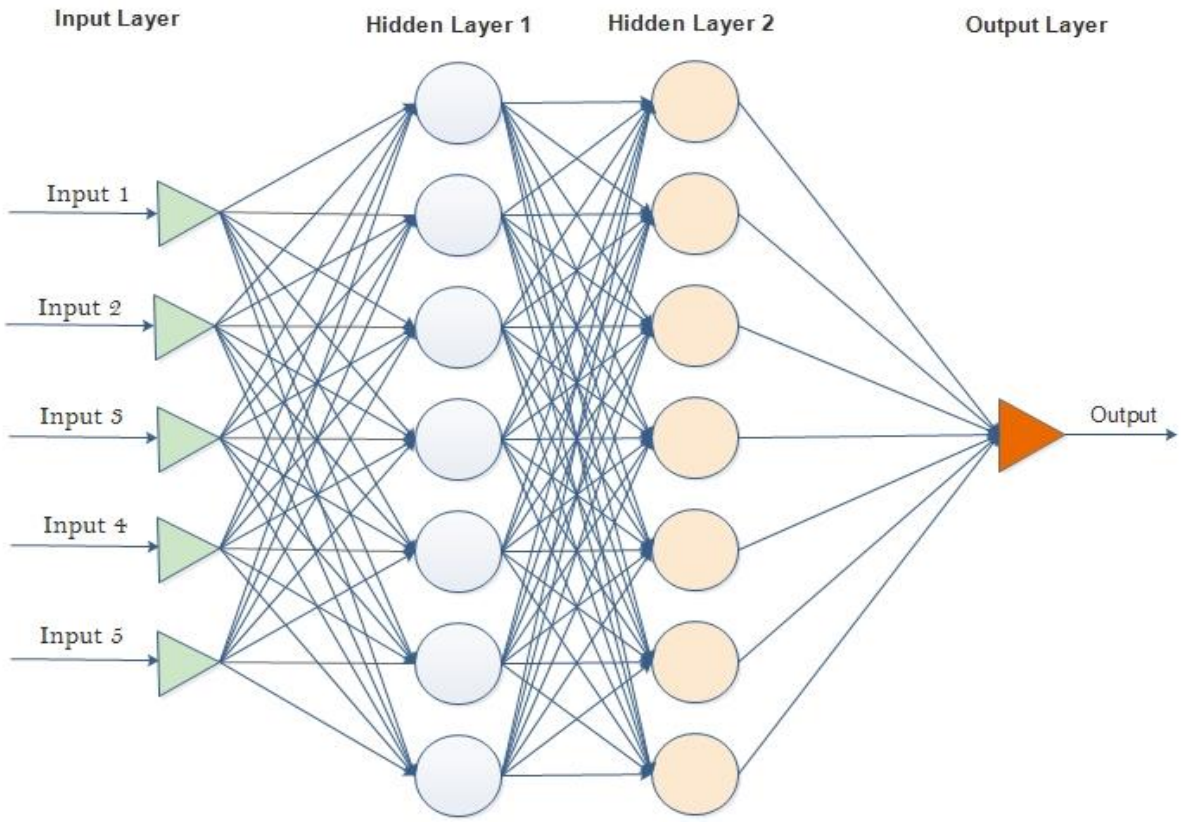

Figure 5.2 General Structure of a multilayer an artificial neural network [190]

ANN is a system that collects the input, works on the data, and gives an output. Mathematically, Figure 5.3 describes this technique more appropriately. All information is added simultaneously and altered by the weights. In Figure 5.3, x_0, x_1, x_2... x_n are the input of neurons from the dendrite. Generally, x_0 is the model's bias input, usually +1. Their synaptic weights wk_1, wk_2, wk_3... wk that measure their importance are labelled accordingly per their inputs. Negative values of the synaptic weights express their inhibitory effect [190]. The excitation level of the neuron is measured by the weighted sum of input values which are as follows:

$$v\kappa = \sum_{j=1}^{p} \omega\kappa j x_j \tag{5.2}$$

When threshold θk is reached, the value of excitation level entices a neuron output Yk, which models the electric impulse produced by the biological axon. The activation function $\varphi(v\kappa)$ gives the non-linear output value by controlling the amplitude of the output. The arithmetical expression of neuron function can be shown according to

$$\gamma\kappa = \varphi(v\kappa) = \begin{cases} 1 & if \quad v\kappa \geq 0 \\ 0 & if \quad v\kappa \angle 0 \end{cases} \text{ Where, } v\kappa = \sum_{j=1}^{p} \omega\kappa j x_j \tag{5.3}$$

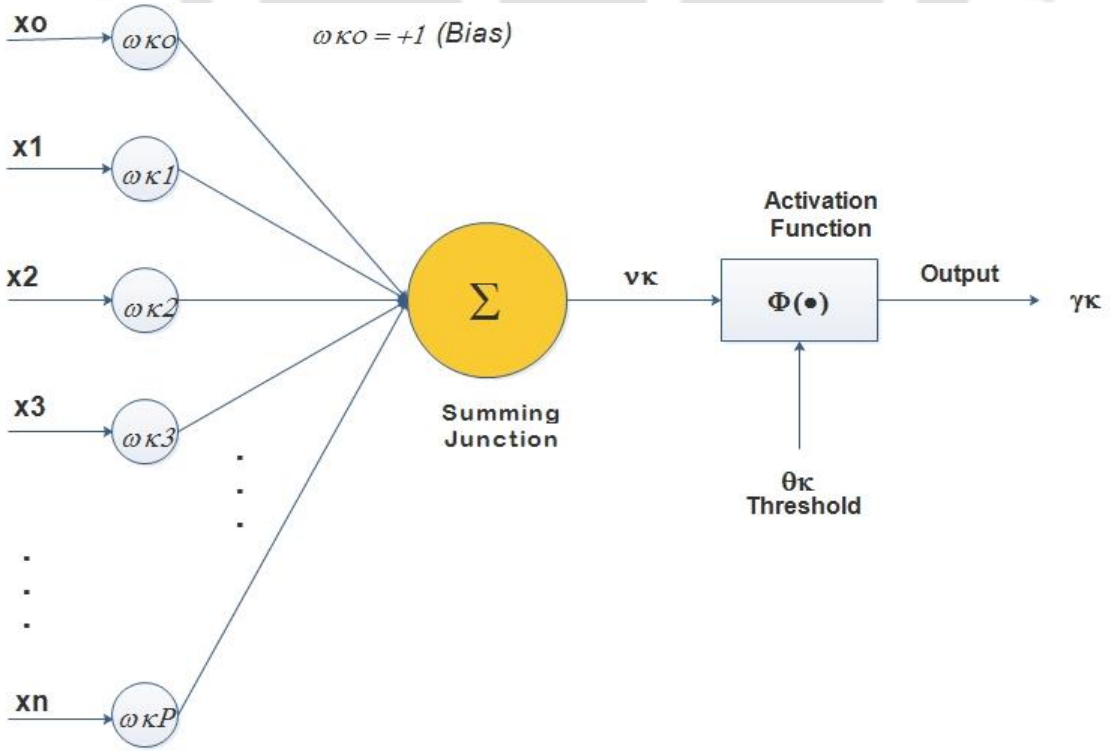

Figure 5.3 Mathematical model of artificial neuron [190]

5.2.7.2. Statistical analysis of data

Minitab16 software was used to conduct a Statistical Analysis of all the results, representing the mean, standard error (mean standard deviation). To better understand the performance of ANN models, statistical expressions based on root mean square error (RMSE) and determination coefficient were employed (R^2).

5.2.8. Microbial fermentation

Xylitol production was carried out by preparing fermentative media (shown in Figure 5.1) from the pH 10 detoxified hydrolysate (PD10), pH 5.5 detoxified hydrolysate (PD5.5), charcoal detoxified hydrolysate (CDH), resin detoxified hydrolysate (RDH) and standard synthetic solution (SSS). Xylose concentration (g/L) in case of PD10, PD5.5, CD, RD and SSS were 6.25, 7.707, 7.386, 7.060 and 8.00 respectively. Xylose concentration act as main sugar substrate in the hydrolysate and was supplemented with yeast extract,10 g/L; $(NH_4)_2SO_4$, 5 g/L; KH_2PO_4, 15 g/L; and $MgSO_4 \cdot 7H_2O$, 1 g/L. pH of the fermentative medium was kept between 4.5 and 5. 4.0% (v/v) yeast strain culture were trasferred (inoculated) into the fermentation medium prepared from the various detoxified hydrolyzate. Fermentation was carried out at 30 ± 1 °C for 90 h, 200 rpm. Samples were collected after every 6 h of time interval and stored in cold place after centrifugation for 15 min, 10,000 rpm.

5.2.9. Fluorescence Microscopy

Candida cells were visualized under Inverted Microscope with Fluorescence (Nikon, Ti-S with camera, Model: DS-Fi2-U3). For fluorescent labeling, stock solution of Methylene Blue (MB) was prepared. This solution was diluted two fold followed by filtration by passing through a 0.22 µm membrane filter (MILLEX GP 0.22 µm; Merck Millipore Ltd., India). A 2.5 µL sample volume was pipetted onto a glass slide (VWR, India) and mixed with 2.5 µL filtered MB solution to a final concentration of 25 µg/mL. Imaging was performed for PD10, PD5.5, CD, RD, SSS, and YPD samples under constant laser irradiation.

5.2.10. High-Performance Liquid Chromatography (HPLC) Analysis

Quantitative determination of various components such as, xylose, glucose, phenols, HMF and furfural were performed by HPLC using an AMINEX ion exchange column (BioRad, HPX87C, Richmond) and a refractometer (BioRad, 1770, Richmond). A 5 mM sulfuric acid (H_2SO_4) - aqueous solution was used for the analysis as a mobile phase media. The analysis was performed on 0.6 mL min^{-1} flow rate at 60 °C.

5.2.11. Total phenolic content (TPC) determination

The TPC of the hydrolysate was quantified using the Folin-Ciocalteu assay method, which has been previously described in the literature. The absorbance of the sample at 765 nm was measured using a UV-Visible spectrophotometer (Make: Thermo Fisher Scientific, Waltham, Massachusetts, USA; Model: UV-2600), and the TPC was determined in units of mg gallic acid equivalent per 100 g of the sample.

5.3. Results and discussion

5.3.1. Process optimization for production maximum hemicellulosic hydrolysate

5.3.1.1. Experimental design for hemicellulosic hydrolysate

Areca nut husk were considered having great potential of hemicellulosic fraction was hydrolyzed to their constituents sugar by performing dilute sulfuric acid hydrolysis. This hydrolysis was performed under mild operating condition to obtain areca nut hemi-cellulosic hydrolysate. In order to higher yield of xylose from areca nut husk for production of xylitol, it is necessary to optimize hydrolysis condition. Optimum hydrolysis condition supports higher yiled of xylitol, which does not required too much of treatment before fermentation. Therefore, this study evaluated the effects of three operating parameters (such as; solid-liquid ratio, acid concentration, and hydrolysis time) on dilute sulfuric acid hydrolysis of areca nut husk hemicellulose fraction.

5.3.1.2. Analysis of solid to liquid ratio on the recovery of xylose from areca nut husk

Impact of solid to liquid ratio (% w/v) on the recovery of xylose concentration from areca nut husk hemicellulose was reported in Table 5.2. The lowest xylose concentration 3.31 g/L was observed when the lowest concentration of biomass (1% w/v biomass in 5% v/v in sulfuric acid for 60 min) was used. The highest xylose concentration 37.20 g/L was observed when 15% w/v of biomass was used in 2% v/v of sulfuric acid for 60 min. Therefore, from Table 5.2, the major components of the hydrolysates i.e., xylose concentration increases initially with increase in solid loading and then decreases with further increases in solid loading. However, the concentration of toxic components also increase simultaneously but the rate of formation is low as compare to xylose rate.

5.3.1.3. Analysis of acid concentration on the recovery of xylose from areca nut husk

The hydrolysis experiment was further conducted by hydrolyzing hemicellulose with sulfuric acid at a concentration in the range of of 1.35 to 5.0% at a solid loading of 1% w/v.

This hydrolysis was continued untill the optimum operating conditions for maximum recovery of xylose concentration in the hydrolysates were achieved. The effect of acid concentrations on areca nut hemicellulosic hydrolysis and concentration of xylose in hydrolysates were reported in Table 5.2. About 3.78 g/L of xylose was obtained from areca nut with a solid loading of 1% w/v in liquid solution by using 1.35% v/v sulphuric acid at 121 °C for 20 mins. However, as there is increase in sulfuric acid concentration during acid hydrolysis, xylose concentration decreased slightly. Whereas amount of toxic components increases by increasing the concentration of acid. This decrease in xylose concentration may be happened due to the degration of xylose by furfural and this is consistent with with the previous analysis. Compared to glucose, xylose is highly susceptible to degradation to furfural. This is particularly noticeable when the concentration of acid exceeds 1% and the reaction temperature exceeds 121 °C [263]. Torget et al. also showed that degradation of xylose at 160 °C is proportional to reaction time and acid concentration [264]. It can be observed that the concentrations of HMF and furfural increased with increasing acid concentration reaction time.

5.3.1.4. Analysis of reaction time on the recovery of xylose from areca nut husk

The effect of reaction time on the xylose concentration present in the hydrolysate during hydrolysis of areca nut husk was reported in Table 5.2. The total concentration of xylose increases as there was increase in reaction time for low acid concentration (i.e., 1.35% v/v). But, as the concentration of acid increases from 1.35 to 2 % v/v, no major change in xylose concentration was noticed by increasing the reaction time. However, slight incresase in inhibtors compounds concentration was noticed. This analysis shows that the maximum extaction of xylose from areca nut husk biomass takes place at 1.35% v/v sulfuric acid concentration and the formation of toxic components at this condition is minimum.

Table 5.2 Influence of different parameters during acid hydrolysis of Areca nut husk

Biomass Conc. (w/v)	Acid Conc. (v/v)	Hydrolysis Time (min)	Glucose (g/L)	Xylose (g/L)	Arabinose (g/L)	TPC (g/L)	HMF (g/L)	Furfural (g/L)
1%	1.35%	20	0.060 ± 0.7	3.783 ± 0.6	0.777 ± 0.5	0.477 ± 0.3	0.211 ± 0.4	0.065 ± 0.6
1%	1.35%	40	0.080 ± 0.5	4.899 ± 0.8	0.945 ± 0.6	0.684 ± 0.4	0.644 ± 0.2	0.073 ± 0.3
1%	1.35%	60	0.095 ± 0.4	5.665 ± 1.1	1.118 ± 0.5	1.903 ± 0.3	0.710 ± 0.8	0.084 ± 0.7
1%	2.70%	20	ND	2.344 ± 0.4	1.052 ± 0.4	0.391 ± 0.4	0.468 ± 0.4	0.027 ± 0.8
1%	2.70%	40	ND	2.506 ± 0.6	1.433 ± 0.5	0.135 ± 0.7	0.707 ± 0.4	0.054 ± 0.5
1%	2.70%	60	ND	2.972 ± 0.6	0.408 ± 0.4	0.778 ± 0.8	0.782 ± 0.1	0.018 ± 0.9
1%	5%	20	ND	2.926 ± 0.4	2.144 ± 0.5	0.564 ± 0.5	0.793 ± 1	0.086 ± 0.6
1%	5%	40	ND	2.895 ± 0.6	1.927 ± 0.6	0.638 ± 0.9	0.511 ± 0.9	0.109 ± 0.4
1%	5%	60	0.020 ± 0.2	3.310 ± 0.3	2.280 ± 0.5	2.644 ± 0.6	0.563 ± 0.4	0.234 ± 0.2
5%	2%	60	2.171± 0.4	10.701 ± 0.7	1.019 ± 0.8	8.148 ± 0.4	4.054 ± 0.7	0.465 ± 0.8
10%	2%	60	2.082 ± 0.2	33.727 ± 0.8	0.767 ± 0.4	9.393 ± 0.2	7.742 ± 0.4	0.382 ± 0.3
15%	2%	60	1.440 ± 0.8	37.202 ± 0.5	0.569 ± 0.3	12.777 ± 0.8	9.360 ± 1.9	0.407 ± 1
5%	5%	60	1.665 ± 0.4	24.225 ± 0.9	3.701 ± 0.7	22.002 ± 0.3	6.428 ± 0.6	0.805 ± 0.8
10%	5%	60	2.915 ± 0.4	16.909 ± 0.6	2.151 ± 0.3	7.538 ± 0.2	4.084 ± 0.4	0.570 ± 0.6
15%	5%	60	1.962 ± 0.3	28.053 ± 0.4	1.779 ± 0.3	13.044 ± 0.3	7.211 ± 0.8	0.551 ± 0.9

TPC: Total phenolic compounds; **HMF**: Hydroxymethylfurfural; **ND**: Not detected

5.3.2. Detoxification of hemicellulosic acid hydrolysate

Table 5.2 summarizes the major components of areca nut husk hydrolysates prior to treatment with different modes of detoxification and after detoxification. The major problem encountered when treating the lignocellulose with acids. Formation of TPC, HMF, furfural and other unidentified toxic products were formed during acid treatment. Therefore, it is necessary to minimize the concentration of these toxic prior used for the fermentation. Otherwise it will inhabit the growth of microorganism which will not result the better fermentability of the hydrolysate and causes to reduce the yield of xylitol. Thus, obtained areca nut hemicellulosic hydrolysate was mainly treated with chemical (pH adjustment), activated charcoal and ion exchange resins which causes to reduce toxic components in the hydrolysate.

5.3.2.1. Detoxification by pH adjustment

The detoxification of areca nut husk hydrolysate by adjusting pH value initially to 10 followed by 5.5, results no major loss of xylose. Toxic components, such as TPC, HMF and furfural, were slightly reduced by these steps. However, phenolic compounds do not substantially remove by this process. Huang et al. researched that the sugar content gets lowered by alkalization, which reduce the fermentation efficiency of hydrolysate [265]. Though, this causes to require additional technique for the removal of calcium sulfate and phosphate precipitate [266].

5.3.2.2. Detoxification by activated charcoal

Detoxification by treatment with activated charcoal (CD) leads to decrease the phenolic compound by 78% and about 0.164 g/L of TPC concentration still remained in the solution. It shows that activated charcoal detoxification was the basic step for detoxifying acid hydrolysates. Misra et al. observed that treatment of acid hydrolysate with activated charcoal was basic step, which mainly helps in the reduction of TPC which formed during acid hydrolysis [267]. Ge et al. analyzed that detoxification by adjusting pH and treatment with activated charcoal entirely removed the furfural, whereas phenolic compounds and acetic acid gets lowered by 96.6% and 62.4% correspondingly [268].

5.3.2.3. Detoxification by ion exchange resin

The resin treatment removed almost all phenolic compounds, furfural, HMF, and arabinose present in the areca nut hydrolysate. After treatment with an ion exchange resin,

there was no major loss of xylose concentration. Canilha et al. observed that treatment with ion exchange resins causes loss of sugar as compared to pH adjustment and the use of activated charcoal [269]. The methods used for detoxification of acid hydrolysate in the present study was like above reported methods with minor modifications. The present study, the reduction in HMF and furfural concentrations using the same procedure was observed about 99%.

5.3.3. FTIR Analysis of hemicellulosic hydrolysate

FTIR spectroscopy was performed in the region of 500 – 4000 cm^{-1} to compare the molecular conformational changes of the dilute sulphuric acid (H_2SO_4) treated areca nut hemicellulosic hydrolysate and hydrolysate obtained after various detoxification technique. FTIR profile was mentioned in Figure 5.4, the absorbance at 3315 cm^{-1} was due to the hydroxyl group. This usually occurs as a result of bonding between polymers and its strength is affected by the sample concentration [245]. Moreover, a band was detected at 2347 cm^{-1}, indicating CH expansion and contraction vibrations because of presence of CH_3 and CH_2 functional groups. In contrast, band at 1369 cm^{-1} was due to the presence of CH bending vibration in hemicelluloses and cellulose chemical structures [270]. Absorbance signal around 1630 cm^{-1} was observed due to water absorbed by xylan type polysaccharides [247]. The sharp absorption peak around at 1087 cm^{-1} depicted typically for xylan which was mainly arises due to the CO and CC stretching oscillations having glycosidic bonds. The low-intensity wavenumber at 1222 cm^{-1} was detected only in the birchwood fraction and showed a connection with the arabinosyl side chain [271]. In contrast, the extracted hemicellulose signal appeared at 1757 cm^{-1}. This was due to the hemicellulose fraction dissolved during the water treatment and contains a small amount of acetyl, ester bonds of the carboxyl groups [270]. In addition, the lower absorbance at 1526 cm^{-1} appeared due to aromatic skeletal oscillations of the associated lignin [245]. FTIR spectral analysis confirmed that toxic components (such as ester and carboxyl groups) were significantly removed after various detoxification modes.

Table 5.3 Characterization of Areca nut husk hydrolysates according to the treatments applied for detoxification.

Treatment	Glucose (g/L)	Xylose (g/L)	Arab. (g/L)	TPC (g/L)	HMF (g/L)	Furfural (g/L)
ANH	0.161 ± 1.02	7.293 ± 1.13	1.013 ± 0.78	1.021 ± 0.23	0.426 ± 0.01	0.132 ± 0.210
PD10	0.114 ± 1.01	6.252 ± 1.57	0.922 ± 1.07	0.582 ± 0.07	0.026 ± 0.03	0.039 ± 0.024
PD5.5	0.165 ± 0.57	7.707 ± 1.09	0.979 ± 0.87	0.784 ± 0.17	0.087 ± 0.07	0.048 ± 0.034
CDH	0.139 ± 0.83	7.386 ± 1.97	0.744 ± 0.62	0.164 ± 0.07	0.047 ± 0.07	0.029± 0.006
RDH120	0.131 ± 0.004	7.122 ± 0.87	0.685 ± 0.42	0.046 ± 0.11	0.042 ± 0.11	0.016± 0.003
RDH410	0.126 ± 0.003	7.060 ± 0.62	0.649 ± 0.57	0.027 ± 0.04	0.037 ± 0.108	0.011 ± 0.005

Arab: Arabinose; **FUR**: Furfural; **HMF**: Hydroxymethylfurfural; **TPC**: Total phenolic compounds

AH: Acid hydrolyzate without any treatment.

pH 10 and pH 5.5: Hydrolyzate with pH adjusted to 10 and then bring back to pH 5.5.

Activated Charcoal: Treatment with activated charcoal.

Resin IRA 120 and IRA 410: Treated hydrolyzate after the use of ion exchange resin IRA 120 & IRA 410, respectively.

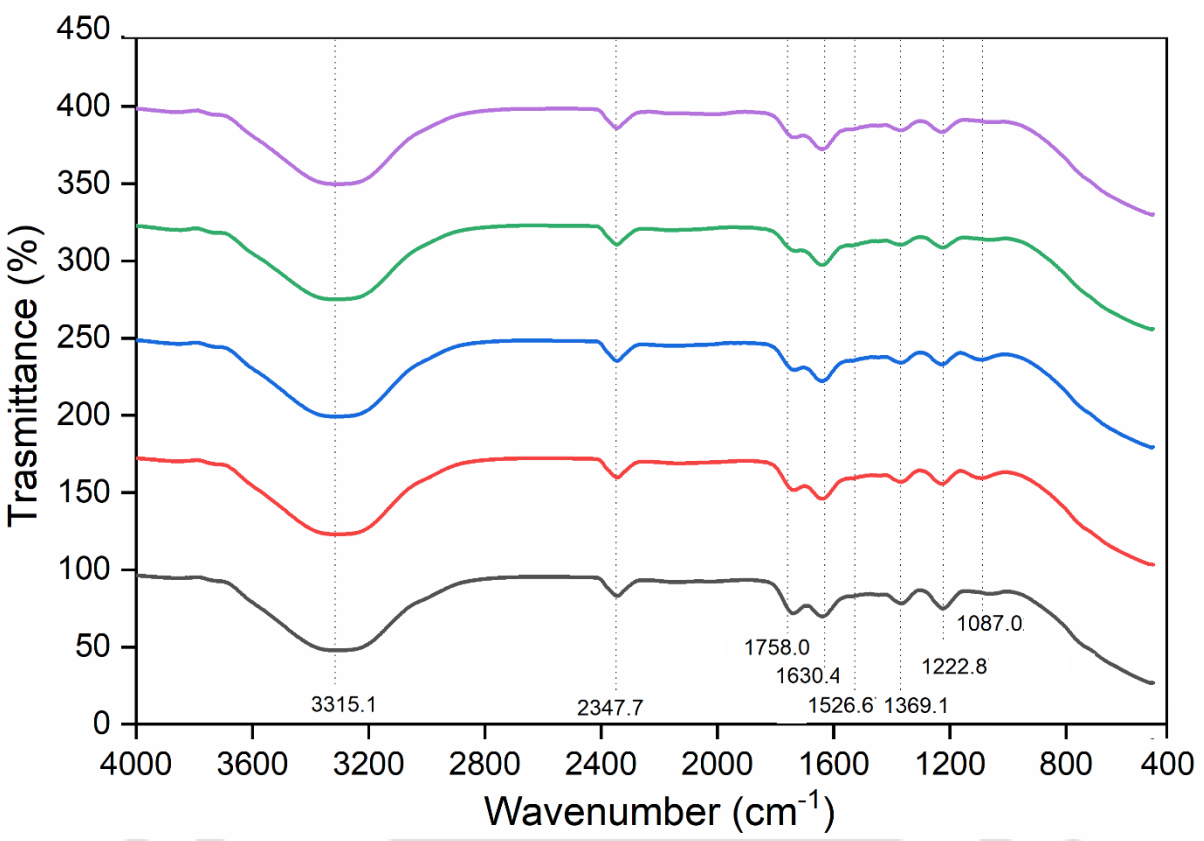

Figure 5.4 FTIR analysis of Hydrolysate; RDH, CDH, PD5.5, PD10, ANH

5.3.4. Cell growth analysis of *C. tropicalis*

The growth behavior of *C. tropicalis* in YPD media and various fermentative media, including PD10, PD5.5, CDH, RDH, and SSS, was investigated and graphically represented in Figure 5.5. It was observed that *C. tropicalis* reached its maximum growth of approximately 11 g/L after 30 hours of incubation in YPD, but the growth rate eventually became stationary over time. However, the presence of toxic components in the media impeded the growth rate of *C. tropicalis*. In fact, the concentration of cells decreased by 46%, 38%, 10%, and 6% for PD10, PD5.5, CDH, and RDH, respectively, in comparison to SSS. Toxic components, such as phenol, HMF, and furfural, were found to significantly prolong the lag phase of *C. tropicalis*, as shown by the growth curve in Figure 5.5. Interestingly, in the case of PD10 and PD5.5, there was a significant difference in pH which caused about an 11% reduction in the concentration of cell biomass (change of weight from 3.65 to 4.15 g/L for PD10 and PD5.5 respectively). Treatment with activated charcoal makes a significant increase in *C. tropicalis* growth and it increases from 4.13 to 6.05 g/L for PD5.5 and CDH

respectively. While in the case of PD5.5 and RDH, there is about a 34 % difference in the concentration of cell biomass. However, all samples PD10, PD5.5, CDH, RDH, SSS and YPD attained the stationary phase at the same time. The final weight of biomass for PD10, PD5.5, CDH, RDH, and SSS in the stationary phase is about 3.65 g/L, 4.13 g/L, 6.05 g/L, 6.28 g/L and 6.71 g/L respectively. The observed growth inhibition and decrease in xylitol yield in the presence of toxic components highlight the need for effective detoxification methods in hydrolysate fermentation [266].

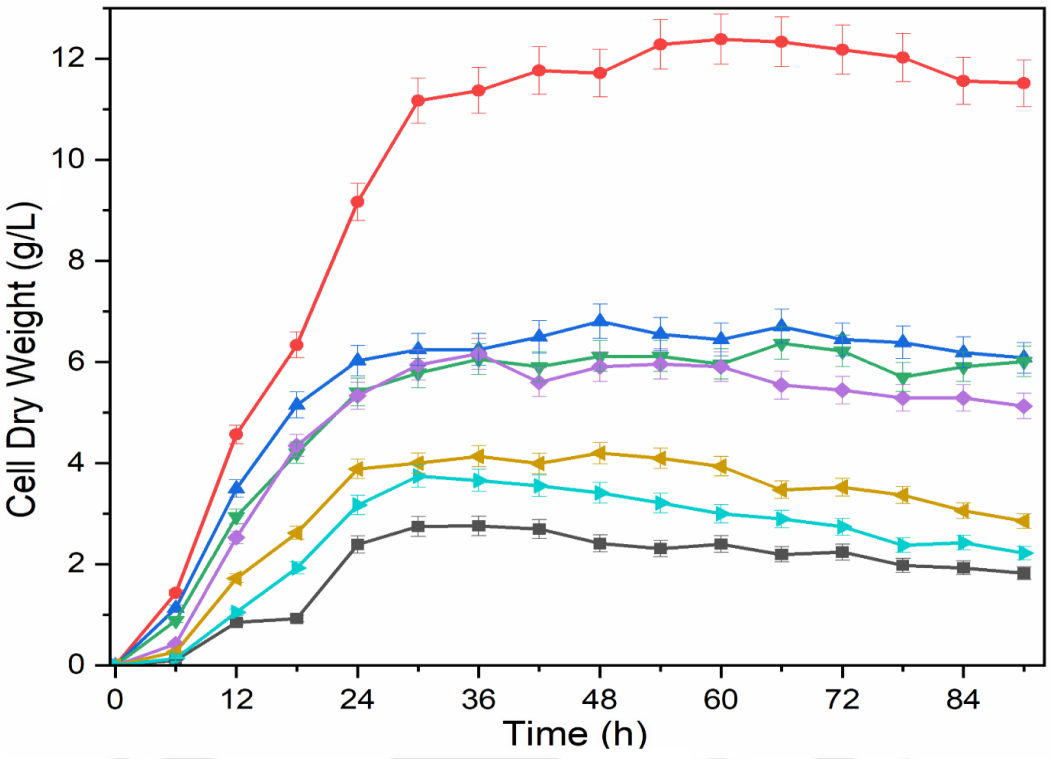

Figure 5.5 Growth curve of *C. tropicalis* in fermentative and YPD medium; YPD, SSS, RDH, CDH, PD5.5, PD10, ANH

Treatment with activated charcoal makes significant increase in *C. tropicalis* growth and it increases from 4.13 to 6.05 g/L for PD5.5 and CD respectively. While in the case of PD 5.5 and RD, there is about 34 % difference in concentration of cell biomass. However, all samples PD 10, PD 5.5, CD, RD, SSS and YPD attained the stationary phase at the same time. The final weight of biomass for PD 10, PD 5.5, CD, RD, SSS in stationary phase is about 3.65 g/L, 4.13 g/L, 6.05 g/L, 6.28 g/L and 6.71 g/L respectively. This may be the possible reason which clarify that growth of *C. tropicalis* get hampered in presence toxic components. Subsequentelly, inhabitation in growth of *C. tropicalis* during fermentation of hydrolysate causes decrease in xylitol yield [266].

5.3.5. Optimization of fermentation process

5.3.5.1. RSM modelling

Fermentation was carried out as per the design matrix mentioned in Table 5.1. After completion of each run, the amount of xylitol produced was noted in the Table 5.4. The coefficients for experimental variables were derived using linear interactive and quadratic coefficients. The consecutive sum of squares and descriptive statistics were used to determine the regression model's limitation and strength. For developing predictive models for xylitol concentration, a second-order polynomial regression analysis was performed. Experimental data were used to derive a coded polynomial equation, describing xylitol concentration as a simultaneous function of agitation, pH, temperature, time of operation and xylose concentration. The coefficient of each parameter is represented in Table 5.5. The quadratic model thus obtained was assessed using the Analysis of Variance (ANOVA), and the results are presented in Table 5.6. From that data and RSM plots, it can be observed that all the factor (both linear and quadratic) has a significant effect on xylitol production, but the interaction effect of agitation with other parameters was not significant, although the interaction effect of temperature with pH and time was significant. Observation revealed that a good interaction effect on pH of the fermentation broth and agitation speed maintained in the reactor. Increasing the pH of the medium reduces the yield of xylitol (Figure 5.6a). The surface plot (Figure 5.6b) revealed that a sudden change in temperature has a negative effect on xylitol yield. To obtain the maximum yield of xylitol, an optimum pH and temperature should always maintain in the reactor. With increasing time of operation, the yield of xylitol increases, but once the xylitol concentration reaches around 9 g/L, the effect of agitation in the reactor becomes less significant (Figure 5.6c). There is no significant interaction effect on xylitol yield for varying agitation, pH, temperature, time with varying xylose concentration present in the fermentation broth. Solubility of xylose may be the probable reason for this (Figure 5.6d, 5.6g, 5.6h, 5.6j). A bell-shaped graph (Figure 5.6e) showed that a proper combination of pH and temperature could only facilitate the growth of *Candida tropicalis*, which leads to the maximum yield of xylitol. Increasing operation time won't improve the yield of xylitol if the pH and temperature of the broth are not properly maintained (Figure 5.6f, 5.6i).

Table 5.4 Design Matrix and experimental variables and their corresponding experimental and RSM and ANN predicted values

Run no	Parameters					Experimental Result	Predicted Result	
	A	B	C	D	E	Xylitol (g/L)	RSM	ANN
1	-1	-1	-1	-1	-1	6.32	6.09	6.48
2	1	-1	-1	-1	-1	6.39	6.56	6.37
3	-1	1	-1	-1	-1	6.96	6.55	6.63
4	1	1	-1	-1	-1	7.01	7.09	7.27
5	-1	-1	1	-1	-1	8.39	7.93	9.03
6	1	-1	1	-1	-1	8.42	8.31	9.32
7	-1	1	1	-1	-1	8.49	8.03	8.09
8	1	1	1	-1	-1	8.62	8.49	8.44
9	-1	-1	-1	1	-1	7.01	6.98	6.76
10	1	-1	-1	1	-1	7.14	7.52	6.71
11	-1	1	-1	1	-1	7.27	7.25	6.99
12	1	1	-1	1	-1	7.57	7.87	7.48
13	-1	-1	1	1	-1	8.56	8.40	8.33
14	1	-1	1	1	-1	8.61	8.87	9.26
15	-1	1	1	1	-1	8.66	8.32	8.34
16	1	1	1	1	-1	8.72	8.86	8.51
17	-1	-1	-1	-1	1	6.35	6.17	6.58
18	1	-1	-1	-1	1	6.41	6.64	6.09
19	-1	1	-1	-1	1	6.98	6.62	6.85
20	1	1	-1	-1	1	7.02	7.16	6.85
21	-1	-1	1	-1	1	8.44	8.03	8.89
22	1	-1	1	-1	1	8.42	8.42	8.30
23	-1	1	1	-1	1	8.54	8.13	8.71
24	1	1	1	-1	1	8.7	8.59	8.59
25	-1	-1	-1	1	1	7.02	7.06	6.32
26	1	-1	-1	1	1	7.17	7.60	6.84
27	-1	1	-1	1	1	7.26	7.33	7.15
28	1	1	-1	1	1	7.6	7.95	7.26
29	-1	-1	1	1	1	8.64	8.52	8.70
30	1	-1	1	1	1	8.69	8.98	8.33
31	-1	1	1	1	1	8.71	8.43	8.59
32	1	1	1	1	1	8.75	8.97	8.60
33	0	0	0	0	0	9.8	10.01	9.67
34	0	0	0	0	0	9.8	10.01	9.67
35	0	0	0	0	0	9.9	10.01	9.67
36	0	0	0	0	0	10	10.01	9.67
37	0	0	0	0	0	9.8	10.01	9.67
38	0	0	0	0	0	9.9	10.01	9.67
39	0	0	0	0	0	9.9	10.01	9.67
40	0	0	0	0	0	9.85	10.01	9.67

41	-2.366	0	0	0	0	6.2	7.65	6.78
42	2.366	0	0	0	0	10.1	8.84	6.44
43	0	-2.366	0	0	0	6.02	5.84	6.23
44	0	2.366	0	0	0	5.98	6.36	7.10
45	0	0	-2.366	0	0	2.09	1.54	2.62
46	0	0	2.366	0	0	4.17	4.92	7.85
47	0	0	0	-2.366	0	6.96	7.94	10.55
48	0	0	0	2.366	0	10.21	9.43	9.87
49	0	0	0	0	-2.366	8.81	9.10	8.46
50	0	0	0	0	2.366	9.41	9.32	7.66
51	0	0	0	0	0	9.82	9.63	9.67
52	0	0	0	0	0	9.93	9.63	9.67
53	0	0	0	0	0	9.91	9.63	9.67
54	0	0	0	0	0	9.86	9.63	9.67

Table 5.5 Estimated Regression Coefficients for Xylitol (g/L)

Term	**Coefficient**
Constant	9.81
Block	0.18
Agitation (rpm)	0.25
pH	0.11
Temperature	0.71
Time (hr)	0.31
Xylose (g/L)	0.04
Agitation (rpm)*Agitation (rpm)	-0.24
pH*pH	-0.63
Temperature*Temperature	-1.14
Time (hr)*Time (hr)	-0.16
Xylose (g/L)*Xylose (g/L)	-0.07
Agitation (rpm)*pH	0.01
Agitation (rpm)*Temperature	-0.02
Agitation (rpm)*Time (hr)	0.01
Agitation (rpm)*Xylose (g/L)	7.59
pH*Temperature	-0.08
pH*Time (hr)	-0.04
pH*Xylose (g/L)	-0.001
Temperature*Time (hr)	-0.10
Temperature*Xylose (g/L)	0.008
Time (hr)*Xylose (g/L)	0.001

Table 5.6 Analysis of Variance for RSM Model

Source	DF	Seq SS	Adj SS	Adj MS	F
Blocks	1	1.462	1.467	1.467	5.14
Regression	20	130.092	130.092	6.504	22.81
Linear	5	29.606	29.606	5.921	20.76
Agitation (rpm)	1	2.734	2.734	2.734	9.59
pH	1	0.53	0.53	0.530	1.86
Temperature	1	21.963	21.963	21.963	77
Time (hr)	1	4.288	4.288	4.287	15.03
Xylose (g/L)	1	0.091	0.091	0.090	0.32
Square	5	99.792	99.792	19.958	69.98
Agitation (rpm)*Agitation (rpm)	1	1.562	3.636	3.635	12.75
pH*pH	1	19.458	23.74	23.739	83.23
Temperature*Temperature	1	76.795	77.989	77.988	273.43
Time (hr)*Time (hr)	1	1.638	1.707	1.707	5.99
Xylose (g/L)*Xylose (g/L)	1	0.339	0.339	0.339	1.19
Interaction	10	0.695	0.695	0.069	0.24
Agitation (rpm)*pH	1	0.011	0.011	0.011	0.04
Agitation (rpm)*Temperature	1	0.013	0.013	0.012	0.04
Agitation (rpm)*Time (hr)	1	0.011	0.011	0.011	0.04
Agitation (rpm)*Xylose (g/L)	1	0	0	0	0
pH*Temperature	1	0.252	0.252	0.252	0.88
pH*Time (hr)	1	0.068	0.068	0.068	0.24
pH*Xylose (g/L)	1	0	0	0	0
Temperature*Time (hr)	1	0.336	0.336	0.336	1.18
Temperature*Xylose (g/L)	1	0.002	0.002	0.002	0.01
Time (hr)*Xylose (g/L)	1	0	0	0	0
Residual Error	32	9.127	9.127	0.285	
Lack-of-Fit	22	9.085	9.085	0.413	98.12
Pure Error	10	0.042	0.042	0.004	
Total	53	140.681			

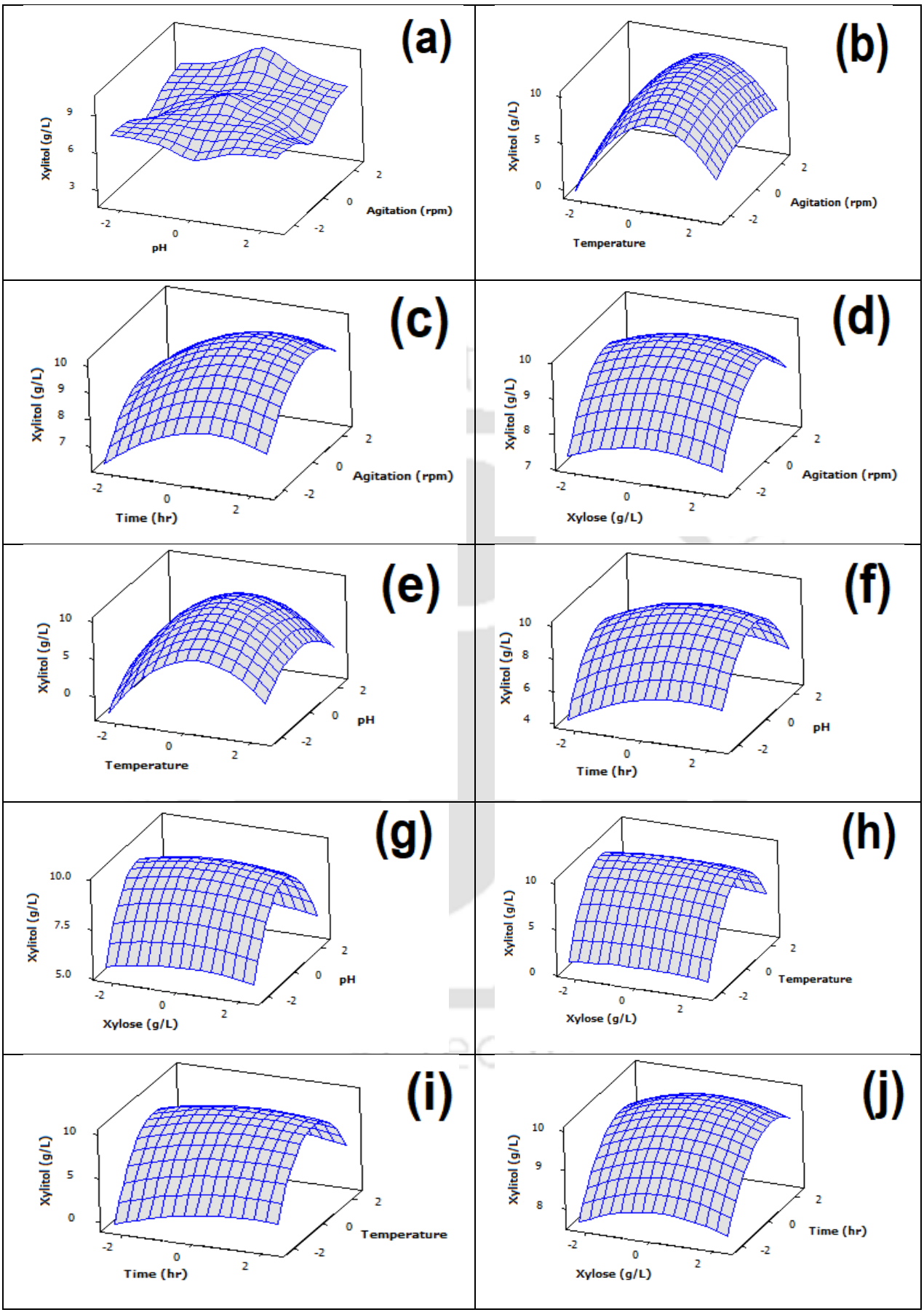
(a)
Xylitol (g/L)
9
6
3
-2
0
2
pH
2
0
-2
Agitation (rpm)
(b)
Xylitol (g/L)
10
5
0
-2
0
2
Temperature
2
0
-2
Agitation (rpm)
(c)
Xylitol (g/L)
10
9
8
7
-2
0
2
Time (hr)
2
0
-2
Agitation (rpm)
(d)
Xylitol (g/L)
10
9
8
7
-2
0
2
Xylose (g/L)
2
0
-2
Agitation (rpm)
(e)
Xylitol (g/L)
10
5
0
-2
0
2
Temperature
2
0
-2
pH
(f)
Xylitol (g/L)
10
8
6
4
-2
0
2
Time (hr)
2
0
-2
pH
(g)
Xylitol (g/L)
10.0
7.5
5.0
-2
0
2
Xylose (g/L)
2
0
-2
pH
(h)
Xylitol (g/L)
10
5
0
-2
0
2
Xylose (g/L)
2
0
-2
Temperature
(i)
Xylitol (g/L)
10
5
0
-2
0
2
Time (hr)
2
0
-2
Temperature
(j)
Xylitol (g/L)
10
9
8
-2
0
2
Xylose (g/L)
2
0
-2
Time (hr)

Figure 5.6 Response surface plots showing the interaction of different parameters during xylitol fermentation process. **(a)** Surface Plot of Xylitol (g/L) vs Agitation (rpm), pH **(b)** Surface Plot of Xylitol (g/L) vs Agitation (rpm), Temperature **(c)** Surface Plot of Xylitol (g/L) vs Agitation (rpm), Time (h) **(d)** Surface Plot of Xylitol (g/L) vs Agitation (rpm), Xylose(g/L) **(e)** Surface Plot of Xylitol (g/L) vs pH, Temperature **(f)** Surface Plot of Xylitol (g/L) vs pH, Time (h) **(g)** Surface Plot of Xylitol (g/L) vs pH, Xylose (g/L) **(h)** Surface Plot of Xylitol (g/L) vs Temperature, Xylose (g/L) **(i)** Surface Plot of Xylitol (g/L) vs Temperature, Time (h) **(j)** Surface Plot of Xylitol (g/L) vs Time (h), Xylose (g/L)

5.3.5.2. ANN modelling

Multi-layer perceptron (MLP) with the logistic sigmoid function was used to develop ANN-based process models. An MLP with feed-forward architecture comprised of five input nodes (agitation, pH, temperature, incubation period, xylose concentration) and one output node (xylitol concentration) was used. The first step was to optimize the ANN model to minimize the number of dimensions and errors during the training and testing of the data sets. The experiment's design and the resulting experimental yield were fed into the neural network during training. To minimize over-training and over-parameterization, the data were segregated into training, validation, and test sets. The hidden layers of neurons were varied, as were the initialization and learning rate parameters, during the data training process. Selecting the parameter weights with the lowest RMSE values proved the model's ability to generalize. The RMSE for the test set was lowest for the MLP with 10 nodes in its hidden layer. The predicted and experimental sets had a correlation coefficient of 0.998.

5.3.5.3. Validation of model's forecasts

The predictive models were validated by doing tests in triplicate under the optimal conditions and comparing the results. The optimized predicted conditions were agitation speed 227 rpm, pH 5.01, temperature 31 ℃, time of operation 79 h and xylose concentration 26.55 g/L with the desirability of 99%. Using such recommended conditions experiment was conducted, and the average value of xylitol was observed to be around 9.96 g/L. Compared to the models' predictions, this was a close match to the actual results. Following optimization, it was observed that there was a strong correlation between the anticipated and experimental values, which further supported the validity of the models.

5.3.5.4. Model comparison between RSM and ANN

The use of statistical techniques enabled the determination of the optimal fermentation conditions that result in the highest possible output of xylitol. The present study examined the

forecasting abilities of RSM and ANN models to see which was more accurate. Modelling using RSM is simpler than modelling with ANN because ANN requires a greater number of inputs to make better predictions than RSM (Figure 5.7). Although the present study observed that there is not a statistically significant difference (P = 0.872) observed between these two models. In terms of prediction and optimization capabilities, ANN outperforms RSM, whereas sensitivity analysis is more exact in RSM. RSM is advised for the modelling of a new process, whereas ANN is best suited for the modelling of non-linear systems with interactions greater than quadratic in nature. Furthermore, there is no requirement for a prior formulation of an appropriate fitting function in ANN.

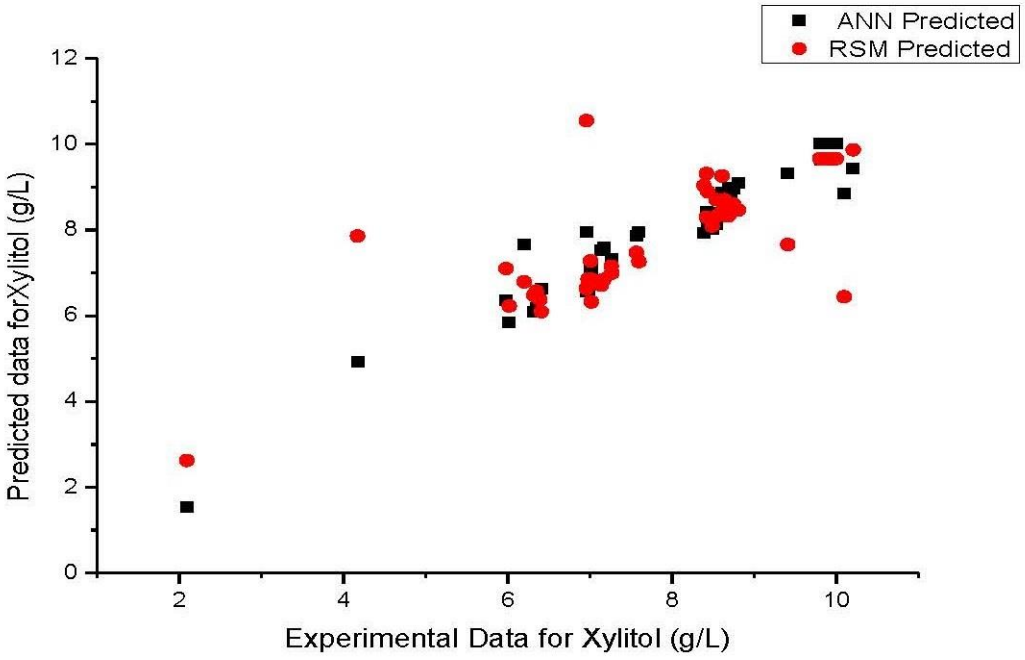

Figure 5.7 Comparison of experimental and projected xylitol production values

5.3.6. Xylitol production by fermentation

5.3.6.1. Fermentation process

To study the possibility of xylitol production from areca nut hemicellulose hydrolysates submerged fermentation was performed using *C. tropicalis* and hemicellulose hydrolysate of areca nut husk (such as PD10, PD5.5, CD, RD, and SSS) as a substrate. Although some researcher reported that yeast can produce xylitol from non-detoxified (only pH adjusted) hemicellulosic acidic hydrolysate. However, reported yield was about 0.38 g/g which is very low. Therefore, production of xylitol still requires detoxification of the hemicellulose hydrolysates for higher yield [272]. Many methods have been attempted to

detoxify hemicellulose hydrolysates with respect to the fermentability of detoxified hemicellulose hydrolysates, the different methods used in detoxifying hemicellulose hydrolysates can be significantly different. Out of these methods, pH adjustment, treatment with activated charcoal followed by ion exchange resins are considered to be the most economical procedure for removing toxic compounds from hydrolysates [175,177].

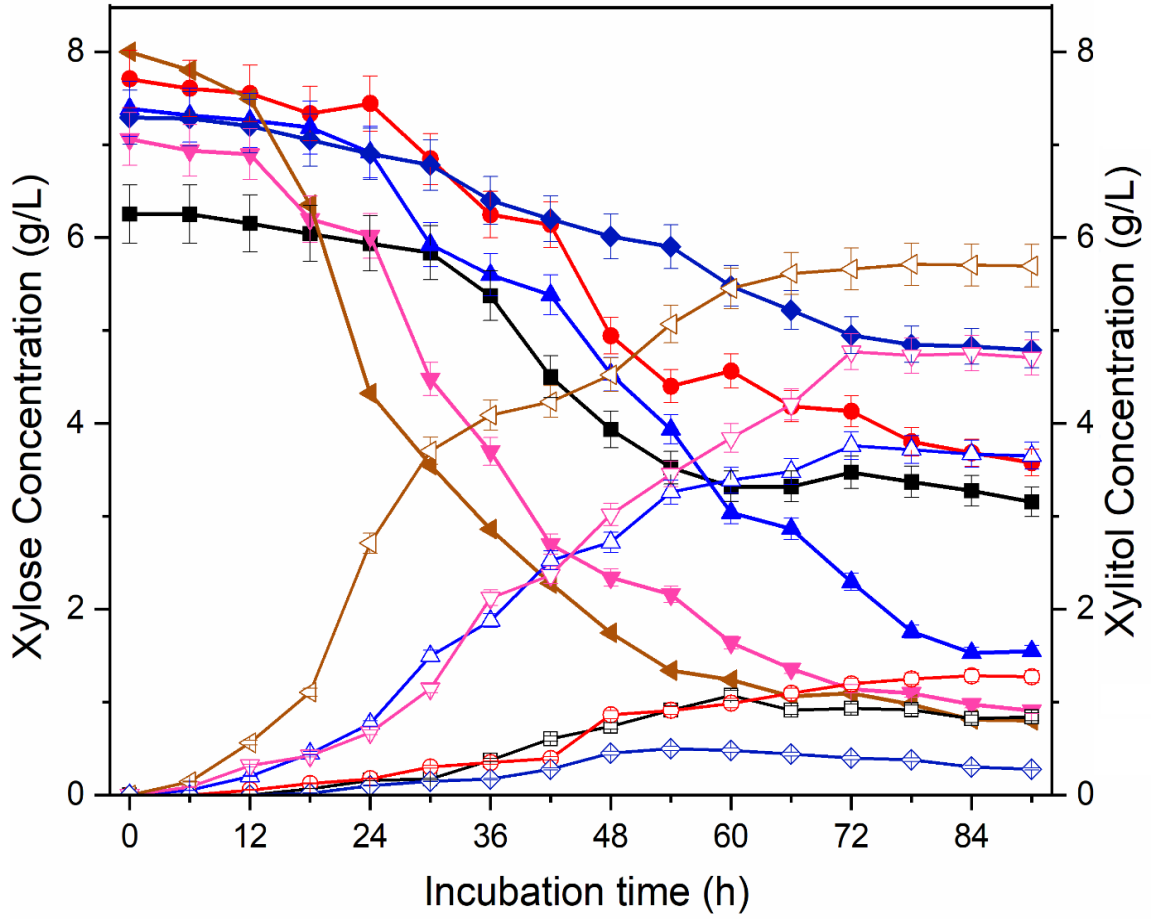

Figure 5.8 Fermentation media xylose consumption; SSS, RDH, CDH, PD5.5, PD10, ANH and corresponding xylitol production; SSS, RDH, CDH, PD5.5, PD10, ANH

The results shown in Figure 5.8 and tabulated in Table 5.7 revealed the production of xylitol from pH treated areca nut hemicellulosic hydrolysate. The maximum yields of xylitol from PD10 and PD5.5 were 0.13 g/g and 0.19 g/g respectively, noted after fermentation of 90 h. About 46% increase in xylitol yield was observed when the pH of the fermentative solution was reduced from 10 to 5.5. This finding is consistent with other studies, where *C. tropicalis* was able to produce xylitol from pH-adjusted corn fiber hemicellulosic acid hydrolysates with comparatively lower yield of 0.17 g/g [273]. Converti et al. 2000 carried out similar type of research by fermenting pH adjusted hemicellulosic wood hydrolysate with *Pachysolen*

tannophilus, and reported the yield of xylitol about 0.46 g/g [135]. Considerably, xylitol yield increase may be due to the addition of sodium sulfite. Other researcher also reported that the fermentation efficiency of hydrolysate could be enhance by addition of reducing reagents (such as, sodium sulfite) [173].

Xylitol fermentation profile for activated charcoal treated areca nut hemicellulosic hydrolysate was shown in Figure 5.8. The maximum yield of xylitol was observed around 0.49 g/g which is higher than the yield observed for PD5.5 hydrolysate. Canilha et al. reported the xylitol yield of about 0.54 g/g can be produced by using activated charcoal treated hemicellulosic wheat straw acid hydrolysate as a starting material for *Candida guilliermondii* FTI20037 [274]. de Albuquerque et al. conducted similar type of experiment and estimated the xylitol production by using *Kluyveromyces marxianus* CCA510 when fermenting activated charcoal treated cashew apple bagasse hydrolysate as a substrate [275]. These analyses revealed that activated charcoal can minimize the presence of toxic compounds (such as TPC, HMF and furfural) from areca nut hemicellulosic hydrolysate and an optimum yield of xylitol 0.49 g/g was obtained. Correspondingly, Parajó et al. fermented activated charcoal treated wood hydrolysate by *Debaryomyces hansenii* NRRL Y-7426 and reported maximum yield of xylitol about 0.32–0.35 g/g [276].

Figure 5.8 revealed that yield of the xylitol from areca nut hemicellulosic hydrolysate treated with cation anion exchange resins is about 0.66 g/g. This yield is the highest among all the detoxified hydrolysates and is 34% greater than the yield obtained from the charcoal-detoxified hydrolysate (CDH). However, this yield is 15% lower than the yield from the standard synthetic solution (SSS) (fermentation of pure xylose with additive nutrients), which is approximately 0.71 g/g. The possible reason for a lower yield in the case of RDH may be due to the potential presence of slightly toxic components in the RDH fermentation media. Ko et al. performed similar type of work and reported the yield of xylitol about 0.73 g/g after fermentation of Hardwood hydrolysate by *C. tropicalis* BCRC 20520 [277]. Santana et al. carried out the similar work and reported that a maximum yield of xylitol is about 0.52 g/g, when fermenting cocoa pod hydrolysate by *C. boidinii* after treatment with cation anion exchange resins [266].

In accordance with the above research work analysis, pH adjustment, activated charcoal treatment, and ion exchange resin were combined to detoxify the hemicellulose hydrolysate of areca nut husk and maximize the yield of xylitol production. From Figure 5.8 analyzed that a maximum production of xylitol was 0.66 g/g attained by fermenting these

hydrolysates with *C. tropicalis*. Xylitol production from areca nut acid hydrolysate was increased significantly after combination of all detoxification techniques. The increase in xylitol yield was mainly due to removal of inhibitors like phenolic compounds, furfural and hydroxy-methyl-furfural. All these compounds generated during lignin degradation process [35]. All such chemicals inhibit the growth of microorganism during fermentation because of its toxic nature. This inhibition greatly impacts the yield of the xylitol production. In this study, it was observed that potential inhibitors formed during hemicellulose extraction of xylose and acid hydrolysis have a significant impact on xylitol production from untreated hemicellulose hydrolysates.

Table 5.7 Comparative analysis of cell biomass, xylose and xylitol

Fermentative substrate	Xylose concentration in fermentative media (g/L)	Concentration of cell biomass in fermentative media (g/L)	Xylitol yield (g/g)
YPD	-	11 ± 0.94	-
ANH	7.29 ± 1.18	2.43 ± 1.07	0.08 ± 0.77
PD10	6.25 ± 1.08	3.65 ± 1.57	0.14 ± 0.47
PD5.5	7.70 ± 1.13	4.13 ± 1.06	0.19 ± 0.65
CDH	7.38 ± 0.89	6.05 ± 0.68	0.49 ± 0.75
RDH	7.06 ± 1.02	6.28 ± 0.76	0.66 ± 0.35
SSS	8.00 ± 1.05	6.71 ± 0.84	0.71 ± 0.45

Table 5.8 Comparison of xylitol production in literature survey.

Feedstocks	Micro-organisms	Methods of detoxification	Xylitol yield (g/g)	References
corncob	*C. tropicalis*	pH adjustment	0.61	[272]
cocoa pod husk	*C. boidinii*	pH adjustment, activated charcoal & ion exchange resins treatment	0.52	[266]
Synthetic medium	*C. boidinii*	Activated carbon and cationic ion exchange resins adsorption	0.48	[278]
Corncob hemicellulosi	*C. tropicalis*	pH adjustment and activated charcoal treatment	0.77	[262]

c hydrolysate				
Hemicellulosic liquor from sugarcane bagasse	*C. tropicalis*	pH adjustment, activated charcoal & ion exchange resins treatment	0.68	[279]
Eucalyptus hemicellulose hydrolysate	*C. guilliermondii FTI 20037*	Ion exchange resins treatment	0.68	[280]
Hardwood hydrolysate	*C. tropicalis BCRC 20520*	Activated charcoal & ion exchange resins treatment	0.73	[277]
Sugarcane bagasse hydrolysate	*C. guilliermondii FTI 20037*	Over liming and activated charcoal treatment	0.75	[281]
Corn fiber hydrolysate	*C. tropicalis*	pH adjustment and activated charcoal treatment	0.4	[273]
Areca nut hemicellulosic hydrolysate	*C. tropicalis*	pH adjustment, activated charcoal & ion exchange resins treatment	0.74	In this study

The important process (like pH adjusted, treated with charcoal and resins) for xylitol production by fermenting hemicellulose hydrolysate was also evaluated. All the different methods of xylitol production from various materials were listed in Table 5.8. Different combination of detoxification technique was performed to eliminate the toxic components present in the hemicellulosic hydrolysate. Further fermentation was conducted by using this detoxified hydrolysate. Comparison analysis of results reveled that yield of xylitol get differs from process to process of detoxification. Combination of detoxification technique such as, pH adjustment, treatment with activated charcoal and ion exchange resin has been used in many processes as a process of superior operability at minimal cost. Rao et al. 2016 researched by following this protocol and reported that *C. tropicalis* could easily fermentate this detoxified hemicellulosic hydrolysate to optimum yield of xylitol about 0.48 g/g [278]. Jia et al. in 2016 reported comparable results that maximum 0.77 g / g of xylitol yield was achieved when corncob detoxified (detoxification was conducted in combination with pH adjustment, activated charcoal and resin-treated) hemicellulose hydrolysates was fermentated

by using *C. tropicalis* [265]. In present research, by using this (pH adjusted, treated with charcoal and resins) protocol, highest xylitol yield was obtained than the all above results. After analyzing this result, it can be concluded that detoxification by pH adjustment, activated charcoal and ion exchange resins treatment plays crucial role for removal of toxins and fermentation of detoxified hemicellulosic hydrolysate becomes more easier by *C. tropicalis*.

5.3.6.2. Viability analysis of *C. tropicalis* in fermentation media

The findings presented in Figure 5.9 (a, b, c, d, e, and f) showcase the growth dynamics of *C. tropicalis* during its stationary growth phase, which occurs after 36 hours of incubation. The cell viability analysis was carried out using the methylene blue staining (MBS) technique, which revealed varying degrees of viability among different concentrations of toxic components present in PD10, PD5.5, CDH, and RDH. The MBS test results demonstrated that cell growth was severely hindered in the presence of toxic components, leading to the death of about 80% cells in the early stages of fermentation, as depicted in Figure 5.9 (a) and Figure 10. This made the continuation of fermentation arduous. PD10 and PD5.5, both containing a considerable number of toxic components, exhibited poor growth of *C. tropicalis* in fermentative media. In addition, a high pH level resulted in increased cell death during pH detoxification (as shown in Figure 5.9 and Figure 10), whereas lowering the pH from 10 to 5.5 led to an increase in the proportion of living cells. However, upon increasing the level of detoxification, from pH adjustment to activated charcoal, and subsequently to resin detoxification, living cells increased accordingly from 60% to 92%, due to the depletion of toxic components in the hydrolysate. The highest proportion of living cells about 88% and 92% was observed in resins RDH and SSS, as depicted in Figure 5.9 (d), Figure 5.9 (e) and Figure 10 respectively, with the maximum living cells (about 97%) recorded in YPD media growth. The findings from Table 5.7 indicate that as the detoxification level increases, resulting in a decrease in toxic components, the growth of cells increases correspondingly, as confirmed by cell viability analysis. The study notes the inhibitory impact of high concentrations of toxic components on the growth of *C. tropicalis* in fermentation broth, leading to cell death and reduced xylitol yield. Nevertheless, the results suggest that changing the detoxification technique can significantly increase the proportion of living cells by decreasing the level of toxic components (as shown in Figure 5.9 and Figure 10), resulting in higher xylitol yield [282].

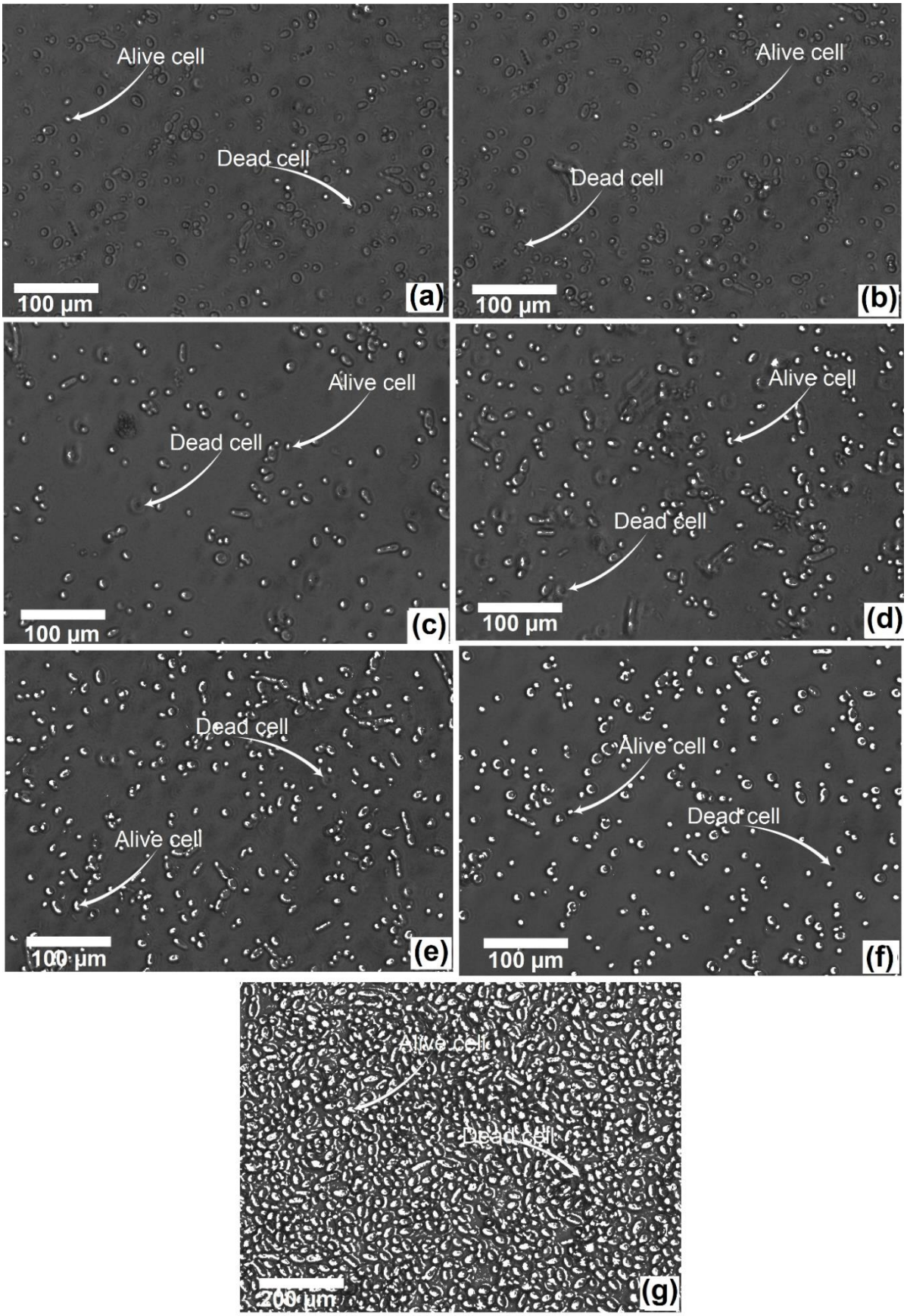

Figure 5.9 Viability analysis of *C. Tropicalis* in growth media;(a) ANH, (b) PD10, (c) PD5.5, (d) CDH, (e) RDH, (f) SSS, (g) YPD

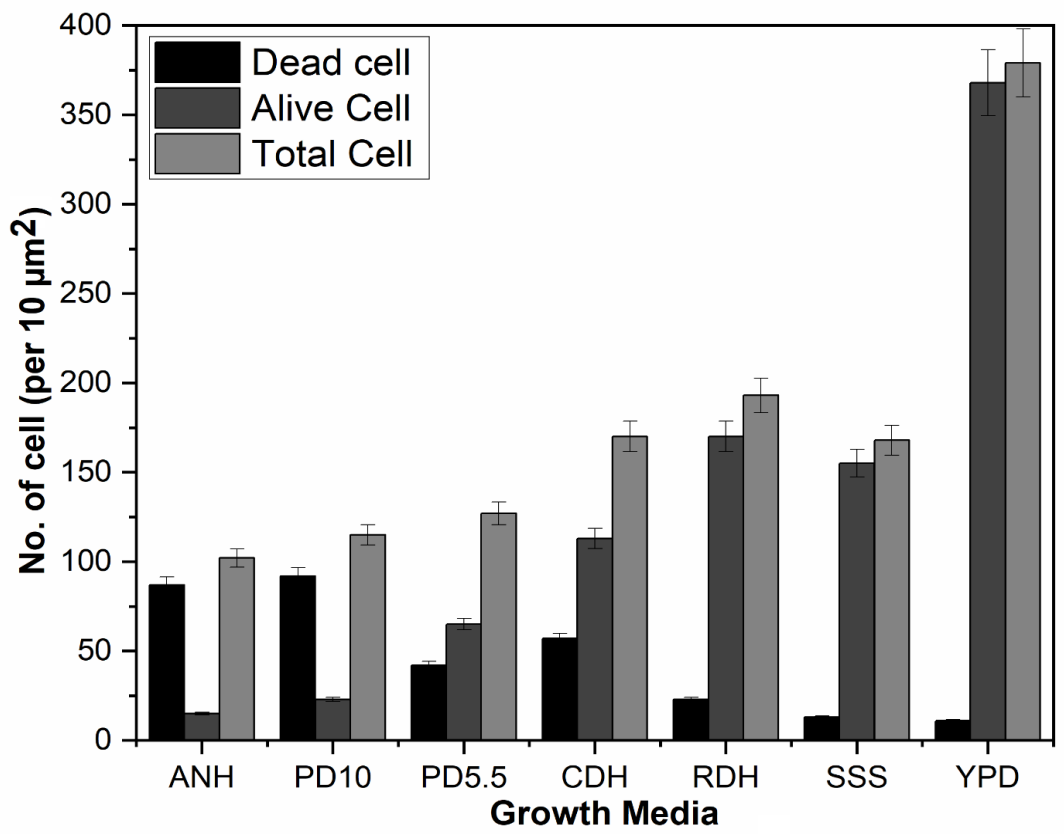

Figure 5.10 Quantitative viability analysis of *C. Tropicalis* in growth media

5.4. Conclusions

Xylitol production is gaining more attention due to the growing demand in the food and pharmaceutical industry, given that it has the same sweetness as sucrose. Researchers have been working on improving the yield of xylitol to make the process more economical and competitive. In this study, the focus was on extracting hemicellulose from areca nut husk through dilute sulfuric acid (H_2SO_4) hydrolysis. Optimal recovery of xylose from areca nut husk hemicellulosic fraction was achieved by using a mixture of 1% w/v solid and 1.35% v/v sulfuric acid at 120 °C reaction temperature for 20 min. Detoxification methods, such as pH adjustment, treatment with activated charcoal, and ion exchange resins, were employed to remove toxic components. More than 99% of toxic components, including TPC, HMF, and furfural, were removed after detoxification. The optimized conditions were used for submerged fermentation process using C. tropicalis for xylitol production, resulting in an optimal yield of 0.13, 0.19, 0.49, and 0.66 g/g for PD10, PD5.5, CDH, and RDH, respectively. It was concluded that the combination of all detoxification techniques, such as pH adjustment, treatment with activated charcoal, and ion exchange resins, increased the yield of xylitol up to 0.66 g/g.

भारतीय प्रौद्योगिकी संस्थान गुवाहाटी
Indian Institute of Technology Guwahati

Chapter 6

Downstream process for separation of xylitol from fermentation broth and crystallization

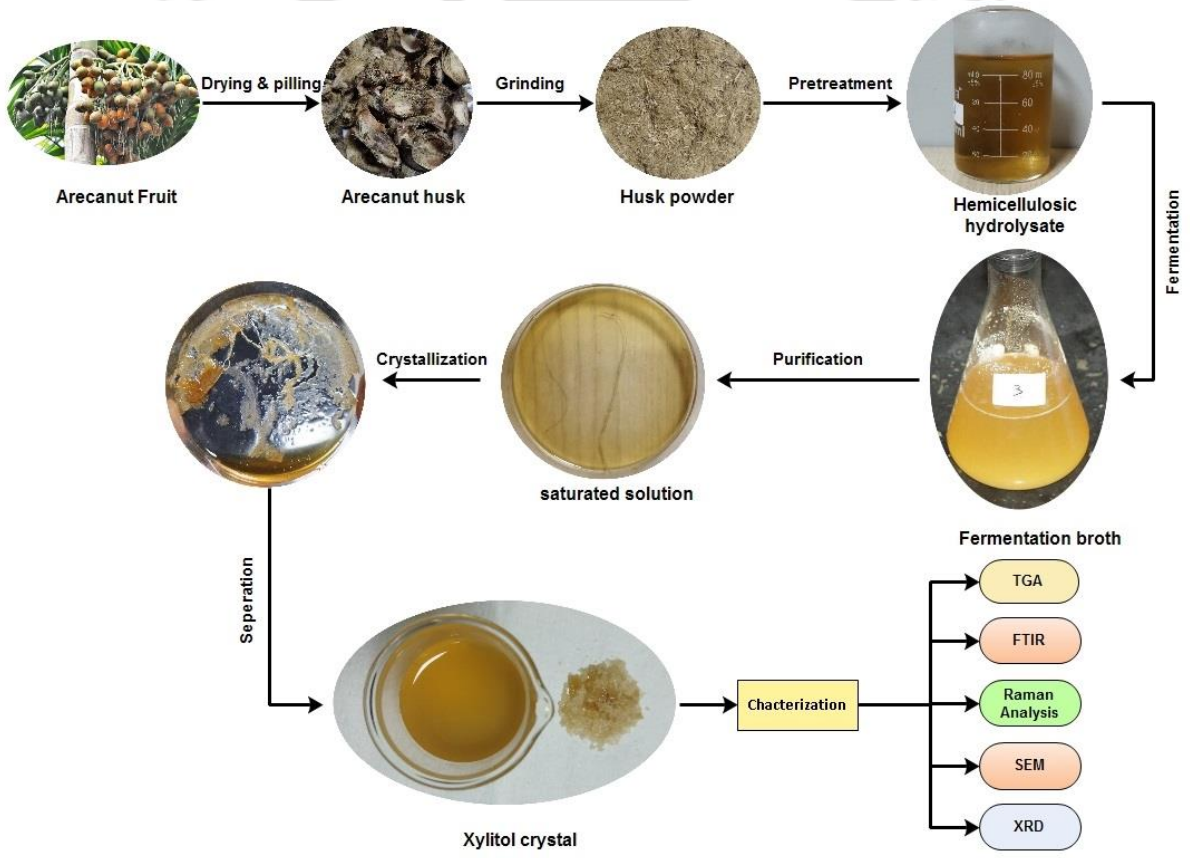

6.1. Overview

Xylitol is a sugar substitute that is becoming increasingly popular in the food and pharmaceutical industry due to its benefits. Researchers have been striving to improve the yield of xylitol to make the production process more cost-effective and competitive. Fermentation is a sustainable approach for producing xylitol using agro-industrial by-products, and it has the potential to lower the production cost. However, the purification process to obtain the final product has not been fully developed yet. This study focused on the optimization of xylitol production via fermentation, followed by the purification and characterization of xylitol crystals. X-ray diffraction, thermogravimetric analysis, differential scanning calorimetry, and Raman analysis were performed to study the properties of the xylitol crystals. The analysis showed that the melting process of commercial xylitol crystals after crystallization and xylitol crystals from fermentation broth was almost the same, with melting points at 93.71 °C and 91.73 °C, respectively, and enthalpies of 210.7 J/g and 220 J/g, respectively.

6.2. Materials and Methods

6.2.1. Microorganism and Inoculum preparation

Candida tropicalis (MTCC 6192) was obtained from MTCC Chandigarh. The culture was maintained at 4 °C on agar slants comprising of 1 % (w/w) peptone, 1 % (w/w) glucose, 0.5 % (w/w) yeast extract and 2 % (w/w) agar. The inoculation medium contained: xylose, 20 g/L; yeast extract,10 g/L; KH_2PO_4, 15 g/L; $(NH_4)_2SO_4$, 5 g/L; and $MgSO_4 \cdot 7H_2O$, 1 g/L. Colonies were transferred from the plate to a 500 mL Erlenmeyer flask containing 100 mL inoculum. The Erlenmeyer flask was incubated on a rotary shaker at 200 rpm and maintained at 30 °C for 24 h. Yeast extract, xylose and salt solution were sterilised individually in an autoclave at 121 °C for 20 minutes.

6.2.2. Substrate

The areca nut husk used in this study was obtained from the local market of Guwahati, Assam. The substrate was washed, dried at 60 °C for 48 h, and then ground into fine powder followed by sieving (mesh size-BSS 30) to get particles of about 1–5 mm long and 1 mm thick. The powdered substrate was then pre-treated using dilute sulfuric acid, as described in a previous study [6]. The powdered pre-treated substrate was stored at room temperature in an airtight container.

6.2.3. Experimental design and fermentation process

The fermentation process was carried out in a 5 L bioreactor containing a 1.5 L fermentation medium. The Response Surface Methodology (RSM) was used for the modelling and optimisation process (Minitab 16) with input parameters of temperature (18–42 °C), substrate loading (13-37 g/L), pH of the medium (3.8-6.1), time of operation (46-96 h) and agitation (82-318 rpm) (Table 5.1). The corresponding range of input parameters has been carefully selected according to previous studies on lignocellulosic waste [7]. The inoculum loading was fixed at 10% (w/v) since it is the standard acceptable quantity usually implemented for xylose fermentation processes [262]. The central composite design was generated using MINITAB 16 software. The design matrix had 32 cubic points, eight centre points in a cube and ten axis points. The α value was calculated to be 2.366. A total of 54 independent runs with different combinations of parameters at different levels were designed. Each experiment (run) was experimentally evaluated, and xylitol concentration was recorded, respectively. Experimental data was used to fit the polynomial model equations to explain the effect of the considered parameters on xylitol concentration.

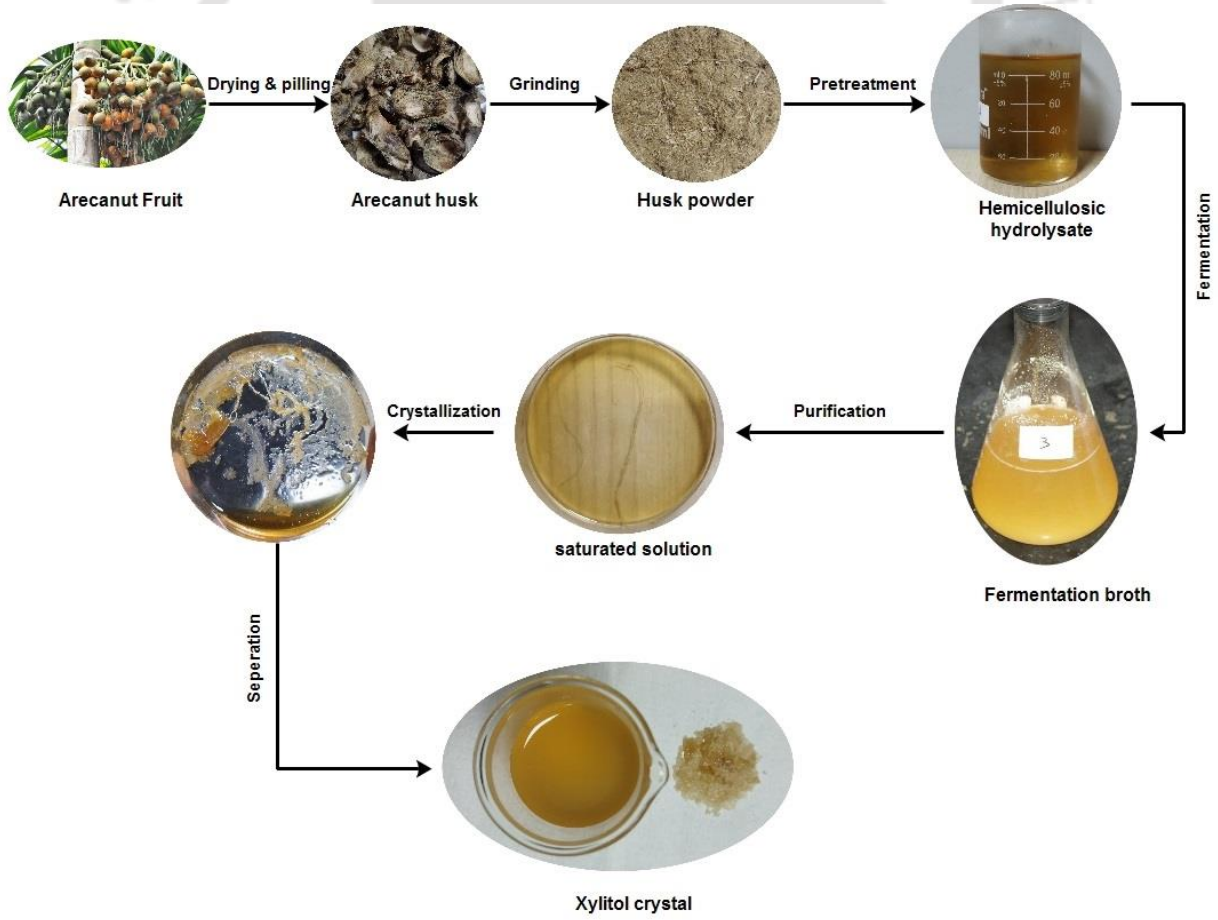

Figure 6.1 Different steps involved in the production of xylitol from lignocellulosic biomass

6.2.4. Downstream process

6.2.4.1. Fermented broth processing and concentration

After production of xylitol by fermentation, the fermentation medium was centrifuged at 2000 X g for 15 minutes using a centrifuge (Model number: 216P, Manufacturer: Sigma, Germany) as shown in Figure 6.1. The fermented broth was collected and treated with 3N NaOH to pH 7.00, followed by filtration through a 0.5 µm filter (Whatman no. 41). The xylitol-rich liquor was then treated with AmberLite™ IRC120 cationic exchange resin and AmberLite™ IRA410 anionic exchange resins, concentrated using a Rotavapor (Model No.: R 300, Make: Buchi, Switzerland) at 65 °C until the xylitol concentration level reaches about 150 g/L.

6.2.4.2. Crystallization of xylitol syrup

The following methodology performed the xylitol crystallization experiment. Initially, the liquid temperature was raised to 10 °C, above the saturation temperature, and maintained at this temperature for 5 minutes to allow the crystals to dissolve completely. The aliquot of the concentrated solution was then transferred to a glass petri dish in which commercially available xylitol (1.0 g/L) was added to favour the nucleation of the crystals [283]. Petri dishes were kept at room temperature for three days for crystal formation. After crystallization, the precipitated crystals were removed from the mother liquor by filtration using a 0.5 µm filter (Whatman No. 41) and dried on filter paper at room temperature. Pre-weighed crystals were dissolved in water and xylitol, and their purity was measured using HPLC. Finally, xylitol crystals were separated by suction filtration through a filter with a pore size of 0.45 µm. The crystals were washed with 100 mL of distilled water and vacuum dried at room temperature for 24 h. After drying, the crystals were weighed on a digital balance (Model Number: ME204, Brand: Mettler Toledo, Switzerland).

6.2.5. Analytical analysis

The xylitol concentration in the fermented hemicellulose hydrolysate or synthetic solution was calculated by HPLC using an AMINEX ion exchange column (BioRad, HPX87C, Richmond). A 5 mM sulfuric acid – the aqueous solution was used as the mobile phase. The calibration curve was obtained by injecting a standard solution with concentrations of 200 ppm, 400 ppm, 600 ppm, 800 ppm and 100 ppm xylitol. The analysis was performed on flow rate at the 0.6 mL min^{-1} at 60 °C.

6.2.5.1. Thermal stability/degradation

Thermogravimetric measurement is performed using a TA Instruments thermogravimetric analyzer (Hitachi, TA7000) by using a pure form of nitrogen (99.9%) at a constant heating rate of 10 °C min^{-1} with a flow rate of 50 mL min^{-1}. The mass of the sample used for analysis was kept between 5 mg to 10 mg in an open platinum pan. The temperature range was kept between ambient temperature to 600 °C. The first derivative (T_{der}) of the TGA scan at the highest temperature was also used to measure the decomposition temperature.

6.2.5.2. Raman spectroscopy analysis

Sample of commercial xylitol crystals after crystallization (CXCAC) and Xylitol crystals obtained from fermentation broth (XCFB) were scanned from 4000 cm^{-1} to 500 cm^{-1} using a Laser Micro Raman system equipped with JobinVyon, Model LabRam HR spectrometer. The analysis was performed using a low power (10 mW) near-infrared diode laser that emits at 785 nm with an incident power of 5 mW at room temperature. The equipment was calibrated using a Neon line and regularly checked on silicon wafers focused under the objective of 20 microscopes. The astatic spectrum cantered at 520 cm^{-1} for 1 s was obtained. All spectra were recorded as 3 scans of 20 seconds each. Three spectra were obtained from each sample.

6.2.5.3. X-Ray diffraction experiments

X-ray diffraction (XRD) measurements were performed to compare the diffraction patterns of the commercial xylitol crystals after crystallization (CXCAC) and Xylitol crystals obtained from fermentation broth (XCFB). Diffractograms were obtained by using a broad angle X-ray diffractometer (9KW Powder X-Ray Diffraction System, Make: Rigaku Technologies, JAPAN, Model: Smartlab). The radiation (X-ray) was generated at a voltage of 40 kV and 40 mA current flow. The spectrum of the scan was set in the range of 10–60° with a step size of 0.02°, and residence time was set at 1 s/0.02°. Figure 6.7 shows the data points of the experimental X-ray diffraction patterns of CXCAC and XCFB.

$$Crystallinity\ Index = \frac{I_{cr}}{I_{cr} + I_{am}} \times 100 \quad (6.1)$$

Where I_{cr} = Area of all Crystalline peaks and I_{am} = Area of all amorphous peaks

6.2.5.4. Differential scanning calorimetry

The melting temperature (Tm), the heat of fusion (ΔHf), and glass transition temperature of CXCAC and XCFB were determined by DSC. DSC measurements were performed on the DSC1 STARe System Mettler Toledo instrument using a 40 µL aluminium crucible with capillary holes under inert nitrogen (N_2) gas. The use of inert gases helps prevent gas build-up, prevent explosions, and remove volatile chemicals that may be present under atmospheric conditions. DSC temperature calibration was performed using standard indium material. The heat flow was calibrated by the melting and heat of fusion of the indium standard. The mass of the sample used for analysis was kept between 5-10 mg, and the calibration was performed at a heating rate of 1 °C min^{-1} with a nitrogen gas flow rate of 40 mL min^{-1}. The empty pan was covered and used as a reference crucible. The temperature range was - 40 °C to 150 °C during the melting process. The analysis was performed in triplicate, and the average value is shown.

6.2.5.5. Field emission Scanning electron microscopy (FESEM)

A field emission scanning electron microscope (Gemini 500 FESEM) was used to evaluate the shape and surface topography of various xylitol. The device was equipped with a LaB6 field emission electron gun and three types of detectors: InLens, SE2 and ESB. Prior to observation, the samples were fixed on an aluminium stub (G301, Agar Scientific, UK) with double-sided adhesive carbon tabs (G3347N, Agar Scientific, UK), and the powder sample was sputtered with chromium under an argon vacuum using a sputter coater (Edwards S 150B sputter coater, layer thickness 12 nm). The FESEM was operated with an acceleration voltage of 5 kV and a probe current of 10 mA. The photos were taken at different magnifications with utmost concern to ascertain their representativeness.

6.3. Results and discussion

6.3.1. Downstream process of fermented broth

The xylitol-rich fermentation broth containing fragments of yeast along with other contaminants (such as culture medium components, residual substrates, and fermentation by-products) were shown in Figure 6.2(A). To remove some of these impurities, the fermentation solution was centrifuged, followed by the addition of 3N NaOH in supernatant solution to maintain the pH 7.00 (Initial pH about 4.5) [283]. It was then subjected to a centrifugation process, which results from the removal of about 3% cell biomass from the fermented broth.

When the fermented liquor was concentrated and treated with Amber Lite ™ IRC120 cation exchange resin and Amber Lite ™ IRA410 anion exchange resin, a 20% reduction in arabinose concentration (HPLC), a decrease in color (visual) and about 9.23% decrease in concentration (HPLC) of xylitol were observed. Other researchers reported higher levels of xylitol loss (15.23%) during the treatment of fermented broth with ion exchange resins [284]. To obtain suitable xylitol concentration conditions for crystallization, the liquid was concentrated under a vacuum to give a syrup containing 150 g/L xylitol (Figure 6.2(B). After completion of the crystallization process (Figure 6.2(C)), the xylitol crystals were separated and stored in a dry place. The crystal obtained from XCFB was pale yellow in colour, whereas CXCAC was colorless (Figure 6.2(D)). XCFB was pale yellow in colour because of the presence of some impurities [283].

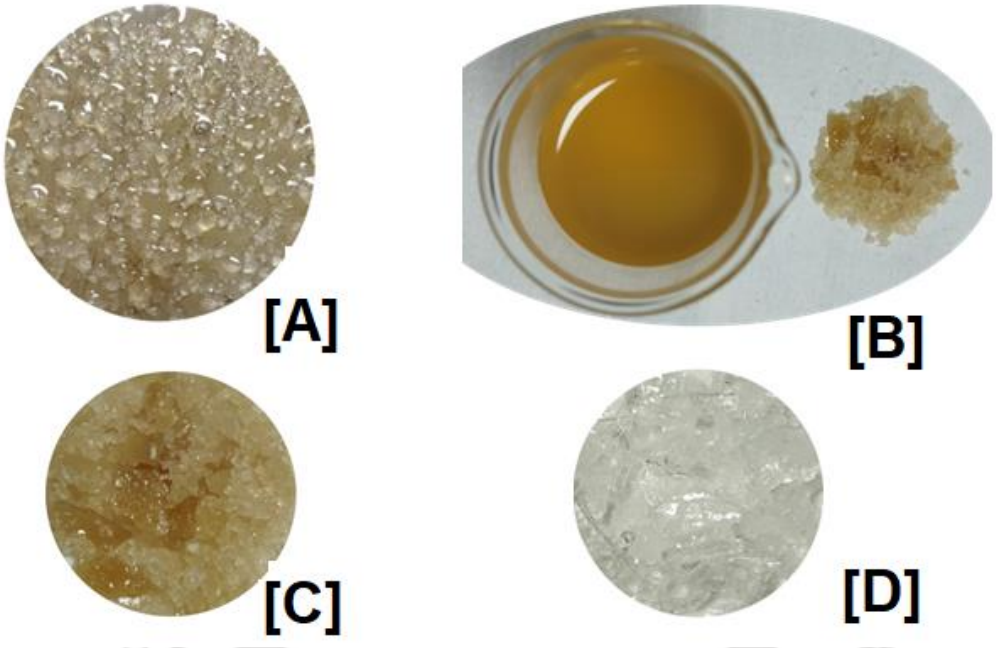

Figure 6.2 Xylitol crystals in fermentation broth (A), Xylitol crystal after separation from fermentation broth (B) and Xylitol crystals from fermentation broth (XCFB) (C) and commercial xylitol crystals after crystallization (CXCAC) (D)

The crystallization process greatly affected the shape and surface morphology of the xylitol particles. FESEM analysis is widely conducted to observe the change in microstructure after crystallization [285]. The micrographs of CXCAC and XCFB are shown in Figure 6.3. From these micrographs, it can be seen that the formation of aggregates and hexagonal xylitol crystals has been confirmed. These agglomerates resulted from the random grouping of crystals, which after growing together, adhered to interpenetrated each other, creating irregular forms. Similar results were reported by [284].

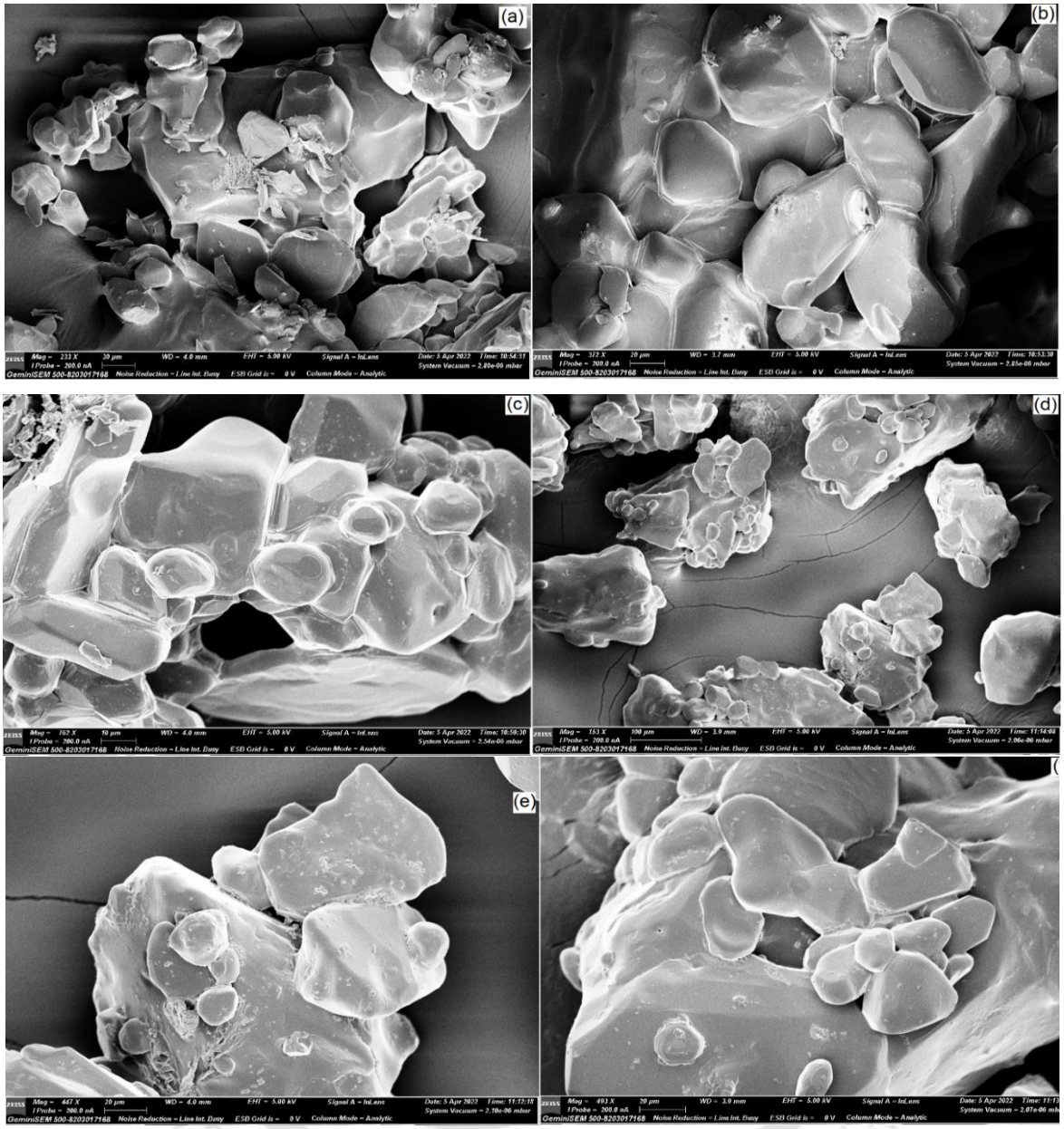

Figure 6.3 SEM images of xylitol crystals. (a), (b) and (c) commercial xylitol crystals after crystallization (CXCAC); (d), (e) and (f) for Xylitol crystals from fermentation broth (XCFB)

6.3.2. Raman Spectroscopy

Raman spectra for commercial xylitol crystals after crystallization (CXCAC) and Xylitol crystals from fermentation broth (XCFB) were obtained in the spectral region 500-2000 cm^{-1} were shown in Figure 6.4. The main peaks of CXCAC and XCFB were labelled in Figure 6.4, revealed that five strong vibrations were stretching vibration of the CO to Raman bands at 855 cm^{-1} and 887 cm^{-1}, O-H to Raman bands at 1060 cm^{-1} and 1092 cm^{-1}, and CH_2 to Raman bands at 1460 cm^{-1}. The strong band at 1459 cm^{-1} ascribed to the C–H bending modes, including CH_2 scissors (Puppels et al., 1991) and CH_3 degenerate deformation [287].

The CH_2 and CH_3 bands are primarily from lipids [288]. The most intense Raman band is at 1060 cm^{-1} and 1092 cm^{-1}; it can be attributed to asymmetric stretching vibration, the character of absorbing spectral were high peak and narrow-band frequency-domain. Moderate intensity of the vibrations appeared at 1002 cm^{-1}, 1109 cm^{-1} and 1316 cm^{-1}. The light intensity of the vibrations appeared at 750 cm^{-1}, 912 cm^{-1}, 1146 cm^{-1}, 1239 cm^{-1}, 1339 cm^{-1}, 1408 cm^{-1}, 1643 $cm^{-1}$and 1831 cm^{-1} [289]. The CH_2 Out-of-plane bending mode for the structural and vibrational analyses of xylitol conformer is assigned to the band at 1239 cm^{-1} in the Raman spectrum, and these shifts are attributed to bond angle changes; the bond length did not change the vertical direction in the spatial, associated band at the same direction and modes corresponding to a distorted oscillation of two parts o hydrogen. Moderate intensity of the vibrations appeared at 1002 cm^{-1}, 1109 cm^{-1} and 1316 cm^{-1}, which corresponds to the stretching vibration mode. The 1308 cm^{-1} band corresponds to the amide III [290]. Raman bands are ascribable to phenylalanine that forms a sharp peak at 1003 cm^{-1} throughout the course of fermentation.

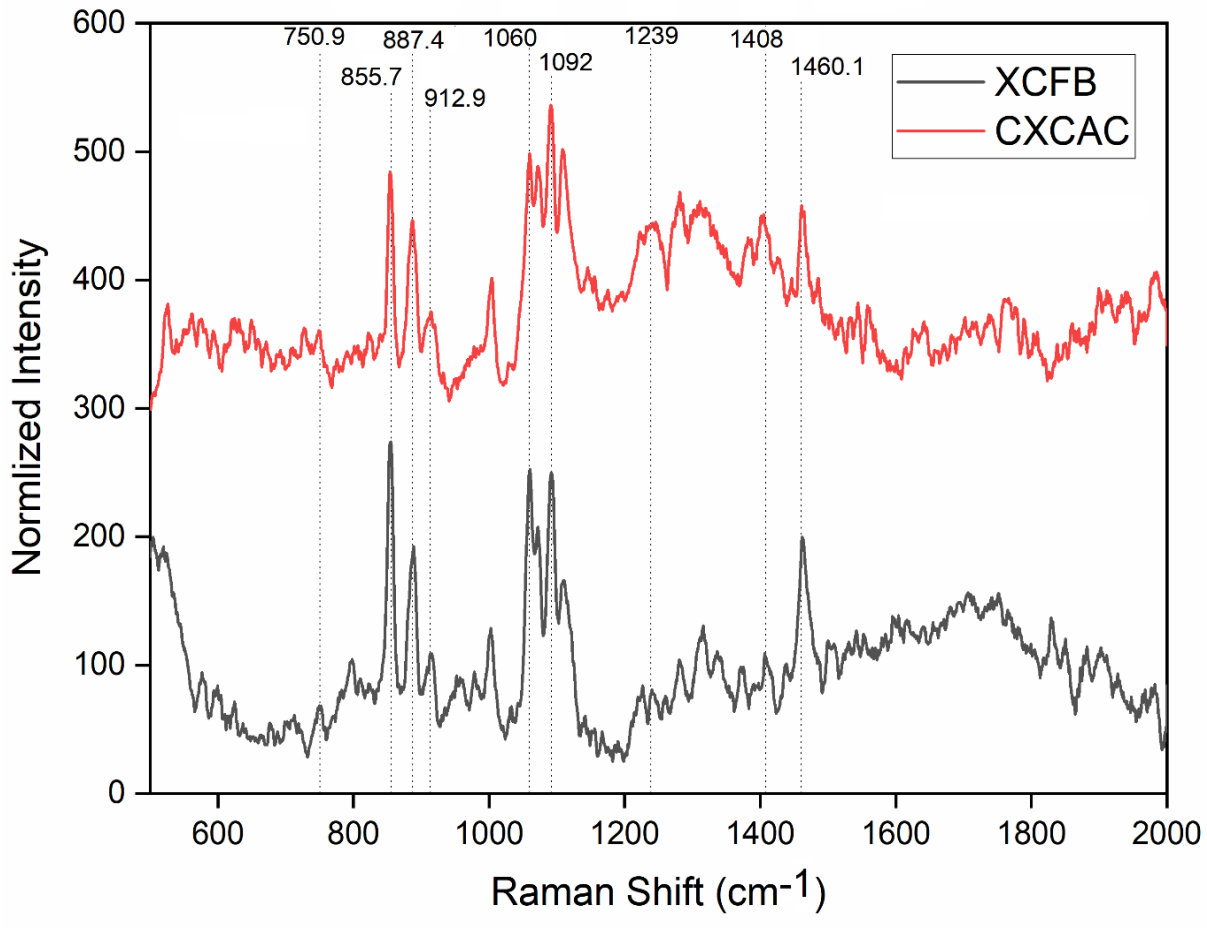

Figure 6.4 Raman curve of CXCAC and XCFB

From this analysis, it can be concluded that both XCFB and CXCAC show similar behaviour and peak position in Figure 6.4. Reduction in intensity was observed in the case of XCFB as compared to CXCAC. This reduction in intensity was most probably due to pretreatment and the presence of a small number of impurities in the case of XCFB as compared to CXCAC [92]. The Raman spectroscopy response for XCFB and CXCAC can be closely correlated to the XRD crystallinity result (Figure 6.7). Higher the crystallinity, the higher the Raman intensity for CXCAC as compared to XCFB [291].

6.3.3. Thermogravimetric Analysis

The TG and DTG curves of xylitol crystals from fermented broth (XCFB) are shown in Figure 6.5. The thermogram shows the mass loss of commercial xylitol crystals after crystallization (CXCAC) was completed in one step. The sample maintains thermal stability below 180 °C. The weight of crystals started decreasing at 210 °C, the maximum mass loss rate was observed at 324 °C, and the mass diminished completely when the temperature reached 332 °C. Similar results were reported by another researcher [258]. The mass loss was completed in single steps for CXCAC and XCFB, respectively. The main steps in the decomposition of xylitol take place between 200 °C and 400 °C. Decomposition and depolymerization of polyurethane polymers and oligomers were observed from 280 °C [292]. This step was followed by recombination to the urea oligomer, which was degraded at high temperatures. Both Samples show one peak between 200 °C and 300 °C, with almost all mass loss within this range. By comparison, the mass loss temperature of CXCAC is higher than the mass loss temperature of XCFB xylitol. In addition, the thermal stability of XCFB from 200 °C to 320 °C was higher than that of CXCAC. Therefore, the presence of residual impurities affects the thermal stability of the particles.

The DSC-thermograms of commercial xylitol crystals after crystallization (CXCAC) and xylitol crystals obtained from fermentation broth (XCFB) have shown in Figure 6.6. Thermal characteristics such as phase change temperature, phase change enthalpy and glass transition temperature are calculated with a DSC instrument, and the results are shown in Table 6.1. DSC analysis of CXCAC and XCFB showed a well-performed endothermic enthalpy change during heating between -40 °C to 150 °C. From the DSC curves of CXCAC and XCFB in Figure 6.6, sharp endothermic peaks correspond to the melting process appear at 93.71 °C and 91.73 °C, with enthalpies of 210.7 J/g and 220 J/g, respectively, which is consistent with those stated in the literature [293,294]. The glass transition temperatures (Tg)

of CXCAC and XCFB are -23.36 °C and -24.27 °C, respectively. Other researchers reported a decrease in Tg of itraconazole loaded on mesoporous silica particles, and the decrease was due to the incarceration of itraconazole in the pores of the supporting material and the increased surface area-to-volume ratio of the adsorbed itraconazole phase [295]. In the case of XCFB, the glass transition temperature shifts to a slightly lower temperature due to the plasticizing effect of the remaining impurities. Similar behaviour was observed by other researchers [296]. The tendency of the polyol to crystallize can be estimated from the ratio of Tm to Tg (Tm / Tg). The encapsulation step can increase this ratio from 1.47 to 1.5. However, no exothermic peak was detected by DSC at a cooling rate of 1K min^{-1}.

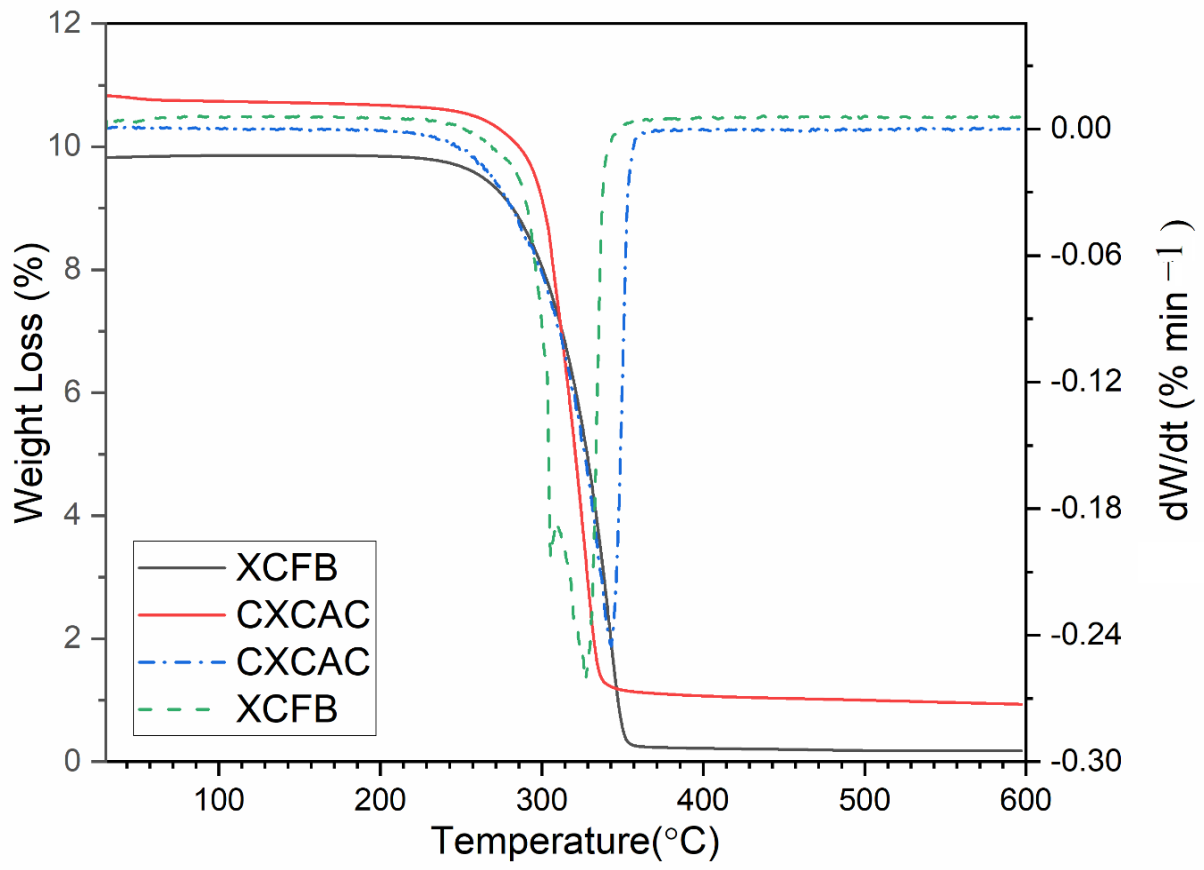

Figure 6.5 TGA and DTG curve of CXCAC and XCFB

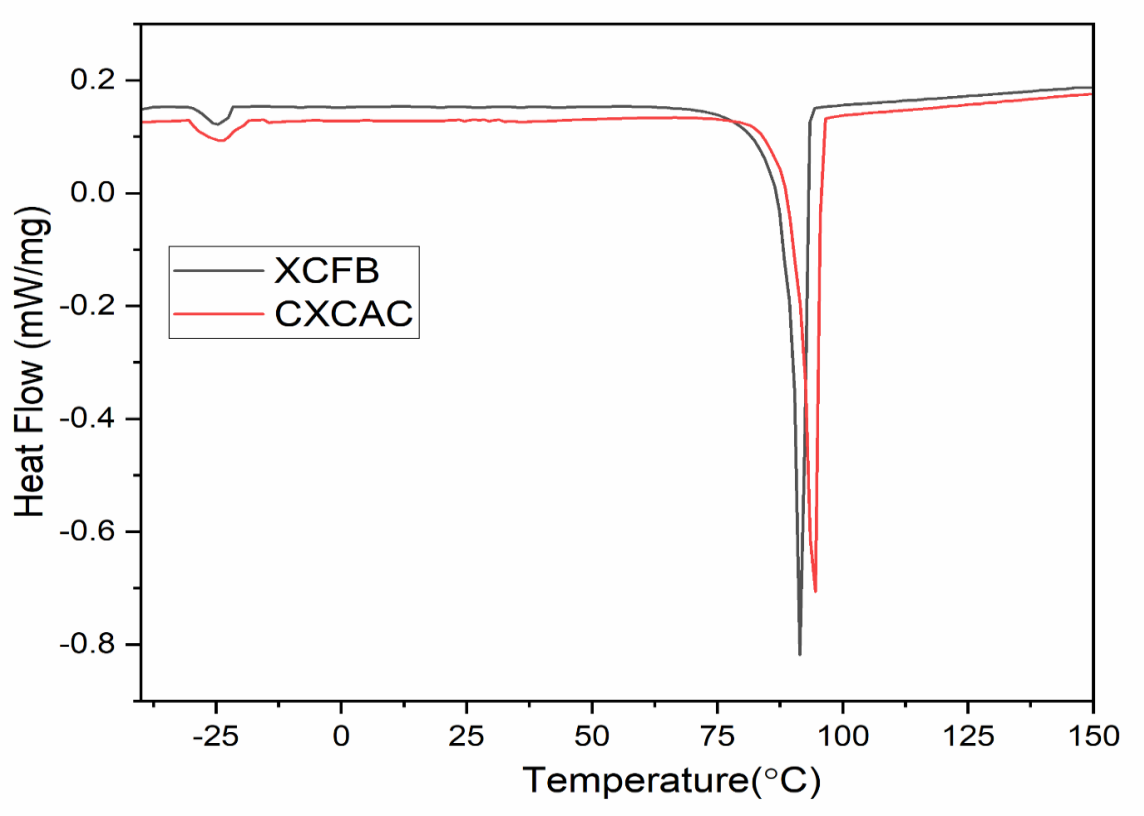

Figure 6.6 DSC curve of CXCAC and XCFB

Table 6.1 Thermal properties of CXCAC and XCFB in this study

Sample	Enthalpy of fusion (J/g)	Delta Cp J/(g*K)	T_g (°C)	T_m (°C)	T_m/T_g
XCFB	-220	0.574	-24.3	91.69	1.46
CXCAC	-210.7	1.372	-23.4	94.4	1.47

6.3.4. XRD analysis

X-ray diffraction of CXCAC and XCFB crystals was performed to determine their crystallinity (Figure 6.7). The peaks of crystals obtained by CXCAC were used as a reference, and the crystals were obtained in XCFB showed characteristic xylitol peaks. It was also observed that in assay XCFB, peaks similar to those in assay CXCAC were observed at 21.60°, 26.41°, 28.76°, 36.6°, 41.40° and 44.78° [297]. The XRD results revealed crystalline peaks, indicating that the processes occurred with complete crystallization under the present experimental conditions. The xylitol obtained from fermentation broth (XCFB) in this study had a crystallinity index of about 76.85%, which is more similar to the commercial xylitol

crystals (CXCAC), having a crystallinity index of 81.44 % (Figure 6.1(a)). Based on these results, the crystallization process fermentation broth resulted in good recovery of xylitol with a level of purity around 85%. Also, in contrast with other methods of purification of xylitol produced by fermented media [42,298,299], this process has the advantage of being carried out in a single step and having a lower cost. Also, the process proposed makes use of non-toxic antisolvents, unlike the process reported by another researcher, who used methanol as an antisolvent [300].

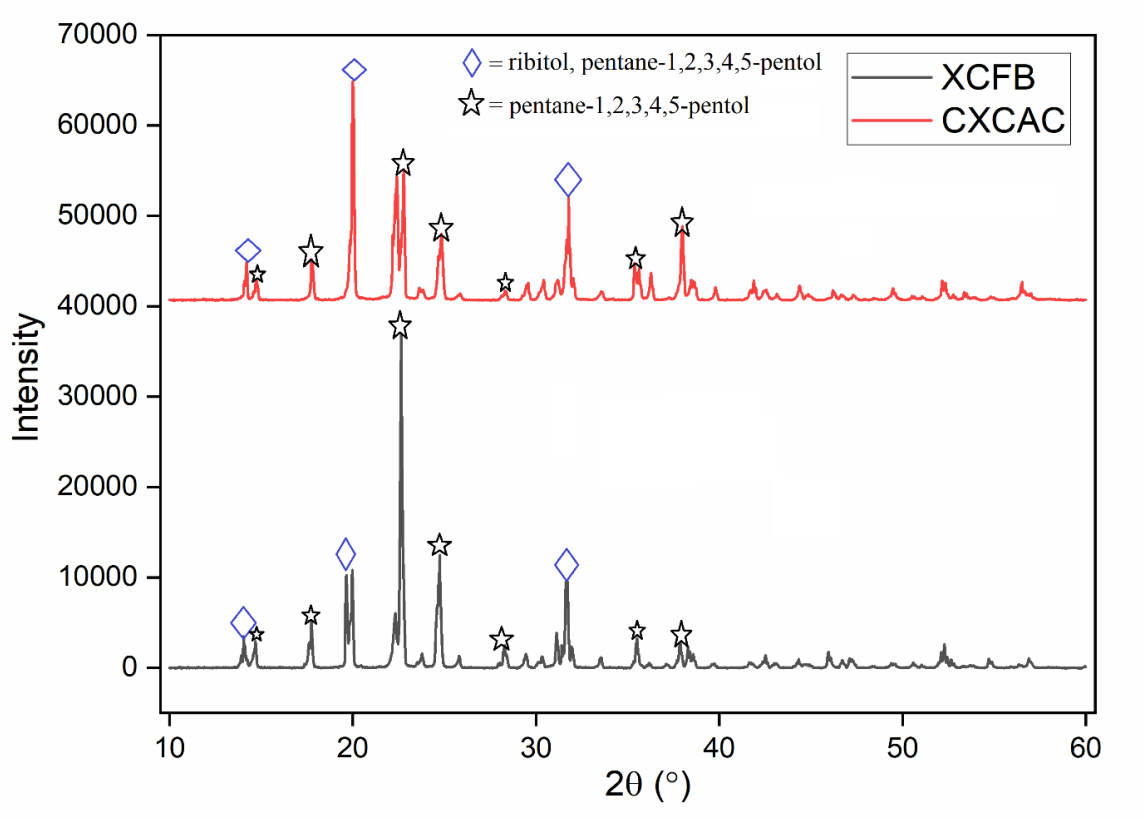

Figure 6.7 XRD curve of CXCAC and XCFB

6.3.5. Comparison of Xylitol Crystals Obtained from XCFB and CXCAC

This section details the dissimilarities between CXCAC and XCFB with regards to their color, microstructure, and Raman spectra. CXCAC is colorless, while XCFB is a pale yellow-colored crystal. Analysis of their microstructure via FESEM showed that both contain hexagonal xylitol crystals and aggregates, but XCFB possesses impurities, which lead to an irregular form. On the other hand, Raman spectra analysis revealed that while both exhibit similar behavior and peak positions, XCFB has reduced intensity compared to CXCAC. Both CXCAC and XCFB exhibit five strong vibrations, including stretching vibration of CO, O-H, and CH_2. Moderate intensity vibrations correspond to stretching vibration mode, and the amide

III is assigned to the 1308 cm^{-1} band. Additionally, the CH_2 Out-of-plane bending mode is assigned to the band at 1239 cm^{-1} in the Raman spectrum. The divergence between CXCAC and XCFB can be ascribed to the purification process, with XCFB's pale-yellow color and lower intensity in Raman spectra resulting from the presence of impurities.

6.4. Conclusions

Lignocellulosic biomass-derived chemicals are an eco-friendly and sustainable source of ingredients for the nutraceutical and pharmaceutical industries. Xylitol, a valuable commodity molecule, holds significant promise in both industries. Microbial xylitol synthesis is a greener alternative to current industry practices, and the present study investigated the crystallization of xylitol from both synthetic solutions and fermented hemicellulose broth. The results obtained were promising, with the best results obtained at a relatively high temperature and fairly concentrated solution (150 g/L). From the experiments, it was observed that the crystallization rate was influenced by the total solute concentration and supersaturation. The xylitol crystals obtained from the crystallization process were characterized and found to be similar to commercial xylitol crystals.

भारतीय प्रौद्योगिकी संस्थान गुवाहाटी
Indian Institute of Technology Guwahati

भारतीय प्रौद्योगिकी संस्थान गुवाहाटी
Indian Institute of Technology Guwahati

Chapter 7

Overall Conclusions and Future Scope

7

The main aim of this research is to utilize agricultural bio-waste, specifically areca nut husk, which is abundantly available in India, particularly in the northeastern region. The objective is to produce xylitol through biotechnological methods, utilizing optimized conditions. This chapter outlines the key findings of the current research and suggests future research that can be undertaken to further advance this field.

7.1. Conclusions

Lignocellulosic biomass is increasingly recognized as a valuable resource that has the potential to replace chemical-based products through integrated biotechnological production methods. To improve the efficiency and economics of this process, global efforts have focused on researching renewable and sustainable energy technologies. The present study specifically focuses on utilizing lignocellulosic agricultural waste biomass for the biotechnological production of xylitol.

The Northeastern region of India boasts a diverse range of indigenous tree and shrub species, offering ample opportunity for researchers to produce bio-based chemicals and valuable products. Areca nut husk (Areca catechu) is a particularly promising lignocellulosic biomass, widely available in this region. The biomass was characterized and pretreated for xylose production, and physical and chemical characterizations were conducted using various techniques, such as thermogravimetric analysis, XRD, Raman spectroscopy, and FTIR. The analysis revealed that the areca nut husk fiber had a crystallinity of approximately 43.38%. Pretreatment is a crucial step in converting lignocellulosic biomass into fermentable sugar. The recalcitrant structure of the biomass must be efficiently disrupted to make it more amenable to enzymatic hydrolysis. Two pretreatment techniques, lime and dilute acid, were conducted on areca nut husk fiber.

In the case of dilute acid pretreatment, the crystallinity of the areca nut husk lignocellulosic biomass decreased from 43.38% to 37.35%, while in the case of lime pretreatment, a reduction in crystallinity was observed from 43.38% to 39.31%. Similarly, the hemicellulose content decreased from 29.17% to 11.2% in the acid-treated sample, while in the lime-treated sample, the reduction in hemicellulose content was noted to be about 29.17% to 23.50%.

The enzymatic hydrolysis of pretreated biomass samples involved using xylanase enzymes that break down structural carbohydrates into monosaccharides, such as xylose and glucose. Saccharification was used as a benchmark to compare the efficiency of different pretreatment processes. Upon analyzing the saccharification efficiency of different pretreatment methods, it was found that the lime-pretreated sample exhibited the highest saccharification efficiency compared to the acid-treated and raw samples. It was also observed that the sugar yield increased with enzyme loading from 2 to 15 IU/g of biomass. Hence, it can be concluded from the saccharification study that the lime-pretreated biomass samples are suitable for the next step of xylitol production, i.e., the fermentation process, and an enzyme loading of 15 IU/g biomass is recommended as the optimum enzyme loading for the enzymatic hydrolysis or saccharification process.

The hydrolysis experiments conducted on areca nut husk hemicellulosic fraction showed that the optimal recovery of xylose was achieved under specific conditions. The optimal condition was achieved by mixing 1.35% v/v sulfuric acid in a mixture of 1% w/v solid at a reaction temperature of 121 °C for 20 minutes of reaction time. To remove the toxic components, various detoxification methods such as pH adjustment, treatment with activated charcoal and ion exchange resins were employed. After detoxification, toxic components such as TPC, HMF and furfural were removed by more than 99%. Furthermore, the fermentation parameters were optimized using RSM and ANN techniques. The results of the ANN model indicated that it is more precise and robust in estimating the values of dependent variables compared to the RSM model. Although RSM is useful for obtaining insight information such as interactions between different components, ANN has been found to be equally useful in sensitivity analysis and predicting optimal conditions and yields. RSM is recommended for modelling new processes, while ANN is better suited for modelling non-linear systems with non-quadratic interactions. Ultimately, under the optimized conditions, submerged fermentation process was carried out using C. tropicalis which resulted in an optimum yield of 0.66 g/g of xylitol.

Crystallization experiments were carried out on both the synthetic solution and the fermented hemicellulose broth, yielding promising results. Optimal conditions were achieved using a relatively high concentration solution (150 g/L) at a high temperature. Based on the experimental findings, it can be concluded that the rate of crystallization is dependent on the total solute concentration and supersaturation. Additionally, the study involved characterizing the xylitol crystals obtained from the crystallization process, and it was observed that the crystals had similar properties to commercial xylitol crystals.

This study provides a comprehensive report on the characterization and saccharification of lignocellulosic biomass from the North-East region of India for the biotechnological production of xylitol. The research also aimed to enhance the yield of xylitol by optimizing fermentation techniques. Additionally, the study included the characterization of xylitol crystals obtained after the crystallization process, and it was found that the resulting crystals resembled commercial xylitol crystals.

7.2. Scopes for Future Work

Although the present study demonstrated promising results in the production of xylitol from areca nut husk using biotechnological approaches, there are still several bottlenecks that need to be addressed to move these findings to industrial applications. One of the main bottlenecks is the scale-up of the process, which requires optimization of the process parameters for large-scale production. For instance, the present study used a batch fermentation process, which may not be suitable for industrial applications. Therefore, future studies should focus on developing continuous fermentation processes that can be easily scaled up. Additionally, cost-effectiveness and the availability of the raw materials should be taken into consideration to ensure the commercial viability of the process.

One of the challenges faced in this process is improving its efficiency. Although the current study has shown promising results, there is still scope for enhancing the yield and purity of xylitol. One approach to address this challenge is through the optimization of fermentation conditions and the adoption of additional purification techniques such as recrystallization. Future research efforts should aim to develop efficient strategies to enhance the yield of xylitol, such as genetic engineering of microorganisms used in the fermentation process, or further optimization of fermentation conditions. The use of mixed culture systems and metabolic flux analysis can also provide valuable insights for the optimization of fermentation processes.

Furthermore, the present study focused on only one type of lignocellulosic biomass as a

raw material for xylitol production. However, Northeast India is known for its richness in various biomass resources. Therefore, future studies should explore the potential of other biomass resources available in the region for the production of fermentable products such as xylitol. This would provide a more sustainable and cost-effective approach for large-scale production.

Finally, for moving these findings to industrial applications, the process needs to be economically feasible, environmentally friendly, and competitive with existing xylitol production methods. Thus, future studies should also focus on developing a comprehensive techno-economic analysis of the process to assess its commercial viability and identify potential areas for improvement.

भारतीय प्रौद्योगिकी संस्थान गुवाहाटी
Indian Institute of Technology Guwahati

भारतीय प्रौद्योगिकी संस्थान गुवाहाटी
Indian Institute of Technology Guwahati

Appendix-A

Xylitol yield (by enzymatic hydrolysis) comparison from literature with different biomass feedstock

Raw materials	Pretreatment	Hydrolysis	Xylose	Detoxification	Xylitol yield (g /g)	Ref.
OPEFB	Autohydrolysis (120 °C; 15 min)	EH	0.08 g/g	No	0.41	[251]
OPEFB	Autohydrolysis (120 °C; 15 min)	EH	4.63 g/L	No	0.24	[252]
Corn cob	Non-isothermal autohydrolysis to reach 202 °C followed by post hydrolysis with 0.5% H_2SO_4 (125 °C; 165 min)	AH with 2% H_2SO_4 (130 °C; 15 min)	35.30 g/L	Yes	0.73	[253]
Corn cob	-	AH with 1% H_2SO_4 (121 °C; 60 min)	0.25 g/g	Yes	0.75	[254]
Cashew apple bagasse	-	AH with 6% H_2SO_4 (121 °C; 15 min)	19.02 g/L	No	0.32	[255]
Corn cob	-	AH with 1% H_2SO_4 (121 °C; 40 min)	31.25 g/L	Yes	0.74	[21]
Brewery spent grain	-	AH with 3% H_2SO_4 (130 °C; 15 min	24 g/L	No	0.58	[256]
Rice straw	-	AH with 1.5% H_2SO_4 (130 °C; 20 min)	17.40 g/L	Yes	0.53	[257]
Corn cob	0.1% H_2SO_4 (room temperature;24 h)	HTS (160 °C; 120 min)	0.18 g/g	Yes	0.71	[258]
Sugarcane straw	-	AH with 1% H_2SO_4 (121 °C; 20 min)	18.60 g/L	Yes	0.67	[259]
Corn cob	Soaking in 10% aqueous ammonia (70 °C; 10 h)	AH with 1% H_2SO_4	33.42 g/L	No	0.60	[260]
Corn cob	-	AH with 1% H_2SO_4 (121 °C; 30 min)	21.98 g/L	Yes	0.37	[261]
Areca nut	Dilute Acid pretreatment (H_2SO_4)	EH	3.83 g/L	Yes	0.76	This study
Areca nut	Lime pretreatment	EH	5.88 g/L	Yes	0.79	-Do-

EH- Enzymatic Hydrolysis; AH- Acid Hydrolysis; HTS- High temperature steaming

Appendix-B

Xylitol yield (by acid hydrolysis) comparison from literature with different biomass feedstock

Feedstocks	Micro-organisms	Methods of detoxification	Xylitol yield (g/g)	References
corncob	*C. tropicalis*	pH adjustment	0.61	[272]
cocoa pod husk	*C. boidinii*	pH adjustment, activated charcoal & ion exchange resins treatment	0.52	[266]
Synthetic medium	*C. boidinii*	Activated carbon and cationic ion exchange resins adsorption	0.48	[278]
Corncob hemicellulosic hydrolysate	*C. tropicalis*	pH adjustment and activated charcoal treatment	0.77	[262]
Hemicellulosic liquor from sugarcane bagasse	*C. tropicalis*	pH adjustment, activated charcoal & ion exchange resins treatment	0.68	[279]
Eucalyptus hemicellulose hydrolysate	*C. guilliermondii* FTI 20037	Ion exchange resins treatment	0.68	[280]
Hardwood hydrolysate	*C. tropicalis* BCRC 20520	Activated charcoal & ion exchange resins treatment	0.73	[277]
Sugarcane bagasse hydrolysate	*C. guilliermondii* FTI 20037	Over liming and activated charcoal treatment	0.75	[281]
Corn fiber hydrolysate	*C. tropicalis*	pH adjustment and activated charcoal treatment	0.4	[273]
Areca nut hemicellulosic hydrolysate	*C. tropicalis*	pH adjustment, activated charcoal & ion exchange resins treatment	0.74	In this study

भारतीय प्रौद्योगिकी संस्थान गुवाहाटी
Indian Institute of Technology Guwahati

भारतीय प्रौद्योगिकी संस्थान गुवाहाटी
Indian Institute of Technology Guwahati

References

[1] Xylitol Uses, Benefits & Dosage - Drugs.com Herbal Database, (n.d.). https://www.drugs.com/npp/xylitol.html (accessed September 12, 2022).

[2] XYLITOL - NATURE'S HEALTHY SWEETENER - DCNutrition.com, (n.d.). https://www.dcnutrition.com/miscellaneous-nutrients/xylitol-natures-healthy-sweetener/ (accessed September 12, 2022).

[3] Xylitol Market Size & Share | Industry Report, 2020-2028, (n.d.). https://www.grandviewresearch.com/industry-analysis/xylitol-market (accessed September 12, 2022).

[4] Xylitol Market Size, Trends, Growth (2022 - 27) | Industry Report, (n.d.). https://www.mordorintelligence.com/industry-reports/xylitol-market (accessed September 12, 2022).

[5] D. Umai, R. Kayalvizhi, V. Kumar, S. Jacob, Xylitol: Bioproduction and Applications-A Review, Front. Sustain. 3 (2022) 1–16. https://doi.org/10.3389/frsus.2022.826190.

[6] H. Vardhan, R.B. Mahato, S. Sasmal, K. Mohanty, Production of Xylose from Pre-treated Husk of Areca Nut, J. Nat. Fibers. 19 (2022) 131–144. https://doi.org/10.1080/15440478.2020.1731905.

[7] Dry Mouth: Causes, Side Effects, Symptoms, and More, (n.d.). https://www.webmd.com/oral-health/ss/slideshow-dry-mouth (accessed September 12, 2022).

[8] R. Dasgupta, R. Pillai, R. Kumar, N.K. Arora, Sugar, Salt, Fat, and Chronic Disease Epidemic in India: Is There Need for Policy Interventions?, Indian J. Community Med. 40 (2015) 71. https://doi.org/10.4103/0970-0218.153858.

[9] What is Xylitol | Supports and Benefits of Xylitol | Xylitol.org, (n.d.). https://xylitol.org/what-is-xylitol/ (accessed September 12, 2022).

[10] E.R. Froesch, Comparison between the metabolism of xylitol, sorbitol, fructose and glucose., Int. Z. Vitam. Ernahrungsforsch. Beih. 15 (1976) 239–241. https://europepmc.org/article/med/1066330 (accessed September 12, 2022).

[11] N.J. Cao, R. Tang, C.S. Gong, L.F. Chen, The effect of cell density on the production of xylitol fromd-xylose by yeast, Appl. Biochem. Biotechnol. 1994 451. 45 (1994) 515–519. https://doi.org/10.1007/BF02941826.

[12] J.C. Parajó, H. Domínguez, J.M. Domínguez, Biotechnological production of xylitol. Part 1: Interest of xylitol and fundamentals of its biosynthesis, Bioresour. Technol. 65 (1998) 191–201. https://doi.org/10.1016/S0960-8524(98)00038-8.

[13] P. Mattila, A.M. Lampi, R. Ronkainen, J. Toivo, V. Piironen, Sterol and vitamin D2 contents in some wild and cultivated mushrooms, Food Chem. 76 (2002) 293–298. https://doi.org/10.1016/S0308-8146(01)00275-8.

[14] M.M. Hämäläinen, K.K. Mäkinen, Polyol-mineral interactions in the diet of the rat with special reference to the stabilities of polyol-metal complexes, Nutr. Res. 9 (1989) 801–811. https://doi.org/10.1016/S0271-5317(89)80023-5.

[15] H. Heikkilä, J. Nurmi, Method for the production of xylitol, (1990).

[16] X. Chen, Z.H. Jiang, S. Chen, W. Qin, Microbial and Bioconversion Production of D-xylitol and Its Detection and Application, Int. J. Biol. Sci. 6 (2010) 834. https://doi.org/10.7150/IJBS.6.834.

[17] J.N. Counsell, Xylitol; (proceedings of an international symposium organized and sponsored by Roche Products Ltd. and Xyrofin Ltd. at the Europa Hotel, London, 5 May 1977), (1978). https://doi.org/10.3/JQUERY-UI.JS.

[18] A. Tangri, R. Singh, Xylitol : Production and Applications, Int. J. Eng. Sci. Res. 5 (2017).

[19] H.A. Spat Etal, Production of crystalline xylose, (1971).

[20] I.S.M. Rafiqul, A.M.M. Sakinah, Processes for the Production of Xylitol—A Review, Https://Doi.Org/10.1080/87559129.2012.714434. 29 (2013) 127–156. https://doi.org/10.1080/87559129.2012.714434.

[21] M. Li, X. Meng, E. Diao, F. Du, Xylitol production by Candida tropicalis from corn cob hemicellulose hydrolysate in a two-stage fed-batch fermentation process, J. Chem. Technol. Biotechnol. 87 (2012) 387–392. https://doi.org/10.1002/JCTB.2732.

[22] N.L. Mohamad, S.M. Mustapa Kamal, M.N. Mokhtar, Xylitol Biological Production: A Review of Recent Studies, Food Rev. Int. 31 (2015) 74–89. https://doi.org/10.1080/87559129.2014.961077.

[23] T. PEPPER, P.M. OLINGER, Xylitol in sugar-free confections, Food Technol. 42 (1988) 98–106.

[24] L. Hyvönen, P. Koivistoinen, F. Voirol, Food Technological Evaluation of Xylitol, Adv. Food Res. 28 (1982) 373–403. https://doi.org/10.1016/S0065-2628(08)60114-7.

[25] E. Winkelhausen, S. Kuzmanova, (No Title), Microb. Pentose Util. 86 (1995) 1–14. https://doi.org/10.1016/S0922-338X(98)80026-3.

[26] P. Nigam, D. Singh, Processes of fermentative production of Xylitol — a sugar substitute, Process Biochem. 30 (1995) 117–124. https://doi.org/10.1016/0032-9592(95)80001-8.

[27] B.C. Saha, R.J. Bothast, Microbial Production of Xylitol, ACS Symp. Ser. 666 (1997) 307–319. https://doi.org/10.1021/BK-1997-0666.CH017.

[28] H. Horitsu, Y. Yahashi, K. Takamizawa, K. Kawai, T. Suzuki, N. Watanabe, Production of xylitol from D-xylose by candida tropicalis: Optimization of production rate, Biotechnol. Bioeng. 40 (1992) 1085–1091. https://doi.org/10.1002/BIT.260400912.

[29] C.T. Evans, C. Ratledge, Induction of xylulose-5-phosphate phosphoketolase in a variety of yeasts grown ond-xylose: the key to efficient xylose metabolism, Arch. Microbiol. 1984 1391. 139 (1984) 48–52. https://doi.org/10.1007/BF00692711.

[30] J. Yoshitake, H. Ishizaki, M. Shimamura, T. Imai, Xylitol production by an enterobacter species, Agric. Biol. Chem. 37 (1973) 2261–2267. https://doi.org/10.1080/00021369.1973.10861002.

[31] K.B. Taylor, M.J. Beck, D.H. Huang, T.T. Sakai, The fermentation of xylose: studies by carbon-13 nuclear magnetic resonance spectroscopy, J. Ind. Microbiol. 6 (1990) 29–41. https://doi.org/10.1007/BF01576174.

[32] B.A. Prior, S.G. Kilian, J.C. du Preez, Fermentation of smallcap˜D-xylose by the yeasts Candida shehatae and Pichia stipitis., Process Biochem. 24 (1989) 21–32.

[33] T.W. Jeffries, Conversion of xylose to ethanol under aerobic conditions by Candida tropicalis, Biotechnol. Lett. 1981 35. 3 (1981) 213–218. https://doi.org/10.1007/BF00154647.

[34] B. Hahn-Hägerdal, H. Jeppsson, K. Skoog, B.A. Prior, Biochemistry and physiology of xylose fermentation by yeasts, Enzyme Microb. Technol. 16 (1994) 933–943. https://doi.org/10.1016/0141-0229(94)90002-7.

[35] J.C. Parajó, H. Domínguez, J.M. Domínguez, Biotechnological production of xylitol. Part 3: Operation in culture media made from lignocellulose hydrolysates, Bioresour. Technol. 66 (1998) 25–40. https://doi.org/10.1016/S0960-8524(98)00037-6.

[36] E. Vandeska, S. Kuzmanova, T.W. Jeffries, Xylitol formation and key enzyme activities in Candida boidinii under different oxygen transfer rates, J. Ferment. Bioeng. 80 (1995) 513–516. https://doi.org/10.1016/0922-338X(96)80929-9.

[37] M.F.S. Barbosa, M.B. de Medeiros, I.M. de Mancilha, H. Schneider, H. Lee, Screening of yeasts for production of xylitol fromd-xylose and some factors which affect xylitol yield in Candida guilliermondii, J. Ind. Microbiol. 3 (1988) 241–251. https://doi.org/10.1007/BF01569582.

[38] J.C. du Preez, Process parameters and environmental factors affecting d-xylose fermentation by yeasts, Enzyme Microb. Technol. 16 (1994) 944–956. https://doi.org/10.1016/0141-0229(94)90003-5.

[39] J.S. Dahiya, Xylitol production by Petromyces albertensis grown on medium containing D-xylose, Https://Doi.Org/10.1139/M91-003. 37 (2011) 14–18. https://doi.org/10.1139/M91-003.

[40] P.P. Ueng, C. shung Gong, Ethanol production from pentoses and sugar-cane bagasse hemicellulose hydrolysate by Mucor and Fusarium species, Enzyme Microb. Technol. 4 (1982) 169–171. https://doi.org/10.1016/0141-0229(82)90111-9.

[41] C. Chiang, S.G. Knight, Metabolism of D-Xylose by Moulds, Nat. 1960 1884744. 188 (1960) 79–81. https://doi.org/10.1038/188079a0.

[42] F.C. Sampaio, F.M.L. Passos, F.J.V. Passos, D. De Faveri, P. Perego, A. Converti, Xylitol crystallization from culture media fermented by yeasts, Chem. Eng. Process. Process Intensif. 45 (2006) 1041–1046. https://doi.org/10.1016/J.CEP.2006.03.012.

[43] S.J. Kalil, F. Maugeri, M.I. Rodrigues, Response surface analysis and simulation as a tool for bioprocess design and optimization, Process Biochem. 35 (2000) 539–550. https://doi.org/10.1016/S0032-9592(99)00101-6.

[44] V. Nolleau, L. Preziosi-Belloy, J.P. Delgenes, J.M. Navarro, Xylitol production from xylose by two yeast strains: Sugar tolerance, Curr. Microbiol. 1993 274. 27 (1993) 191–197. https://doi.org/10.1007/BF01692875.

[45] T. Walther, P. Hensirisak, F.A. Agblevor, The influence of aeration and hemicellulosic sugars on xylitol production by Candida tropicalis, Bioresour. Technol. 76 (2001) 213–220. https://doi.org/10.1016/S0960-8524(00)00113-9.

[46] Y. Yahashi, H. Horitsu, K. Kawai, T. Suzuki, K. Takamizawa, Production of xylitol from d-xylose by Candida tropicalis: the effect of d-glucose feeding, J. Ferment. Bioeng. 81 (1996) 148–152. https://doi.org/10.1016/0922-338X(96)87593-3.

[47] S.S. Silva, I.C. Roberto, M.G.A. Felipe, I.M. Mancilha, Batch fermentation of xylose for xylitol production in stirred tank bioreactor, Process Biochem. 31 (1996) 549–553. https://doi.org/10.1016/S0032-9592(96)00002-7.

[48] M. Soleimani, L. Tabil, S. Panigrahi, E. Alberta, The Canadian Society for Bioengineering The Canadian society for engineering in agricultural, food, environmental, and biological systems. La Société Canadienne de Génie Agroalimentaire et de Bioingénierie Bio-production of a Polyalcohol (Xylitol) from Lignocellulosic Resources: A Review Written for presentation at the CSBE/SCGAB 2006 Annual Conference, (n.d.).

[49] W.J. Lee, Y.W. Ryu, J.H. Seo, Characterization of two-substrate fermentation processes for xylitol production using recombinant Saccharomyces cerevisiae containing xylose reductase gene, Process Biochem. 35 (2000) 1199–1203. https://doi.org/10.1016/S0032-9592(00)00165-5.

[50] E. Winkelhausen, S. Kuzmanova, Microbial conversion of d-xylose to xylitol, J. Ferment. Bioeng. 86 (1998) 1–14. https://doi.org/10.1016/S0922-338X(98)80026-3.

[51] J.C. Parajó, H. Domínguez, J.M. Domínguez, Biotechnological production of xylitol. Part 2: Operation in culture media made with commercial sugars, Bioresour. Technol. 65 (1998) 203–212. https://doi.org/10.1016/S0960-8524(98)00036-4.

[52] E. Vandeska, S. Amartey, S. Kuzmanova, T. Jeffries, Effects of environmental conditions on production of xylitol byCandida boidinii, World J. Microbiol. Biotechnol. 1995 112. 11 (1995) 213–218. https://doi.org/10.1007/BF00704652.

[53] M.G.A. Felipe, L.A. Alves, S.S. Silva, I.C. Roberto, I.M. Mancilha, J.B. Almeida e

Silva, Fermentation of eucalyptus hemicellulosic hydrolysate to xylitol by Candida guilliermondii, Bioresour. Technol. 56 (1996) 281–283. https://doi.org/10.1016/0960-8524(96)00031-4.

[54] M.J. Pfeifer, S.S. Silva, M.G.A. Felipe, I.C. Roberto, I.M. Mancilha, Effect of Culture Conditions on Xylitol Production by FTI 20037, Seventeenth Symp. Biotechnol. Fuels Chem. (1996) 423–430. https://doi.org/10.1007/978-1-4612-0223-3_39.

[55] N.J. Cao, R. Tang, C.S. Gong, L.F. Chen, The effect of cell density on the production of xylitol fromd-xylose by yeast, Appl. Biochem. Biotechnol. 1994 451. 45 (1994) 515–519. https://doi.org/10.1007/BF02941826.

[56] S.S. da Silva, A.S. Afschar, Microbial production of xylitol from D-xylose using Candida tropicalis, Bioprocess Eng. 1994 114. 11 (1994) 129–134. https://doi.org/10.1007/BF00518734.

[57] V. Ahuja, M. Macho, D. Ewe, M. Singh, S. Saha, K. Saurav, Biological and Pharmacological Potential of Xylitol: A Molecular Insight of Unique Metabolism, Foods (Basel, Switzerland). 9 (2020). https://doi.org/10.3390/FOODS9111592.

[58] Y.P. Cen, D.H. Turpin, D.B. Layzell, Whole-Plant Gas Exchange and Reductive Biosynthesis in White Lupin, Plant Physiol. 126 (2001) 1555–1565. https://doi.org/10.1104/PP.126.4.1555.

[59] R.C. Kuhad, A. Singh, Lignocellulose Biotechnology: Current and Future Prospects, Https://Doi.Org/10.3109/07388559309040630. 13 (2008) 151–172. https://doi.org/10.3109/07388559309040630.

[60] P. Bajpai, Pretreatment of Lignocellulosic Biomass, (2016) 17–70. https://doi.org/10.1007/978-981-10-0687-6_4.

[61] Biochemistry by Reginald H. Garrett | Goodreads, (n.d.). https://www.goodreads.com/en/book/show/134296.Biochemistry (accessed September 13, 2022).

[62] T. Heinze, T. Liebert, Unconventional methods in cellulose functionalization, Prog. Polym. Sci. 26 (2001) 1689–1762. https://doi.org/10.1016/S0079-6700(01)00022-3.

[63] C. Olsson, G. Westman, Direct Dissolution of Cellulose: Background, Means and Applications, Cellul. - Fundam. Asp. (2013). https://doi.org/10.5772/52144.

[64] FENGEL D, Ideas on the ultrastructural organization of the cell wall components, J. Polym. Sci. Part C Polym. Symp. 36 (1971) 383–392. https://doi.org/10.1002/POLC.5070360127.

[65] V.B. Agbor, N. Cicek, R. Sparling, A. Berlin, D.B. Levin, Biomass pretreatment: Fundamentals toward application, Biotechnol. Adv. 29 (2011) 675–685. https://doi.org/10.1016/J.BIOTECHADV.2011.05.005.

[66] H.V. Scheller, P. Ulvskov, Hemicelluloses, Http://Dx.Doi.Org/10.1146/Annurev-Arplant-042809-112315. 61 (2010) 263–289. https://doi.org/10.1146/ANNUREV-

ARPLANT-042809-112315.

[67] A.T.W.M. Hendriks, G. Zeeman, Pretreatments to enhance the digestibility of lignocellulosic biomass, Bioresour. Technol. 100 (2009) 10–18. https://doi.org/10.1016/J.BIORTECH.2008.05.027.

[68] F.G. Calvo-Flores, J.A. Dobado, Lignin as Renewable Raw Material, ChemSusChem. 3 (2010) 1227–1235. https://doi.org/10.1002/CSSC.201000157.

[69] A.J. Ragauskas, G.T. Beckham, M.J. Biddy, R. Chandra, F. Chen, M.F. Davis, B.H. Davison, R.A. Dixon, P. Gilna, M. Keller, P. Langan, A.K. Naskar, J.N. Saddler, T.J. Tschaplinski, G.A. Tuskan, C.E. Wyman, Lignin Valorization: Improving Lignin Processing in the Biorefinery, Science (80-.). (2014). https://doi.org/10.1126/SCIENCE.1246843.

[70] W. Boerjan, J. Ralph, M. Baucher, Lignin Biosynthesis, Annu. Rev. Plant Biol. 54 (2003) 519–546. https://doi.org/10.1146/annurev.arplant.54.031902.134938.

[71] F. Guo, W. Shi, W. Sun, X. Li, F. Wang, J. Zhao, Y. Qu, Differences in the adsorption of enzymes onto lignins from diverse types of lignocellulosic biomass and the underlying mechanism, Biotechnol. Biofuels. 7 (2014) 1–10. https://doi.org/10.1186/1754-6834-7-38/TABLES/5.

[72] A.U. Buranov, G. Mazza, Lignin in straw of herbaceous crops, Ind. Crops Prod. 28 (2008) 237–259. https://doi.org/10.1016/J.INDCROP.2008.03.008.

[73] S.I. Mussatto, J.A. Teixeira, Lignocellulose as raw material in fermentation processes, Appl. Microbiol. an Microb. Biotechnol. 2 (2011) 897–907. https://repositorium.sdum.uminho.pt/handle/1822/16762 (accessed September 13, 2022).

[74] J. Martinez, P. Szeto, T. Stewart, The Relationship Between Structural Parameters and Mechanical Properties of Cactus Spines, Mater. Eng. (2017). https://digitalcommons.calpoly.edu/matesp/171 (accessed September 13, 2022).

[75] C. Xiao, C.T. Anderson, Roles of pectin in biomass yield and processing for biofuels, Front. Plant Sci. 4 (2013) 67. https://doi.org/10.3389/FPLS.2013.00067/XML/NLM.

[76] M. Dash, V. Venkata Dasu, K. Mohanty, Physico-chemical characterization of Miscanthus, Castor, and Jatropha towards biofuel production, J. Renew. Sustain. Energy. 7 (2015) 043124. https://doi.org/10.1063/1.4926577.

[77] B. Alriksson, Karlstads universitet. Avdelningen för kemi och biomedicinsk vetenskap., Ethanol from lignocellulose : management of by-products of hydrolysis, (2009).

[78] T. Abbasi, S.A. Abbasi, Biomass energy and the environmental impacts associated with its production and utilization, Renew. Sustain. Energy Rev. 14 (2010) 919–937. https://doi.org/10.1016/J.RSER.2009.11.006.

[79] P. Joshi, N. Sharma, P. Manab Sarma, Assessment of Biomass Potential and Current Status of Bio-fuels and Bioenergy Production in India, (n.d.).

[80] A. Kumar, N. Kumar, P. Baredar, A. Shukla, A review on biomass energy resources, potential, conversion and policy in India, Renew. Sustain. Energy Rev. 45 (2015) 530–539. https://doi.org/10.1016/J.RSER.2015.02.007.

[81] D. Kumar, G.S. Murthy, Impact of pretreatment and downstream processing technologies on economics and energy in cellulosic ethanol production, Biotechnol. Biofuels. 4 (2011) 1–19. https://doi.org/10.1186/1754-6834-4-27/FIGURES/9.

[82] B. Yang, C.E. Wyman, Pretreatment: the key to unlocking low-cost cellulosic ethanol, Biofuels, Bioprod. Biorefining. 2 (2008) 26–40. https://doi.org/10.1002/BBB.49.

[83] G. Brodeur, E. Yau, K. Badal, J. Collier, K.B. Ramachandran, S. Ramakrishnan, Chemical and physicochemical pretreatment of lignocellulosic biomass: A review, Enzyme Res. 2011 (2011). https://doi.org/10.4061/2011/787532.

[84] R.K. Sukumaran, A.K. Mathew, M.K. Kumar, A. Abraham, M. Chistopher, M. Sankar, First- and second-generation ethanol in India: A comprehensive overview on feedstock availability, composition, and potential conversion yields, Sustain. Biofuels Dev. India. (2017) 223–246. https://doi.org/10.1007/978-3-319-50219-9_10/COVER.

[85] B. Jarimopas, S. Niamhom, A. Terdwongworakul, Development and testing of a husking machine for dry betel nut (Areca Catechu Linn.), Biosyst. Eng. 102 (2009) 83–89. https://doi.org/10.1016/J.BIOSYSTEMSENG.2008.09.033.

[86] D.B.T.R. DR. B.T. Ramappa□, Economics of Areca nut Cultivation in Karnataka, a Case Study Of Shivamogga District., IOSR J. Agric. Vet. Sci. 3 (2013) 50–59. https://doi.org/10.9790/2380-0315059.

[87] A. Rajan, J.G. Kurup, T.E. Abraham, Biosoftening of arecanut fiber for value added products, Biochem. Eng. J. 25 (2005) 237–242. https://doi.org/10.1016/J.BEJ.2005.05.011.

[88] S. Krishnaraj, R. Gunaseelan, M. Arunmozhi, C.S.P. Sumandiran, Supply chain perspective and logistics of spices in Indian retail industry, Mater. Today Proc. 48 (2022) 119–124. https://doi.org/10.1016/J.MATPR.2020.02.681.

[89] V. Raghavan, H.K. Baruah, Arecanut: India's popular masticatory —history, chemistry and utilization, Econ. Bot. 1958 124. 12 (1958) 315–345. https://doi.org/10.1007/BF02860022.

[90] G K Nair-The Hindu BusinessLine, (n.d.). https://www.thehindubusinessline.com/profile/author/G-K-Nair/?page=77 (accessed September 13, 2022).

[91] R. Raghupathy, R. Viswanathan, C. Devadas, Quality of paper boards from arecanut leaf sheath, Bioresour. Technol. 82 (2002) 99–100. https://doi.org/10.1016/S0960-8524(01)00141-9.

[92] S. Sasmal, V. V. Goud, K. Mohanty, Characterization of biomasses available in the region of North-East India for production of biofuels, Biomass and Bioenergy. 45 (2012) 212–220. https://doi.org/10.1016/j.biombioe.2012.06.008.

[93] G. Narayanamurthy, Y.L. Ramachandra, S.P. Rai, Y.N. Manohara, B.T. Kavitha, Areca husk: An inexpensive substrate for citric acid production by Aspergillus niger under solid state fermentation, Indian J. Biotechnol. 7 (2008) 99–102.

[94] The Kambatik Park, Bintulu.: Views of the Park, (n.d.). https://kambatikpark.blogspot.com/p/palm-views.html?m=1 (accessed September 13, 2022).

[95] N. Das, P.K. Jena, D. Padhi, M. Kumar Mohanty, G. Sahoo, A comprehensive review of characterization, pretreatment and its applications on different lignocellulosic biomass for bioethanol production, Biomass Convers. Biorefinery 2021. (2021) 1–25. https://doi.org/10.1007/S13399-021-01294-3.

[96] H. Chen, J. Liu, X. Chang, D. Chen, Y. Xue, P. Liu, H. Lin, S. Han, A review on the pretreatment of lignocellulose for high-value chemicals, Fuel Process. Technol. 160 (2017) 196–206. https://doi.org/10.1016/J.FUPROC.2016.12.007.

[97] L. Cadoche, G.D. López, Assessment of size reduction as a preliminary step in the production of ethanol from lignocellulosic wastes, Biol. Wastes. 30 (1989) 153–157. https://doi.org/10.1016/0269-7483(89)90069-4.

[98] H. Zabed, J.N. Sahu, A. Suely, A.N. Boyce, G. Faruq, Bioethanol production from renewable sources: Current perspectives and technological progress, Renew. Sustain. Energy Rev. 71 (2017) 475–501. https://doi.org/10.1016/J.RSER.2016.12.076.

[99] S. Larsson, A. Quintana-Sáinz, A. Reimann, N.-O. Nilvebrant, L.J. Jönsson, Influence of Lignocellulose-Derived Aromatic Compounds on Oxygen-Limited Growth and Ethanolic Fermentation by, Twenty-First Symp. Biotechnol. Fuels Chem. (2000) 617–632. https://doi.org/10.1007/978-1-4612-1392-5_47.

[100] P. Kitchaiya, P. Intanakul, M. Krairiksh, Enhancement of Enzymatic Hydrolysis of Lignocellulosic Wastes by Microwave Pretreatment Under Atmospheric Pressure, Http://Dx.Doi.Org/10.1081/WCT-120021926. 23 (2007) 217–225. https://doi.org/10.1081/WCT-120021926.

[101] M.M. de S. Moretti, D.A. Bocchini-Martins, C. da C.C. Nunes, M.A. Villena, O.M. Perrone, R. da Silva, M. Boscolo, E. Gomes, Pretreatment of sugarcane bagasse with microwaves irradiation and its effects on the structure and on enzymatic hydrolysis, Appl. Energy. 122 (2014) 189–195. https://doi.org/10.1016/J.APENERGY.2014.02.020.

[102] J. Cheng, H. Su, J. Zhou, W. Song, K. Cen, Microwave-assisted alkali pretreatment of rice straw to promote enzymatic hydrolysis and hydrogen production in dark- and photo-fermentation, Int. J. Hydrogen Energy. 36 (2011) 2093–2101. https://doi.org/10.1016/J.IJHYDENE.2010.11.021.

[103] M.E. Himmel, W.S. Adney, J.O. Baker, R. Elander, J.D. McMillan, R.A. Nieves, J.J. Sheehan, S.R. Thomas, T.B. Vinzant, M. Zhang, Advanced Bioethanol Production Technologies: A Perspective, ACS Symp. Ser. 666 (1997). https://doi.org/10.1021/BK-1997-0666.CH001.

[104] L. Wang, B. Zhao, B. Liu, B. Yu, C. Ma, F. Su, D. Hua, Q. Li, Y. Ma, P. Xu, Efficient

production of l-lactic acid from corncob molasses, a waste by-product in xylitol production, by a newly isolated xylose utilizing Bacillus sp. strain, Bioresour. Technol. 101 (2010) 7908–7915. https://doi.org/10.1016/J.BIORTECH.2010.05.031.

[105] Y.H.P. Zhang, S.Y. Ding, J.R. Mielenz, J.B. Cui, R.T. Elander, M. Laser, M.E. Himmel, J.R. McMillan, L.R. Lynd, Fractionating recalcitrant lignocellulose at modest reaction conditions, Biotechnol. Bioeng. 97 (2007) 214–223. https://doi.org/10.1002/BIT.21386.

[106] S. Aslanzadeh, A. Berg, M.J. Taherzadeh, I. Sárvári Horváth, Biogas production from N-Methylmorpholine-N-oxide (NMMO) pretreated forest residues, Appl. Biochem. Biotechnol. 172 (2014) 2998–3008. https://doi.org/10.1007/S12010-014-0747-Z/FIGURES/3.

[107] M.J. Taherzadeh, K. Karimi, Pretreatment of Lignocellulosic Wastes to Improve Ethanol and Biogas Production: A Review, Int. J. Mol. Sci. 2008, Vol. 9, Pages 1621-1651. 9 (2008) 1621–1651. https://doi.org/10.3390/IJMS9091621.

[108] P. Alvira, E. Tomás-Pejó, M. Ballesteros, M.J. Negro, Pretreatment technologies for an efficient bioethanol production process based on enzymatic hydrolysis: A review, Bioresour. Technol. 101 (2010) 4851–4861. https://doi.org/10.1016/J.BIORTECH.2009.11.093.

[109] T. Kobayashi, B. Kohn, L. Holmes, R. Faulkner, M. Davis, G.E. MacIel, Molecular-level consequences of biomass pretreatment by dilute sulfuric acid at various temperatures, Energy and Fuels. 25 (2011) 1790–1797. https://doi.org/10.1021/EF1017219/SUPPL_FILE/EF1017219_SI_001.PDF.

[110] R. Kumar, C.E. Wyman, Access of cellulase to cellulose and lignin for poplar solids produced by leading pretreatment technologies, Biotechnol. Prog. 25 (2009) 807–819. https://doi.org/10.1002/BTPR.153.

[111] L. Shuai, Q. Yang, J.Y. Zhu, F.C. Lu, P.J. Weimer, J. Ralph, X.J. Pan, Comparative study of SPORL and dilute-acid pretreatments of spruce for cellulosic ethanol production, Bioresour. Technol. 101 (2010) 3106–3114. https://doi.org/10.1016/J.BIORTECH.2009.12.044.

[112] C. Li, B. Knierim, C. Manisseri, R. Arora, H. V. Scheller, M. Auer, K.P. Vogel, B.A. Simmons, S. Singh, Comparison of dilute acid and ionic liquid pretreatment of switchgrass: Biomass recalcitrance, delignification and enzymatic saccharification, Bioresour. Technol. 101 (2010) 4900–4906. https://doi.org/10.1016/J.BIORTECH.2009.10.066.

[113] Y. Zhang, L. Teng, Y. Quan, H. Tian, Y. Dong, Q. Meng, J. Lu, F. Lin, X. Zheng, Artificial intelligence based optimization of fermentation medium for β-glucosidase production from newly isolated strain Tolypocladium cylindrosporum, Lect. Notes Comput. Sci. (Including Subser. Lect. Notes Artif. Intell. Lect. Notes Bioinformatics). 6330 LNBI (2010) 325–332. https://doi.org/10.1007/978-3-642-15615-1_39/COVER.

[114] M. Shafiei, R. Kumar, K. Karimi, Pretreatment of Lignocellulosic Biomass, (2015) 85–154. https://doi.org/10.1007/978-3-319-14033-9_3.

[115] Y.S. Cheng, Y. Zheng, C.W. Yu, T.M. Dooley, B.M. Jenkins, J.S. Vandergheynst, Evaluation of high solids alkaline pretreatment of rice straw, Appl. Biochem. Biotechnol. 162 (2010) 1768–1784. https://doi.org/10.1007/S12010-010-8958-4/TABLES/7.

[116] M. Balat, H. Balat, C. Öz, Progress in bioethanol processing, Prog. Energy Combust. Sci. 34 (2008) 551–573. https://doi.org/10.1016/J.PECS.2007.11.001.

[117] C. Wan, Y. Zhou, Y. Li, Liquid hot water and alkaline pretreatment of soybean straw for improving cellulose digestibility, Bioresour. Technol. 102 (2011) 6254–6259. https://doi.org/10.1016/J.BIORTECH.2011.02.075.

[118] B.W. Koo, B.C. Min, K.S. Gwak, S.M. Lee, J.W. Choi, H. Yeo, I.G. Choi, Structural changes in lignin during organosolv pretreatment of Liriodendron tulipifera and the effect on enzymatic hydrolysis, Biomass and Bioenergy. 42 (2012) 24–32. https://doi.org/10.1016/J.BIOMBIOE.2012.03.012.

[119] S. Ostovareh, K. Karimi, A. Zamani, Efficient conversion of sweet sorghum stalks to biogas and ethanol using organosolv pretreatment, Ind. Crops Prod. 66 (2015) 170–177. https://doi.org/10.1016/J.INDCROP.2014.12.023.

[120] S. Haghighi Mood, A. Hossein Golfeshan, M. Tabatabaei, G. Salehi Jouzani, G.H. Najafi, M. Gholami, M. Ardjmand, Lignocellulosic biomass to bioethanol, a comprehensive review with a focus on pretreatment, Renew. Sustain. Energy Rev. 27 (2013) 77–93. https://doi.org/10.1016/J.RSER.2013.06.033.

[121] E. Varga, K. Réczey, G. Zacchi, Optimization of Steam Pretreatment of Corn Stover to Enhance Enzymatic Digestibility, Proc. Twenty-Fifth Symp. Biotechnol. Fuels Chem. Held May 4–7, 2003, Breckenridge, CO. (2004) 509–523. https://doi.org/10.1007/978-1-59259-837-3_43.

[122] N. Mosier, C. Wyman, B. Dale, R. Elander, Y.Y. Lee, M. Holtzapple, M. Ladisch, Features of promising technologies for pretreatment of lignocellulosic biomass, Bioresour. Technol. 96 (2005) 673–686. https://doi.org/10.1016/J.BIORTECH.2004.06.025.

[123] T.H. Kim, F. Taylor, K.B. Hicks, Bioethanol production from barley hull using SAA (soaking in aqueous ammonia) pretreatment, Bioresour. Technol. 99 (2008) 5694–5702. https://doi.org/10.1016/J.BIORTECH.2007.10.055.

[124] G.P. Van Walsum, S.G. Allen, M.J. Spencer, M.S. Laser, M.J. Antal, L.R. Lynd, Conversion of Lignocellulosics Pretreated with Liquid Hot Water to Ethanol, Seventeenth Symp. Biotechnol. Fuels Chem. (1996) 157–170. https://doi.org/10.1007/978-1-4612-0223-3_14.

[125] M. Laser, D. Schulman, S.G. Allen, J. Lichwa, M.J. Antal, L.R. Lynd, A comparison of liquid hot water and steam pretreatments of sugar cane bagasse for bioconversion to ethanol, Bioresour. Technol. 81 (2002) 33–44. https://doi.org/10.1016/S0960-8524(01)00103-1.

[126] Y. Sun, J. Cheng, Hydrolysis of lignocellulosic materials for ethanol production: a review, Bioresour. Technol. 83 (2002) 1–11. https://doi.org/10.1016/S0960-

8524(01)00212-7.

[127] C. Sánchez, Lignocellulosic residues: Biodegradation and bioconversion by fungi, Biotechnol. Adv. 27 (2009) 185–194. https://doi.org/10.1016/J.BIOTECHADV.2008.11.001.

[128] L. Magnusson, R. Islam, R. Sparling, D. Levin, N. Cicek, Direct hydrogen production from cellulosic waste materials with a single-step dark fermentation process, Int. J. Hydrogen Energy. 33 (2008) 5398–5403. https://doi.org/10.1016/J.IJHYDENE.2008.06.018.

[129] P.C. Badger, Ethanol From Cellulose: A General Review, (2002).

[130] S. Kalia, A. Dufresne, B.M. Cherian, B.S. Kaith, L. Avérous, J. Njuguna, E. Nassiopoulos, Cellulose-based bio- and nanocomposites: A review, Int. J. Polym. Sci. 2011 (2011). https://doi.org/10.1155/2011/837875.

[131] S.S. Hassan, G.A. Williams, A.K. Jaiswal, Emerging technologies for the pretreatment of lignocellulosic biomass, Bioresour. Technol. 262 (2018) 310–318. https://doi.org/10.1016/J.BIORTECH.2018.04.099.

[132] J. Iranmahboob, F. Nadim, S. Monemi, Optimizing acid-hydrolysis: a critical step for production of ethanol from mixed wood chips, Biomass and Bioenergy. 22 (2002) 401–404. https://doi.org/10.1016/S0961-9534(02)00016-8.

[133] R.J. Magee, N. Kosaric, Bioconversion of hemicellulosics., Adv. Biochem. Eng. Biotechnol. 32 (1985) 61–93. https://doi.org/10.1007/BFB0009525/COVER.

[134] L. Olsson, B. Hahn-Hägerdal, Fermentation of lignocellulosic hydrolysates for ethanol production, Enzyme Microb. Technol. 18 (1996) 312–331. https://doi.org/10.1016/0141-0229(95)00157-3.

[135] B.A. Converti, J.M. Domínguez, P. Perego, S. Silvørio, M. Zilli, Wood Hydrolysis and Hydrolysate Detoxification for Subsequent Xylitol Production, 23 (2000) 1013–1020.

[136] R.S. Pereira, S.I. Mussatto, I.C. Roberto, Inhibitory action of toxic compounds present in lignocellulosic hydrolysates on xylose to xylitol bioconversion by Candida guilliermondii, J. Ind. Microbiol. Biotechnol. 38 (2011) 71–78. https://doi.org/10.1007/S10295-010-0830-6.

[137] M.J. Taherzadeh, K. Karimi, ACID-BASED HYDROLYSIS PROCESSES FOR ETHANOL FROM LIGNOCELLULOSIC MATERIALS: A REVIEW, BioResources. 2 (2007) 472–499. https://ojs.cnr.ncsu.edu/index.php/BioRes/article/view/BioRes_2_3_472_499_Taherzadeh_K_AcidHydrolysis_BioEthanol (accessed September 14, 2022).

[138] M. Galbe, G. Zacchi, A review of the production of ethanol from softwood, Appl. Microbiol. Biotechnol. 2003 596. 59 (2002) 618–628. https://doi.org/10.1007/S00253-002-1058-9.

[139] B.K. Sung, J.K. Hyun, J.K. Chang, Enhancement of the enzymatic digestibility of waste

newspaper using tween, Appl. Biochem. Biotechnol. 2006 1301. 130 (2006) 486–495. https://doi.org/10.1385/ABAB:130:1:486.

[140] M. Alkasrawi, T. Eriksson, J. Börjesson, A. Wingren, M. Galbe, F. Tjerneld, G. Zacchi, The effect of Tween-20 on simultaneous saccharification and fermentation of softwood to ethanol, Enzyme Microb. Technol. 33 (2003) 71–78. https://doi.org/10.1016/S0141-0229(03)00087-5.

[141] D. DODD, I.K.O. CANN, Enzymatic deconstruction of xylan for biofuel production, GCB Bioenergy. 1 (2009) 2–17. https://doi.org/10.1111/J.1757-1707.2009.01004.X.

[142] J. Shekiro, E.M. Kuhn, M.J. Selig, N.J. Nagle, S.R. Decker, R.T. Elander, Enzymatic conversion of xylan residues from dilute acid-pretreated corn stover, Appl. Biochem. Biotechnol. 168 (2012) 421–433. https://doi.org/10.1007/S12010-012-9786-5/TABLES/5.

[143] S.G. Nair, S. R, S. Shashidhar, Fungal xylanase production under solid state and submerged fermentation conditions, African J. Microbiol. Res. 2 (2008) 82–86. https://doi.org/10.5897/AJMR.9000334.

[144] M.L.T.M. Polizeli, A.C.S. Rizzatti, R. Monti, H.F. Terenzi, J.A. Jorge, D.S. Amorim, Xylanases from fungi: properties and industrial applications, Appl. Microbiol. Biotechnol. 2005 675. 67 (2005) 577–591. https://doi.org/10.1007/S00253-005-1904-7.

[145] S. Singh, C.H. Tyagi, D. Dutt, J.S. Upadhyaya, Production of high level of cellulase-poor xylanases by wild strains of white-rot fungus Coprinellus disseminatus in solid-state fermentation, N. Biotechnol. 26 (2009) 165–170. https://doi.org/10.1016/J.NBT.2009.09.004.

[146] M.G. Godoy, G.M. Amorim, M.S. Barreto, D.M.G. Freire, Agricultural Residues as Animal Feed, Elsevier B.V., 2018. https://doi.org/10.1016/b978-0-444-63990-5.00012-8.

[147] E. Palmqvist, B. Hahn-Hägerdal, Fermentation of lignocellulosic hydrolysates. I: inhibition and detoxification, Bioresour. Technol. 74 (2000) 17–24. https://doi.org/10.1016/S0960-8524(99)00160-1.

[148] Y. Tadele, Y. Tadele, G. Animut, Effect of Exogenous Enzymes on Ruminal degradation of Feed and Animal Performance: A review, (n.d.). http://130.203.136.95/viewdoc/summary?doi=10.1.1.674.7347 (accessed September 14, 2022).

[149] W.Z. Yang, K.A. Beauchemin, L.M. Rode, Effects of an Enzyme Feed Additive on Extent of Digestion and Milk Production of Lactating Dairy Cows, J. Dairy Sci. 82 (1999) 391–403. https://doi.org/10.3168/JDS.S0022-0302(99)75245-8.

[150] V.J.H. Sewalt, W.G. Glasser, K.A. Beauchemin, Lignin Impact on Fiber Degradation. 3. Reversal of Inhibition of Enzymatic Hydrolysis by Chemical Modification of Lignin and by Additives, J. Agric. Food Chem. 45 (1997) 1823–1828. https://doi.org/10.1021/JF9608074/ASSET/IMAGES/LARGE/JF9608074F00003.JPEG.

[151] J.K. Alicja Niewiadomska, A. Niewiadomska, J. Klama, Polish Journal of Microbiology,

Polish J. Microbiol. 54 (2005) 43–48.

[152] M.L. Sinnott, Catalytic Mechanisms of Enzymic Glycosyl Transfer, Chem. Rev. 90 (1990) 1171–1202. https://pubs.acs.org/sharingguidelines (accessed September 14, 2022).

[153] J.A. Kelly, A.R. Sielecki, B.D. Sykes, M.N.G. James, D.C. Phillips, X-ray crystallography of the binding of the bacterial cell wall trisaccharide NAM-NAG-NAM to lysozyme, Nat. 1979 2825741. 282 (1979) 875–878. https://doi.org/10.1038/282875a0.

[154] J.A. Thoma, J.E. Spradlin, S. Dygert, 6 Plant and Animal Amylases, Enzymes. 5 (1971) 115–189. https://doi.org/10.1016/S1874-6047(08)60089-X.

[155] A.M. Hashem, M.M. Rashad, Production of ethanol by yeasts grown on hydrolysate of Egyptian sweet potato., Egypt. J. Food Sci. 21 (1993) 171–180.

[156] J.L. Jones, K.T. Semrau, Wood hydrolysis for ethanol production — previous experience and the economics of selected processes, Biomass. 5 (1984) 109–135. https://doi.org/10.1016/0144-4565(84)90052-0.

[157] *,† Mohammad J. Taherzadeh, ‡ Robert Eklund, § Lena Gustafsson, † and Claes Niklasson, G. Lidén†, Characterization and Fermentation of Dilute-Acid Hydrolyzates from Wood, (1997). https://doi.org/10.1021/IE9700831.

[158] N. Qureshi, G.J. Manderson, Bioconversion of Renewable Resources into Ethanol: An Economic Evaluation of Selected Hydrolysis, Fermentation, and Membrane Technologies, Http://Dx.Doi.Org/10.1080/00908319508946081. 17 (2007) 241–265. https://doi.org/10.1080/00908319508946081.

[159] B.C. Saha, Hemicellulose bioconversion, J. Ind. Microbiol. Biotechnol. 30 (2003) 279–291. https://doi.org/10.1007/S10295-003-0049-X.

[160] J. Xu, J.J. Cheng, Pretreatment of switchgrass for sugar production with the combination of sodium hydroxide and lime, Bioresour. Technol. 102 (2011) 3861–3868. https://doi.org/10.1016/J.BIORTECH.2010.12.038.

[161] S. Larsson, A. Reimann, N.O. Nilvebrant, L.J. Jönsson, Comparison of different methods for the detoxification of lignocellulose hydrolyzates of spruce, Appl. Biochem. Biotechnol. 1999 771. 77 (1999) 91–103. https://doi.org/10.1385/ABAB:77:1-3:91.

[162] R.J. Ulbricht, S.J. Northup, J.A. Thomas, A Review of 5-Hydroxymethylfurfural (HMF) in Parenteral Solutions, Toxicol. Sci. 4 (1984) 843–853. https://doi.org/10.1093/TOXSCI/4.5.843.

[163] J.J. Bozell, L. Moens, D.C. Elliott, Y. Wang, G.G. Neuenscwander, S.W. Fitzpatrick, R.J. Bilski, J.L. Jarnefeld, Production of levulinic acid and use as a platform chemical for derived products, Resour. Conserv. Recycl. 28 (2000) 227–239. https://doi.org/10.1016/S0921-3449(99)00047-6.

[164] M.J. López, J. Moreno, N.N. Nichols, B.S. Dien, R.J. Bothast, Isolation of microorganisms for biological detoxification of lignocellulosic hydrolysates, Appl.

Microbiol. Biotechnol. 64 (2004) 125–131. https://doi.org/10.1007/S00253-003-1401-9/FIGURES/5.

[165] L.J. Jönsson, E. Palmqvist, N.O. Nilvebrant, B. Hahn-Hägerdal, Detoxification of wood hydrolysates with laccase and peroxidase from the white-rot fungus Trametes versicolor, Appl. Microbiol. Biotechnol. 1998 496. 49 (1998) 691–697. https://doi.org/10.1007/S002530051233.

[166] A.K. Chandel, S.S. da Silva, O. V. Singh, Detoxification of Lignocellulosic Hydrolysates for Improved Bioethanol Production, Biofuel Prod. Dev. Prospect. (2011). https://doi.org/10.5772/16454.

[167] N.N. Nichols, L.N. Sharma, R.A. Mowery, C.K. Chambliss, G.P. van Walsum, B.S. Dien, L.B. Iten, Fungal metabolism of fermentation inhibitors present in corn stover dilute acid hydrolysate, Enzyme Microb. Technol. 42 (2008) 624–630. https://doi.org/10.1016/J.ENZMICTEC.2008.02.008.

[168] W. Parawira, M. Tekere, Biotechnological strategies to overcome inhibitors in lignocellulose hydrolysates for ethanol production: review, Http://Dx.Doi.Org/10.3109/07388551003757816. 31 (2011) 20–31. https://doi.org/10.3109/07388551003757816.

[169] A. Coz, T. Llano, E. Cifrián, J. Viguri, E. Maican, H. Sixta, Physico-Chemical Alternatives in Lignocellulosic Materials in Relation to the Kind of Component for Fermenting Purposes, Mater. 2016, Vol. 9, Page 574. 9 (2016) 574. https://doi.org/10.3390/MA9070574.

[170] P. Reddy Shetty, R.S. Prakasham, R. Sreenivas Rao, P.J. Hobbs, Current trends in biotechnological production of xylitol and future prospects, (n.d.).

[171] B. Alriksson, I.S. Horváth, A. Sjöde, N.O. Nilvebrant, L.J. Jönsson, Ammonium hydroxide detoxification of spruce acid hydrolysates, Appl. Biochem. Biotechnol. - Part A Enzym. Eng. Biotechnol. 124 (2005) 911–922. https://doi.org/10.1007/978-1-59259-991-2_78/COVER.

[172] T.D. Ranatunga, J. Jervis, R.F. Helm, J.D. McMillan, R.J. Wooley, The effect of overliming on the toxicity of dilute acid pretreated lignocellulosics: the role of inorganics, uronic acids and ether-soluble organics, Enzyme Microb. Technol. 27 (2000) 240–247. https://doi.org/10.1016/S0141-0229(00)00216-7.

[173] B. Alriksson, A. Cavka, L.J. Jönsson, Improving the fermentability of enzymatic hydrolysates of lignocellulose through chemical in-situ detoxification with reducing agents, Bioresour. Technol. 102 (2011) 1254–1263. https://doi.org/10.1016/J.BIORTECH.2010.08.037.

[174] N.O. Nilvebrant, A. Reimann, S. Larsson, L.J. Jönsson, Detoxification of lignocellulose hydrolysates with ion-exchange resins, Appl. Biochem. Biotechnol. 2001 911. 91 (2001) 35–49. https://doi.org/10.1385/ABAB:91-93:1-9:35.

[175] A.K. Chandel, R.K. Kapoor, A. Singh, R.C. Kuhad, Detoxification of sugarcane bagasse hydrolysate improves ethanol production by Candida shehatae NCIM 3501, Bioresour.

Technol. 98 (2007) 1947–1950. https://doi.org/10.1016/J.BIORTECH.2006.07.047.

[176] S. Datta, Y.J. Lin, S.W. Snyder, Current and emerging separations technologies in biorefining, Adv. Biorefineries Biomass Waste Supply Chain Exploit. (2014) 112–151. https://doi.org/10.1533/9780857097385.1.112.

[177] M. Cantarella, L. Cantarella, A. Gallifuoco, A. Spera, F. Alfani, Comparison of different detoxification methods for steam-exploded poplar wood as a substrate for the bioproduction of ethanol in SHF and SSF, Process Biochem. 39 (2004) 1533–1542. https://doi.org/10.1016/S0032-9592(03)00285-1.

[178] S.S. Dalli, S.S. da Silva, B.K. Uprety, S.K. Rakshit, Enhanced Production of Xylitol from Poplar Wood Hydrolysates Through a Sustainable Process Using Immobilized New Strain Candida tropicalis UFMG BX 12-a, Appl. Biochem. Biotechnol. 182 (2017) 1053–1064. https://doi.org/10.1007/S12010-016-2381-4.

[179] S. Mateo, I.C. Roberto, S. Sánchez, A.J. Moya, Detoxification of hemicellulosic hydrolyzate from olive tree pruning residue, Ind. Crops Prod. 49 (2013) 196–203. https://doi.org/10.1016/J.INDCROP.2013.04.046.

[180] J. Zhuang, Y. Liu, Z. Wu, Y. Sun, L. Lin, HYDROLYSIS OF WHEAT STRAW HEMICELLULOSE AND DETOXIFICATION OF THE HYDROLYSATE FOR XYLITOL PRODUCTION, BioResources. 4 (2009) 674–686. https://ojs.cnr.ncsu.edu/index.php/BioRes/article/view/BioRes_04_2_0674_Hydrolysis_Wheat_Straw_Hemi (accessed September 14, 2022).

[181] J.J. Wilson, L. Deschatelets, N.K. Nishikawa, Comparative fermentability of enzymatic and acid hydrolysates of steam-pretreated aspenwood hemicellulose by Pichia stipitis CBS 5776, Appl. Microbiol. Biotechnol. 1989 315. 31 (1989) 592–596. https://doi.org/10.1007/BF00270801.

[182] R.C.L.B. Rodrigues, M.G.A. Felipe, J.B. Almeida e Silva, M. Vitolo, P. V. Gómez, The influence of pH, temperature and hydrolyzate concentration on the removal of volatile and nonvolatile compounds from sugarcane bagasse hemicellulosic hydrolyzate treated with activated charcoal before or after vacuum evaporation, Brazilian J. Chem. Eng. 18 (2001) 299–311. https://doi.org/10.1590/S0104-66322001000300009.

[183] S.S. Dalli, M. Patel, S.K. Rakshit, Development and evaluation of poplar hemicellulose prehydrolysate upstream processes for the enhanced fermentative production of xylitol, Biomass and Bioenergy. 105 (2017) 402–410. https://doi.org/10.1016/J.BIOMBIOE.2017.08.001.

[184] K. Nath, D. Das, Modeling and optimization of fermentative hydrogen production, Bioresour. Technol. 102 (2011) 8569–8581. https://doi.org/10.1016/J.BIORTECH.2011.03.108.

[185] J.K. Whiteman, E.B. Gueguim Kana, Comparative Assessment of the Artificial Neural Network and Response Surface Modelling Efficiencies for Biohydrogen Production on Sugar Cane Molasses, Bioenergy Res. 7 (2014) 295–305. https://doi.org/10.1007/S12155-013-9375-7/FIGURES/8.

[186] S. Hussain, H. Khan, S. Gul, J.R. Steter, A.J. Motheo, Modeling of photolytic degradation of sulfamethoxazole using boosted regression tree (BRT), artificial neural network (ANN) and response surface methodology (RSM); energy consumption and intermediates study, Chemosphere. 276 (2021) 130151. https://doi.org/10.1016/J.CHEMOSPHERE.2021.130151.

[187] E. Franco-Lara, H. Link, D. Weuster-Botz, Evaluation of artificial neural networks for modelling and optimization of medium composition with a genetic algorithm, Process Biochem. 41 (2006) 2200–2206. https://doi.org/10.1016/J.PROCBIO.2006.06.024.

[188] W. Feng, T. Zhao, Y. Zhou, F. Li, Y. Zou, S. Bai, W. Wang, L. Yang, X. Wu, Optimization of enzyme-assisted extraction and characterization of collagen from Chinese sturgeon (Acipenser sturio Linnaeus) skin, Pharmacogn. Mag. 9 (2013) S32. https://doi.org/10.4103/0973-1296.117859.

[189] E.B. Gueguim Kana, J.K. Oloke, A. Lateef, M.O. Adesiyan, Modeling and optimization of biogas production on saw dust and other co-substrates using Artificial Neural network and Genetic Algorithm, Renew. Energy. 46 (2012) 276–281. https://doi.org/10.1016/J.RENENE.2012.03.027.

[190] Y. Sewsynker-Sukai, F. Faloye, E.B.G. Kana, Artificial neural networks: an efficient tool for modelling and optimization of biofuel production (a mini review), Http://Mc.Manuscriptcentral.Com/Tbeq. 31 (2016) 221–235. https://doi.org/10.1080/13102818.2016.1269616.

[191] H. Abu Qdais, K. Bani Hani, N. Shatnawi, Modeling and optimization of biogas production from a waste digester using artificial neural network and genetic algorithm, Resour. Conserv. Recycl. 54 (2010) 359–363. https://doi.org/10.1016/J.RESCONREC.2009.08.012.

[192] V.K. Garlapati, R. Banerjee, Evolutionary and swarm intelligence-based approaches for optimization of lipase extraction from fermented broth, Eng. Life Sci. 10 (2010) 265–273. https://doi.org/10.1002/ELSC.200900086.

[193] J.W. (Jan W. Gooch, Encyclopedic dictionary of polymers, (2010).

[194] L.R. Lynd, M.S. Laser, D. Bransby, B.E. Dale, B. Davison, R. Hamilton, M. Himmel, M. Keller, J.D. McMillan, J. Sheehan, C.E. Wyman, How biotech can transform biofuels, Nat. Biotechnol. 2008 262. 26 (2008) 169–172. https://doi.org/10.1038/nbt0208-169.

[195] C.A. Cardona, Ó.J. Sánchez, Fuel ethanol production: Process design trends and integration opportunities, Bioresour. Technol. 98 (2007) 2415–2457. https://doi.org/10.1016/J.BIORTECH.2007.01.002.

[196] E. Gnansounou, A. Dauriat, C.E. Wyman, Refining sweet sorghum to ethanol and sugar: economic trade-offs in the context of North China, Bioresour. Technol. 96 (2005) 985–1002. https://doi.org/10.1016/J.BIORTECH.2004.09.015.

[197] Bioconversion of Waste Materials to Industrial Products, Bioconversion Waste Mater. to Ind. Prod. (1998). https://doi.org/10.1007/978-1-4615-5821-7.

[198] W. Carvalho, J.C. Santos, L. Canilha, J.B. Almeida E Silva, M.G.A. Felipe, I.M. Mancilha, S.S. Silva, A study on xylitol production from sugarcane bagasse hemicellulosic hydrolysate by Ca-alginate entrapped cells in a stirred tank reactor, Process Biochem. 39 (2004) 2135–2141. https://doi.org/10.1016/J.PROCBIO.2003.11.021.

[199] W. Carvalho, J.C. Santos, L. Canilha, S.S. Silva, P. Perego, A. Converti, Xylitol production from sugarcane bagasse hydrolysate: Metabolic behaviour of Candida guilliermondii cells entrapped in Ca-alginate, Biochem. Eng. J. 25 (2005) 25–31. https://doi.org/10.1016/J.BEJ.2005.03.006.

[200] J.C. Santos, A. Converti, W. De Carvalho, S.I. Mussatto, S.S. Da Silva, Influence of aeration rate and carrier concentration on xylitol production from sugarcane bagasse hydrolyzate in immobilized-cell fluidized bed reactor, Process Biochem. 40 (2005) 113–118. https://doi.org/10.1016/J.PROCBIO.2003.11.045.

[201] P. V. Gurgel, I.M. Mancilha, R.P. Peçanha, J.F.M. Siqueira, Xylitol recovery from fermented sugarcane bagasse hydrolyzate, Bioresour. Technol. 52 (1995) 219–223. https://doi.org/10.1016/0960-8524(95)00025-A.

[202] K. Kiyosawa, Volumetric properties of polyols (ethylene glycol, glycerol, meso-erythritol, xylitol and mannitol) in relation to their membrane permeability: Group additivity and estimation of the maximum radius of their molecules, Biochim. Biophys. Acta - Biomembr. 1064 (1991) 251–255. https://doi.org/10.1016/0005-2736(91)90309-V.

[203] S.S. Silva, R.M. Ramos, C.G.A. Rodrigues, I.M. Mancilha, Downstream Processing for Xylitol Recovery from Fermented Sugar Cane Bagasse Hydrolysate Using Aluminium Polychloride, Zeitschrift Für Naturforsch. C. 55 (2000) 10–15. https://doi.org/10.1515/ZNC-2000-1-204.

[204] J.W. Mullin, Crystallization: Chpater 5- Nucleation, Crystallization. (2001) 181–215.

[205] E. Aamir, Population balance model-based optimal control of batch crystallisation processes for systematic crystal size distribution design, (2010). /articles/thesis/Population_balance_model-based_optimal_control_of_batch_crystallisation_processes_for_systematic_crystal_size_distribution_design/9239399/1 (accessed September 15, 2022).

[206] Crystallization Technology Handbook - Google Books, (n.d.). https://books.google.co.in/books?hl=en&lr=&id=l839DwAAQBAJ&oi=fnd&pg=PP1&dq=Mersmann,+A.,+2001.+Crystallization+Technology+Handbook+-+Second+Edition+Revised+and++Expanded,+Marcel+Dekker+Inc.&ots=E_2YrDzcTs&sig=cE1Nj52DF0SucbTU2N_H2M79tIU&redir_esc=y#v=onepage&q&f=false (accessed September 15, 2022).

[207] A.M. Schwartz, A.S. Myerson, Solutions and solution properties, Handb. Ind. Cryst. (2002) 1–31. https://doi.org/10.1016/B978-075067012-8/50003-3.

[208] T. Panagiotou, R.J. Fisher, Enhanced Transport Capabilities via Nanotechnologies: Impacting Bioefficacy, Controlled Release Strategies, and Novel Chaperones, J. Drug

Deliv. 2011 (2011) 1–14. https://doi.org/10.1155/2011/902403.

[209] A. Sluiter, B. Hames, R. Ruiz, C. Scarlata, J. Sluiter, D. Templeton, D. Crocker, Determination of Structural Carbohydrates and Lignin in Biomass Laboratory Analytical Procedure (LAP) Issue Date: 7/17/2005, (2008). www.nrel.gov (accessed July 23, 2022).

[210] L. Segal, J.J. Creely, A.E. Martin, C.M. Conrad, An Empirical Method for Estimating the Degree of Crystallinity of Native Cellulose Using the X-Ray Diffractometer, Text. Res. J. 29 (1959) 786–794. https://doi.org/10.1177/004051755902901003.

[211] S. V. Vassilev, C.G. Vassileva, V.S. Vassilev, Advantages and disadvantages of composition and properties of biomass in comparison with coal: An overview, Fuel. 158 (2015) 330–350. https://doi.org/10.1016/J.FUEL.2015.05.050.

[212] D. Lynch, A.M. Henihan, B. Bowen, D. Lynch, K. McDonnell, W. Kwapinski, J.J. Leahy, Utilisation of poultry litter as an energy feedstock, Biomass and Bioenergy. 49 (2013) 197–204. https://doi.org/10.1016/J.BIOMBIOE.2012.12.009.

[213] V. Sóti, S. Lenaerts, I. Cornet, Of enzyme use in cost-effective high solid simultaneous saccharification and fermentation processes, J. Biotechnol. 270 (2018) 70–76. https://doi.org/10.1016/J.JBIOTEC.2018.01.020.

[214] A.A. Guilherme, P.V.F. Dantas, E.S. Santos, F.A.N. Fernandes, G.R. Macedo, EVALUATION OF COMPOSITION, CHARACTERIZATION AND ENZYMATIC HYDROLYSIS OF PRETREATED SUGAR CANE BAGASSE, Brazilian J. Chem. Eng. 32 (2015) 23–33. https://doi.org/10.1590/0104-6632.20150321S00003146.

[215] M. Asgher, Z. Ahmad, H.M.N. Iqbal, Alkali and enzymatic delignification of sugarcane bagasse to expose cellulose polymers for saccharification and bio-ethanol production, Ind. Crops Prod. 44 (2013) 488–495. https://doi.org/10.1016/J.INDCROP.2012.10.005.

[216] K. Guo, B. Gao, Q. Yue, X. Xu, R. Li, X. Shen, Characterization and performance of a novel lignin-based flocculant for the treatment of dye wastewater, Int. Biodeterior. Biodegradation. 133 (2018) 99–107. https://doi.org/10.1016/J.IBIOD.2018.06.015.

[217] C.J. Chirayil, J. Joy, L. Mathew, M. Mozetic, J. Koetz, S. Thomas, Isolation and characterization of cellulose nanofibrils from Helicteres isora plant, Ind. Crops Prod. 59 (2014) 27–34. https://doi.org/10.1016/J.INDCROP.2014.04.020.

[218] M. Brebu, C. Vasile, THERMAL DEGRADATION OF LIGNIN-A REVIEW, Cellul. Chem. Technol. Cellul. Chem. Technol. 44 (2010) 353–363.

[219] E. Cárdenas- Aguiar, G. Gascó, J. Paz-Ferreiro, A. Méndez, The effect of biochar and compost from urban organic waste on plant biomass and properties of an artificially copper polluted soil, Int. Biodeterior. Biodegradation. 124 (2017) 223–232. https://doi.org/10.1016/J.IBIOD.2017.05.014.

[220] C.S. Julie Chandra, N. George, S.K. Narayanankutty, Isolation and characterization of cellulose nanofibrils from arecanut husk fibre, Carbohydr. Polym. 142 (2016) 158–166. https://doi.org/10.1016/J.CARBPOL.2016.01.015.

[221] M.N. Mahamad, M.A.A. Zaini, Z.A. Zakaria, Preparation and characterization of activated carbon from pineapple waste biomass for dye removal, Int. Biodeterior. Biodegradation. 102 (2015) 274–280. https://doi.org/10.1016/J.IBIOD.2015.03.009.

[222] S. Sasmal, V. V. Goud, K. Mohanty, Determination of salutary parameters to facilitate bio-energy production from three uncommon biomasses using thermogravimetric analysis, J. Therm. Anal. Calorim. 111 (2013) 1649–1655. https://doi.org/10.1007/S10973-011-1891-0/TABLES/4.

[223] W.G. Glasser, Comprehensive Cellulose Chemistry Edited by D. Klemm, (University of Jena), B. Philipp (Max Planck Institute Teltow-Seehof), T. Heinze (University of Jena), U. Heinze (University of Jena), and W. Wagenknecht (Max Planck Institute Teltow-Seehof). Wiley-VCH, Weinheim, Germany, 1998. Volume 1, xxii + 260 pp. 16.5 × 24 cm. $170.00. ISBN 3-527-29413-9. Volume 2, xvi + 390 pp. 16.5 × 24 cm. $188.00. ISBN 3-527-29489-9., J. Nat. Prod. 62 (1999) 800–800. https://doi.org/10.1021/NP980254M.

[224] Y. Li, L. Xia, J.F.T. Vazquez, S. Song, Optimization of Supercritical CO2 Extraction of Essential Oil from Artemisia annua L. by Means of Response Surface Methodology, Http://Dx.Doi.Org/10.1080/0972060X.2017.1298475. 20 (2017) 314–327. https://doi.org/10.1080/0972060X.2017.1298475.

[225] S. Sasmal, V. V. Goud, K. Mohanty, Optimisation of the acid catalysed pretreatment of areca nut husk fibre using the Taguchi design method, Biosyst. Eng. 110 (2011) 465–472. https://doi.org/10.1016/J.BIOSYSTEMSENG.2011.09.013.

[226] F. Meddeb-Mouelhi, J.K. Moisan, M. Beauregard, A comparison of plate assay methods for detecting extracellular cellulase and xylanase activity, Enzyme Microb. Technol. 66 (2014) 16–19. https://doi.org/10.1016/J.ENZMICTEC.2014.07.004.

[227] Z. Li, X. Guo, X. Feng, C. Li, An environment friendly and efficient process for xylitol bioconversion from enzymatic corncob hydrolysate by adapted Candida tropicalis, Chem. Eng. J. 263 (2015) 249–256. https://doi.org/10.1016/J.CEJ.2014.11.013.

[228] A.S.A. Da Silva, H. Inoue, T. Endo, S. Yano, E.P.S. Bon, Milling pretreatment of sugarcane bagasse and straw for enzymatic hydrolysis and ethanol fermentation, Bioresour. Technol. 101 (2010) 7402–7409. https://doi.org/10.1016/J.BIORTECH.2010.05.008.

[229] M. Martins, M. Henriques, J. Azeredo, S.M. Rocha, M.A. Coimbra, R. Oliveira, Morphogenesis control in Candida albicans and Candida dubliniensis through signaling molecules produced by planktonic and biofilm cells, Eukaryot. Cell. 6 (2007) 2429–2436. https://doi.org/10.1128/EC.00252-07/ASSET/372A4F99-9812-40E2-9A8A-D1DB245418CE/ASSETS/GRAPHIC/ZEK0120730350003.JPEG.

[230] A. Waheed Khan, J.P. Labrie, J. McKeown, Electron beam irradiation pretreatment and enzymatic saccharification of used newsprint and paper mill wastes, Int. J. Radiat. Appl. Instrumentation. Part C. Radiat. Phys. Chem. 29 (1987) 117–120. https://doi.org/10.1016/1359-0197(87)90044-0.

[231] R. Chosdu, N. Hilmy, Erizal, T.B. Erlinda, B. Abbas, Radiation and chemical

pretreatment of cellulosic waste, Radiat. Phys. Chem. 42 (1993) 695–698. https://doi.org/10.1016/0969-806X(93)90354-W.

[232] J.S. Bak, J.K. Ko, Y.H. Han, B.C. Lee, I.G. Choi, K.H. Kim, Improved enzymatic hydrolysis yield of rice straw using electron beam irradiation pretreatment, Bioresour. Technol. 100 (2009) 1285–1290. https://doi.org/10.1016/J.BIORTECH.2008.09.010.

[233] J. Lamaming, R. Hashim, O. Sulaiman, C.P. Leh, T. Sugimoto, N.A. Nordin, Cellulose nanocrystals isolated from oil palm trunk, Carbohydr. Polym. 127 (2015) 202–208. https://doi.org/10.1016/J.CARBPOL.2015.03.043.

[234] H. Gao, B. Duan, A. Lu, H. Deng, Y. Du, X. Shi, L. Zhang, Fabrication of cellulose nanofibers from waste brown algae and their potential application as milk thickeners, Food Hydrocoll. 79 (2018) 473–481. https://doi.org/10.1016/J.FOODHYD.2018.01.023.

[235] H. Zhang, S. Wu, J. Xie, Evaluation of the effects of isolated lignin on enzymatic hydrolysis of cellulose, Enzyme Microb. Technol. 101 (2017) 44–50. https://doi.org/10.1016/J.ENZMICTEC.2017.03.001.

[236] A. Mandal, D. Chakrabarty, Isolation of nanocellulose from waste sugarcane bagasse (SCB) and its characterization, Carbohydr. Polym. 86 (2011) 1291–1299. https://doi.org/10.1016/J.CARBPOL.2011.06.030.

[237] N. Ahmad, S. Sultana, A. Azam, S. Sabir, M.Z. Khan, Novel bio-nanocomposite materials for enhanced biodegradability and photocatalytic activity, New J. Chem. 41 (2017) 10198–10207. https://doi.org/10.1039/C7NJ00842B.

[238] P. Kumari, G. Pathak, R. Gupta, D. Sharma, A. Meena, Cellulose nanofibers from lignocellulosic biomass of lemongrass using enzymatic hydrolysis: characterization and cytotoxicity assessment., DARU, J. Pharm. Sci. 27 (2019) 683–693. https://doi.org/10.1007/S40199-019-00303-1/FIGURES/7.

[239] and J.S. Heitner, Cyril, Don Dimmel, No Title, CRC Press Taylor Fr. Gr. 9 (2016) 322–341.

[240] K.L. Larsen, S. Barsberg, Theoretical and Raman Spectroscopic Studies of Phenolic Lignin Model Monomers, J. Phys. Chem. B. 114 (2010) 8009–8021. https://doi.org/10.1021/JP1028239/ASSET/IMAGES/MEDIUM/JP-2010-028239_0009.GIF.

[241] U.P. Agarwal, S.A. Ralph, FT-Raman spectroscopy of wood: Identifying contributions of lignin and carbohydrate polymers in the spectrum of black spruce (Picea mariana), Appl. Spectrosc. 51 (1997) 1648–1655. https://doi.org/10.1366/0003702971939316.

[242] M. Kačuráková, N. Wellner, A. Ebringerová, Z. Hromádková, R.H. Wilson, P.S. Belton, Characterisation of xylan-type polysaccharides and associated cell wall components by FT-IR and FT-Raman spectroscopies, Food Hydrocoll. 13 (1999) 35–41. https://doi.org/10.1016/S0268-005X(98)00067-8.

[243] J.H. Wiley, R.H. Atalla, Band assignments in the raman spectra of celluloses, Carbohydr. Res. 160 (1987) 113–129. https://doi.org/10.1016/0008-6215(87)80306-3.

[244] S.D. Kshirsagar, P.R. Waghmare, P. Chandrakant Loni, S.A. Patil, S.P. Govindwar, Dilute acid pretreatment of rice straw, structural characterization and optimization of enzymatic hydrolysis conditions by response surface methodology, RSC Adv. 5 (2015) 46525–46533. https://doi.org/10.1039/C5RA04430H.

[245] X.F. Sun, F. Xu, R.C. Sun, P. Fowler, M.S. Baird, Characteristics of degraded cellulose obtained from steam-exploded wheat straw, Carbohydr. Res. 340 (2005) 97–106. https://doi.org/10.1016/J.CARRES.2004.10.022.

[246] F. Peng, J.L. Ren, F. Xu, J. Bian, P. Peng, R.C. Sun, Comparative study of hemicelluloses obtained by graded ethanol precipitation from sugarcane bagasse, J. Agric. Food Chem. 57 (2009) 6305–6317. https://doi.org/10.1021/JF900986B/ASSET/IMAGES/LARGE/JF-2009-00986B_0007.JPEG.

[247] E.E. Oliveira, A.E. Silva, T.N. Júnior, M.C.S. Gomes, L.M. Aguiar, H.R. Marcelino, I.B. Araújo, M.P. Bayer, N.M.P.S. Ricardo, A.G. Oliveira, E.S.T. Egito, Xylan from corn cobs, a promising polymer for drug delivery: Production and characterization, Bioresour. Technol. 101 (2010) 5402–5406. https://doi.org/10.1016/J.BIORTECH.2010.01.137.

[248] C. Cai, Y. Bao, F. Li, Y. Pang, H. Lou, Y. Qian, X. Qiu, Using highly recyclable sodium caseinate to enhance lignocellulosic hydrolysis and cellulase recovery, Bioresour. Technol. 304 (2020) 122974. https://doi.org/10.1016/J.BIORTECH.2020.122974.

[249] J. Yan, W. Jianping, L. Hongmei, Y. Suliang, H. Zongding, The biodegradation of phenol at high initial concentration by the yeast Candida tropicalis, Biochem. Eng. J. 24 (2005) 243–247. https://doi.org/10.1016/J.BEJ.2005.02.016.

[250] J.M. Tavares, L.C. Duarte, M.T. Amaral-Collaço, F.M. Gírio, The influence of hexoses addition on the fermentation of d-xylose in Debaryomyces hansenii under continuous cultivation, Enzyme Microb. Technol. 26 (2000) 743–747. https://doi.org/10.1016/S0141-0229(00)00166-6.

[251] B.M. Harahap, M.T.A.P. Kresnowati, Moderate pretreatment of oil palm empty fruit bunches for optimal production of xylitol via enzymatic hydrolysis and fermentation, Biomass Convers. Biorefinery. 8 (2018) 255–263. https://doi.org/10.1007/S13399-017-0299-X/TABLES/3.

[252] E. Mardawati, N. Maharani, D.W. Wira, B.M. Harahap, T. Yuliana, E. Sukarminah, Xylitol Production from Oil Palm Empty Fruit Bunches (OPEFB) Via Simultaneous Enzymatic Hydrolysis and Fermentation Process, J. Ind. Inf. Technol. Agric. 2 (2020) 29–36. https://doi.org/10.24198/JIITA.V2I1.25064.

[253] B. Rivas, J.M. Domínguez, H. Domínguez, J.C. Parajó, Bioconversion of posthydrolysed autohydrolysis liquors: An alternative for xylitol production from corn cobs, Enzyme Microb. Technol. 31 (2002) 431–438. https://doi.org/10.1016/S0141-0229(02)00098-4.

[254] K. Tada, J.I. Horiuchi, T. Kanno, M. Kobayashi, Microbial xylitol production from corn cobs using Candida magnoliae, J. Biosci. Bioeng. 98 (2004) 228–230. https://doi.org/10.1016/S1389-1723(04)00273-7.

[255] T.L. de Albuquerque, S.D.L. Gomes, J.E. Marques, I.J. da Silva, M.V.P. Rocha, Xylitol production from cashew apple bagasse by Kluyveromyces marxianus CCA510, Catal. Today. 255 (2015) 33–40. https://doi.org/10.1016/J.CATTOD.2014.10.054.

[256] F. Carvalheiro, L.C. Duarte, R. Medeiros, F.M. Gírio, Xylitol production by Debaryomyces hansenii in brewery spent grain dilute-acid hydrolysate: effect of supplementation, Biotechnol. Lett. 29 (2007) 1887–1891. https://doi.org/10.1007/S10529-007-9468-5.

[257] S.C. Baek, Y.J. Kwon, Optimization of the pretreatment of rice straw hemicellulosic hydrolyzates for microbial production of xylitol, Biotechnol. Bioprocess Eng. 2007 124. 12 (2007) 404–409. https://doi.org/10.1007/BF02931063.

[258] B. Tong, Z.C. Tan, Q. Shi, Y.S. Li, D.T. Yue, S.X. Wang, Thermodynamic investigation of several natural polyols (I): Heat capacities and thermodynamic properties of xylitol, Thermochim. Acta. 457 (2007) 20–26. https://doi.org/10.1016/J.TCA.2007.02.022.

[259] J.E. Marques Júnior, M.V.P. Rocha, Development of a purification process via crystallization of xylitol produced for bioprocess using a hemicellulosic hydrolysate from the cashew apple bagasse as feedstock, Bioprocess Biosyst. Eng. 44 (2021) 713–725. https://doi.org/10.1007/S00449-020-02480-9/FIGURES/9.

[260] L.H. Deng, Y. Tang, Y. Liu, Detoxification of corncob acid hydrolysate with SAA pretreatment and xylitol production by immobilized Candida tropicalis, Sci. World J. 2014 (2014). https://doi.org/10.1155/2014/214632.

[261] S. Misra, S. Raghuwanshi, R.K. Saxena, Evaluation of corncob hemicellulosic hydrolysate for xylitol production by adapted strain of Candida tropicalis, Carbohydr. Polym. 92 (2013) 1596–1601. https://doi.org/10.1016/J.CARBPOL.2012.11.033.

[262] H. Jia, T. Shao, C. Zhong, H. Li, M. Jiang, H. Zhou, P. Wei, Evaluation of xylitol production using corncob hemicellulosic hydrolysate by combining tetrabutylammonium hydroxide extraction with dilute acid hydrolysis, Carbohydr. Polym. 151 (2016) 676–683. https://doi.org/10.1016/J.CARBPOL.2016.06.013.

[263] P. Jeevan, R. Nelson, A.E. Rena, Optimization studies on acid hydrolysis of Corn cob hemicellulosic hydrolysate for Microbial production of xylitol, J. Microbiol. Biotechnol. Res. Sch. Res. Libr. J. Microbiol. Biotech. Res. 1 (2011) 114–123. http://scholarsresearchlibrary.com/archive.html (accessed August 6, 2022).

[264] R. Torget, P. Walter, M. Himmel, K. Grohmann, Dilute-Acid Pretreatment of Corn Residues and Short-Rotation Woody Crops, Appl. Biochem. Biotechnol. 1991 281. 28 (1991) 75–86. https://doi.org/10.1007/BF02922590.

[265] C.F. Huang, Y.F. Jiang, G.L. Guo, W.S. Hwang, Development of a yeast strain for xylitol production without hydrolysate detoxification as part of the integration of co-product generation within the lignocellulosic ethanol process, Bioresour. Technol. 102 (2011) 3322–3329. https://doi.org/10.1016/J.BIORTECH.2010.10.111.

[266] N.B. Santana, J.C. Teixeira Dias, R.P. Rezende, M. Franco, L.K. Silva Oliveira, L.O. Souza, Production of xylitol and bio-detoxification of cocoa pod husk hemicellulose

hydrolysate by Candida boidinii XM02G, PLoS One. 13 (2018) e0195206. https://doi.org/10.1371/JOURNAL.PONE.0195206.

[267] S. Misra, S. Raghuwanshi, R.K. Saxena, Evaluation of corncob hemicellulosic hydrolysate for xylitol production by adapted strain of Candida tropicalis, Carbohydr. Polym. 92 (2013) 1596–1601. https://doi.org/10.1016/J.CARBPOL.2012.11.033.

[268] G. Jing Ping, C. Bai Yan, L. Guo Ming, L. Hong Zhi, F. Bao Zhu, S. Gang, Y. Xiao Feng, P. Wen Xiang, Comparison of different detoxification methods for corn cob hemicelluose hydrolysate to improve ethanol production by Candida shehatae ACCC 20335, African J. Microbiol. Res. 5 (2011) 1163–1168. https://doi.org/10.5897/ajmr10.744.

[269] L. Canilha, J.B. De Almeida E Silva, A.I.N. Solenzal, Eucalyptus hydrolysate detoxification with activated charcoal adsorption or ion-exchange resins for xylitol production, Process Biochem. 39 (2004) 1909–1912. https://doi.org/10.1016/J.PROCBIO.2003.09.009.

[270] F. Peng, J.L. Ren, F. Xu, J. Bian, P. Peng, R.C. Sun, Comparative study of hemicelluloses obtained by graded ethanol precipitation from sugarcane bagasse, J. Agric. Food Chem. 57 (2009) 6305–6317. https://doi.org/10.1021/JF900986B/ASSET/IMAGES/LARGE/JF-2009-00986B_0007.JPEG.

[271] H.A. Ruiz, M.A. Cerqueira, H.D. Silva, R.M. Rodríguez-Jasso, A.A. Vicente, J.A. Teixeira, Biorefinery valorization of autohydrolysis wheat straw hemicellulose to be applied in a polymer-blend film, Carbohydr. Polym. 92 (2013) 2154–2162. https://doi.org/10.1016/J.CARBPOL.2012.11.054.

[272] Y. Ping, H.Z. Ling, G. Song, J.P. Ge, Xylitol production from non-detoxified corncob hemicellulose acid hydrolysate by Candida tropicalis, Biochem. Eng. J. 75 (2013) 86–91. https://doi.org/10.1016/J.BEJ.2013.03.022.

[273] J. Buhner, F.A. Agblevor, Effect of detoxification of dilute-acid corn fiber hydrolysate on xylitol production, Appl. Biochem. Biotechnol. 2004 1191. 119 (2004) 13–30. https://doi.org/10.1385/ABAB:119:1:13.

[274] L. Canilha, W. Carvalho, J.B. Almeida E Silva, Xylitol bioproduction from wheat straw: hemicellulose hydrolysis and hydrolyzate fermentation, J. Sci. Food Agric. 86 (2006) 1371–1376. https://doi.org/10.1002/JSFA.2524.

[275] T.L. de Albuquerque, S.D.L. Gomes, J.E. Marques, I.J. da Silva, M.V.P. Rocha, Xylitol production from cashew apple bagasse by Kluyveromyces marxianus CCA510, Catal. Today. 255 (2015) 33–40. https://doi.org/10.1016/J.CATTOD.2014.10.054.

[276] J.C. Parajó, H. Dominguez, J.M. Dominguez, Study of charcoal adsorption for improving the production of Xylitol from wood hydrolysates, Bioprocess Eng. 1996 161. 16 (1996) 39–43. https://doi.org/10.1007/S004490050285.

[277] C.H. Ko, P.N. Chiang, P.C. Chiu, C.C. Liu, C.L. Yang, I.L. Shiau, Integrated xylitol production by fermentation of hardwood wastes, J. Chem. Technol. Biotechnol. 83

(2008) 534–540. https://doi.org/10.1002/JCTB.1828.

[278] L. Venkateswar Rao, J.K. Goli, J. Gentela, S. Koti, Bioconversion of lignocellulosic biomass to xylitol: An overview, Bioresour. Technol. 213 (2016) 299–310. https://doi.org/10.1016/J.BIORTECH.2016.04.092.

[279] M.E. Vallejos, M. Chade, E.B. Mereles, D.I. Bengoechea, J.G. Brizuela, F.E. Felissia, M.C. Area, Strategies of detoxification and fermentation for biotechnological production of xylitol from sugarcane bagasse, Ind. Crops Prod. 91 (2016) 161–169. https://doi.org/10.1016/J.INDCROP.2016.07.007.

[280] M.L.M. Villarreal, A.M.R. Prata, M.G.A. Felipe, J.B. Almeida E Silva, Detoxification procedures of eucalyptus hemicellulose hydrolysate for xylitol production by Candida guilliermondii, Enzyme Microb. Technol. 40 (2006) 17–24. https://doi.org/10.1016/J.ENZMICTEC.2005.10.032.

[281] R.C.L.B. Rodrigues, M.G.A. Felipe, I.C. Roberto, M. Vitolo, Batch xylitol production by Candida guilliermondii FTI 20037 from sugarcane bagasse hemicellulosic hydrolyzate at controlled pH values, Bioprocess Biosyst. Eng. 26 (2003) 103–107. https://doi.org/10.1007/S00449-003-0332-2/FIGURES/2.

[282] J. Zhang, A. Geng, C. Yao, Y. Lu, Q. Li, Effects of lignin-derived phenolic compounds on xylitol production and key enzyme activities by a xylose utilizing yeast Candida athensensis SB18, Bioresour. Technol. 121 (2012) 369–378. https://doi.org/10.1016/J.BIORTECH.2012.07.020.

[283] E.A. Martínez, E. V Canettieri, J.A. C Bispo, M. Giulietti, J.B. de Almeida Silva, A. Converti, J.B. de Almeida, Strategies for Xylitol Purification and Crystallization: A Review, Sep. Sci. Technol. 50 (2015) 2087–2098. https://doi.org/10.1080/01496395.2015.1009115.

[284] E.A. Martínez, J.B. de Almeida e Silva, M. Giulietti, A.I.N. Solenzal, Downstream process for xylitol produced from fermented hydrolysate, Enzyme Microb. Technol. 40 (2007) 1193–1198. https://doi.org/10.1016/J.ENZMICTEC.2006.09.003.

[285] H. Yang, Y. Fu, Y. Zhang, J. Zhou, D. Wang, Z. Gao, Y. Ke, Q. Lv, B. Ding, X. Wang, Evaluation of mannitol and xylitol on the quality of wheat flour and extruded flour products, Int. J. Food Sci. Technol. 56 (2021) 4119–4128. https://doi.org/10.1111/IJFS.15040.

[286] G.J. Puppels, J.H.F. Olminkhof, G.M.J. Segers-Nolten, C. Otto, F.F.M. de Mul, J. Greve, Laser irradiation and Raman spectroscopy of single living cells and chromosomes: Sample degradation occurs with 514.5 nm but not with 660 nm laser light, Exp. Cell Res. 195 (1991) 361–367. https://doi.org/10.1016/0014-4827(91)90385-8.

[287] Y. Takai, T. Masuko, H. Takeuchi, Lipid structure of cytotoxic granules in living human killer T lymphocytes studied by Raman microspectroscopy, Biochim. Biophys. Acta - Gen. Subj. 1335 (1997) 199–208. https://doi.org/10.1016/S0304-4165(96)00138-9.

[288] C. Matthäus, B. Bird, M. Miljković, T. Chernenko, M. Romeo, M. Diem, Chapter 10 Infrared and Raman Microscopy in Cell Biology, Methods Cell Biol. 89 (2008) 275–308.

https://doi.org/10.1016/S0091-679X(08)00610-9.

[289] K.C. Schuster, E. Urlaub, J.R. Gapes, Single-cell analysis of bacteria by Raman microscopy: spectral information on the chemical composition of cells and on the heterogeneity in a culture, J. Microbiol. Methods. 42 (2000) 29–38. https://doi.org/10.1016/S0167-7012(00)00169-X.

[290] N. Uzunbajakava, A. Lenferink, Y. Kraan, B. Willekens, G. Vrensen, J. Greve, C. Otto, Nonresonant Raman imaging of protein distribution in single human cells, Biopolymers. 72 (2003) 1–9. https://doi.org/10.1002/BIP.10246.

[291] P. Stacey, S. Hall, S. Stagg, F. Clegg, C. Sammon, Raman spectroscopy and X-ray diffraction responses when measuring health-related micrometre and nanometre particle size fractions of crystalline quartz and the measurement of quartz in dust samples from the cutting and polishing of natural and artificial stones, J. Raman Spectrosc. 52 (2021) 1095–1107. https://doi.org/10.1002/JRS.6110.

[292] F. Salaün, G. Bedek, E. Devaux, D. Dupont, D. Deranton, Investigation of Water Absorption and Diffusion in Microparticles Containing Xylitol to Provide a Cooling Effect by Thermal Analysis, Int. J. Thermophys. 2009 304. 30 (2009) 1242–1256. https://doi.org/10.1007/S10765-009-0649-4.

[293] D. Robl, P. da S. Delabona, C.M. Mergel, J.D. Rojas, P. dos S. Costa, I.C. Pimentel, V.A. Vicente, J.G. da Cruz Pradella, G. Padilla, The capability of endophytic fungi for production of hemicellulases and related enzymes, BMC Biotechnol. 13 (2013) 1–12. https://doi.org/10.1186/1472-6750-13-94/FIGURES/6.

[294] C. Huang, Z. Chen, Y. Gui, C. Shi, G.G.Z. Zhang, L. Yu, Crystal nucleation rates in glass-forming molecular liquids: D-sorbitol, D-arabitol, D-xylitol, and glycerol, J. Chem. Phys. 149 (2018) 054503. https://doi.org/10.1063/1.5042112.

[295] R. Mellaerts, J.A.G. Jammaer, M. Van Speybroeck, C. Hong, J. Van Humbeeck, P. Augustijns, G. Van Den Mooter, J.A. Martens, Physical state of poorly water soluble therapeutic molecules loaded into SBA-15 ordered mesoporous silica carriers: A case study with itraconazole and ibuprofen, Langmuir. 24 (2008) 8651–8659. https://doi.org/10.1021/LA801161G/ASSET/IMAGES/LARGE/LA-2008-01161G_0009.JPEG.

[296] P. Kinnari, E. Mäkilä, T. Heikkilä, J. Salonen, J. Hirvonen, H.A. Santos, Comparison of mesoporous silicon and non-ordered mesoporous silica materials as drug carriers for itraconazole, Int. J. Pharm. 414 (2011) 148–156. https://doi.org/10.1016/J.IJPHARM.2011.05.021.

[297] J.E. Marques Júnior, M.V.P. Rocha, Development of a purification process via crystallization of xylitol produced for bioprocess using a hemicellulosic hydrolysate from the cashew apple bagasse as feedstock, Bioprocess Biosyst. Eng. 44 (2021) 713–725. https://doi.org/10.1007/S00449-020-02480-9/FIGURES/9.

[298] J. Wei, Q. Yuan, T. Wang, L. Wang, Purification and crystallization of xylitol from fermentation broth of corncob hydrolysates, Front. Chem. Eng. China 2010 41. 4 (2010) 57–64. https://doi.org/10.1007/S11705-009-0295-1.

[299] M.T.A.P. Kresnowati, D. Regina, C. Bella, A.K. Wardani, I.G. Wenten, Combined ultrafiltration and electrodeionization techniques for microbial xylitol purification, Food Bioprod. Process. 114 (2019) 245–252. https://doi.org/10.1016/J.FBP.2019.01.005.

[300] X. Zhao, L. Zhang, D. Liu, Biomass recalcitrance. Part I: the chemical compositions and physical structures affecting the enzymatic hydrolysis of lignocellulose, Biofuels, Bioprod. Biorefining. 6 (2012) 465–482. https://doi.org/10.1002/BBB.1331.

भारतीय प्रौद्योगिकी संस्थान गुवाहाटी
Indian Institute of Technology Guwahati

भारतीय प्रौद्योगिकी संस्थान गुवाहाटी
Indian Institute of Technology Guwahati

List of Publications

Published in peer-reviewed journal

- Vardhan, H., Mahato, R.B., Sasmal, S., Mohanty, K., 2020. Production of Xylose from Pre-treated Husk of Areca Nut. J. Nat. Fibers 19, 131–144. https://doi.org/10.1080/15440478.2020.1731905

- Vardhan, H., Sasamal, S., Mohanty, K., 2022. Fermentation process optimisation based on ANN and RSM for xylitol production from areca nut husk followed by xylitol crystal characterisation. Process Biochem. 122, 146–159. https://doi.org/10.1016/j.procbio.2022.10.005

- Vardhan, H., Sasamal, S., Mohanty, K., 2023. Xylitol Production by Candida tropicalis from Areca Nut Husk Enzymatic Hydrolysate and Crystallization. Appl. Biochem. Biotechnol. 2023 1–24. https://doi.org/10.1007/S12010-023-04469-Y

- Vardhan, H., Sasamal, S., Mohanty, K., 2023. Detoxification of areca nut acid hydrolysate and production of xylitol by Candida tropicalis (MTCC 6192). Prep. Biochem. Biotechnol. 0, 1–12. https://doi.org/10.1080/10826068.2023.2207093

Submitted in peer-reviewed journal

- Harsh Vardhan, Soumya Sasmal & Kaustubha Mohanty (2023) Enzymatic Saccharification of Areca nut husk by Xylanase enzyme and Characterization of saccharified biomass.

भारतीय प्रौद्योगिकी संस्थान गुवाहाटी
Indian Institute of Technology Guwahati

Curriculum Vitae

NAME	Harsh Vardhan
DATE OF BIRTH	07/07/1992
ADDRESS	Department of Chemical Engineering Indian Institute of Technology, Guwahati Guwahati, Assam-781039
Email:	harshvardhan865@gmail.com; harsh.vardhan@iitg.ac.in

EDUCATION QUALIFICATIONS

2010-2014	**Bachelor of Technology**
Institute	National Institute of Technology Agartala
Specialization	Chemical Engineering
CGPA	8.36/10
2015-2017	**Master of Technology**
Institute	Indian Institute of Technology Guwahati
Specialization	Chemical Engineering
CGPA	8.16/10
2017-Till Now	**Doctor of Philosophy**
Institute	Indian Institute of Technology Guwahati
Specialization	Chemical Engineering
Registration Date	01/01/2018

WORK EXPERIENCE

OCT 2022-TILL NOW	**Assistant Professor**
Institute	Golaghat Engineering College (GEC), Bogorijeng, Assam 785621

JAN 2018-AUG 2022	**Assistant Professor (TEQIP-III)**
Institute	Bineswar Brahma Engineering College, Kokrajhar Kokrajhar, Assam-783370

SEP 2017-NOV 2017	**Junior Research Fellow (JRF)**
Institute	Indian Institute of Technology Guwahati
Department	Chemical Engineering
Project Title	Low-cost Process Development for the Production of Xylitol from Waste Agricultural Biomass with Special Focus on Delignification and Downstream Processing, Sponsored Research Project funded by DBT, 2017-2020.

WORKSHOPS / SEMINARS ORGANIZED

- As a coordinator of Industrial visit (Digboi Refinery) with the 3rd semester students, Department of chemical engineering, Bineswar Brahma Engineering College (BBEC), Kokrajhar, held on 31st October 2018.
- Organized "**Stakeholders meeting"** in Bineswar Brahma Engineering College (BBEC), Kokrajhar, held on 27th October 2018.
- Organized, TEQIP-III funded Two-Weeks Faculty Development Program on "**Developing Teaching & Learning Techniques on Engineering Education**" Organized by BBEC, Kokrajhar from 30 Dec. 2019- 11th Jan 2020
- Conducted "**IT ITeS NASSCOM Training on future skill: Internet of Thing (IoT)"** for Beginners from 18th October 2020 to 15th November 2020

WORKSHOPS / SEMINARS ATTENDED

- Attended 5 days **"Faculty Induction Workshop**" at Indian Institute of Technology Kharagpur, on 06th - 10th February, 2018.
- Attended 3 days "**Outcomes Based Education and NBA Accreditation**" workshop held on 28-30th June 2018 at Govt. of College of Engineering, Bargur (Tamilnadu).

- Attended 5 days workshop on "**Recent Advances in Materials, Energy and Environmental Engineering**" conducted under TEQIP sponsored by MHRD, Government of India held on 16-20th July 2018 at IIT Guwahati.

- Attended 2 days "NBA Workshop" at Bineswar Brahma Engineering College, on 30th to 31st March, 2018.

- Attended 2 days **"National Symposium cum Workshop on Effectiveness of using natural filtration in water treatment**" at Bineswar Brahma Engineering College, on 27th to 28th March, 2018.

- Participated in the Faculty Development Program on "**Green Technology For Sustainable Development**" at AEC, Jalukbari from 17th to 21st December, 2018.

- Participated in International Workshop on "**Energy, Power & Environment (IWEPE 2019)**" organized by NIT Kurukshetra from March 17-19th, 2019

- Participated in the TEQIP-III Training Program on "**Advanced Pedagogy & Digital Tool**" for TEQIP Faculty Members organized by IIT Kharagpur, during July 01-05th, 2019

- Participated in the "**Professional Development Training**" under TEQIP-III held from 14th to 18th 2019 at Indian Institute of Management Tiruchirappalli.

- Participated in the TEQIP-III funded Two Day National Level Workshop titled "**Patents & IPR-Methodologies**" for generating Revenue from Research at BBEC, Kokrajhar held on the 20th & 21st June 2019.

- Participated in Short Term Course on " **Clean Energy Technologies**" held on 10th-14th June 2019 at IIT, Guwahati

- Participated in the TEQIP-III funded Two-Weeks Faculty Development Program on "**Developing Teaching & Learning Techniques on Engineering Education**" Organized by BBEC, Kokrajhar from 30 Dec. 2019- 11th Jan 2020

- Attended 5 days Short Term Course on "**Internet of Things (IoT)**" at IIT Bombay, from 27th to 31st Jan, 2020.

ACHIVMENTS AND AWARDS

- Worked as a Training and Placement Officer in BBEC Kokrajhar.
- Secured all India 31st Rank in NPIU Assistant Professor Recruitment under TEQIP-III in December 2017.
- Conducted TEQIP staff recruitment examination at Bineswar Brahma Engineering College.
- Awarded scholarship from Ministry of Human Development, Government of India to pursue post graduate studies for the session 2015-2017.
- Obtained 98.4 percentile in the Graduate Aptitude Test in Engineering (GATE) Examination, 2015.
- Consistent performance in GATE examination from 2015 to 2018.
- Achieved first class with distinction mark in B. Tech (Chemical Engineering).
- Merit Scholarship (by Govt. of Bihar) During B.Tech.

IIT GUWAHATI **Harsh Vardhan**